

AD-A143 233

PLASMA SWITCH DEVELOPMENT(U) JAYCOR ALEXANDRIA VA  
R J COMMISSO 08 JUN 84 JAYCOR-J206-84-000/6220  
N00014-82-C-2114

1/2

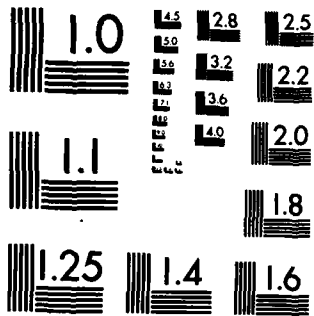
UNCLASSIFIED

F/B 20/7

NL



128  
129  
130  
131  
132  
133  
134  
135  
136  
137  
138  
139  
140  
141  
142  
143  
144  
145  
146  
147  
148  
149  
150  
151  
152  
153  
154  
155  
156  
157  
158  
159  
160  
161  
162  
163  
164  
165  
166  
167  
168  
169  
170  
171  
172  
173  
174  
175  
176  
177  
178  
179  
180  
181  
182  
183  
184  
185  
186  
187  
188  
189  
190  
191  
192  
193  
194  
195  
196  
197  
198  
199  
200



MICROCOPY RESOLUTION TEST CHART  
NATIONAL BUREAU OF STANDARDS-1963-A

12

PLASMA SWITCH DEVELOPMENT

J206-84-008/6220

**JAYCOR**

---

AD-A143 233

DTIC FILE COPY

JUL 26 1984  
A

15  
16  
17  
18

205 South Whiting Street  
Alexandria, Virginia 22304

PLASMA SWITCH DEVELOPMENT

J206-84-008/6220

Final Report  
by  
Robert J. Comisso

June 8, 1984

Prepared for:  
Naval Research Laboratory  
4555 Overlook Avenue, SW  
Washington, DC 20375

NAVY  
JUL 20 1984  
A

Under:  
Contract Number N00014-82-C-2114

This document has been approved  
for public release and sale; its  
distribution is unlimited.

# JAYCOR

6220

June 8, 1984

Mr. Ihor M. Vitkovitsky  
Code 4770  
Naval Research Laboratory  
4555 Overlook Avenue, SW  
Washington, DC 20375

SUBJECT: Final Report, Contract Number N00014-82-C-2114

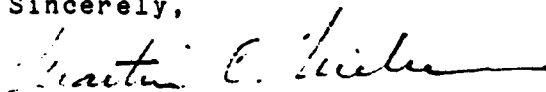
Dear Mr. Vitkovitsky:

JAYCOR is pleased to submit this Final Report entitled, "Plasma Switch Development," in accordance with the subject contract, CDRL Item Number A003.

If the Final Report is acceptable, please sign and forward the enclosed DD Form 250.

Questions of a technical nature should be addressed to Dr. Robert J. Comisso while questions of a contractual nature should be addressed to Mr. Floyd C. Stilley, our Contracts Administrator.

Sincerely,



Martin C. Nielsen  
Vice President and Counsel

ssh-b

Enclosures

cc: Code 4701  
Code 4703  
Code 2627  
DTIC



Accession For	
NO. 1234	
DATE	
BY	
FILE	
SEARCHED	
SERIALIZED	
INDEXED	
FILED	
1A-11	

UNCLASSIFIED

SECURITY CLASSIFICATION OF THIS PAGE (When Data Entered)

REPORT DOCUMENTATION PAGE		READ INSTRUCTIONS BEFORE COMPLETING FORM
1. REPORT NUMBER	2. GOVT ACCESSION NO. <b>AD-A243 233</b>	3. RECIPIENT'S CATALOG NUMBER
4. TITLE (and Subtitle) <b>PLASMA SWITCH DEVELOPMENT</b>	5. TYPE OF REPORT & PERIOD COVERED Final Report: 02/26/82 thru 02/25/84	6. PERFORMING ORG. REPORT NUMBER J206-84-008/6220
		8. CONTRACT OR GRANT NUMBER(s) N00014-82-C-2114
7. AUTHOR(s) Robert J. Comisso	9. PERFORMING ORGANIZATION NAME AND ADDRESS JAYCOR 205 South Whiting Street Alexandria, VA 22304	10. PROGRAM ELEMENT, PROJECT, TASK AREA & WORK UNIT NUMBERS A003
11. CONTROLLING OFFICE NAME AND ADDRESS Naval Research Laboratory 4555 Overlook Avenue, SW Washington, DC 20375	12. REPORT DATE June 8, 1984	
	13. NUMBER OF PAGES 182 pages	
14. MONITORING AGENCY NAME & ADDRESS (if different from Controlling Office)	15. SECURITY CLASS. (of this report) UNCLASSIFIED	
	15a. DECLASSIFICATION/DOWNGRADING SCHEDULE	
16. DISTRIBUTION STATEMENT (of this Report) 3 copies - Code 4770 1 copy - Code 4701 1 copy - Code 4703 6 copies - Code 2627 12 copies - DTIC		
17. DISTRIBUTION STATEMENT (of the abstract entered in Block 20, if different from Report)		
18. SUPPLEMENTARY NOTES		
19. KEY WORDS (Continue on reverse side if necessary and identify by block number) Electron-beam controlled switch (EBCS), plasma dynamic switch (PDS)		
20. ABSTRACT (Continue on reverse side if necessary and identify by block number)		

DD FORM 1 JAN 73 1473

EDITION OF 1 NOV 68 IS OBSOLETE  
S/N 0102-LF-014-6401

-i-

UNCLASSIFIED  
SECURITY CLASSIFICATION OF THIS PAGE (When Data Entered)

TABLE OF CONTENTS

I.	INTRODUCTION . . . . .	1
II.	E-BEAM CONTROLLED SWITCH . . . . .	2
III.	PLASMA DYNAMIC SWITCH. . . . .	5
IV.	SUMMARY. . . . .	.15
V.	REFERENCES . . . . .	.16
	APPENDIX I . . . . .	.18
	APPENDIX II. . . . .	165

## I. INTRODUCTION

This document is the Final Report for Contract Number N00014-82-C-2114 (JAYCOR Proposal Number 8206-48).

The work done under this contract relates to two opening switch concepts that may be applied to inductive store/pulse compression techniques for various pulsed power applications, of interest to the Plasma Technology Branch of the Plasma Physics Division at the Naval Research Laboratory.

The opening switch concepts that are the subject of this final report are the electron-beam controlled switch (EBCS) and the plasma dynamic switch, (PDS).

The EBCS work is well documented and will only be briefly discussed here. The details of this work can be found in Appendix I, which is a compilation of a peer reviewed journal article<sup>1</sup>, a journal paper accepted for publication<sup>2</sup>, an NRL report<sup>3</sup>, conference papers<sup>4-7</sup> (one of which was an invited paper<sup>6</sup>) and presentations at various meetings<sup>8-11</sup>. This work was performed in collaboration with NRL and JAYCOR personnel under Contract Number N00014-82-C-2336.

Because the second area of investigation, the PDS, has only been documented in JAYCOR Final Reports J206-83-006/6209 (Contract Number N00014-81-C-2152) and J206-83-010/6224 (Contract Number N00014-82-C-2336) and in one conference presentation<sup>12</sup> (see Appendix II), the progress to date will be detailed here.

## II. E-BEAM CONTROLLED SWITCH

The EBCS is an opening switch concept that has the potential for fast (~10 kHz) repetitive operation<sup>1-4</sup>. The work performed in this area includes:

- a systems study that incorporates load pulse requirements and EBCS physics self-consistently<sup>2,3,6</sup>;
- experimental study of the scaling of various switch parameters with comparison to theory<sup>1,5-9,11</sup>;
- investigations into optimizing gas mixtures for opening switch applications<sup>1,4,6,7,10,11</sup>; and
- preliminary study of the discharge stability<sup>3,6,10,11</sup>.

In addition, a new experimental facility for generating a long (>1 $\mu$ s) e-beam pulse was designed, fabricated, assembled and successfully operated. This device was necessary to demonstrate EBCS operation in the ~1 $\mu$ s conduction regime and is illustrated in Figure 1. Figure 2 shows a typical current and voltage waveform for the generator. EBCS experiments using this facility are now being planned.

References 1-11 appear in Appendix I. The engineering drawings for the EBCS to be used with the long pulse generator can be found in JAYCOR Final Report J206-83-010/6224.



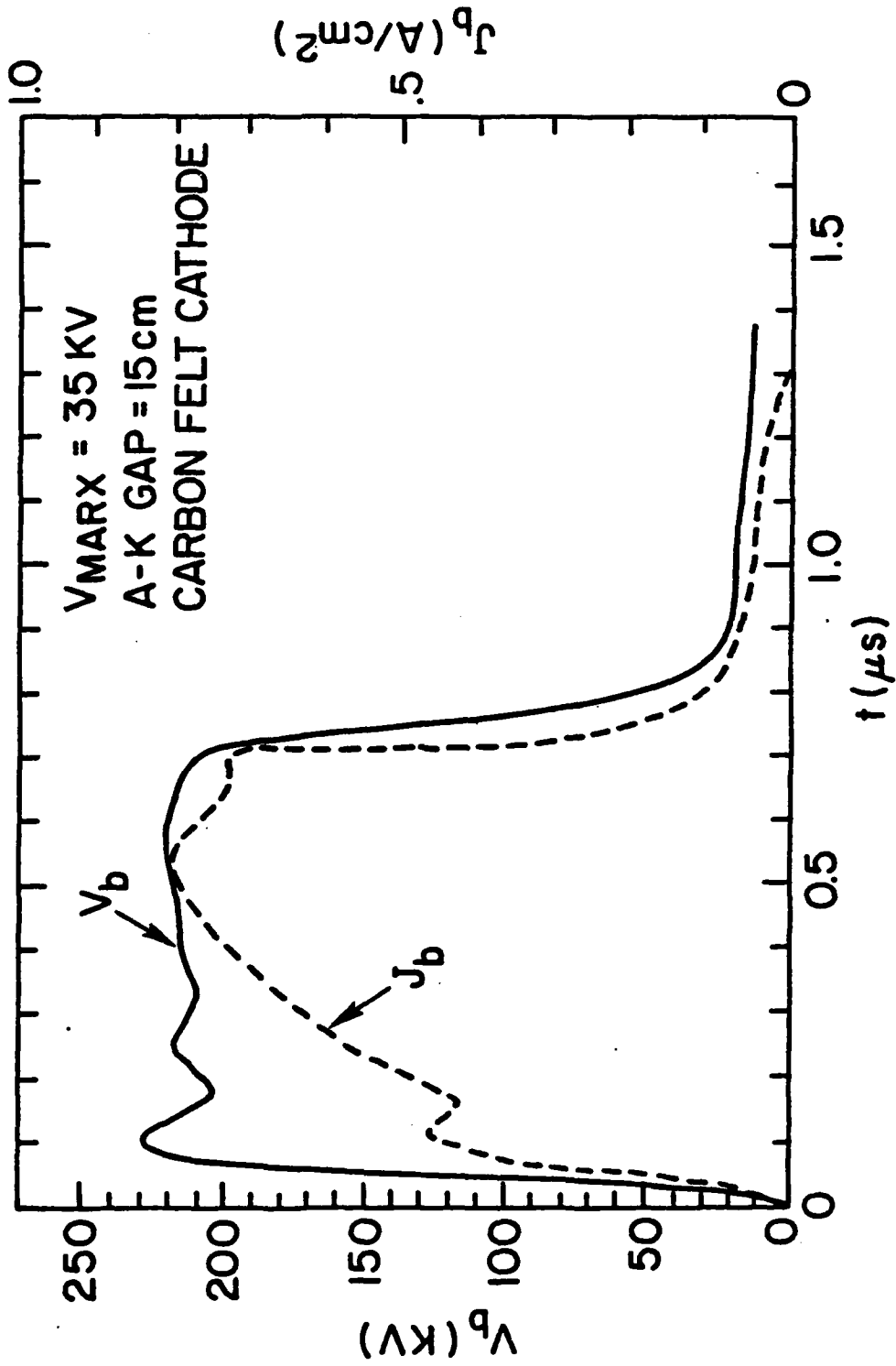


Figure 2. Electron beam accelerating voltage  $V_b$  and current density  $J_b$  as a function of time.

### III. PLASMA DYNAMIC SWITCH

The plasma dynamic switch concept is illustrated in Figure 3. A switch plasma produced by a plasma source moves with speed  $v_p$  toward two electrodes held at a relative electrical potential difference (Figure 3a). The switch circuit conducts when the plasma is between the switch electrodes (Figure 3b). Conduction ceases (the switch opens) when the plasma leaves the interelectrode region (Figure 1c). The crucial areas of investigation for this switch concept are:

- the nature of the switch plasma density gradients at the plasma leading and trailing edges;
- the interaction between the plasma and switch electrodes; and
- the formation of an arc discharge between the electrodes and how this might be avoided.

Experimental investigations into this switching concept have been carried out in fulfillment of this contract. They are a continuation of work done under Contract Number N00014-81-C-2152 and N00014-82-C-2336. The results to date have been mixed. There is some indication that the switch opens; however, the discharge soon goes into an arc mode from which there is no recovery.

Some of the initial results have been reported at a conference<sup>1,2</sup> and the conference presentation comprises Appendix II. The remainder of this section deals with most recent results.

The PDS is an exploratory concept which makes use of the high directed energy acquired by a gun produced plasma. An important aspect of this concept is the plasma spatial distribution. Earlier measurements with Faraday

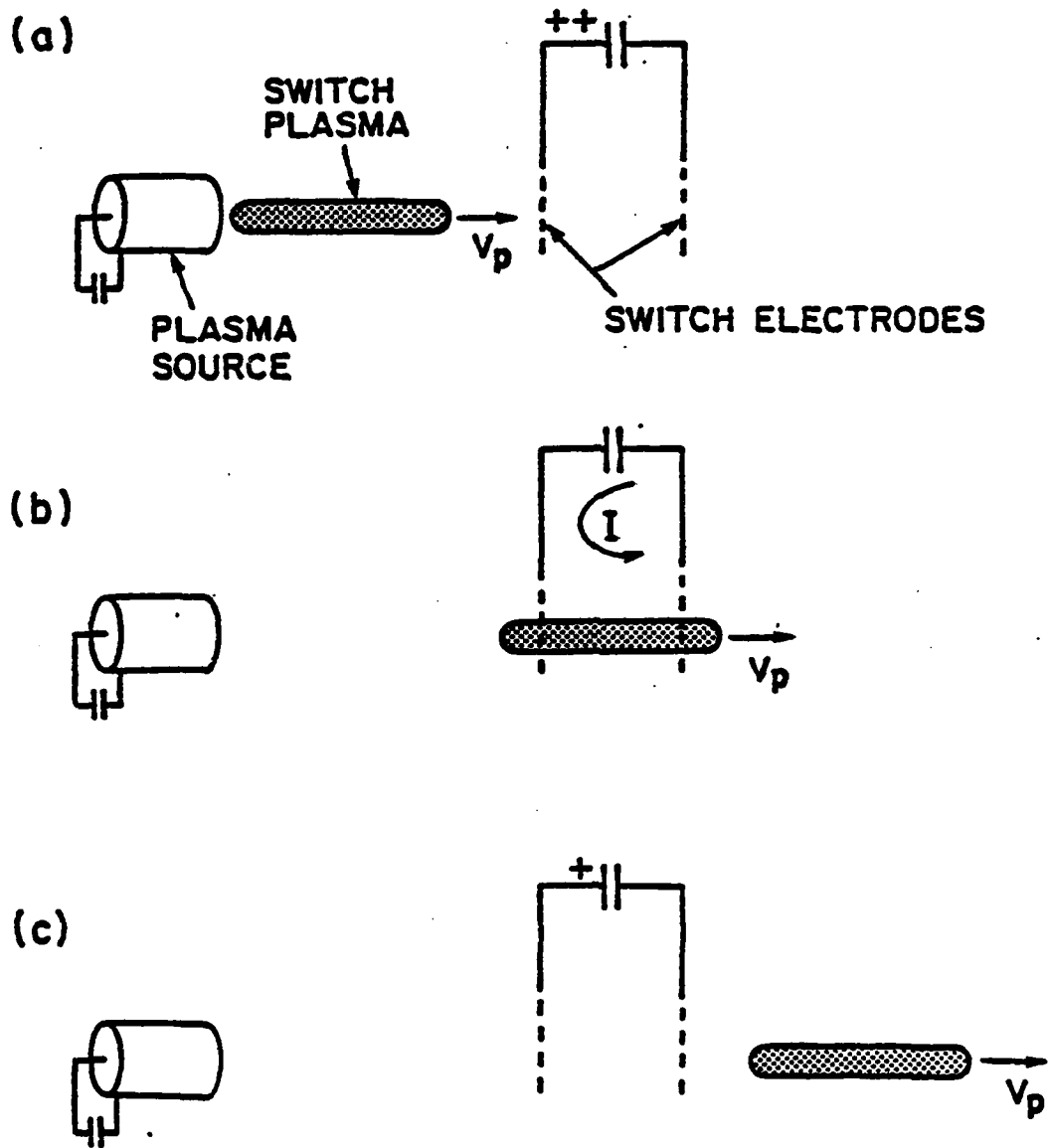


Figure 3. Schematic depiction of plasma dynamic switch concept.

cups indicated that the plasma filled the interelectrode region for times long compared to the desired conduction time ( $\sim 5\mu\text{s}$ )(cf. JAYCOR Final Report J206-83-006/6209). To ascertain the plasma distribution, several measurements were made. Witness plates (aluminum disks) were placed at various distances from the gun. Shots were taken both with the without a fuse in series with the gun. Photographs of the plates appear in Figure 4. There is a decrease in the damage when a fuse is used. Also, the azimuthally asymmetric nature of the gun plasma, particularly at the longer distances from the gun ( $\Delta Z$ ) is apparent.

A detailed set of Faraday cup measurements was taken with screen attenuators. Figure 5 is a schematic of the geometry used. The Faraday cups were of the same design as described in JAYCOR Final Report J206-82-009/ 6215, modified by the addition of permanent magnets. The magnets provided a magnetic field measured to be  $\approx 500$  G to help prevent plasma electrons from entering the cup and secondaries from leaving the cup. The aperture diameter of the Faraday cups was  $64\mu\text{m}$ .

The results with no screens were difficult to interpret because the gun plasma has such a high ion flux. However, with two attenuating screens, one of which (the one closer to the gun) is grounded, the signals can be interpreted in some cases. In Figure 6 the data from the Faraday cups both with and without a fuse wire used in series with the gun are plotted. The fuse consisted of eight 28-gauge wires in parallel, each 11.4 cm in length. There appear to be two plasma "blobs" early in time, the ion flux without fuse being  $\sim 2-3$  times higher than the case without fuse. This is a situation close to what is desired

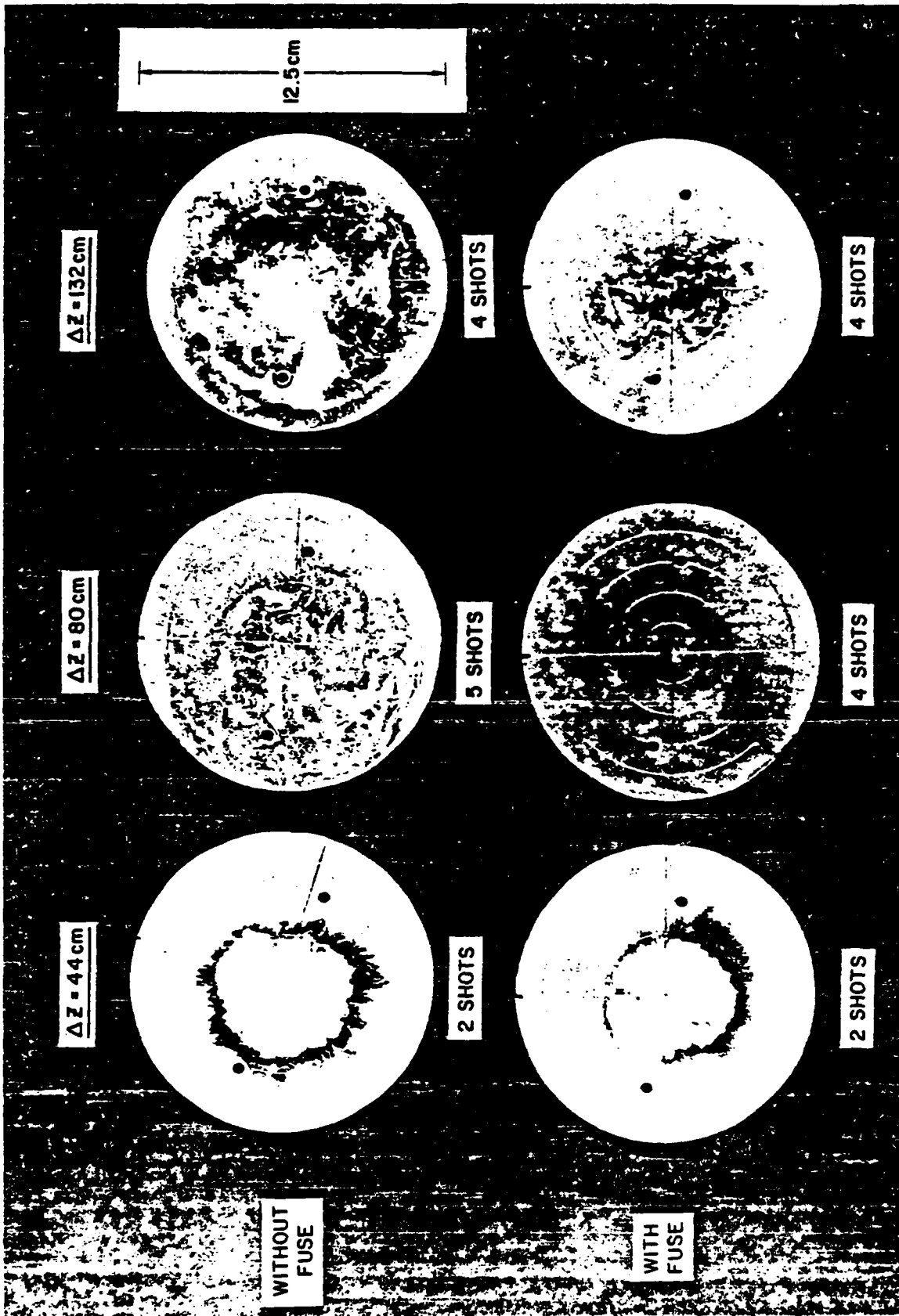


Figure 4. Photographs of the witness plates placed at various distances from the gun ( $\Delta Z$ ). Shots with and without a series fuse are displayed.

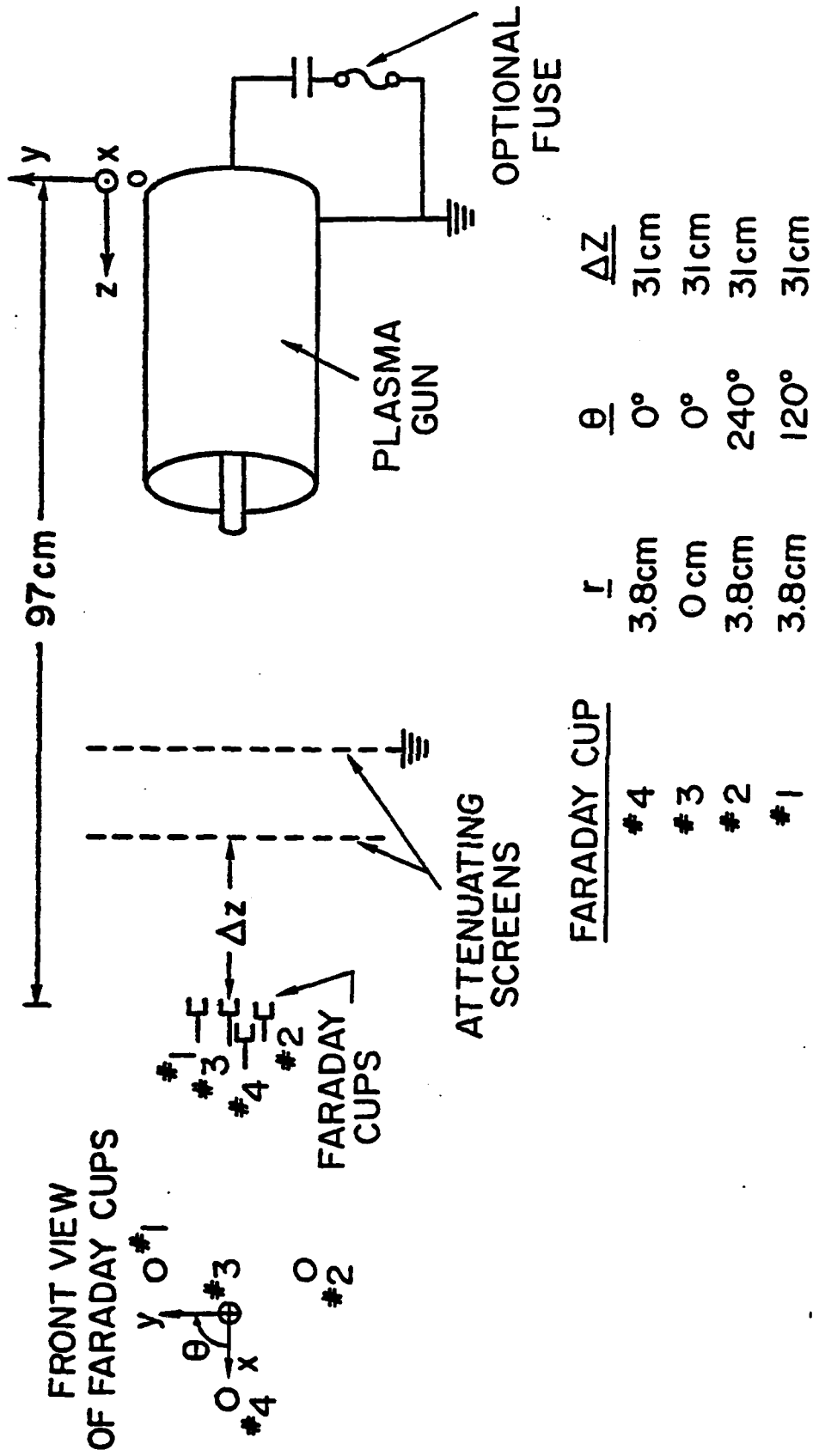


Figure 5. Schematic of geometrical arrangement for Faraday cup measurements.

# FARADAY CUP SIGNALS

Z=97cm  $\Delta Z=31\text{cm}$

$V_{FC} = -175\text{V}$

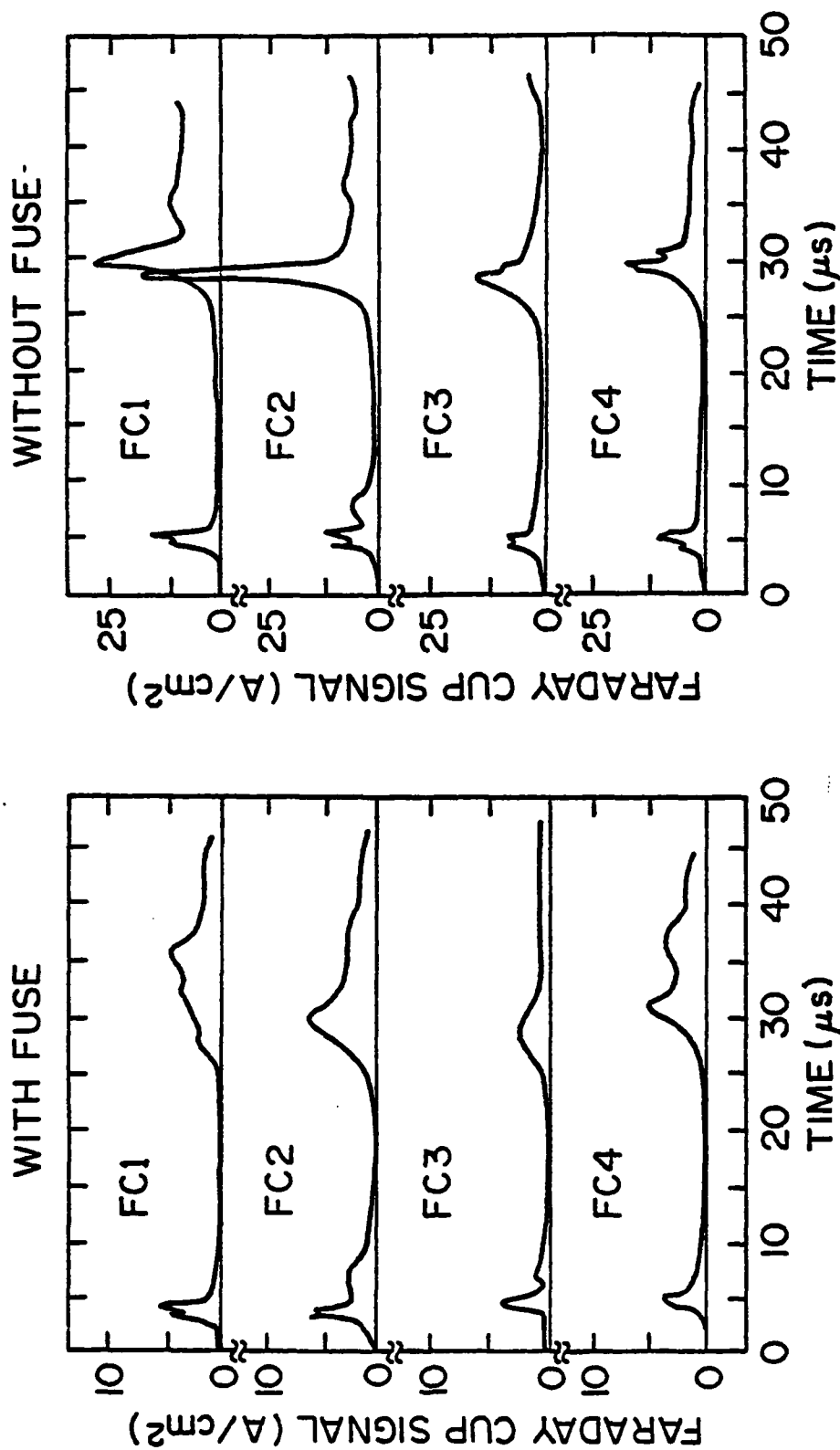


Figure 6. Faraday cup data for two attenuating screens with and without fuse.

for switching. Figure 7 has the same data plotted but on a less sensitive scale and for a longer time. Late in time the plasma ion flux for the case with no fuse is so high that only the RC decay of the Faraday cup is observed. Note that the fuse opens after one half cycle of gun current. The late time signals for the case with fuse have disappeared. If no screens are present, the signals look like the no fuse case of Figures 6 and 7, both with and without the fuse and the early time portion is very irreproducible.

A new electrode geometry was designed, assembled and successfully tested. New experiments were undertaken using the attenuating screens, the new switch geometry and a fused gun, together. A schematic of this system is given in Figure 8. The coaxial geometry was chosen for better definition of the switch electrode surface. The gun circuit was standard with  $C_G = 55 \mu\text{F}$ ,  $L_G = 184 \text{ nH}$  and  $C_G$  charged to 12kV (see Figure 8). The capacitor driving the switch was made up of two 13.4  $\mu\text{F}$  capacitors in parallel charged to 10 kV and the switch circuit inductance was  $\approx 750 \text{ nH}$ .

The results of these experiments indicate that even with attenuating screens and fuse, the switch always developed a short circuit. This behavior is most likely due to a combination of improper plasma spatial and temporal profile and electrode plasma resulting from gun plasma-electrode interaction. Investigations<sup>1,3</sup> carried out in connection with the PEOS indicate the electrode plasma expansion velocities can be  $\geq 1 \text{ cm}/\mu\text{s}$ . This means the interelectrode region would be filled with such plasma in  $\leq 10 \mu\text{s}$ . To accurately assess the viability of this scheme, more effort than what was provided to date is required.

# FARADAY CUP SIGNALS

Z = 97 cm  $\Delta Z = 31$  cm

$V_{FC} = -175$  V

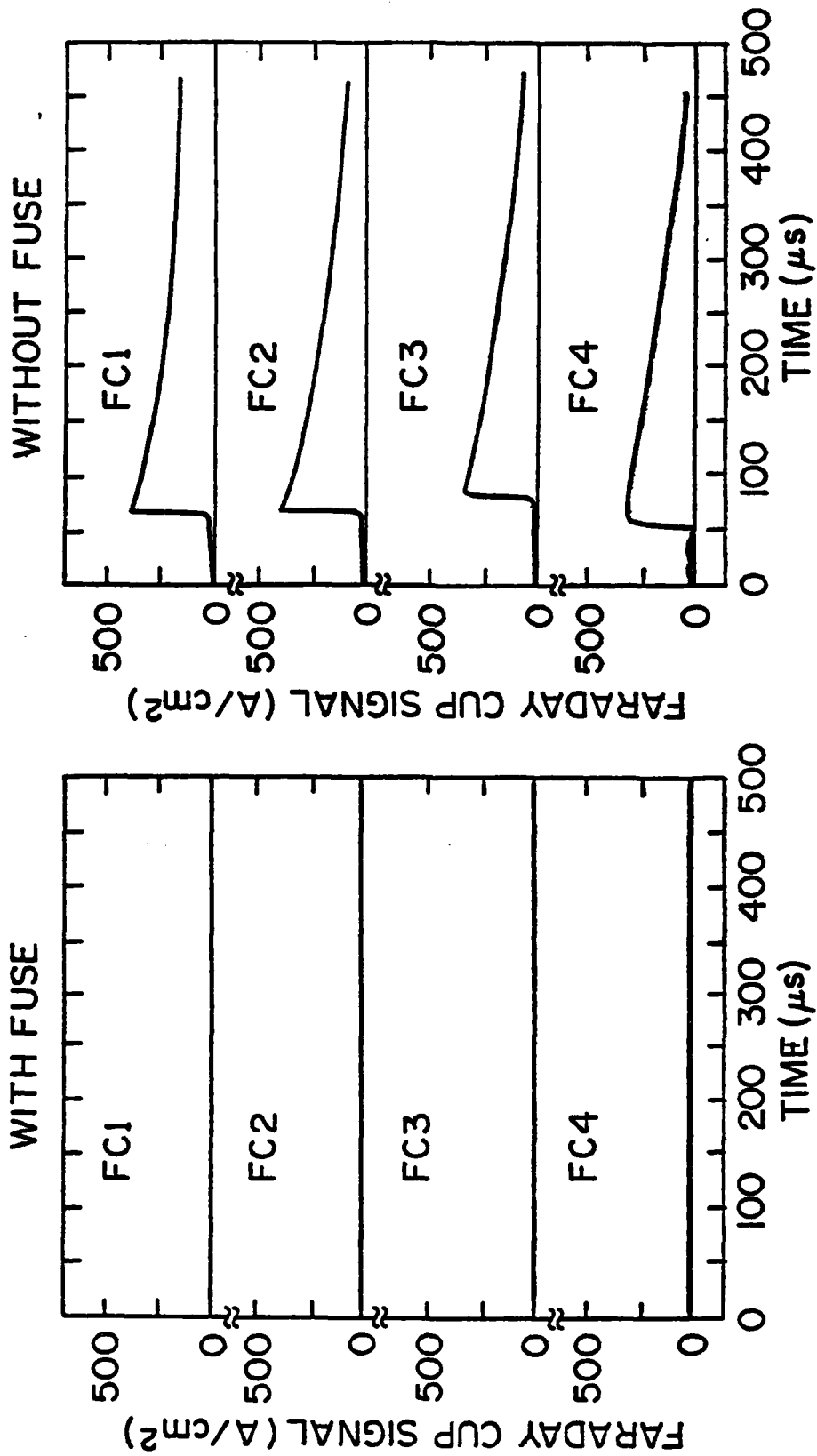


Figure 7. Faraday cup data for two attenuating screens with and without fuse on a long time scale.

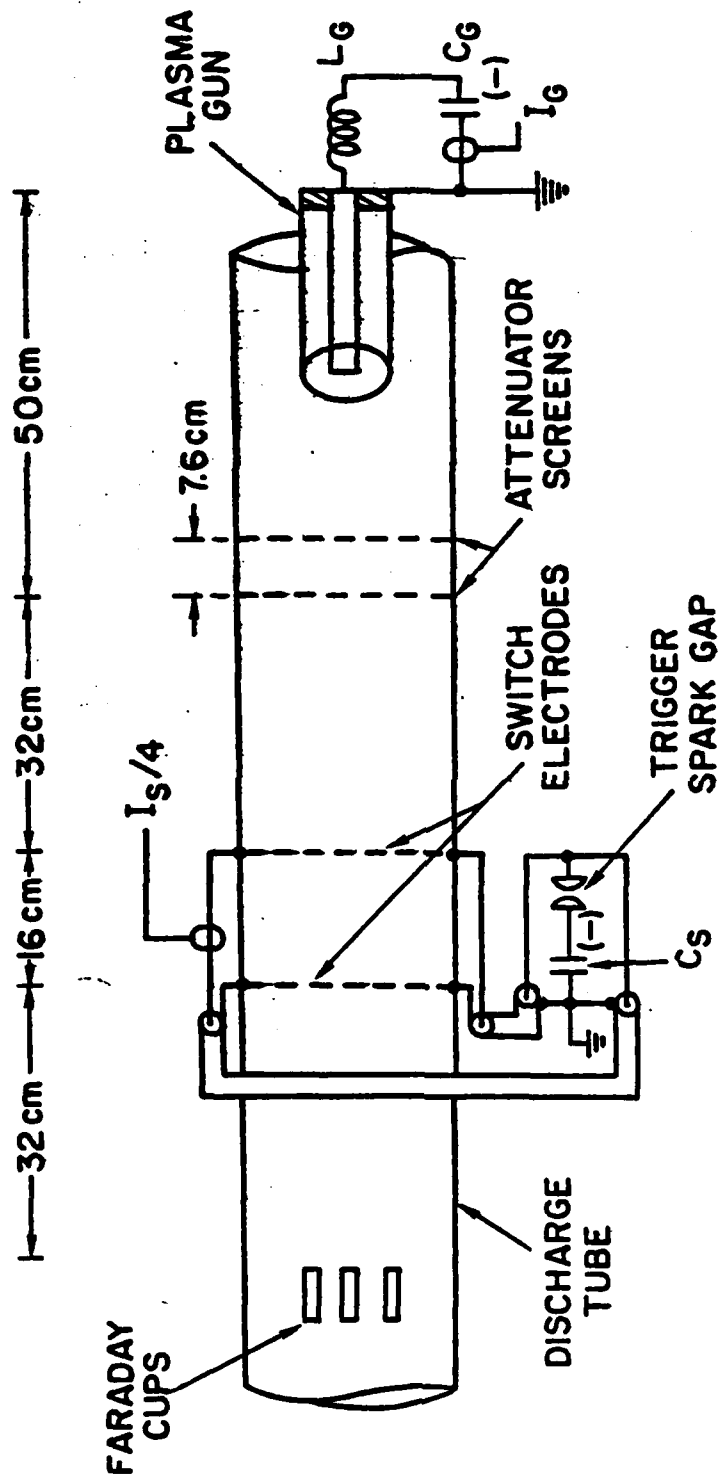


Figure 8. Schematic of the coaxial PDS arrangement. The attenuating screens are floating.

If interest in this scheme is rekindled there are several improvements that could be incorporated into the experiment:

- use of plasma source with a lower density, more uniform plasma that can be controlled more easily;
- use more transparent screens made of a highly refractory material for the electrodes;
- clean electrodes (perhaps heating);
- implement better diagnostics so that the plasma distribution can be well characterized; and
- reverse the polarity of the switch electrodes.

#### IV. SUMMARY

The tasks performed under this contract relate to the development and understanding of opening switch concepts that can be applied to inductive energy storage schemes for pulsed power applications. These concepts are the EBCS and PDS. For all of these switching schemes, JAYCOR has provided diagnostics for characterizing the switching plasma and the opening process, provided technical guidance in the design of experiments, carried out analysis aimed at understanding the physical mechanisms governing the switch behavior, and prepared all the written documentation. In addition, JAYCOR contributed to the establishment of a long pulse ( $\geq 1 \mu\text{s}$ ) e-beam facility.

The EBCS appears to be a viable switch concept for moderately high power ( $\sim 10^{10}\text{W}$ ) particularly when fast, repetitive operation ( $\sim 1 \text{ kHz}$ ) is required. The PDS has not shown great promise; however, there are several improvements which could be attempted.

V. REFERENCES

1. R. J. Commisso, R. F. Fernsler, V. E. Scherrer and I. M. Vitkovitsky, IEEE Trans. Plasma Sci. PS-10, 241 (1982).
2. R. J. Commisso, R. F. Fernsler, V. E. Scherrer and I. M. Vitkovitsky, accepted for publication, Rev. Sci. Instrum., (1984).
3. R. J. Commisso, R. F. Fernsler, V. E. Scherrer and I. M. Vitkovitsky, NRL Memo. Rep. 4975 (1982).
4. V. E. Scherrer, R. J. Commisso, R. F. Fernsler, L. Miles and I. M. Vitkovitsky, Gaseous Dielectrics III, L. G. Christophorou, ed., Pergamon Press, New York (1983), pp. 34-39.
5. V. E. Scherrer, R. J. Commisso, R. F. Fernsler and I. M. Vitkovitsky, 1982 Fifteenth Power Modulation Symposium, Baltimore, MD, IEEE Cat. No. 82CH1785-5, pp. 146 (1982).
6. R. J. Commisso, R. F. Fernsler, V. E. Scherrer and I. M. Vitkovitsky, Fourth IEEE Pulsed Power Conference, Albuquerque, NM, IEEE Cat. No. 83CH1908-3, 87 (1983).
7. V. E. Scherrer, R. J. Commisso, R. F. Fernsler and I. M. Vitkovitsky, Fourth International Symposium on Gaseous Dielectrics, Knoxville, TN, (1984), to be published, L. G. Christophorou, ed.
8. V. E. Scherrer, R. J. Commisso, R. F. Fernsler and I. M. Vitkovitsky, 1982 IEEE International Conference on Plasma Science, Ottawa, Ontario, IEEE Cat. No. 82CH1770-7, 153 (1982).
9. V. E. Scherrer, R. J. Commisso, R. F. Fernsler and I. M. Vitkovitsky, Bull. Am. Phys. Soc. 27, 982 (1982).
10. V. E. Scherrer, R. J. Commisso, R. F. Fernsler and I. M. Vitkovitsky, 1983 IEEE International Conference on Plasma Science, San Diego, CA, IEEE Cat. No. 83CH1847-3, 88 (1983).

11. V. E. Scherrer, R. J. Commisso, R. F. Fernsler and I. M. Vitkovitsky, Bull. Am. Phys. Soc. 28, 1148 (1983).
12. R. J. Commisso and I. M. Vitkovitsky, 1982 IEEE International Conference on Plasma Science, Ottawa, Ontario, IEEE Cat. No. 82CH1770-7, 154 (1982).
13. J. M. Neri, R. J. Commisso, Y. A. Goldstein, R. A. Meger, P. F. Ottinger, B. V. Weber and F. C. Young, 1983 IEEE International Conference on Plasma Science, San Diego, CA, IEEE Cat. No. 83CH1847-3, 124 (1983).

**APPENDIX I**

PAPERS ON EBCS  
REFERENCES 1-11

# Electron-Beam Controlled Discharges

R. J. COMMISSO, R. F. FERNSLER, V. E. SCHERRER, AND I. M. VITKOVITSKY

**Abstract**—When an electron beam (*e*-beam) is injected into a gas located between two electrodes, a volume discharge, which turns on and off in association with the beam, can be generated. We present a review of the theory and new experimental data for such a discharge relevant to potential applications for high-power switching. The data suggest that an optimum balance between the contradictory requirements of low resistivity and short opening time may be realized by proper choice of gas mixture.

## I. INTRODUCTION

**A**DVANCES in electrical high-power ( $\geq 10^{10}$  W) technology are necessary for the successful development of such areas as charged particle beam production and propagation, high-power lasers, and inertial confinement fusion. One task to be addressed in the improvement of high-power technology is the realization of rapid ( $> 1$  kHz) repetitive switching that is compatible with an inductive energy store. At present, the state-of-the-art of high-power repetitive opening or closing switches is limited to repetition rates of  $\leq 1$  kHz. Several authors [1]–[7] have reported on experiments and theoretical investigations in which an electron beam (*e*-beam) was used to control the resistivity of a gas mixture between two switch electrodes. This concept has been shown theoretically to have application as a repetitive opening and closing switch of high-repetition rate (in a burst mode) and high-power level [5].

An important distinguishing feature of this switch is the ability to open (cease conduction) under high applied voltage. This is achieved by using an external agent—in this case, the *e*-beam—to control the gas ionization. Initially, avalanche ionization is avoided by keeping the applied voltage across the switch below the self-sparking threshold. As the discharge evolves, cumulative gas heating also must be constrained so that thermal ionization and, more importantly, hydrodynamic reduction in gas density do not significantly lower the self-sparking threshold. A self-sustained discharge is thus prevented. Under these conditions, the fractional gas ionization, and thus the switch resistivity, at any time is determined by the competition between ionization provided by the beam and the various recombination and attaching processes characteristic of the specific gas mixture, pressure, and applied electric field. A second important feature of this switch is the volume discharge property. This characteristic makes it possible to avoid excessive heating of electrodes and the switch gas. These two features permit the discharge to return to its initial state

Manuscript received April 28, 1982; revised July 2, 1982. This work was supported by the Naval Surface Weapons Center at Dahlgren, VA 22448.

R. J. Comisso and R. F. Fernsler are with JAYCOR, Inc., Alexandria, VA 22304.

V. E. Scherrer and I. M. Vitkovitsky are with the Naval Research Laboratory, Washington, DC 20375.

of high resistivity very quickly once the source of ionization is removed. Unlike an arc discharge, this transition can be accomplished rapidly under an applied voltage.

In this paper, we present some measurements of discharge resistivity and opening time in a regime that can be scaled to high-power applications. These measurements are necessary to understand the relevant basic physical processes, to provide a bench mark for comparison with theory for scaling purposes, and also to provide data that are important in the design considerations of an actual device (e.g., switch size, ohmic heating losses, ratio of applied electric field to gas pressure, etc.). The fundamental theoretical considerations are reviewed in Section II and the experimental apparatus is described in Section III. In Section IV we present and discuss the results of our measurements and in Section V the implications and conclusions are summarized.

## II. THEORY

When an *e*-beam is injected into a chamber containing a mixture of attaching and nonattaching gases, the ionization associated with the *e*-beam competes with attachment and recombination processes, thereby controlling the conductivity of the gas. For heuristic purposes, and because of the availability of data, we consider a mixture of  $O_2$  as an attaching gas and  $N_2$  as a nonattaching gas. Then the dominant atomic and molecular processes involved in our parameter regime are outlined in what follows.

### Ionization

The number of discharge plasma electrons produced per cubic centimeter per second as a result of ionization associated with the beam can be expressed as

$$S_b = \frac{J_b}{e} \sum_A \sigma_{iA} n_A \quad (1)$$

Here  $J_b$  is the *e*-beam current density,  $e$  the electronic charge,  $n_A$  the neutral gas density of species  $A$ , and  $\sigma_{iA}$  the total effective ionization cross section associated with the beam for species  $A$ . This cross section includes the ionization caused by primary beam electrons, as well as that done by all secondaries. Such secondary processes may account for a substantial fraction of the total ionization. Ionization by discharge plasma electrons accelerated by the applied electric field (i.e., avalanche ionization) is constrained to be small compared to ionization associated with the *e*-beam.

### Recombination

The most rapid recombination process for our parameter regime is that of two-body dissociative recombination



where  $A_2^+$  is, in general, any positive molecular ion (simple or cluster) of species  $A$ . We define the effective rate at which this process occurs as  $\beta$  ( $s^{-1}$ ) and note that  $\beta$  is proportional to the density of positive molecular ions, which in turn is related to the density of discharge plasma electrons through the charge neutrality condition (see (6)). Thus this process proceeds at a progressively slower rate as the plasma electron density decreases.

The recombination rate between electrons and atomic ions (created by the  $e$ -beam) is much slower than for recombination with molecular ions. For a situation where recombination is the dominant process in the recovery of a switch, the presence of atomic ions may slow the recovery process. This is an undesirable effect, for example, in a fast opening switch. We further note that process two can rapidly heat the gas as a result of the relatively low dissociation energies ( $\sim 7$  eV) of the molecules compared to their typical ionization energies ( $\sim 15$  eV). Such heating is generally undesirable for switch applications.

#### Attachment

Two attachment processes must be considered: 1) two-body dissociative attachment



and 2) three-body attachment



We define an effective rate for these processes as  $\alpha$  ( $s^{-1}$ ) and note that  $\alpha$  is proportional to the density of the attaching gas. Because the gas is only weakly ionized,  $\alpha$  is essentially independent of the discharge plasma electron density. This type of behavior is desired for fast opening switch applications.

Assuming spatial gradients are unimportant, the continuity equation along with processes two, three, and four and (1) result in a differential equation governing the time history of the discharge plasma electron density  $n_p$

$$\frac{dn_p}{dt} = \frac{J_b}{e} \sum_A \sigma_{iA} n_A - (\alpha + \beta) n_p. \quad (5)$$

(In ignoring spatial gradients, we have also assumed electrode effects are not important, which is the case for applied voltages much greater than the sheath potential). Equation (5) is coupled to a set of rate equations, one for the density of each ionic species, so that the conservation of charge is self-consistently satisfied, i.e.,

$$n_p + \sum_A n_A^+ = \sum_A n_A^- \quad (6)$$

where  $n_A^+$  and  $n_A^-$  are the densities of positive and negative ionic species, respectively.

The electron density  $n_p$  is related to the gas resistivity through

$$\rho = (en_p \mu)^{-1} \quad (7)$$

where  $\rho$  is the gas resistivity, which is dominated by electron-

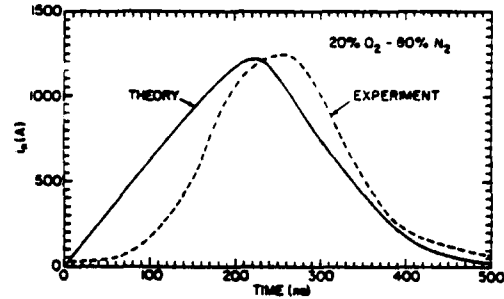


Fig. 1. Comparison of measured net current in discharge circuit  $i_n$  and numerical simulation.

neutral collisions, and  $\mu$  is the electron mobility. If  $E$  is the applied electric field, then  $\mu$  is defined by

$$\mu = \frac{v}{E} \quad (8)$$

where  $v$  is the electron drift speed.

Equations (5) and (7) are closed by the circuit equation (see (10)) and the appropriate Ohm's law for the discharge

$$E = \frac{J_p}{\rho - 1} \quad (9)$$

where  $J_p = n_p e v$  is the current density associated with the discharge plasma electrons only. Note that  $J_p$  is never measured directly; rather  $J_n$ , the net current density flowing in the discharge circuit, is directly measurable.  $J_n$  is related to  $J_p$  by  $J_n = J_p + J_b$ . For switch applications, we desire that  $J_p \gg J_b$ ; however, this condition is not satisfied in all cases.

By experimentally determining  $\rho$  or  $J_p$  for a specific choice of gas mixtures, geometry, and discharge circuit parameters, a comparison can be made with the calculated values of  $\rho$  or  $J_p$ . We have assumed that on the time scale of the experiment the bulk of the ions remain immobile.

Using the air chemistry code CHMAIR [8], the appropriate beam and circuit parameters may be coupled with the air chemistry to provide a numerical simulation of the experiment for one representative gas mixture. In this case, many more atomic and molecular physics processes than those previously outlined can be included self-consistently. Fig. 1 illustrates such a comparison. The measured net current  $i_n$  (geometrically proportional to  $J_n$ ) as a function of time is compared to the calculated value. Because  $J_b$  was not measured directly, but rather inferred from other measurements, there is a degree of uncertainty in the initial conditions used in the code. Moreover, even for air, many of the rates used in the code are not well known. Nevertheless, the comparison confirms the general validity of the physical model used.

Other calculations have been performed, for a variety of gas mixtures, in which a Boltzmann analysis was used to derive the required transport coefficients and reaction rates [9]. Simulations have also been performed incorporating axial spatial variations to assess the effects of the cathode sheath and related phenomena [10]. We note that considerably altered behavior of  $\rho$  can often be obtained by choosing gases in which  $\mu$  decreases and  $\alpha$  increases rapidly with applied field.

This point is discussed again in Section IV. Although such changes tend to complicate our understanding of the basic ionization and deionization processes and can additionally result in unstable behavior [11], they can significantly improve switch response, and therefore can be very useful in certain applications.

An important issue for long time conduction and repetitive switch applications is the heating of the gas during conduction. This heating has been addressed theoretically [5] and is included in the present simulations.

### III. EXPERIMENT

An inductively driven *e*-beam diode system, in which two exploding wire fuses are used in sequence as opening switches to produce a high-voltage pulse across the diode, provides the *e*-beam for the gas discharge studies. This system has been discussed in detail elsewhere [12]. A general schematic of the system appears in Fig. 2. Generation of a second *e*-beam pulse can be accomplished by switching in a second set of fuses and switches (not shown in the figure), which are similar to the set used in generating the first pulse [12]. The central 16 cm<sup>2</sup> of the anode is provided with holes to allow the beam to enter the discharge region at a specified average current density.

Fig. 3 depicts, with arbitrary amplitude and time scales, the current and voltage waveforms associated with single pulse operation of the inductively driven *e*-beam diode. The voltage pulse across the diode is generated by triggering spark gap  $S_1$  (Fig. 2) at time  $t_0$ . Current  $i_1$  then begins to flow in the first stage of the circuit, charging the inductor  $L_0$ . Fuse  $F_1$  acts as an opening switch that diverts the current  $i_1$ , in time short compared to the rise time of  $i_1$ , into the second stage of the system via the self-breakdown of spark gap  $S_2$  at time  $t_1$ . Because of the rapid rise of  $i_2$ , the fuse  $F_2$  can be of smaller diameter than  $F_1$  and thus responds to the current  $i_2$  by opening in a time short compared to the opening of  $F_1$ . This generates the high-voltage pulse across the diode after self-breakdown of sharpening gap  $S_D$  at time  $t_2$ . The fuse  $F_D$  interrupts the diode current at time  $t_3$ , allowing the diode to recover from the whisker and arc plasmas associated with the first pulse so that a second *e*-beam may be generated. Typically, voltages of  $\approx 180$  kV, currents of  $\approx 1$  kA at densities of  $\approx 50$  A/cm<sup>2</sup>, and beam widths of  $\approx 200$  ns were obtained with a 3-cm diameter sawblade cathode, an anode-cathode spacing of 1.5 cm, and an initial charging voltage on the capacitor  $C_0$  (56  $\mu$ F) of  $\approx 9$  kV.

Also illustrated in Fig. 2 are the driving circuit and electrode structure for the gas discharge. The gas discharge vessel was operated at a pressure of 760 torr with an electrode separation of 1.3 cm. The applied voltage on the capacitor was  $\approx 8$  kV below the static breakdown voltage for the various mixtures of gases used. A 50- $\mu$ m mylar window maintained the pressure differential between the discharge vessel and the evacuated *e*-beam diode while allowing the high-energy portion of *e*-beam to enter the discharge chamber. The values of the discharge circuit capacitance  $C$  and inductance  $L$  were 1  $\mu$ F and  $\approx 1$   $\mu$ H, respectively.

The resistance of the cell is determined by measuring the

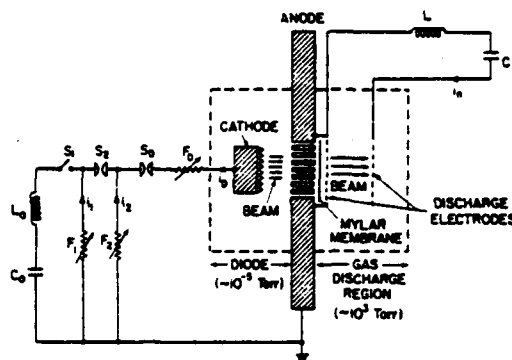


Fig. 2. Schematic of apparatus for investigating *e*-beam controlled discharges.

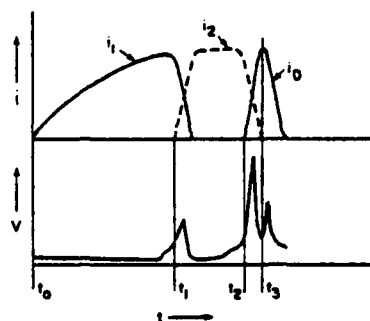


Fig. 3. Depiction of inductively driven pulser current and voltage behavior.

current through and the voltage across it. The circuit is described by

$$V_0 = R(i_n - i_b) + L \frac{di_n}{dt} + \frac{1}{C_p} \int i_n dt \quad (10)$$

where  $i_n$  is the net current flowing in the discharge circuit,  $V_0$  is the initial voltage on capacitor  $C$ ,  $L$  is the circuit inductance, and  $i_b$  is the *e*-beam current. Note that the beam current not only provides ionization, but also enters as a current source in (10).  $\rho$ ,  $J_n$ , and  $J_b$  are geometrically proportional to the gas resistance,  $R$ ,  $i_n$ , and  $i_b$ , respectively.

Representative data obtained from this apparatus with calibrated Rogowski loops and voltage dividers appear in Fig. 4. Plotted as a function of time for 20-percent O<sub>2</sub>-80-percent N<sub>2</sub> at 760 torr are: the diode voltage and current,  $V_D$  and  $i_D$ , respectively; the voltage across the discharge  $V_d$ ; the net current in the discharge circuit  $i_n$ ; and the *e*-beam current  $i_b$ . As noted in the previous section,  $i_b$  was not measured directly but was inferred from other measurements and assumed to change proportionally to  $i_D$  from shot to shot. Hence, there is some uncertainty in the determination of  $i_b$ , especially its detailed time history.

### IV. RESULTS AND DISCUSSION

When considering the design of an actual *e*-beam controlled switch, the following parameters are important: the rise time, jitter, efficiency or current gain ( $J_p/J_b$ ), resistivity, discharge

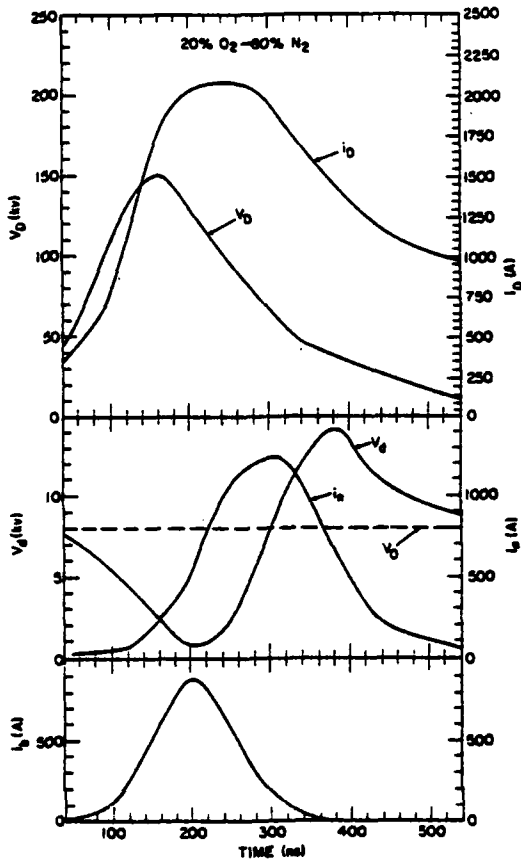


Fig. 4. Representation of the measured diode voltage  $V_D$ , diode current  $i_D$ , voltage across discharge  $V_d$ , and net current in the discharge  $i_n$  as a function of time. Also included is the inferred  $e$ -beam current in the discharge  $i_b$ .

current decay time and recovery characteristics, and the effects of energy deposition on these parameters. Rise times of  $\sim 2.5$  ns with jitter less than the response time of the instrumentation ( $\leq 0.2$  ns) [4] and current gains [6] of  $\sim 1000$  have been reported under a wide variety of operating conditions. Little data have yet been accumulated, however, on the discharge resistivity  $\rho$  and its scaling with gas mixture,  $J_b$ , beam energy, and  $E/P$ . For example, the ohmic heating power dissipation in the switch, which may have deleterious effects on switch recovery [5] may be controlled by varying the switch size and thus its resistance, for a given  $\rho$ .

For opening switch applications, it is also important to know the discharge current decay time (opening time) and the discharge recovery characteristics. Although one investigator [3] reports that a current of  $\sim 150$  kA was interrupted in  $\sim 1$   $\mu$ s at  $J_b = 1.5$  A/cm<sup>2</sup>, no systematic empirical or theoretical scaling of these parameters in an applicable regime for use as a component in a high-power inductive store pulser exists (i.e., for a parameter range of  $i_p \sim 10^5$ - $10^6$  A,  $V_d \sim 10^6$  V, opening time  $\leq 100$  ns, conduction time  $\geq 1$   $\mu$ s).

Measurements of resistivity and opening time as a function of percent attaching gas for a variety of gas mixtures at a total pressure of 760 torr have been performed using the apparatus

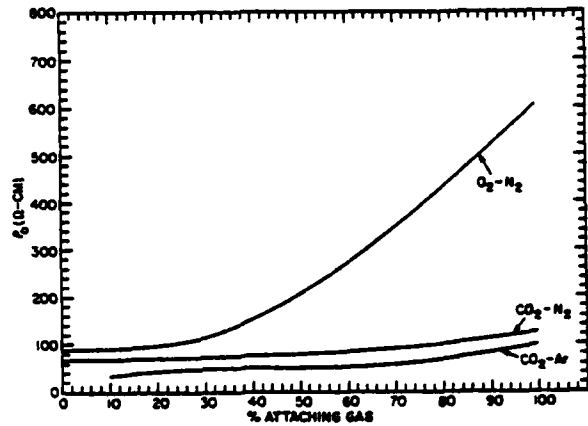


Fig. 5. Plot of resistivity at peak net current  $\rho_0$  as a function of percent attaching gas for various gas mixtures. Attaching gases are  $\text{CO}_2$  and  $\text{O}_2$ .

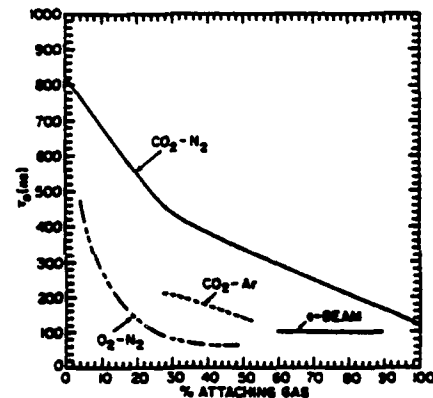


Fig. 6. Plot of discharge current decay time (opening time)  $\tau_0$ , as a function of percent attaching gas for various gas mixtures. Attaching gases are  $\text{CO}_2$  and  $\text{O}_2$ .

described in Section III. Neglecting the last term in (10) ( $< 5$ -percent correction) we have at the time of peak  $i_n$ , i.e., when  $di_n/dt = 0$ , a switch resistance of

$$R_0 = \frac{V_0}{(i_n - i_b)} \quad (11)$$

$\rho_0$  is then related to  $R_0$  through the switch geometry. In Fig. 5 we present a summary of  $\rho_0$  as a function of attaching gas for  $10 \text{ A} \leq J_b \leq 30 \text{ A/cm}^2$ . Over this range of  $J_b$ , the data varies less than a factor of 2, typically  $\sim 40$  percent. The attaching gases are  $\text{O}_2$  and  $\text{CO}_2$ . These results illustrate the relative merit of the gas combinations and percentages for producing low resistivity. The discharge current decay time  $\tau_0$  is presented in Fig. 6 for the same gas combinations and for the same incident  $e$ -beam current density as the previous figure. As a reference, the decay time of the  $e$ -beam is also given. The decay times and rise times may be governed by circuit parameters, as well as the amplitude variation of the beam current and the attachment rate.

Note that, in general, one would expect the gas combinations which give the shortest  $\tau_0$  have the highest  $\rho_0$  (assuming  $\alpha$  and

$\mu$  are only weak functions of  $E/P$ , where  $P$  is the ambient gas pressure). The curves in Figs. 5 and 6 illustrate this point. This effect also has been observed for a recombination dominated regime [6]. However, a gas mixture whose attachment rate is low for low applied field (during conducting phase) but high for high applied field (during opening phase) and whose mobility behaves just oppositely, can partially offset this trade-off between  $\tau_0$  and  $\rho_0$  [5]-[7]. We see some evidence that this situation may be realized in practice from our data. Although  $\rho_0$  for  $\text{CO}_2$ -Ar is comparable (or somewhat less) than  $\rho_0$  for  $\text{CO}_2$ - $\text{N}_2$ , the decay time for  $\text{CO}_2$ -Ar is clearly smaller than for  $\text{CO}_2$ - $\text{N}_2$ . Note that Ar is known to exhibit the Ramsauer-Townsend effect [1], [13].

These data were obtained at up to 75 percent of the self-breakdown voltage for some mixtures with no post-discharge breakdown observed. The gas recovers to a dielectric stress of  $\sim 7$  kV/cm. The current gains observed varied between 1 and 10.

#### V. SUMMARY AND CONCLUSIONS

We have reviewed the fundamental theory and presented experimental data for an  $e$ -beam controlled discharge from the perspective of high-power switching application. The data suggest that an optimum balance between the contradictory requirements of low resistivity and short opening time may be realized by proper choice of gas mixture. Comparison of theory and experiment confirms the general validity of the physical model used.

Issues yet to be addressed for the successful development of

a high-power switch include: 1) the impact of energy deposition on switch performance; and 2) the tradeoff between current gain (switch efficiency) and other switch parameters.

#### ACKNOWLEDGMENT

We wish to acknowledge the expert assistance of H. Hall and L. Miles in obtaining the data.

#### REFERENCES

- [1] R. O. Hunter, in *Proc. IEEE First Int. Pulsed Power Conf.*, Lubbock, TX, 1976, IC8: pp. 1-6.
- [2] J. P. O'Loughlin, in *Proc. IEEE First Int. Pulsed Power Conf.*, Lubbock, TX, 1976, IC8: pp. 1-6.
- [3] B. M. Kovalchuk and G. A. Mesyats, *Sov. Tech. Phys. Lett.*, vol. 2, p. 252, 1976.
- [4] K. McDonald, *et al.*, *IEEE Trans. Plasma Sci.*, vol. PS-8, p. 181, 1980.
- [5] R. F. Fernsler, D. Conte, and I. M. Vitkovitsky, *IEEE Trans. Plasma Sci.*, vol. PS-8, p. 176, 1980.
- [6] P. Bletzinger, in *Proc. Workshop Repetitive Opening Switches*, Tamaron, CO, Texas Tech Univ. Rep., Apr. 1981, p. 128.
- [7] L. E. Kline, in *Proc. Workshop Repetitive Opening Switches*, Tamaron, CO, Texas Tech Univ. Rep., Apr. 1981, p. 121.
- [8] R. F. Fernsler, A. W. Ali, J. R. Greig, and I. M. Vitkovitsky, *Naval Res. Lab Memo Rep.* 4110, 1979.
- [9] J. W. Drimianski and L. E. Kline, *Westinghouse Electric Corp. Rep.* DYD-555-85-AA, 1979.
- [10] J. J. Lowke and D. K. Davies, *J. Appl. Phys.*, vol. 48, p. 4991, 1977.
- [11] D. H. Douglas-Hamilton and S. A. Mani, *Appl. Phys. Lett.*, vol. 23, p. 508, 1973.
- [12] B. Fell, R. J. Commisso, V. E. Scherrer, and I. M. Vitkovitsky, *J. Appl. Phys.*, vol. 53, p. 2818, 1982.
- [13] S. C. Brown, *Basic Data of Plasma Physics*, 1966, 2nd. Ed. revised. Cambridge, MA: MIT Press, 1967, p. 27.

**HIGH POWER ELECTRON-BEAM CONTROLLED SWITCHES**

**R.J. Comisso, R.F. Fernsler, V.E. Scherrer  
and I.M. Vitkovitsky**

**Naval Research Laboratory  
Washington, DC 20375**

### Abstract

The application of an electron beam controlled diffuse discharge to high power ( $> 10^9$ W), repetitive opening switches is analytically formulated under a set of assumptions. Basic physics considerations are combined with energy transfer requirements to obtain analytical estimates of the e-beam controlled switch parameters for given circuit requirements. The switch design is optimized by minimizing the switch pressure subject to the constraint of system efficiency. The result of this optimization is that each of the major energy losses - conduction, opening, and electron beam production - are roughly equal to each other. This formulation is used to relate the switch parameters to the desired operating characteristics for an arbitrary number of pulses. As an example, the formalism is utilized in outlining the design of a single pulse, high power ( $\approx 10^{10}$ W) inductive storage system. A judicious choice of gas or gas mixture results in desirable changes in the system design or efficiency.

## HIGH POWER ELECTRON-BEAM CONTROLLED SWITCHES

R.J. Comisso, R.F. Fernsler, V.E. Scherrer and I.M. Vitkovitsky

Naval Research Laboratory

Washington, D.C. 20375

### I. List of Symbols

$A$	=	switch area
$E$	=	electric field across the switch
$E_C$	=	$E$ during conduction
$E_C^0$	=	$E_C$ when $I_{SW}$ is maximum
$(E/P)_B$	=	reduced breakdown field strength
$e$	=	electronic charge
$f_0$	=	$eS_b \mu P$
$g_b$	=	ratio of e-beam energy to load energy
$g_C$	=	ratio of energy dissipated during switch conduction to load energy
$g_0$	=	ratio of energy dissipated during switch opening to load energy
$I_b$	=	e-beam current
$I_L$	=	load current
$I_L^0$	=	maximum $I_L$
$I_{SW}$	=	switch plasma current

$I_{SW}^0$	=	maximum $I_{SW}$
$J_b$	=	e-beam current density
$J_{SW}$	=	switch plasma current density
$k_b$	=	fraction of total e-beam energy deposited in switch gas from inelastic processes
$k_I$	=	ratio of average switch current during conduction to $I_L^0$
$k_O$	=	fraction of peak load power dissipated by switch during opening
$k_P$	=	$\tau_O/\tau_P$
$L$	=	inductance of storage inductor
$l$	=	switch length
$N^+$	=	positive ion density
$N_a$	=	attaching gas density
$N_o$	=	non-attaching gas density
$n$	=	number of pulses
$n_p$	=	switch plasma electron density
$n_p^0$	=	$n_p$ at time e-beam ceases
$P$	=	switch gas pressure
$(P^{-1}dc_b/dx)_b$	=	reduced energy lost per unit length by beam electrons
$R_{SW}$	=	switch resistance
$S_b$	=	e-beam ionization parameter
$s_B$	=	safety factor for static breakdown
$s_H$	=	safety factor for heating
$V_b$	=	e-beam accelerating voltage
$V_L$	=	voltage across the load
$V_L^0$	=	maximum $V_L$
$V_{SW}$	=	voltage across the switch

$V_{SW}^0$	= maximum $V_{SW}$
$v$	= plasma drift velocity
$(W/P)_B$	= reduced critical energy deposited per unit volume of switch
$\alpha$	= effective attachment rate coefficient
$\beta$	= effective recombination rate coefficient
$\epsilon$	= current gain
$\epsilon_b$	= energy of beam electrons
$\epsilon_i$	= energy required for ionization per electron-ion pair
$\eta$	= energy transfer efficiency
$\mu$	= electron mobility
$\xi$	= gain factor
$\rho$	= switch resistivity
$\rho_C$	= $\rho$ during conduction
$\tau_C$	= time interval during which switch is conducting
$\tau_{COM}$	= current commutation time
$\tau_L$	= characteristic load pulse width
$\tau_O$	= time interval during which switch changes from conducting to nonconducting
$\tau_P$	= characteristic loss time for plasma electrons
$\tau_{AP}$	= characteristic loss time for plasma electrons - attachment dominated discharge
$\tau_{RP}$	= characteristic loss time for plasma electrons - recombination dominated discharge

## II. INTRODUCTION:

The successful implementation of inductive energy storage to pulsed power applications<sup>1,2</sup> ( $> 10^9 W$ ) depends critically on the development of an opening

switch. This switch must conduct current for the charging period of an inductor and then become sufficiently resistive to divert the current flowing in the switch to a load. The commutation must occur in a time short compared to the inductor charging time and in the presence of an applied electric field which increases during the commutation process. Some applications additionally require the switch to be capable of repetitively pulsed operation (see, for example, Ref. 3). Such a repetitively pulsed opening switch will more than satisfy the requirements for a repetitively pulsed closing switch of high ( $> 10$  kHz) repetition rate. Several authors<sup>4-9</sup> have reported on experiments and theoretical investigations in which an electron beam (e-beam) is used as an external agent to sustain a diffuse (volumetric) discharge in a gas. The concept as it might be used in an opening switch application is illustrated in Fig. 1. In this scheme the gas resistivity at any time is determined only by a competition between ionization provided by the e-beam and the various recombination and attaching processes characteristic of the specific gas mixture, pressure, and applied electric field. This, along with the volume discharge property, allows the gas to return to its original non-conducting state very quickly once the source of ionization is removed.

A particular design for the e-beam controlled switch (EBCS) must specify the switch gas pressure, gas mixture, area, length and e-beam generator requirements necessary to provide the required electrical characteristics of the output pulse(s) at the desired system efficiency. The design also must insure that an arc discharge is avoided, otherwise the switch will not exhibit a rapid recovery.

In this paper we review the physics of the EBCS that is relevant to the switch design. The energy transfer efficiency for an inductive storage system employing an EBCS is defined and formulated in such a way that it can be

combined with the switch physics to arrive at a set of equations that yield an analytical estimate of EBCS design parameters. This analysis self-consistently includes the switch physics, circuit requirements, and system efficiency. The switch design is optimized by minimizing the switch pressure subject to the constraint of system efficiency. As a result of this analysis, the range of applicability for the EBCS in terms of the switch conduction time and output pulse width for a given system efficiency can be identified. To illustrate this formalism we outline a design for an inductive storage system capable of delivering a single 200 kV, 100 ns full width at half maximum (FWHM), 35 kA pulse into a 6  $\Omega$  load.

The switch physics and energy transfer efficiency are discussed in Secs. III and IV, respectively. These considerations are combined in Sec. V to arrive at general expressions for the switch design parameters. An illustration of this design procedure is presented in Sec. VI.

### III. SWITCH PHYSICS CONSIDERATIONS

Various aspects of the physics associated with controlled diffuse discharges as it relates to EBCS have been discussed.<sup>4-9</sup> Here we review the physical model for the switch and discuss the discharge energetics. In the model a uniform e-beam ionization source produces a very weakly ionized gas between two electrodes across which a potential is applied. Typically,  $n_p \leq 10^{-5} N_0$ , where  $n_p$  is the switch plasma electron density and  $N_0$  is the gas density. The electrodes are perfectly uniform and the applied voltage during the conduction phase is much greater than the sheath potential<sup>6</sup> ( $\sim 1$  kV). The e-beam accelerating potential must similarly be high enough that e-beam electrons can traverse the entire switch region (Ref. 10 suggests the e-beam range should be about twice the switch length). Another assumption is a constant e-beam current and accelerating voltage with decay times that

are very short compared to the switch opening time (Sec. III-B). That these conditions be met is important because any circumstance that allows the presence of nonuniformities in the switch (other than in the cathode and anode sheaths) may result in a nonuniform electric field and degraded switch performance (breakdown).<sup>11</sup> Thus, the gas resistivity of the volumetric discharge is determined by electron-neutral collisions, and the electrical potential in the switch is a linear function of the distance between the electrodes.<sup>10</sup> We further assume for this analysis that the electron mobility and attachment rates are independent of the electron temperature. For switch design purposes this is a conservative approximation and is made to simplify the analysis. The advantages of using temperature dependent mobilities and attachment rates will be discussed in later sections. Because experiments have shown that KBCS closing times can be very short ( $< 2\text{ns}$ ),<sup>12</sup> the closing phase is not considered here.

#### A. Electron Density

We assume that the switch has a two component gas mixture made up of a non-attaching base gas of density  $= N_0$  with a small ( $< 10\%$ ) fraction of attaching gas of density  $N_a$ . Assuming further that density gradients are negligible, the continuity equation for  $n_p$  gives

$$\frac{dn_p}{dt} = S_b J_b P - (\alpha N_a + \beta N^+) n_p. \quad (1)$$

Here  $J_b$  is the e-beam current density,  $\alpha$  is the attachment rate coefficient ( $\text{cm}^3\text{-sec}^{-1}$ ),  $\beta$  is the recombination rate coefficient ( $\text{cm}^3\text{-sec}^{-1}$ ),  $P$  is the total gas pressure, and  $N^+$  is the positive ion density.  $S_b$ , a beam ionization parameter, is given by  $S_b = (e\epsilon_i)^{-1}(P^{-1}d\epsilon_b/dx)_b$  where  $e$  is the electronic charge,  $\epsilon_i = 35\text{ eV}$  is the energy required for ionization per electron-ion

pair, and  $(P^{-1} d\epsilon_p/dx)_p = 3 \text{ keV/cm-atm}$  is the reduced energy lost per unit length for the beam electrons, assumed constant. Because of non-ideal conditions, including reflected electrons at the switch electrodes, this calculation may underestimate the electron production.<sup>9,13</sup>

The time decay of switch plasma electrons can be readily estimated from Eq. (1) for both attachment dominated ( $\alpha N_a \gg \beta N^+$ ) and recombination dominated ( $\alpha N_a \ll \beta N^+$ ) switch recoveries when  $J_p = 0$ . For an attachment dominated case

$$n_p(t) = n_p^0 e^{-t/\tau_p^a}, \quad (2)$$

where  $n_p^0$  is the switch plasma electron density at the time the e-beam ceases ( $t = 0$ ) and  $\tau_p^a \equiv (\alpha N_a)^{-1}$ . Letting  $N^+ = n_p$  in Eq. (1) for the recombination dominated case results in

$$n_p(t) = \frac{n_p^0}{(t/\tau_p^r) + 1}. \quad (3)$$

Here  $\tau_p^r = (\beta n_p^0)^{-1}$ .

Note that  $n_p$  decays exponentially with time in the attachment dominated case and approximately inversely with time in the recombination dominated case. Moreover, because  $\tau_p^a$  is inversely proportional to  $N_a$ , it can be externally controlled by adding more attaching gas.<sup>7</sup> The recombination rate between electrons and atomic ions (created by the e-beam) is much slower than for recombination with molecular ions. For a situation where recombination is dominant, the presence of atomic ions may slow the recovery process. This is an undesirable effect in a fast opening switch. Note further that when molecular dissociative recombination is dominant, the gas can rapidly heat as

a result of the relatively low dissociation energies ( $\sim 7$  eV) of the molecules compared to their typical ionization energies ( $\sim 15$  eV). Such heating is generally undesirable for switching applications.

### B. Switch Resistivity and Opening Time

The switch plasma density is related to the switch plasma current density,  $J_{SW}$ , through

$$J_{SW} = \frac{I_{SW}}{A} = n_p v \quad (4)$$

Here  $I_{SW}$  is the switch plasma current,  $A$  is the switch area, and  $v$  is the electron drift speed,

$$v = \mu E \quad (5)$$

where  $\mu$  is the electron mobility<sup>14</sup> and  $E$  is the electric field across the switch. Thus the switch resistivity is given by

$$\rho = \frac{E}{J_{SW}} = (en_p \mu)^{-1} \quad (6)$$

A useful expression for the switch resistivity during conduction  $\rho_C$  can be obtained for an attachment dominated switch in equilibrium ( $dn_p/dt = 0$ ) by combining Eq. (1) and Eq. (6). Thus

$$\rho_C = \frac{\alpha N_a}{(eS_b J_b \mu P)} \quad (7)$$

A similar expression can be derived for a recombination dominated switch.

The recovery time for attachment and recombination dominated switches may be estimated by using Eqs. (2) and (3), respectively, in Eq. (6) and

determining the time for  $\rho$  to increase by some arbitrary factor, say  $10^2$ . For an attachment dominated recovery, this switch recovery (or opening) time is  $\tau_0 \sim 5\tau_p^a$ , while for recombination dominated recovery this time is  $\tau_0 \sim 10^2 \tau_p^F$ . Thus, because  $\tau_p^a$  can be made less than  $\tau_p^F$  and on the basis of other considerations discussed in Sec. II-A, an attachment dominated switch is generally desirable for these applications.<sup>7</sup>

### C. Scaling Relation

Replacing the last term in Eq. (1) with a phenomenological expression  $n_p/\tau_p$ , where  $\tau_p$  is the characteristic loss time for the switch plasma electrons in the absence of ionization; substituting  $n_p$  from Eq. (6) into Eq. (1); and assuming equilibrium Eq. (1) becomes

$$\frac{\epsilon}{\tau_p} = f_0 \left( \frac{E_C^0}{P} \right) P, \quad (8)$$

where  $f_0 \equiv eS_b \mu P$  is essentially a constant for a given gas composition and  $E_C^0$  is the electric field across the switch during conduction at the time when  $I_{SW}$  is maximum. For most gases  $f_0 \sim 10^5 - 10^6$  cm/V-s. We also define the current gain as  $\epsilon \equiv I_{SW}^0 / I_b$ , where  $I_b$  is the e-beam current and  $I_{SW}^0$  is the maximum switch plasma current. The time history of  $I_{SW}$  will be discussed in Sec. IV. The switch efficiency will depend on  $\epsilon$  (Sec. III). This analytic equilibrium scaling law has particular relevance for fast EBCS applications.

In these applications one desires large

$\epsilon$  and short  $\tau_p$ . For a given gas composition and given  $E_C^0/P$ , Eq. (8)

indicates there is a "trade-off" between high  $\epsilon$  and small  $\tau_p$  while suggesting that operation at high pressure is favorable.

#### D. Discharge Stability

##### 1. Static Breakdown

If the electric field across the switch exceeds the static breakdown field at the ambient switch pressure, the switch may go into an arc mode, which is undesirable because it prevents the switch resistivity from being externally controlled. Assuming uniformity

$$V_{SW}^0 = s_B \left(\frac{E}{P}\right)_B (Pl) , \quad (9)$$

where  $V_{SW}^0 = V_L^0$  is the maximum expected voltage across the switch,  $(E/P)_B$  is the reduced breakdown field strength (typically 20 kV/cm-atm),  $s_B < 1$  is a dimensionless safety factor, and  $l$  is the switch length. This condition can be relaxed somewhat for transient ( $< 1 \mu s$ ) pulses.

##### 2. Cumulative Effects.

Cumulative heating of the gas must be sufficiently constrained so that any reduction in switch gas density does not allow the self-sparking threshold to be exceeded. Energy is deposited in the switch from resistive heating during the conduction phase, resistive heating during the opening phase, and heating of the gas from the electron beam itself. This deposited energy per unit volume of switch must be less than some critical value, required to change the instantaneous value of the gas density such that the self-sparking threshold is exceeded. Assuming this reduced critical energy deposited per unit switch volume is  $(W/P)_B$ , a constant for a given gas, we have

$$\left(\frac{T_0}{T_C} \langle I_{SW}^V \rangle_0 + \langle I_{SW}^V \rangle_C + k_b I_b^V \right) n \tau_C = s_H \left(\frac{W}{P}\right)_B A(Pl) . \quad (10)$$

Here  $n$  is the number of pulses,  $\tau_c$  is the switch conduction time,  $\langle I_{SW} V_{SW} \rangle_C$  is the average power dissipated in the switch during conduction,  $\langle I_{SW} V_{SW} \rangle_O$  is the average power dissipated in the switch during opening,  $I_b$  and  $V_b$  are the e-beam current and accelerating voltage respectively, and  $s_H < 1$  is a dimensionless safety factor. The factor  $k_b$  is the fraction of the e-beam energy deposited in the gas and is estimated as

$$k_b = (P^{-1} \frac{ds_b}{dx})_b \frac{Pl}{eV_b}, \quad (11)$$

Typically  $k_b \sim 0.1$ .

Cumulative heating can also change the chemical properties of the gas which may result in additional detrimental effects. Studies in  $N_2$  have shown that if in Eq. (10)  $(W/P)_B$  is taken to be the reduced thermal energy density of the ambient gas ( $\sim 0.1 \text{ J/cm}^3\text{-atm}$ ), these alterations are unimportant.<sup>15</sup> Such effects caused directly by the e-beam (e.g., direct dissociation) are ignored in this analysis.

### 3. Additional Effects

Assuming that bulk heating is sufficiently constrained, other phenomena may affect the switch discharge stability. For example, when  $\alpha$  is a strongly varying function of  $E$ , an attachment instability has been observed to lead to breakdown in an e-beam controlled discharge.<sup>16-18</sup> Also, inhomogeneities in the discharge or switch electrodes and resulting local heating have been suggested as possible breakdown mechanisms.<sup>8,11,19</sup> These last effects can be minimized if in Eq. (9) we use  $s_B \lesssim 0.7$ .<sup>8,19</sup>

### IV. ENERGY TRANSFER EFFICIENCY

We define the energy transfer efficiency,  $\eta$ , as

$$\eta = \frac{n I_L^{\circ} V_L^{\circ} \tau_L}{(1/2) L I_{SW}^{\circ 2} + n I_b V_b \tau_c} \quad (12)$$

Here  $I_L^{\circ}$  and  $V_L^{\circ}$  are the peak current and voltage delivered to the load, and  $\tau_L$  is the characteristic load pulse width. Note that for  $\tau_0$  and the current rise time into the load small compared to  $L/R$ , where  $L$  is generally the storage inductance and  $R$  is the system resistance after the EBCS is open (Fig.3),  $I_{SW}^{\circ} = I_L^{\circ}$  (although not at exactly the same time).

The energy stored in the storage inductor may be written as

$$\frac{1}{2} L I_{SW}^{\circ 2} = n (\langle I_{SW} V_{SW} \rangle_C \tau_c + \langle I_{SW} V_{SW} \rangle_O \tau_0 + I_L^{\circ} V_L^{\circ} \tau_L) \quad (13)$$

Thus  $\eta$  may be expressed as

$$\eta = \frac{\xi}{\xi + 1} \quad (14)$$

where the gain factor,  $\xi$ , is given by

$$\xi = \frac{I_L^{\circ} V_L^{\circ} \tau_L}{\langle I_{SW} V_{SW} \rangle_O \tau_0 + \langle I_{SW} V_{SW} \rangle_C \tau_c + I_b V_b \tau_c} \quad (15)$$

For energy transfer efficiency comparable to, for example, capacitive store pulsed power generators ( $\eta \gtrsim 0.5$ ), we require  $\xi \gtrsim 1$ . Therefore, each energy loss term in the denominator of Eq. (15) (energy cost for switching) must be sufficiently less than the numerator (energy delivered to the load). Thus with  $V_{SW}^{\circ} = V_L^{\circ}$ ,  $I_{SW}^{\circ} = I_L^{\circ}$ , and  $\langle V_{SW} \rangle_C = R_{SW} \langle I_{SW} \rangle_C$ , we define three dimensionless factors  $g_0$ ,  $g_c$ , and  $g_b$  as follows:

$$g_0 = \frac{\langle I_{SW} V_{SW} \rangle_0}{I_L^0 V_L^0} \left( \frac{\tau_0}{\tau_L} \right) < 1, \quad (16a)$$

$$g_C = \frac{\langle I_{SW} \rangle_C^2 R_{SW}}{I_L^0 V_L^0} \left( \frac{\tau_C}{\tau_L} \right) < 1, \quad (16b)$$

$$g_b = \epsilon^{-1} \left( \frac{v_b}{V_L^0} \right) \left( \frac{\tau_C}{\tau_L} \right) < 1. \quad (16c)$$

Then, the efficiency requirement is

$$\xi = (g_0 + g_C + g_b)^{-1} \geq 1 \quad (17)$$

These equations have straightforward physical interpretations. Eq. (16a) restricts the switch opening time  $\tau_0$ . (The factor  $\langle I_{SW} V_{SW} \rangle_0 / I_L^0 V_L^0$  can be estimated for various loads and will be discussed in Sec. IV.) Equation (16b) restricts the voltage drop across the switch during conduction. (The factor  $\langle I_{SW} \rangle_C / I_L^0$  in Eq. (16b) is estimated in Sec. IV for various applications.) This condition is equivalent to requiring the current decay time of the storage inductor through the switch resistance ( $L/R_{SW}$ ) be long compared to the switch conduction time. Equation (16c) restricts the switch current gain,  $\epsilon$ . At this point the values of the  $g$  factors are arbitrary, consistent with the required efficiency through Eqs. (17) and (14). The arbitrary nature of the  $g$  factors will disappear when the switch pressure is minimized subject to the efficiency constraint, Eq. (17) (Sec. V).

## V. SWITCH DESIGN

The design developed in this section emphasizes the overall energy transfer efficiency of the switch, the fundamental circuit requirements and

the switch physics. We assume all the load pulse current and voltage characteristics,  $\tau_c$ , and the system efficiency  $\eta$  are specified.

Before the results of the two previous sections can be combined to develop a self-consistent EBCS design, some specification of the switch application will be useful. Illustrated in Fig. 2 are two idealized generic examples of how an EBCS might be used to produce a short, high voltage pulse. In Fig. 2(a) the EBCS must carry current for the entire charging time of the storage inductance  $L$ . In some applications this charging time may be too long for one switch to fulfill all the requirements of the system (especially a fast opening time). The example illustrated in Fig. 2(b) employs the EBCS as the last stage in a pulse compression scheme. Here  $L$  is charged through switch  $S1$  - some opening switch that can provide a sufficiently long conduction time. The opening time for  $S1$  is  $\leq \tau_c$  for the EBCS but is long compared with  $\tau_0$  for the EBCS. Thus, the EBCS is employed as a second stage to obtain the desired pulse width and voltage. (A discussion of the relation between conduction time, and load pulse width is presented later in this section.) The current source in both cases may be a low voltage capacitor bank. Switch  $SL$  is a closing switch that may be necessary to isolate the load during the conduction phase.

Keeping Figs. 2(a) and 2(b) in mind, we define a factor

$$k_I = \frac{\langle I_{SW} \rangle C}{I_L^0} \quad (18)$$

The earlier assumption that  $I_L^0 = I_{SW}^0$  results in  $k_I = 0.5$  [Fig. 2(a)] or  $k_I = 1.0$  [Fig. 2(b)]. depending on which case is applicable. It will also be useful to define a factor  $k_0$  for the opening phase,

$$k_0 = \frac{\langle I_{SW} V_{SW} \rangle_0}{I_L^0 V_L^0} \quad (19)$$

During the time interval  $\tau_0$ , the switch current decreases to zero, the load current increases to  $I_L^0$ , and the switch resistance increases. The time history of the voltage across the switch will depend upon the load voltage time behavior. For loads where the load voltage rises to its peak value in a time  $= \tau_0$  (i.e., resistive or inductive loads),  $\langle I_{SW} \rangle_0 = 0.5 I_{SW}^0$  and  $\langle V_{SW} \rangle_0 = 0.5 V_{SW}^0$  so that  $k_0 \sim 0.25$ . For a capacitive load, the load voltage reaches its maximum in the time it takes to charge the capacitor ( $= \tau_L$  for  $\tau_L \gg \tau_0$ ). Assuming in this case that during  $\tau_0$  the current rise in the capacitor is linear and noting that  $V_L(t) = I_L(t)/C$ , where  $V_L(t)$  and  $I_L(t)$  are the instantaneous voltage and current across the load capacitor  $C$ , we obtain  $k_0 = \tau_0 / 8\tau_L$ .

Finally we define the parameter  $k_p$  as

$$k_p = \tau_0 / \tau_p \quad (20)$$

and recall from Sec. II-B that  $k_p \sim 5$  for attachment dominated recovery and  $\sim 10^2$  for a recombination dominated recovery.

The switch pressure may now be computed. Using Eqs. (16a-c) and (9), the definition of the current gain  $\epsilon$ , scaling relation Eq. (8), Eqs. (18) - (20) and recalling that the electric field across the switch at the end of the conduction phase is  $E_C^0 = I_{SW}^0 R_{SW} / l$  results in

$$P^{-1} = \frac{g_0^3 g_C^3 g_b^3 g_B^3 f_0}{k_0 k_p k_I^2} \tau_L \left(\frac{E}{P}\right)_B \left(\frac{V_L^0}{V_b}\right) \left(\frac{\tau_L}{\tau_C}\right)^2 \quad (21a)$$

Once  $P$  is known, Eq. (9) gives the switch length,  $l$ , and Eq. (10) gives

the switch area,  $A$ . Thus, with the help of Eqs. (16 a-c) and (19), we obtain

$$l = \frac{V_L^0}{s_B P(E/P)_B} \quad (21b)$$

and

$$A = \frac{I_L^0 V_L^0 (n \tau_L) g_C}{s_B (W/P)_B P l} \left[ 1 + \frac{g_O}{g_C} + k_b \frac{g_b}{g_C} \right] \quad (21c)$$

The switch dimensions thus computed insure that the switch will be large enough that the breakdown threshold will not be reached.

As long as Eq. (17) is satisfied the  $g$  factors are arbitrary. The arbitrariness of the  $g$  factors in Eq. (21a) can be removed by requiring that the switch pressure be minimum subject to the efficiency constraint, Eq. (17). This requirement is desirable for simplicity of construction. The method of Lagrange undetermined multipliers<sup>20</sup> can be used to do this minimization. The result is  $g_O = g_C = g_b$ . Thus, the switch with the lowest pressure for a given system efficiency is one for which each of the energy dissipation terms (each term in the denominator of Eq. (15)) is equal to each other.

The amount of attaching gas necessary to obtain the required opening time can be estimated from the arguments of Secs. II-A and II-B. For an attachment dominated recovery ( $\tau_0 = 5 \tau_p^a$ )

$$N_a = \frac{5}{\alpha \tau_0} \quad (21d)$$

The e-beam generator requirements are determined from  $V_b$ ,  $I_b$ ,  $\tau_0$ , and  $A$ .  $I_b$  is computed from Eq. (16c) and the definition of  $\epsilon$ . The e-beam

generator must actually provide a higher current than  $I_b$  to account for current lost to the structure supporting the vacuum-high pressure interface. The value chosen for  $V_b$  in Eq. (21a) can be combined with  $P$  and  $l$  to compute  $k_b$  of Eq. (11). Note that for the beam to traverse the switch length  $V_b$  will depend on the product  $Pl$  as does  $V_L^0$ . Therefore, one can show that typically  $V_b \lesssim V_L^0$ .

The performance of an EBCS is primarily limited by the desired switch efficiency and by the ambient switch gas pressure, as indicated by Eqs. (17) and (21a). Choosing  $k_0 = 0.25$ ,  $k_p = 5$ , and  $(E/P)_B = 20\text{kV/cm-atm}$ ; using Eq. (14) and (17) with  $g_0 = g_0 = g_b$ ; and assuming  $V_b = V_L^0$ , Eq. (21a) can be rewritten as

$$\left(\frac{\tau_C}{\tau_L}\right) = 0.6P \left(\frac{1-\eta}{\eta}\right)^3 f_0 \tau_L. \quad (22)$$

Eq. (22) is plotted in Fig. 3 for  $\eta = 0.5$  and  $0.8$ ,  $f_0 = 2 \times 10^6 \text{ cm/V-s}$ , and  $P = 10 \text{ atm}$ . The values of  $f_0$  and  $P$  chosen are representative upper limits for these parameters. Figure 3 gives the effective range of applicability of the EBCS in terms of the ratio of conduction time to load pulse width for a desired load pulse width.

#### V. EXAMPLE

Although the results of Sec. IV can be applied for an arbitrary number of pulses, suppose we desire to generate only a single high voltage pulse in the manner illustrated in Fig. 2(a), using a capacitor bank of capacitance  $C$  for the current source. The desired pulse characteristics are  $I_L^0 = 35 \text{ kA}$ ,  $V_L^0 = 200 \text{ kV}$ ,  $\tau_L = 100 \text{ ns}$ , with  $R_L = 6 \Omega$ . This choice of these parameters is relevant to several pulsed power applications.<sup>3,21</sup> For this problem we choose a conduction time for the switch of  $1 \mu\text{s}$ . The situation depicted in Fig. 2(a) has  $k_I = 0.5$ . Also, for an attachment dominated recovery  $k_p = 5$ .

Referring to suggested gases<sup>5,22</sup> we take for the switch gas a 1:9 N<sub>2</sub>-Ar mixture. This mixture exhibits the Ramsauer-Townsend collision cross section behavior.<sup>5, 22, 23</sup> The addition of N<sub>2</sub> cools the switch plasma electrons through excitation of N<sub>2</sub> vibrational levels, thereby keeping them near the Ramsauer-Townsend minimum. We take for  $f_0$  an average value of  $\approx 2.5 \times 10^5$  cm/V-sec and assume it is constant. Taking  $k_0 = 0.25$ ,  $s_B = 0.75$ ,  $v_L^0 = v_b$ ,  $(E/P)_B = 20$  kV/cm-atm,  $s_H = 0.5$ ,  $(W/P)_B = 0.1$  J/cm<sup>3</sup>-atm,  $\tau_c = 1$   $\mu$ s, and  $\eta = 0.6$ , Eqs. (21a-c) give:  $P = 25$  atm,  $l \sim 0.6$  cm, and  $\Lambda = 335$  cm<sup>2</sup>, respectively. Equation (16a) gives  $\tau_0 = 60$  ns and Eq. (16c) gives  $\epsilon = 70$ . Thus the current densities are  $J_{SW} = 100$  A/cm<sup>2</sup> and  $J_b = 1.5$  A/cm<sup>2</sup>. The fraction  $f$  of attaching gas can be obtained from Eq. (21d) and the (3-body) attachment rate for O<sub>2</sub>;  $f = 0.2\%$ . Finally the switch resistance during conduction comes from either Eq. (7) or Eq.

$$(16b), R_{SW} = 0.35\Omega.$$

With this information one can design the e-beam generator and calculate the required values of C and L. Note that this is an LRC circuit. A finite amount of current (or, equivalently, magnetic flux) is lost during both the conduction and opening phases as a result of the finite switch and load resistances, respectively. This is a direct consequence of having  $\eta < 1$ . Therefore, the choice of L, C, and the initial voltage on C must be such as to compensate for these losses.

The circuit of Fig. 2(a) can be solved analytically. Considering the period during and after opening, using Eqs. (2) and (6) to give the time dependence of the switch resistance  $R_{SW}(t)$ , assuming  $J_b = 0$  at  $t = 0$ , and taking  $C = 0.5$   $\mu$ F and  $L = 0.8$   $\mu$ H we obtain the plots shown in Fig. 4 for the system just described. In this case  $R_{SW}(0) = R_{SW} = 0.35\Omega$  and C is charged to

50 kv.

The use of a gas or gas mixture whose mobility and attachment rate vary rapidly as a function of  $E/N_0$  (i.e., electron temperature) has not been discussed. Gases that have high mobility for low  $E/N_0$  and low mobility for high  $E/N_0$  in combination with gases whose attachment rates behave just oppositely have been suggested.<sup>7, 24</sup> The Ar-N<sub>2</sub> mixture used in the example exhibits this tendency to some degree (factor ~ 2); however, CH<sub>4</sub> shows a strongly increased mobility at low  $E/N_0$  values while having comparable mobility at high  $E/N_0$ .<sup>23</sup> For example, if a mixture of CH<sub>4</sub> and C<sub>3</sub>F<sub>8</sub><sup>24</sup> were used in the example then average values of  $f_0$  and  $\alpha$  give a pressure of ~ 8 atm with  $f = 1\%$  for the same efficiency. This is a factor of ~ 3 decrease in pressure compared with Ar-N<sub>2</sub> and is directly attributable to the factor of ~ 3 increase in average  $f_0$  for CH<sub>4</sub> at the same  $E/N_0$ . Because CH<sub>4</sub> is polyatomic it serves to cool the electrons itself and no additional gas is needed to keep the electron energy near the Ramsauer-Townsend minimum. If the pressure is left at the original 25 atm, then  $\eta$  will increase from 0.6 to ~ 0.75. In the case of CH<sub>4</sub>, however, the procedure of Sec. IV is not nearly as applicable as for  $f_0 = \text{constant}$ . The problem should be done by numerical simulation, which is beyond the scope of this paper.

This work was supported by the Naval Surface Weapons Center, Dahlgren, VA.

#### References

1. R.D. Ford, D. Jenkins, W.H. Lupton, and I.M. Vitkovitsky, Rev. Sci. Inst. 52, 694 (1981).

2. S.A. Nasar and H.H. Woodson, Proceedings of the Sixth Symposium on Engineering Problems of Fusion Research, IEEE Pub. No. 75CH1097-5-NPS (1975), p. 316.
3. W.A. Barletts, Lawrence Livermore Laboratory Report UCRL-87288 (1981).
4. R.J. Comisso, R.F. Fernsler, V.E. Scherrer, and I.M. Vitkovitsky, IEEE Trans. Plasma Sci. PS-10, 241 (1982) and references therein.
5. S.E. Kline, IEEE Trans. Plasma Sci., PS-10, 224 (1982).
6. M. R. Hallada, P. Bletzinger, and W. F. Bailey, IEEE Trans. Plasma Sci., PS-10, 218 (1982).
7. R.F. Fernsler, D. Conte, and I.M. Vitkovitsky, IEEE Trans. Plasma Sci. PS-8, 176 (1980).
8. R.J. Comisso, R.F. Fernsler, V.E. Scherrer and I.M. Vitkovitsky, proceedings of 4th IEEE Pulsed Power Conference, Albuquerque, NM, IEEE Cat. No. 83CH1908-3 (1983), p. 87. ,
9. J.F. Lowry, L.E. Kline and J.V.R. Heberlein, *ibid*, p. 94;  
P. Bletzinger, *ibid*, p. 37.
10. A. M. Orishich, A. G. Ponomarenko and V. G. Posulch, J. Appl. Mech. and Tech. Phys. No.1, XI (1979).
11. Yu, D. Korolev and A. P. Khuzeev, High Temp. Phys. 13, 779 (1975).
12. K. McDonald, M. Newton, E. E. Kundhardt, M. Kristiansen and A. K. Gruenther, IEEE Trans. Plasma Sci. PS-8, 181 (1980).
13. Richard Cecil Smith, Appl. Phys. Lett. 25, 292 (1974).
14. S.C. Brown, Basic Data of Plasma Physics, (MIT Press, Cambridge, 1967), pp. 87-94.
15. T.H. Lee, Physics and Engineering of High Power Devices, (MIT Press, Cambridge, MA. 1975), p. 305.
16. D.H. Douglas-Hamilton and Siva A. Mani, Appl. Phys. Letter. 23, 503

(1973).

17. D.H. Douglas-Hamilton and S.A. Mani, *J. Appl. Phys.* 45, 4406 (1974).
18. M.N. Andreeva, I.G. Persiantsev, V.D. Pis'mennyi, V.M. Polushkin, A. T. Kakhimov, M.A. Timofeev, and E.G. Treeva, *Sov. J. Plasma Phys.* 3 (6), 770 (1977).
19. S.A. Genkin, Yu. D. Korolev, V.G. Rabotkin, and A.P. Khuzeev, *Sov. J. Plasma Phys.* 7 (3), 327 (1981).
20. H. Goldstein, Classical Mechanics, (Addison-Wesley, Reading, 1950), p. 41.
21. R. J. Comisso, R. F. Fernsler, V. E. Scherrer, and I. M. Vitkovitsky, *NRL Memo Rep.* 4975 (1982).
22. Dzimianski and L. E. Kline, *Air Force Wright Aeronautical Laboratory Report AFWAL-TR-80-2041* (1980).
23. J. B. Hasted, Physics of Atomic Collisions (American Elsevier, New York, 1972), pp. 306-310.
24. L. G. Christophorou, S. R. Hunter, J. G. Carter, and R. A. Mathis, *Appl. Phys. Lett.* 41, 147 (1982).

### Figure Captions

Fig. 1. Illustration of opening switch application for an e-beam controlled diffuse discharge.

Fig. 2. Two idealized generic examples of high-voltage short-pulse generation using an EBCS. In case (a) the EBCS is used to charge the storage inductance,  $L$ , and to provide the fast opening. In case (b) the functions of charging the inductor and fast opening are accomplished using two switches, the EBCS providing the fast opening in a pulse compression scheme.  $\tau_{COM}$  is the time for current to be diverted from  $S_1$  to the EBCS.

Fig. 3. Ratio of load pulse width,  $\tau_L$ , to EBCS conduction time,  $\tau_C$ , as a function of load pulse width for system efficiencies of  $\eta=0.5$  and  $0.8$ .

Fig. 4. Plots of instantaneous switch resistance  $R_{SW}(t)$ ; currents  $I_{SW}$ ,  $I_L$ ,  $I = I_{SW} + I_L$ ; and load voltage  $V_L$  normalized to the switch resistance during conduction  $R_{SW}$ ; peak load current  $I_L^0$  and peak load voltage  $R_L I_L^0$ , respectively.

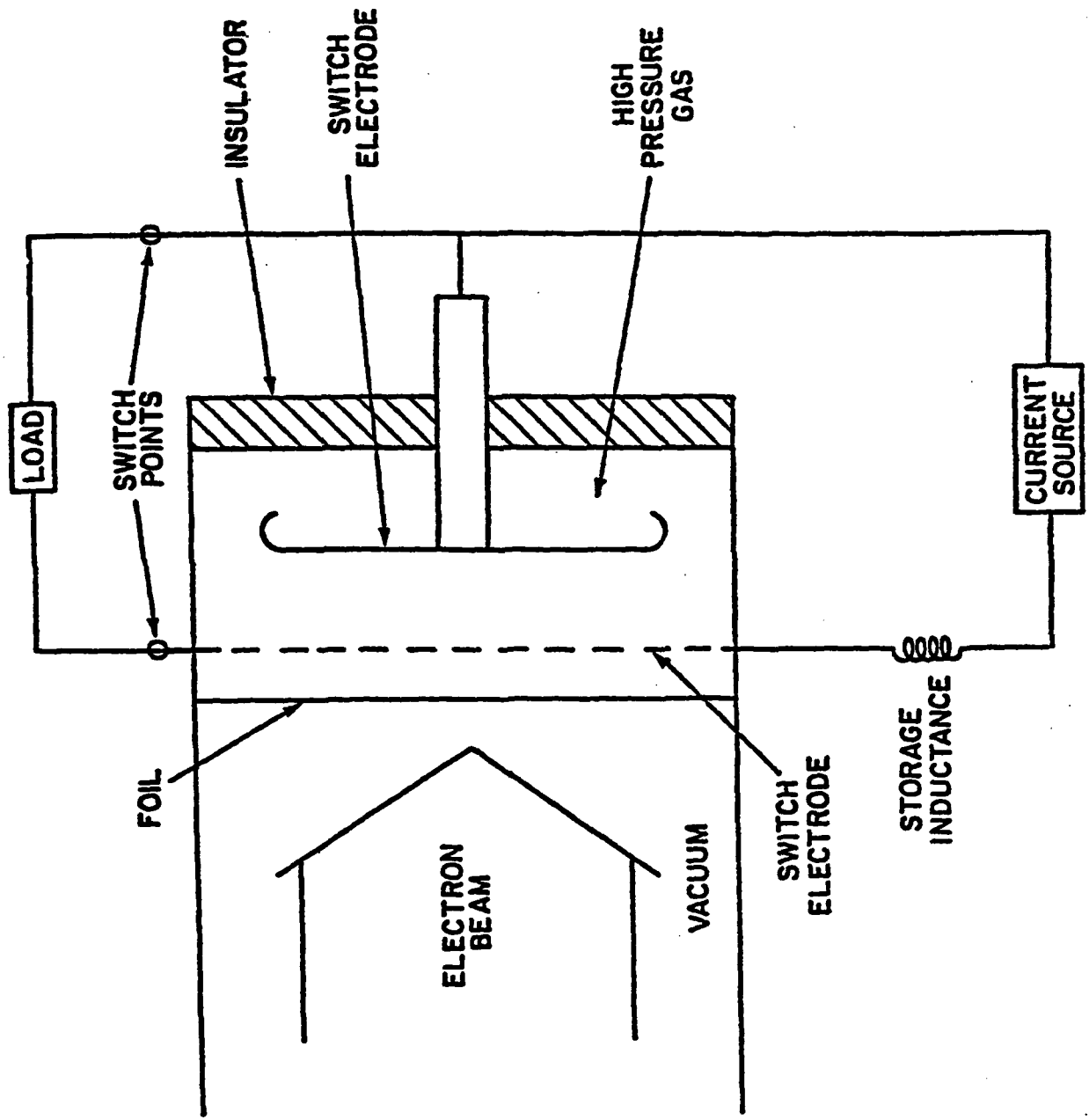


Figure 1

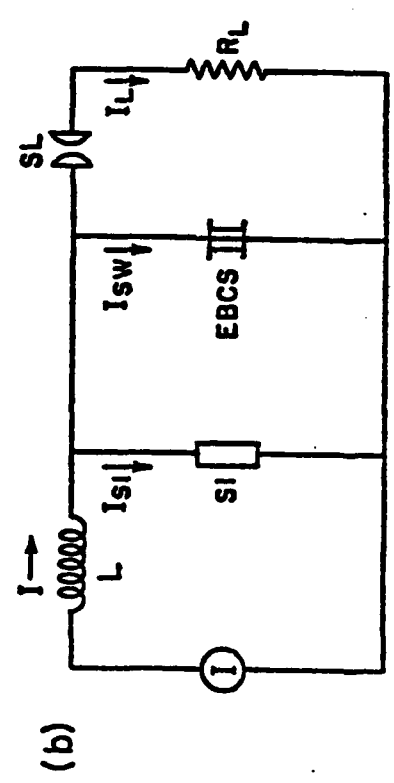
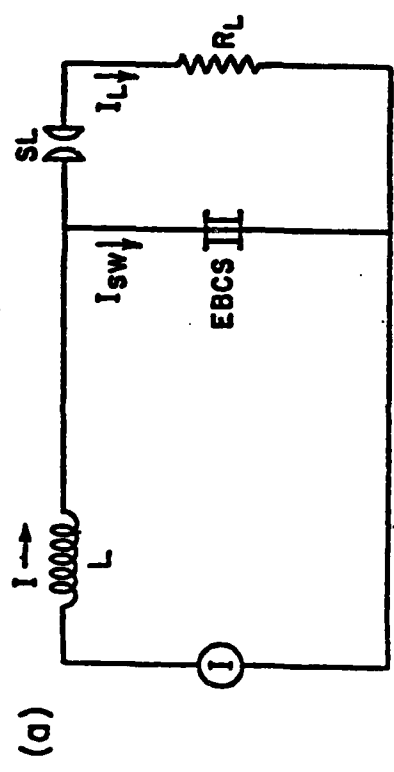
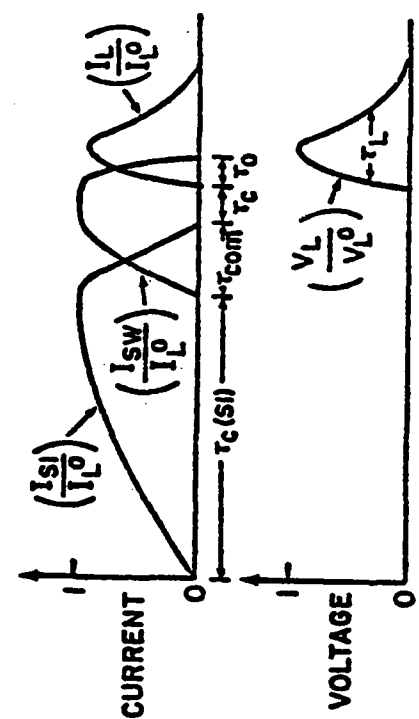
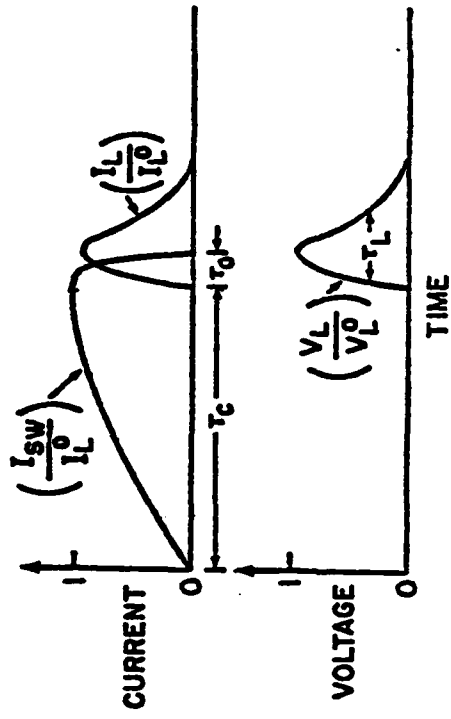


Figure 2

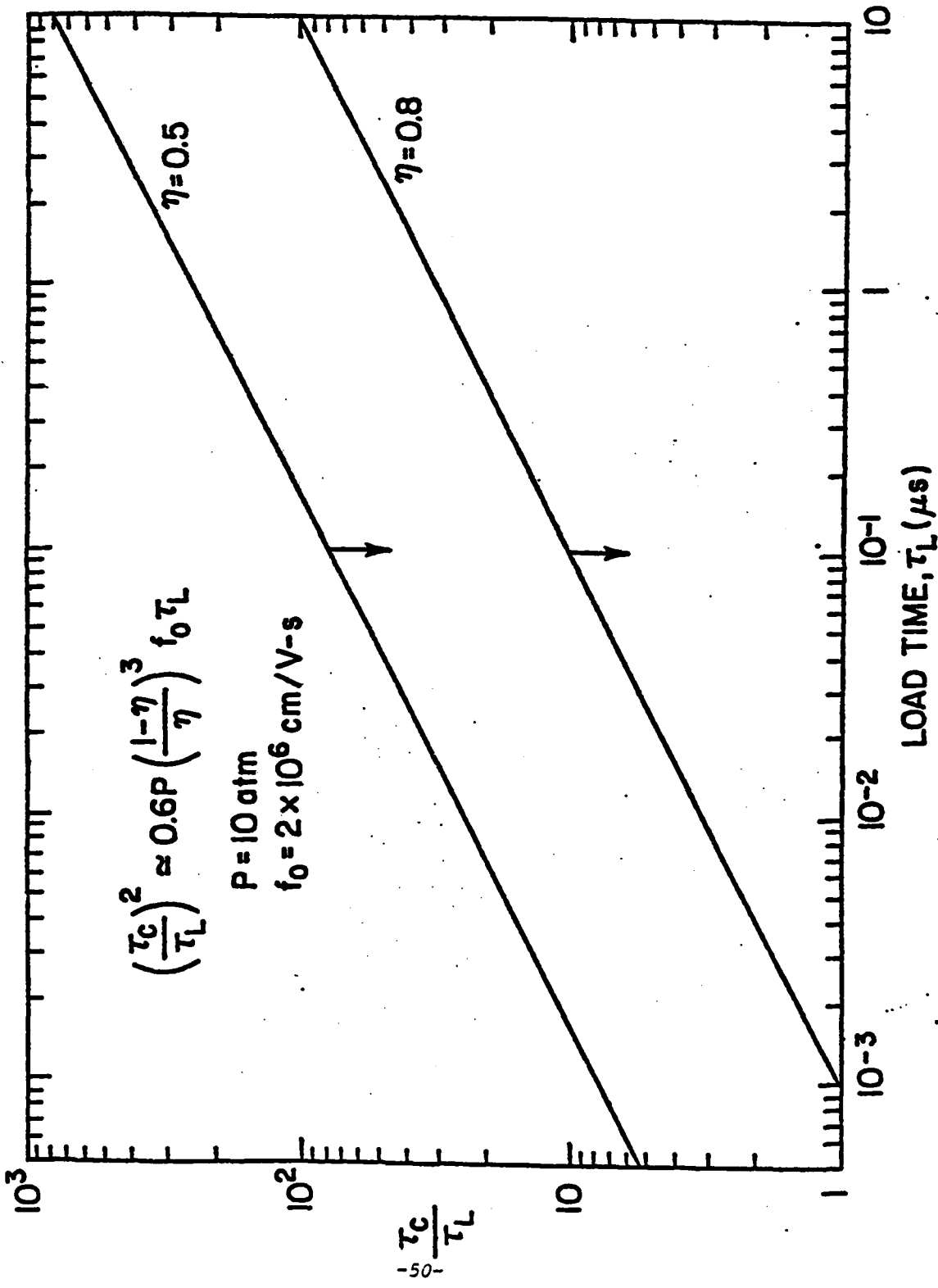


Figure 3

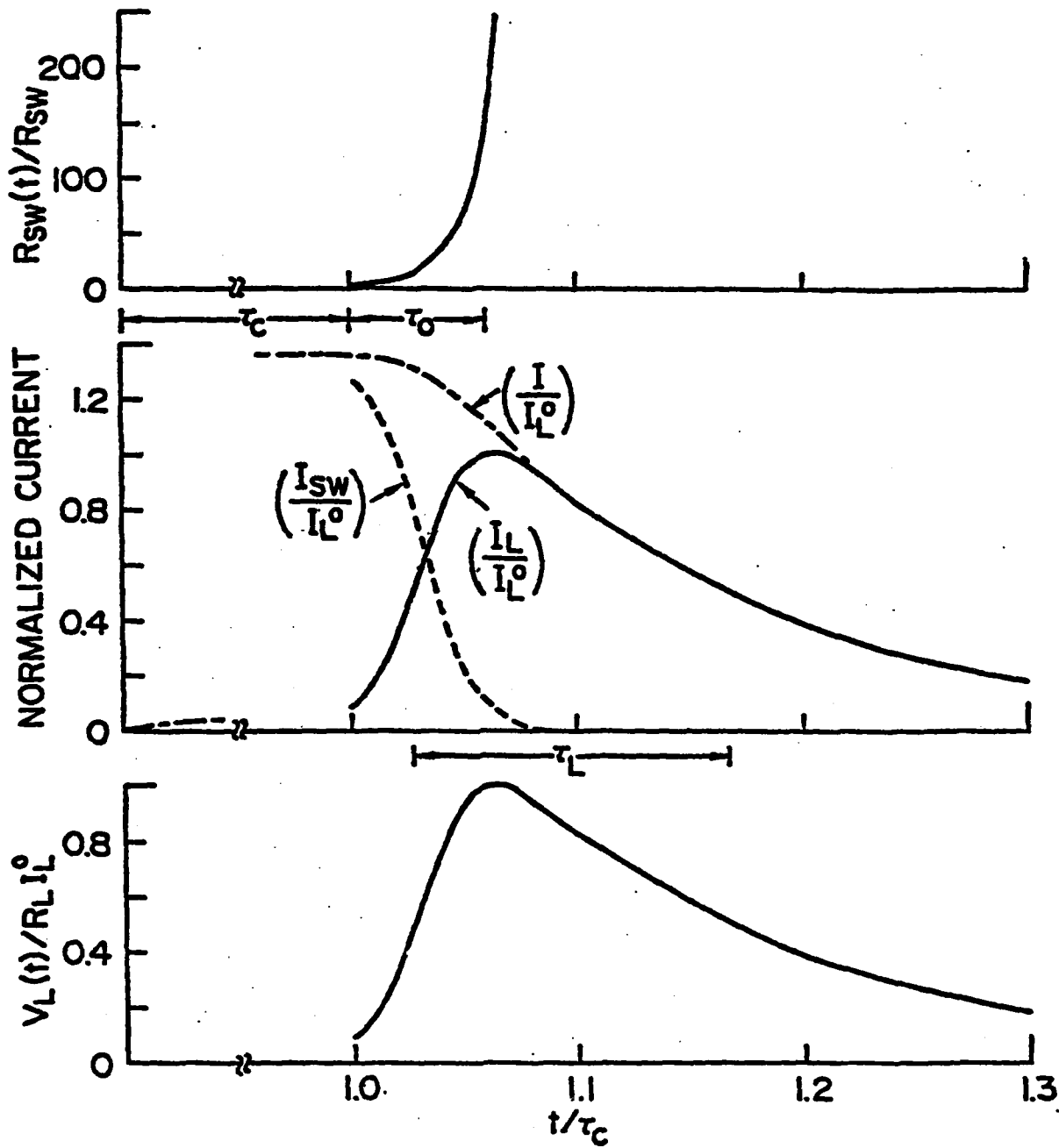


Figure 4

# Design of Electron-Beam Controlled Switches

BY R. G. COMMISSION AND R. F. EHRNSBERG

Naval Research Laboratory

Washington, D.C. 20340

AND S. HERRICK AND M. WILKOWSKI

Naval Research Laboratory

SEP 24 1982



NAVAL RESEARCH LABORATORY  
Washington, D.C.

Approved for public release, distribution unlimited.

SECURITY CLASSIFICATION OF THIS PAGE (When Data Entered)

REPORT DOCUMENTATION PAGE		READ INSTRUCTIONS BEFORE COMPLETING FORM
1. REPORT NUMBER NRL Memorandum Report 4975	2. GOVT ACCESSION NO.	3. RECIPIENT'S CATALOG NUMBER
4. TITLE (and Subtitle) DESIGN OF ELECTRON-BEAM CONTROLLED SWITCHES		5. TYPE OF REPORT & PERIOD COVERED Interim report on a continuing NRL problem.
7. AUTHOR(s) R. J. Commisso,* R. F. Fernsler,* V. E. Scherrer, and L. M. Vitkovitsky		6. PERFORMING ORG. REPORT NUMBER
9. PERFORMING ORGANIZATION NAME AND ADDRESS Naval Research Laboratory Washington, DC 20375		8. CONTRACT OR GRANT NUMBER(s)
11. CONTROLLING OFFICE NAME AND ADDRESS Naval Research Laboratory Washington, DC 20375		10. PROGRAM ELEMENT, PROJECT, TASK AREA & WORK UNIT NUMBERS 61153N, RR0110941 47-0878-0-3
14. MONITORING AGENCY NAME & ADDRESS (if different from Controlling Office)		12. REPORT DATE November 24, 1982
		13. NUMBER OF PAGES 29
		15. SECURITY CLASS. (of this report) Unclassified
		16. DECLASSIFICATION/DOWNGRADING SCHEDULE
18. DISTRIBUTION STATEMENT (of this Report)  Approved for public release, distribution unlimited.		
17. DISTRIBUTION STATEMENT (of the abstract entered in Block 20, if different from Report)		
19. SUPPLEMENTARY NOTES  *Present address: JAYCOR, Inc., 205 S. Whiting Street, Alexandria, VA 22302		
20. KEY WORDS (Continue on reverse side if necessary and identify by block number)  Opening Switch Repetitively Pulsed Operation Electron Beam Diffuse Discharges		
20. ABSTRACT (Continue on reverse side if necessary and identify by block number)  This paper reviews the principles of operation of the electron-beam controlled switch (EBCS) and presents a procedure for its design. The EBCS is compared to other switches which have potential application to repetitively pulsed, high power systems, and is found to have some substantial advantages at high ( $\geq 10$ kHz) repetition rates. Circuit requirements for the application of an EBCS to ETA/ATA like devices are outlined. A self-consistent formalism for optimum switch design is derived. The formalism is applied to the previously outlined circuit requirements using capacitive and capacitive-inductive hybrid energy storage schemes. The required switches are readily designed.		

DD FORM 1473  
1 JAN 73

EDITION OF 1 NOV 65 IS OBSOLETE  
S/N 0102-014-6601

SECURITY CLASSIFICATION OF THIS PAGE (When Data Entered)

## CONTENTS

I.	INTRODUCTION .....	1
II.	PRINCIPLES OF OPERATION .....	1
III.	COMPARISON TO OTHER SWITCHES .....	2
IV.	DESIGN CRITERIA .....	3
	A. Capacitive Systems—Application of the Repetitive Closing Switch Mode .....	4
	1. Electrical Characteristics for Closing Switch .....	4
	2. Electron Beam Requirements .....	6
	B. Inductive Systems—Application of the Repetitive Opening Switch Mode .....	6
	1. Hybrid Pulser .....	6
	2. Inductive Pulser .....	6
	3. Electrical Characteristics for Opening Switch—Hybrid Pulser .....	9
V.	SWITCH DESIGNS .....	10
	A. Switch Parameters .....	10
	1. Breakdown .....	10
	2. Efficiency .....	11
	3. Resistance .....	12
	4. Closing and Opening Time .....	12
	B. Switch Physics .....	16
	C. Design Procedure .....	18
	D. Design for Repetitive Closing Switch—Capacitive System .....	18
	E. Design for Repetitive Opening Switch—Hybrid System .....	20
VI.	CONCLUDING REMARKS .....	20
VII.	REFERENCES .....	24
VIII.	TABLE OF SYMBOLS .....	26

# DESIGN OF ELECTRON-BEAM CONTROLLED SWITCHES

## I. INTRODUCTION

Recent investigations<sup>1-4</sup> into the phenomena associated with electron-beam (*e*-beam) controlled diffuse discharges indicate potential applications for repetitive ( $>10$  kHz in a "burst" mode), high power ( $\sim 10^{10}$  W) switching. Applications include use in both the opening and closing switch mode. The switch requirements may vary considerably depending upon the specific mode used.

There now exists a need for the development of these switches in several areas. One area of focus is the generation and propagation of intense charged particle beams.<sup>9</sup> Here, the repetitive capability of the switch in the closing mode under high power operation is of critical importance. Another category of general interest is the development of a compact, high power inductive energy storage system to replace conventional capacitive systems.<sup>10-12</sup> This application has universal impact on many areas where pulsed power is required, including that of beam generation and propagation. In this case the generation of a high voltage pulse ( $>200$  kV) as a result of the fast increase of an opening switch resistance while the switch is being stressed by high electric fields associated with the pulse is crucial. Depending upon the application, this opening switch may be repetitively pulsed. This would involve a more stringent set of requirements on both the switch gas and the switch *e*-beam driver than is the case for single pulse switching.

In this report we review the principles of operation of the *e*-beam controlled switch (EBCS), highlighting its capability for rapid recovery—the essential requirement for repetitively pulsed systems, whether inductively or capacitively driven. Detailed explanations of the switch physics can be found in Refs. 5, 8, 13, and 14. The EBCS is compared to other candidate switches for repetitive, high power application. Design requirements for two applications of this switch to devices with characteristics similar to either the Experimental Test Accelerator (ETA) or Advanced Test Accelerator (ATA)<sup>15</sup> are then outlined. We next develop a formalism for switch design that combines the circuit requirements with the switch physics. Using this formalism, which is backed by our present data base,<sup>5,8,13,14</sup> the necessary *e*-beam controlled switches are designed. The reader is cautioned that the design examples chosen do not necessarily make optimum use of the potential capabilities of the EBCS switch concept. A full system study in which the EBCS is included as an integral part of the design process from inception would be required for such a task. Rather, the examples chosen serve to illustrate the practical engineering aspects of the switches, define some of the technical requirements necessary for their implementation, and indicate the steps that are necessary for a complete system design.

The results of this study indicate that EBCS's can be readily designed for repetitive ( $>10$  kHz), high power (200 kV, 20 kA) applications. Further research and development concerning gas chemistry and atomic physics, cumulative heating in the switch, and switch *e*-beam driver under repetitive, long conduction time (with respect to the load pulse width) conditions are needed in varying degrees depending upon the specific switch application. The authors believe that such studies will lead to further significant gain in the practicality of EBCS's.

## II. PRINCIPLES OF OPERATION

When an electron beam is injected into a chamber containing a mixture of an attaching and a nonattaching gas, the ionization of the gas produced by the *e*-beam pulse competes with attachment and

recombination processes controlling the conductivity of the gas. The conductivity, and hence the discharge current, is turned on and off in association with the e-beam pulse.

An important distinguishing feature of a switch based on this concept is the ability of the switch to open (cease conduction) under high applied voltage. This is achieved by using the electron beam to control the gas ionization. To avoid avalanche ionization the switch must be designed so that the maximum expected voltage across the switch is below the static self-sparking threshold (for sufficiently transient voltages this requirement may be relaxed). As the discharge evolves, cumulative gas heating also must be constrained so that thermal ionization and, more importantly, local hydrodynamic reduction in gas density do not significantly lower the self-sparking threshold. A self-sustained discharge is thus prevented. Under these conditions, the fractional gas ionization, and thus the switch resistivity, at any time is determined by the competition between ionization provided by the beam and the various recombination and attaching processes characteristic of the specific gas mixture, pressure, and applied electric field. A second important feature of this switch is the volume discharge property. This characteristic makes it possible to avoid excessive heating of electrodes and the switch gas (as well as lessen mechanical shock and minimize the switch inductance). All these features combine to permit the discharge to return to its initial state of high resistivity very quickly once the source of ionization is removed. Unlike an arc discharge, this transition can be accomplished rapidly in the presence of an applied voltage. Some details of the gas chemistry and atomic physics associated with the switch operation and their coupling to the switch circuitry can be found in Ref. 8.

Looked at from a different perspective, the EBCS behaves as a current amplifier. That is, the small ( $\leq 1$  kA) electron beam current can control a large ( $\sim 10$  kA) switch plasma current. The ratio of these two currents is called the current gain,  $\epsilon$ . For  $\epsilon \gg 1$  a substantial energy gain (i.e., energy delivered to the load normalized to the energy dissipated) can be achieved, as discussed in Sec. V.

### III. COMPARISON TO OTHER SWITCHES

Several summaries of high power closing and opening switches with potential application to repetitively pulsed systems exist.<sup>9,16</sup> There are basically six switch types which emerge as candidates for a high power repetitively pulsed switch:<sup>9</sup> (1) the low-pressure gas switch,<sup>17</sup> (2) the surface flashover switch,<sup>18</sup> (3) the thyatron,<sup>9,16</sup> (4) the high pressure spark gap, (5) the magnetic switch,<sup>19,20</sup> and (6) the EBCS.

The ongoing research for both the low pressure gas and surface flashover closing switches has yielded some encouraging results. The technology appears to be simple. At present, however, recovery times of only 100  $\mu$ s have been observed for both devices with no applied voltage. Jitter may also be a problem. Under repetitive burst operation, both switches may have to be cooled. For the surface flashover switch, the insulator may additionally require cooling and the insulator lifetime is likely to be limited.

The thyatron is a well developed device; however, the present limitations in voltage, current, and risetime probably make it unsuitable for implementation in the systems of interest here. Further, the power consumption and long warm up period for the cathode heater are disadvantageous.

The high pressure spark gap is the traditional choice for a closing switch of the pulsed power community. It cannot be used as an opening switch. It is very simple mechanically and has associated with it an extensive data base. The problem areas are the substantial gas flow requirements and energy dissipation associated with this device when used in high frequency repetitive high power applications. Also, a trigger pulse amplitude comparable to the applied switch voltage is necessary for low jitter.

Magnetic switches are now a part of the ATA design. The potential advantages of such a switch are its simplicity, ruggedness, and lifetime. Questions still remain concerning overall size and weight.

evaluation of core materials, limiting output pulse duration, pulse compression ratios, trade-offs in number of stages in cascade, and core bias and/or resetting methods.

An understanding of the physics of the  $e$ -beam switch operation along with the results of recent NRL experiments leads one to conclude that the principal advantages of the EBCS are: (1) rapid recovery (opening) of the switch when the electron beam ceases, and the consequent opening and closing repetitive capability<sup>8,13,14</sup> at high repetition rates; (2) negligible switch jitter;<sup>4,5</sup> (3) volume discharge resulting in low inductance and reduced switch current density (limiting electrode wear, switch gas heating, and mechanical shock); and (4) high power switching capability<sup>5</sup> (for limited pulse bursts).

Potential problem areas for this switch concept include the switch  $e$ -beam driver complexity, the effect of cumulative heating on the switch's repetitive capability, and switch packaging. The  $e$ -beam driver has modest peak power requirements on a per-pulse basis (200 kV, <1 kA, <10<sup>8</sup> W); however, it must provide a beam with the pulse shape and repetition rate required for the desired switching characteristics. Thermionic  $e$ -beam generators, developed for excitation of high power lasers, now provide<sup>21,22</sup> 1-5  $\mu$ s  $e$ -beam pulses with  $\sim$ 100 ns rise and decay times at a 25 Hz repetition and at 10 A/cm<sup>2</sup>. The repetition rate can probably be improved, e.g., if a lower  $e$ -beam current density is desired. With some further development, these devices may indeed provide the desired beam modulation characteristics. Thin film field emission cathodes with molybdenum cones<sup>23</sup> appear attractive because of their low control voltage (100-300 V), high current densities ( $\sim$ 10 A/cm<sup>2</sup>), and continuous operation capability. An inductively driven electron beam system has successfully demonstrated two-pulse "burst" operation, generating two  $\sim$ 1 kA pulses with a 150-200  $\mu$ s (limited by diode closure) interpulse separation.<sup>24</sup> In regard to the EBCS and the role of the  $e$ -beam source we quote from Ref. 9 (pg. 439), "The main application of this switch concept would seem to be as an opening switch. Since it has few rivals in this role, the complexity of the electron beam source becomes less formidable."

The effects of cumulative heating in the switch gas are not well known. Preliminary experiments<sup>14</sup> indicate that at least two-pulse operation is possible at a deposited energy density of  $\sim$ 0.1 J/cm<sup>2</sup>. These experiments also show a favorable (approximately linear) scaling of the maximum energy deposited before switch breakdown occurs with increasing switch ambient pressure. However, more research in this area is needed.

Although a stand-alone switch packaging scheme has been outlined,<sup>25</sup> a complete system design has not yet been addressed. Such a design would be heavily dependent on the specific application and would have to incorporate the switch as an integral part of the system ab initio. At present we see no fundamental limitation resulting from packaging considerations that would prevent integration of this switch into pulse power systems. For example, a compact, high pressure,  $e$ -beam controlled laser system with an  $e$ -beam generator (single pulse) compatible with severe optical requirements has been successfully assembled and operated.<sup>26</sup>

Much work is still needed to develop these concepts into viable repetitively operated switches. In some areas (e.g., recovery) the EBCS has some very substantial advantages when compared to the other switch candidates. It is the only switch discussed here that can open under an applied voltage and, therefore, it is especially promising in applications which require high repetition rate (>10 kHz) opening switches.

#### IV. DESIGN CRITERIA

In this section we outline switch performance characteristics upon which a switch can be designed. These characteristics strongly depend upon the specific application of the switch. Optimum switch performance requires that the switch be incorporated into a system design at its inception. However, to illustrate the practical design considerations for this switch concept we have chosen as an example the

requirements of the ETA/ATA inductive electron beam accelerator.<sup>15</sup> In this context we describe the requirements for application of this switch to three energy storage schemes: capacitive, hybrid, and inductive. Depending upon the specific requirements, each scheme may involve, respectively, a more stringent set of switch performance and *e*-beam driver characteristics and a progressively greater extrapolation from the present data and technology base.

#### A. Capacitive Systems—Application of the Repetitive Closing Switch Mode

The *e*-beam controlled switch based on the principles outlined in Sec. II can be used at high power levels ( $\sim 10^{10}$  W) with capacitive energy storage as a closing switch, in applications where very fast rise-time pulses of short duration ( $< 100$  ns) must be generated at high repetition frequency ( $> 10$  kHz).

##### 1. Switch Electrical Characteristics for Closing Switch

One example of such an application is an output switch of the ETA/ATA. For definition purposes, the load characteristics are assumed to be those summarized in Table I.<sup>15</sup>

The characteristics displayed in Table I imply that the switch *e*-beam driver has sufficiently fast risetime and that the working gas can respond sufficiently fast to the injected beam.

Two circuits which provide the required output for the load are shown in Fig. 1a and b. Both circuits depend on use of switch  $S_1$  for charging. Typically, direct Marx charging as given in Fig. 1a can provide a charge time for capacitor  $C_0$ , of  $\tau_{CH} \sim 1 \mu\text{sec}$ . Using the voltage step-up transformer (Fig. 1b) has no deleterious effect other than to possibly increase  $\tau_{CH}$  to several microseconds.

Electrically, the switch must deliver a peak power  $P = 4 \times 10^9$  W to the load for each pulse. With  $> 10$  kHz repetition rate ( $< 100 \mu\text{sec}$  pulse-to-pulse separation), the average power output of the pulse is  $P_{av} = P(\tau_L/\tau_{pp}) \approx 1 \times 10^6$  W, where  $\tau_L$  is the load pulse width and  $\tau_{pp}$  is the time between pulses. (For those scenarios where large numbers of accelerating modules are needed, the total average output power can be as high as  $1 \times 10^9$  W.) The power transport through the switch leads to some dissipation of energy in the switch. The amount that is dissipated depends on the pulse duration, the current, and the switch voltage drop during conduction and is constrained to be less than the energy delivered to the load (see Sec. V.A.2). The opened state of the switch has negligible conduction in all cases considered in this paper.

Finally, the switch inductance must be limited to  $L_{SW} \ll V_L \tau_R / I_L \approx 100$  nH, as suggested by the parameters in Table I. A schematic representation of the time history of the switch resistance,  $R_{sw}$ , is shown in Fig. 1c.

TABLE I: SUMMARY OF ASSUMED  
LOAD CHARACTERISTICS  
(Closing Switch, Capacitive System)

Type of Load	Electron beam diode
Load Voltage, $V_L$	200 kV
Load Current, $I_L$	20 kA
Equivalent Impedance, $R_L$	10 $\Omega$
Pulse Duration, $\tau_L$	40 ns
Pulse Rise Time, $\tau_R$	10 ns
Pulse-to-Pulse Time, $\tau_{pp}$	$< 100 \mu\text{s}$
Pulses per burst, $n$	$\geq 5$

## CAPACITIVE (CLOSING)

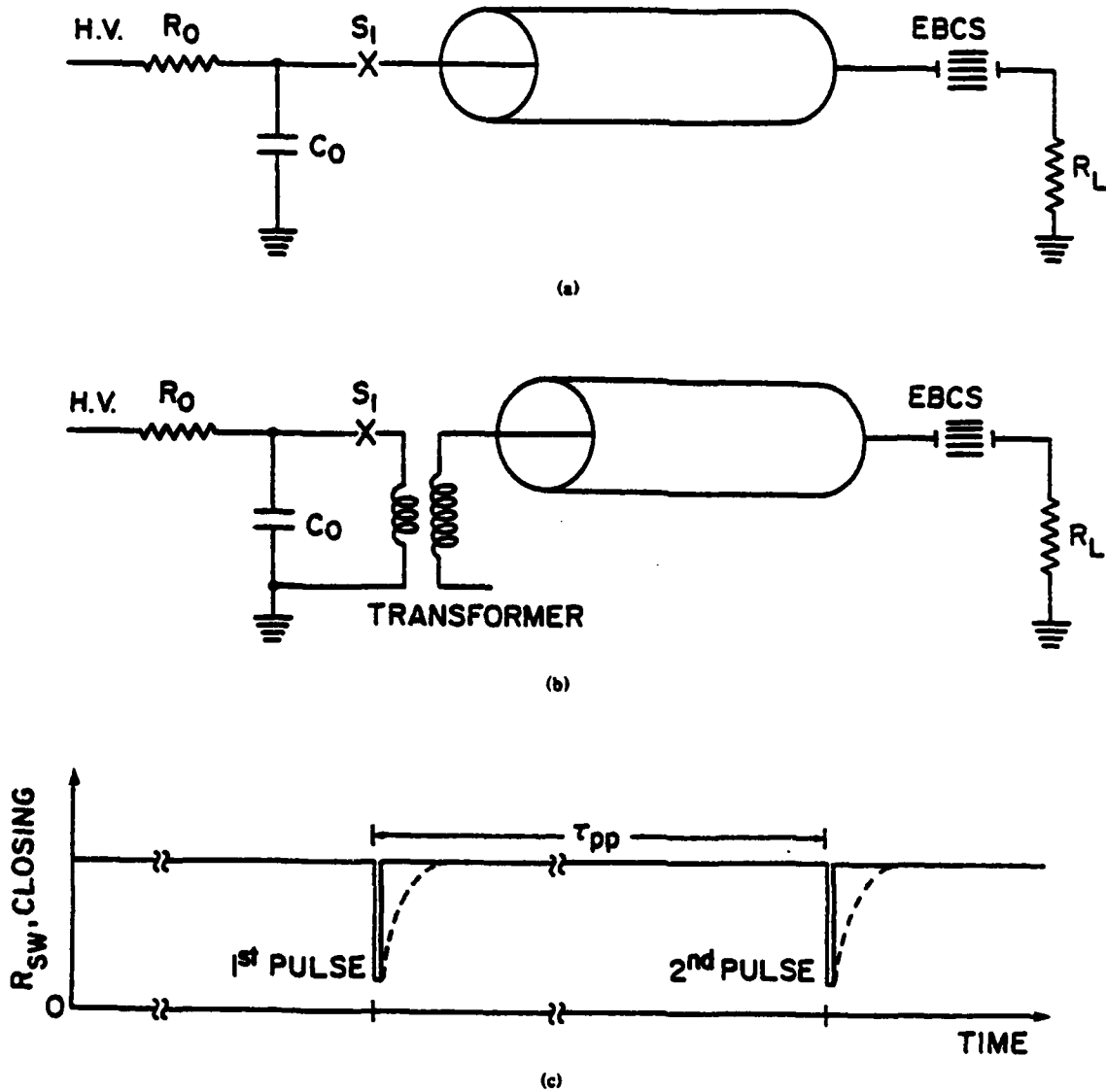


Fig. 1 - Circuit diagram illustrating the application of an EBCS in the closing mode to a capacitive storage system. The circuit is shown both without (a) and with (b) a step-up transformer. Also shown is a representation of the switch resistance time behavior (c).

## 2. Electron Beam Requirements

To obtain the necessary time variation of the gas conductivity, the electron beam injected into the gas must satisfy pulse shape, repetition rate, and current requirements. The  $e$ -beam current is set by a number of factors, as discussed in Sec. V. The beam modulation was discussed in Sec. III. We assume for the remainder of the discussion that an appropriate  $e$ -beam generator exists, or can be developed.

### B. Inductive Systems—Application of Repetitive Opening Switch Mode

In projecting charged particle beam technology to deployable systems, practical size and weight of the system is one of the major considerations in the system design. The power source represents a major component of any of the proposed systems. Because inductive storage offers a potential for much more compact designs than those that would be possible with capacitive systems, there exists a strong incentive to develop the necessary inductive storage components. A repetitive opening switch is a fundamental component that must yet be developed. As in the repetitive closing switch development,  $e$ -beam control of gas conductivity offers a method that can be employed for repetitive opening switching for high power pulse train production.

#### 1. Hybrid Pulser

Continuing with the scenario of an accelerator based on modular accelerating sections requiring 20 kA, 200 kV, and 40 nsec pulses at a burst rate of  $>10$  kHz, the power supply circuits, shown in Figs. 2 and 3, can be employed.

The circuit in Fig. 2a utilizes a pulse-forming line, represented as a capacitor  $C$ , to form a specific pulse shape required by the accelerator (i.e., rise time of 10 nsec and 40 nsec pulse duration). The inductor,  $L_o$ , is initially charged by a current,  $I_o$ , through, in this example, an explosively actuated switch<sup>27-28</sup> (denoted by  $E$ ) for a time  $\tau_{CH}$ . Note that some current generators, e.g., a homopolar, may require earlier, additional stages of pulse compression. When switch  $E$  opens, the current is commutated (in a time  $\tau_{COM}$ ) to the next stage which contains an EBCS operating in the repetitive opening mode (denoted by the letter  $O$  in parenthesis). EBCS( $O$ ) is closed and conducting during  $\tau_{COM}$ . After the commutation time, EBCS( $O$ ) is commanded to open. The opening generates a resistive voltage, and the pulse line  $C$  is charged for the charging time,  $\tau_{CH} = \tau_L$ . At the end of  $\tau_{CH}$ , EBCS( $O$ ) again closes.

The output for the pulse line is an  $e$ -beam controlled device already described in the previous section, i.e., an EBCS operating in the repetitive closing mode (denoted by letter  $C$  in parenthesis). Figure 2b is a schematic representation of the time histories of the resistance of EBCS( $O$ ) and EBCS( $C$ ) of Fig. 2a.

Thus, the circuit in Fig. 2a employs two repetitive EBCS's. The EBCS( $O$ ) has a long conduction time, equal to  $\tau_C = (\tau_{pp} - \tau_{CH})$ , and a short nonconduction time,  $\tau_{NC} = \tau_{CH}$ , during which the capacitor  $C$  is charged. The EBCS( $C$ ) is identical in its operation to the switch discussed in Sec. IV.A.

#### 2. Inductive Pulser

A more compact and simpler pulser would result if a circuit in Fig. 3a could be used. The pulser represented by this circuit is purely inductive, eliminating any need for capacitive storage. However, this scheme represents the farthest extrapolation of the present data and technology base thus far considered. Figure 3b is a schematic representation of the time history of the opening switch resistance for a purely inductive system of Fig. 3a. The EBCS( $O$ ) in Fig. 3a must conduct for the period between pulses,  $\tau_{pp}$ , and open repetitively for a much shorter period,  $\tau_L$ . The output pulse shape, however, imposes stringent performance requirements on EBCS( $O$ ), in terms of pulse risetime and duration.

## HYBRID (OPENING/CLOSING)

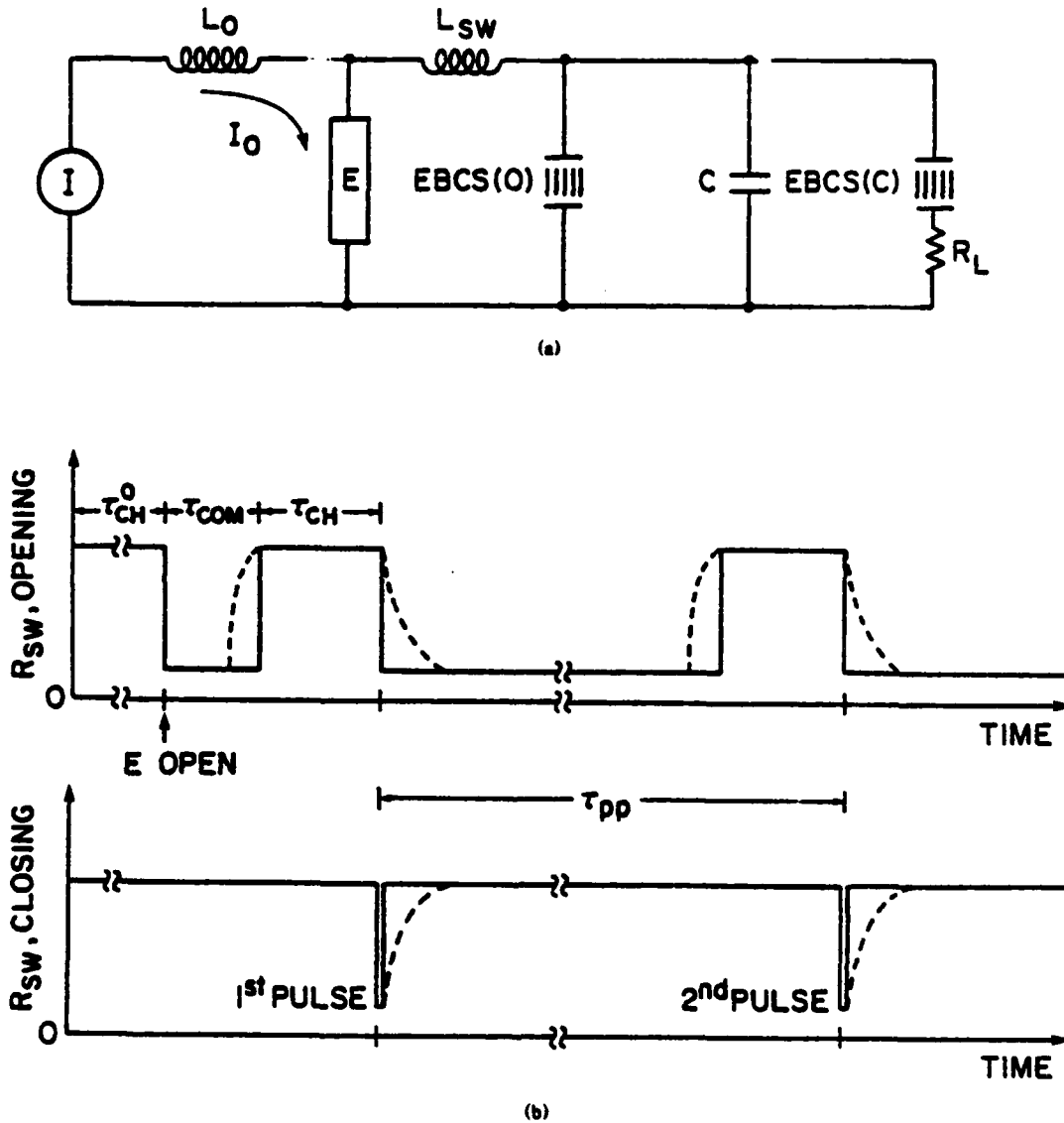


Fig. 2 - Circuit diagram illustrating the application of an EBCS in the opening mode, EBCS(O), and closing mode, EBCS(C), for a hybrid (capacitive-inductive) inductive storage system (a). Also shown are representations of the time behavior of both switch resistances (b).

## INDUCTIVE (OPENING)

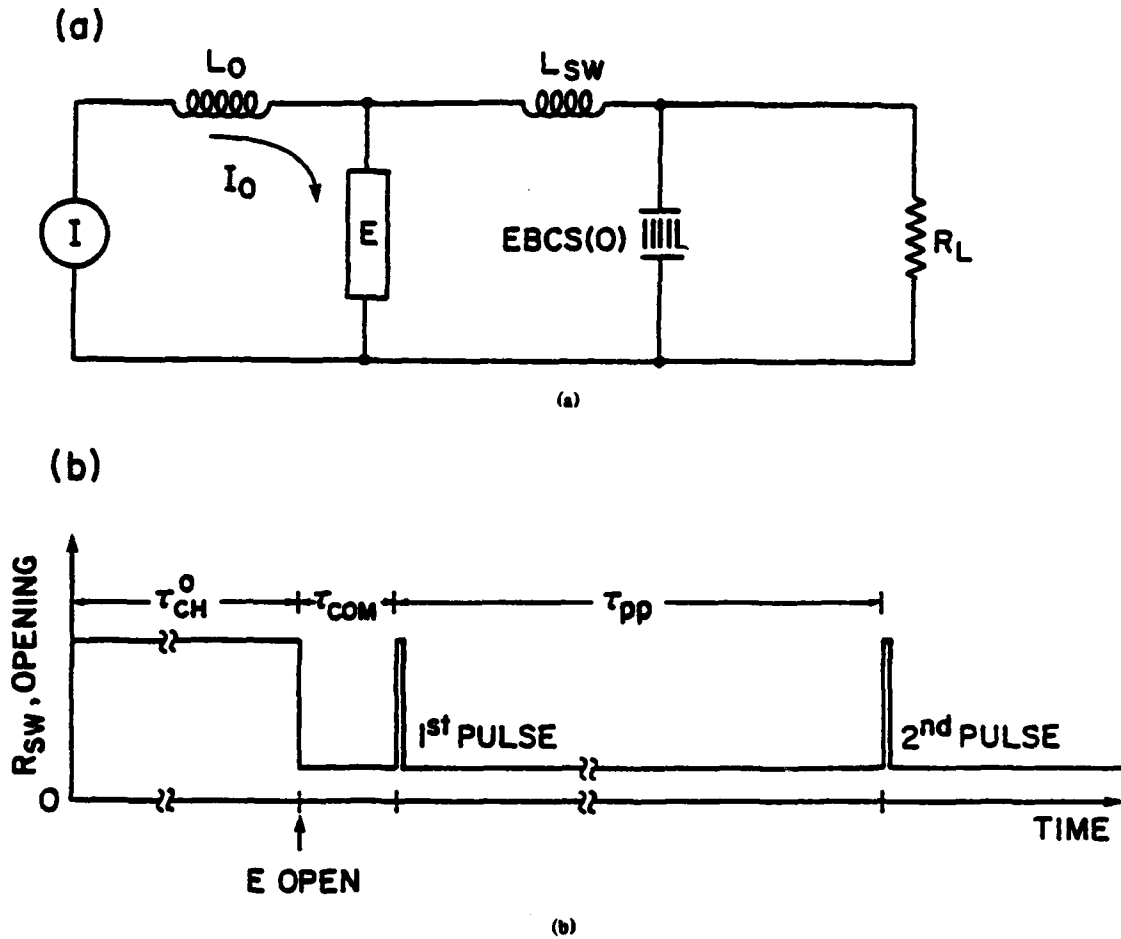


Fig. 3 - Circuit diagram illustrating the application of an EBCS in the opening mode for a purely inductive energy storage system (a). Also shown is a representation of the switch resistance time behavior (b).

Although this scenario is conceptually the simplest, it may be too speculative to assume that a single switch can achieve an opening time of less than 10 ns and a conduction time of greater than 10  $\mu$ s. Thus, this design is not considered for detailed engineering at present. The option of using a purely inductive system is attractive and, therefore, suggests that future effort should be invested in development of switches with opening times of  $\sim 10$  nsec. We note that response times of  $< 10$  ns are theoretically possible<sup>5</sup>; however, an  $e$ -beam driver with the necessary waveform capability needs to be developed.

### 3. Electrical Characteristics for Opening Switch—Hybrid System

The energy associated with a single pulse for a single module delivering 20 kA, at 200 kV, with a 40 nsec pulse width, is very small:  $E_1 = 160$  J. Considering a 10-pulse burst,  $\sim 2$  kJ is required as a minimum to be stored by the inductor. Taking 30% efficiency of conversion from stored to pulse energy,  $\sim 6$  kJ must be handled by a storage system for charging one pulse line. This projects to  $\sim 10^7$  J for a 1000 module accelerator. In considering the engineering of a switching system, one must know the number of modules to be powered by one switch. At this stage of switch development, where little experience with a practical switching device exists, the choice is dictated as much by the need to maintain a reasonable experimental set-up as by the lack of certainty related to the ultimate application. A reasonable first attempt, that would uncover most of the problems of a design, would be a switch design for a 10-module pulse train generator limited to 5-pulses. Circuit, current, and voltage parameters are derived below for the EBCS(O) switch of Fig. 2a.

Using the same final load pulse parameters as in the preceding section, the single pulse line capacity is  $C = 2E_1/V^2 = 8$  nF; i.e., in 10-module operation 80 nF must be charged to 200 kV. Choosing a 5-burst pulse train for an initial switch design (and for experiment design to test the switch), the total stored energy in the ten pulse lines is  $E_2 = 8$  kJ. We assume a 15  $\mu$ s interpulse time ( $\sim 70$  kHz) and a 2- $\mu$ s charge time. The energy stored in the inductor must be about  $E_3 = 3 \times E_2 = 24$  kJ, to account for the inefficiencies ( $\sim 70\%$ ) associated with the circuit and fuses shown in Fig. 2a. This amount of energy suggests that low voltage capacitors can be conveniently used as the source of current (shown in Fig. 2a) to charge the inductor in small laboratory experiments. As previously stated, the time required to pulse-charge the capacity  $C$ , is taken to be  $\tau_{CH} = 2$   $\mu$ sec. This is consistent with compact water-dielectric pulse line requirements. The current needed to charge a capacitance to a given voltage,  $V$ , is  $I_o = dQ/dt = CV/\tau_{CH}$ . For  $C = 80$  nF,  $V = 200$  kV and  $\tau_{CH} = 2$   $\mu$ s,  $I_o = 8$  kA. The storage inductor  $L_o = 2 E_3/I_o^2 = 750$   $\mu$ H. This choice of inductor presents no structural or electrical design problems.

To summarize, the EBCS(O) of Fig. 2a charging the ten pulse-lines must accommodate the circuit performance characteristics shown in Table II.

TABLE II: Summary of Assumed  
Circuit Characteristics  
(Opening Switch, Hybrid System)

Type of Load	Capacitive
Peak voltage, $V_L$	200 kV
Load current, $I_L = I_o$	8 kA
Conduction time, $\tau_C = (\tau_{pp} - \tau_{CH})$	13 $\mu$ s
Nonconduction time, $\tau_{NC} = \tau_{CH}$	2 $\mu$ s
Storage Inductance, $L_o$	750 $\mu$ H
Pulses per burst, $n$	5

## V. SWITCH DESIGNS

In this section we apply the results of experimental and theoretical research at NRL and the switch performance criteria described previously to obtain specific switch designs. First we review the important switch characteristics and their relationship to the system. A simple quantitative model for the switch physics along with scaling relations is then presented. A design procedure is outlined that self-consistently incorporates the switch electrical characteristics with switch physics. Finally, the values of the switch parameters are obtained and the closing and opening switches are designed.

### A. Switch Parameters

The following switch parameter considerations are of importance for opening and closing switch designs.

#### 1. Breakdown

If the electric field across the switch exceeds the static breakdown field at the ambient switch pressure, the switch may go into an arc mode, which is undesirable because it prevents the switch from opening. This leads to the constraint that

$$V_L = s_B \frac{E_B^0}{P_0} (Pl), \quad (1)$$

where  $V_L$  is the maximum expected voltage across the switch (i.e., the load voltage),  $E_B^0$  is the static breakdown field at atmospheric pressure  $P_0$ ,  $s_B < 1$  is a dimensionless safety factor, and  $l$  is the switch length. We have assumed that  $E_B = E_B^0 (P/P_0)$ , where  $E_B$  is the static breakdown field at pressure  $P$ . This condition can be relaxed somewhat for transient,  $< 1 \mu s$ , pulses.

Additionally, cumulative heating of the gas must be sufficiently constrained so that any local reduction in switch gas density does not significantly lower the self-sparking threshold. Energy is deposited in the switch from the following processes:

(1) During the time the switch changes from a conducting to a nonconducting state, i.e., during the opening time  $\tau_O$ , the current in the switch is finite while the switch resistance is large. Thus, the resistive heating during this time may be significant. This cumulative heating is estimated by

$$H_O = k_O I_{SW} V_L n \tau_O, \quad (2)$$

where  $I_{SW}$  is the maximum switch current,  $V_L$  is the maximum switch voltage (load voltage),  $n$  is the number of pulses,  $\tau_O$  is the opening time, and  $k_O \leq 0.5$  is a dimensionless constant which appropriately averages ( $I_{SW} V_L$ ) during  $\tau_O$  (see Sec.V.C). Because  $\tau_O \gg \tau_{SR}$ , where the switch rise time,  $\tau_{SR}$ , is the time for the switch to change from nonconducting to conducting, we will neglect the energy loss during the switch closing phase.

(2) During the total time the switch is conducting,  $n\tau_C$ , there will be some resistive heating. The total energy deposited in the switch as a result of this process is approximated by

$$H_C = I_{SW}^2 R_{SW} n \tau_C. \quad (3)$$

Here  $R_{SW}$  is the switch resistance during conduction.

(3) When the beam is injected, a fraction of the beam energy will be directly deposited in the switch gas as a result of inelastic collision processes. This energy deposition is estimated by

$$H_b = k_b I_b V_b n \tau_C. \quad (4)$$

where  $I_b$  and  $V_b$  are the beam current and voltage respectively, and  $k_b \leq 1$  is the fraction of the beam energy deposited in the switch (determined from  $V_b$ ,  $P$ , and  $D$ ). The conduction time  $\tau_C$  is also the  $e$ -beam pulse duration.

To properly constrain cumulative heating in the switch, we must have

$$H_O + H_C + H_b < W_B A I. \quad (5)$$

Here  $W_B$  is the deposited energy per unit volume at which the self-sparking threshold is altered and  $A$  is the switch area. As shown in Fig. 4,  $W_B$  scales linearly with ambient gas pressure  $P$ .<sup>14</sup> We therefore take  $W_B = (P/P_0) W_B^0$ , where  $W_B^0 = 0.15 \text{ J/cm}^3$  is the breakdown energy density at atmospheric pressure.<sup>5,14,29</sup> Equations (2)-(5) can thus be combined to give

$$\left[ k_O I_{SW} V_L \left( \frac{\tau_O}{\tau_C} \right) + I_{SW}^2 R_{SW} + k_b I_b V_b \right] n \tau_C = s_H \left( \frac{W_B^0}{P_0} \right) A (PI), \quad (6)$$

where  $s_H \leq 1$  is a dimensionless safety factor.

## 2. Efficiency

The switch energy gain,  $\xi$ , is defined as the ratio of the energy delivered to the load to the total energy used in making the switch conduct. Thus, applying the same arguments used in obtaining Eqs. (2)-(4) we have

$$\xi = \frac{I_L V_L \tau_L}{\left[ k_O I_{SW} V_L \left( \frac{\tau_O}{\tau_C} \right) + I_{SW}^2 R_{SW} + I_b V_b \right] \tau_C}, \quad (7)$$

where  $I_L$  is the load current and  $\tau_L$  is the load pulse width e.g.,  $\tau_L = \tau_{CH}$  for the opening switch of the hybrid system in Figs. 2a and 3b, while for closing switch  $\tau_L = \tau_C$ , see Figs. 1 and 3a. In all cases,  $I_{SW} = I_L$  (although not always at the same time).

The switch efficiency,  $\eta$ , is related to  $\xi$  by  $\eta = \xi / (\xi + 1)$ . Thus, to attain a high efficiency,

$$\xi > 1. \quad (8)$$

Upon substitution of  $I_L = I_{SW}$  and using the definition of current gain,  $\epsilon \equiv I_{SW} / I_b$ , Eq. (7) becomes

$$\xi = \frac{(\tau_L / \tau_C) \epsilon}{\left[ (\tau_O / \tau_C) k_O + (I_{SW} R_{SW} / V_L) \right] \epsilon + 1}. \quad (9)$$

Recently obtained measurements of  $\epsilon$  as a function of percent  $O_2$  in  $N_2$  for 1, 2, and 3 atm at an applied  $E/P = 10.5 \text{ V/cm-torr}$  with an  $e$ -beam current density of  $5 \text{ A/cm}^2$  are illustrated in Fig. 5. Because of the short duration (200 ns) and long rise time (100 ns) of the  $e$ -beam pulse used in these measurements, the values of  $\epsilon \leq 15$  at low  $O_2$  concentrations (<20%) should be considered a lower bound.<sup>14</sup>

Equation (7) may be rearranged to yield

$$\xi^{-1} I_L V_L \tau_L = k_O I_{SW} V_L \tau_O + I_{SW} V_L \tau_C + I_b V_b \tau_C. \quad (11)$$

To realize an energy gain, i.e., for  $\xi > 1$ , each term on the right hand side of Eq. (11) must be sufficiently less than  $I_L V_L \tau_L$ . Thus we set

$$k_O I_{SW} V_L \tau_O = g_O I_L V_L \tau_L, \quad (12a)$$

$$I_{SW}^2 R_{SW} \tau_C = g_C I_L V_L \tau_L. \quad (12b)$$

and

$$I_b V_b \tau_C = g_b I_L V_L \tau_L \quad (12c)$$

where  $g_O, g_C, g_b < 1$ , such that

$$\xi^{-1} = g_O + g_C + g_b < 1. \quad (13)$$

Equations (12a)-(12c) can be rewritten (with  $I_{SW} = I_L$ ) as:

$$\tau_O = (g_O/k_O)\tau_L \quad (14a)$$

$$\frac{E_C}{P} = g_C s_B (E_b^2/P_o) \frac{\tau_L}{\tau_C} \quad (14b)$$

and

$$\epsilon = g_b^{-1} \frac{V_b}{V_L} \left( \frac{\tau_C}{\tau_L} \right) \quad (14c)$$

where  $E_C = I_{SW} R_{SW}/l$  is the electric field across the switch during conduction.

### 3. Resistance

The switch resistance during conduction is related to the switch gas resistivity during conduction,  $\rho_o$ , by

$$R_{SW} = \rho_o \frac{l}{A} \quad (15)$$

Plotted in Fig. 6 is the resistivity at peak switch current as a function of percent  $O_2$  in  $N_2$  for 1, 2 and 3 atm at an applied  $E/P = 10.5$  V/cm-torr for an  $e$ -beam current density of  $5$  A/cm<sup>2</sup>. Values of 300-400  $\Omega$ -cm are typical for <20%  $O_2$ . We reiterate that because of the short duration (200 ns) and relatively long rise time (100 ns) of the electron beam used in the experiment, the values of  $\rho_o$  in Fig. 6 for low concentrations of  $O_2$  can be considered as an upper bound (see Ref. 14).

By recalling that  $E_C = I_{SW} R_{SW}/l$  and using Eq. (1) to eliminate  $l$ , we may rewrite Eq. (14b) as

$$R_{SW} = g_C \left( \frac{V_L}{I_{SW}} \right) \frac{\tau_L}{\tau_C} \quad (16)$$

for the switch resistance during conduction. This equation and the condition  $g_C < 1$  is essentially equivalent to the requirement that the characteristic  $L/R$  time of the system be long compared to the switch conduction time, so that the current will not resistively decay from the system.

### 4. Closing and Opening Times

The characteristic time scale for the switch to change from nonconducting to conducting is the switch closing time,  $\tau_{SR}$ . This time is important in closing switch designs (Fig. 1) and for our experiments has been limited by the beam rise time ( $\sim 100$  ns) and the circuit parameters. When fast rising (<5 ns) beams were used, rise times as short as 2 ns have been observed.<sup>4</sup>

The characteristic time scale for the switch to change from a conducting to a nonconducting state is the opening time,  $\tau_O$ . On this time scale the switch current decreases and switch resistance increases by orders of magnitude.

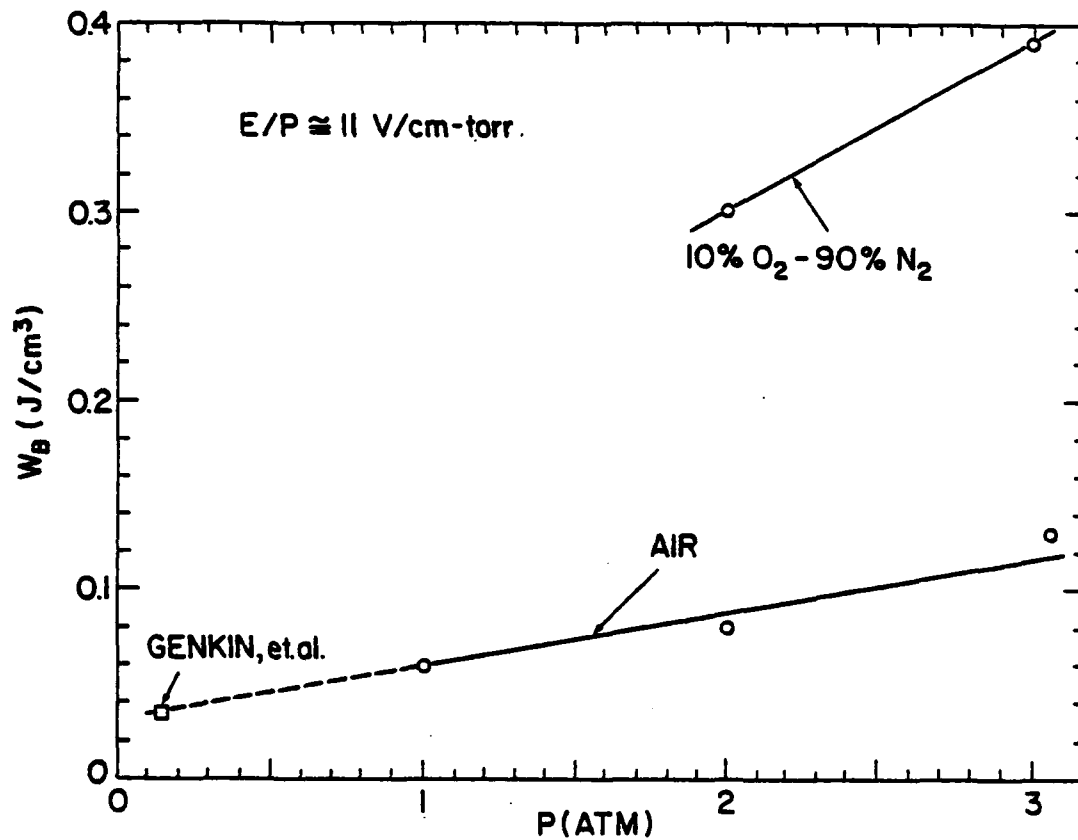


Fig. 4 - Plot of deposited energy density required for breakdown,  $W_B$ , as a function of ambient pressure,  $P$ , for Air and a 10% O<sub>2</sub>-90% N<sub>2</sub> mixture. Genkin, et al. is given in Ref. 29.

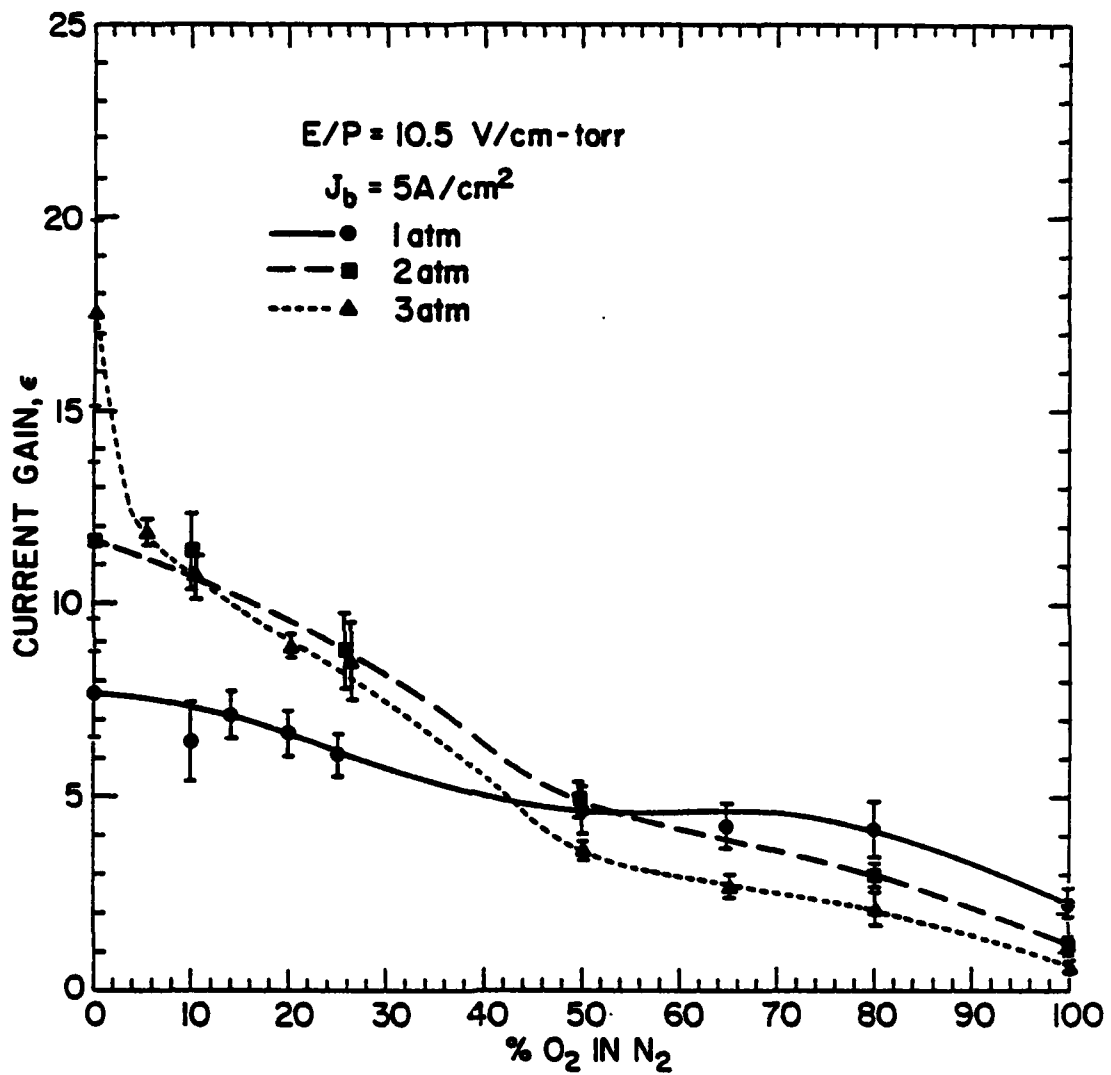


Fig. 5 — Plot of current gain,  $\epsilon$ , as a function of  $O_2$  concentration in  $N_2$  at  $E/P = 10.5 \text{ V/cm-torr}$  and  $J_b = 5 \text{ A/cm}^2$  for ambient pressure  $P = 1, 2$  and  $3 \text{ atm}$ .

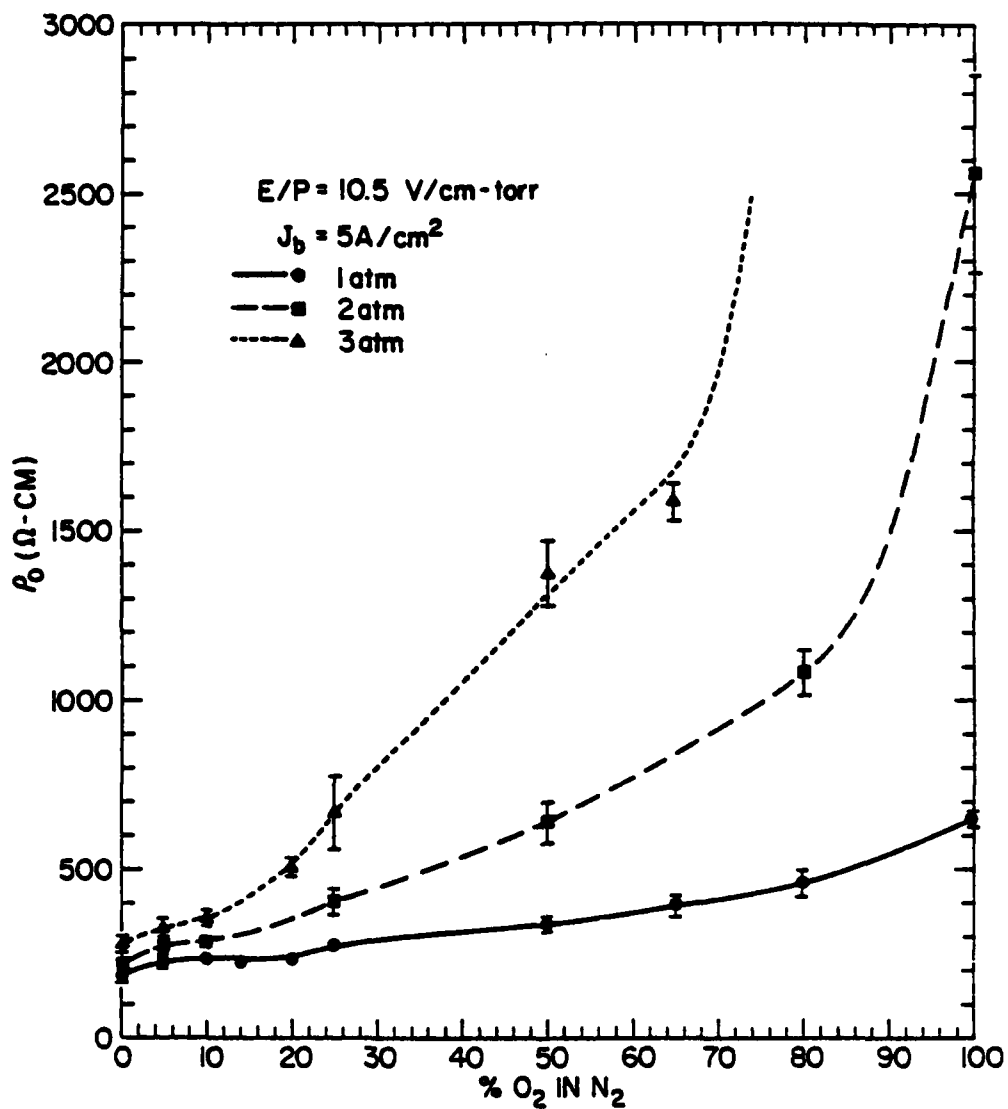


Fig. 6 - Plot of resistivity at peak switch current,  $\rho_0$ , as a function of  $O_2$  concentration in  $N_2$  at  $E/P = 10.5$  V/cm-torr and  $J_b = 5 \text{ A/cm}^2$  for ambient pressure  $P = 1, 2$  and  $3 \text{ atm}$ .

Values of  $\tau_0$  obtained from single pulse experiments<sup>8,13,14</sup> are plotted in Fig. 7 as a function of O<sub>2</sub> concentration in N<sub>2</sub> at 1, 2 and 3 atm with an applied  $E/P = 10.5$  V/cm-torr for an e-beam current density of 5 A/cm<sup>2</sup>. For this plot,  $\tau_0$  was estimated from the inductively generated voltage,  $V_I$ , by  $\tau_0 \approx L\Delta I/V_I$ , where  $\Delta I$  is the change in the system current and  $L$  is the system inductance. Typically, values of  $\tau_0 \leq 300$  ns, limited by the beam decay time ( $\sim 100$  ns) are observed.

## B. Switch Physics

The continuity equation for the switch plasma electron density,  $n_p$ , can be expressed simply as<sup>14</sup>

$$\frac{dn_p}{dt} = S_0 P J_b - \frac{n_p}{\tau_p}, \quad (17)$$

where  $J_b \equiv I_b/A$  is the e-beam current density and  $\tau_p$  is the characteristic loss time for the switch plasma electron density. Several to very many  $\tau_p$  periods are necessary for the switch to open, depending upon the dominant mechanism responsible for switch plasma electron loss. Thus, we have

$$\tau_0 = k_p \tau_p, \quad (18)$$

where  $k_p \approx 5$  for an attachment dominated switch or  $k_p \approx 10^2 - 10^3$  for a recombination dominated switch.<sup>5</sup>

$S_0$  is a beam ionization parameter given by

$$S_0 = \frac{1}{e\epsilon_i P_0} \left( \frac{dE}{dX} \right)_0, \quad (19)$$

where  $e$  is the electronic charge,  $\epsilon_i \approx 35$  eV is the energy required for ionization per electron-ion pair, and  $(dE/dX)_0 \approx 3$  keV/cm is the energy lost per unit length for the beam electrons at 1 atm.

The plasma density is related to the switch plasma current density through

$$J_{SW} \equiv I_{SW}/A = n_p e v, \quad (20)$$

where  $v$  is the electron drift velocity,

$$v = \mu E. \quad (21)$$

Here  $\mu$  is the electron mobility<sup>30</sup> and  $E$  is the electric field across the switch. Thus the resistivity during conduction is given by

$$\rho_0 = \frac{E_C}{J_{SW}} = (en_p \mu)^{-1}. \quad (22)$$

Substituting  $n_p$  from Eq. (22) into Eq. (17), and noting that at equilibrium  $dn_p/dt = 0$ , Eq. (17) becomes

$$J_b \rho_0 \tau_p = f_0^{-1}, \quad (23)$$

where  $f_0 \equiv e S_0 \mu P$  is essentially a constant for a given gas composition. For most gases  $f_0 \sim 10^5 - 10^6$  cm/V-s. Note that Eq. (23) indicates that for a given beam current and gas with a constant  $f_0$ , there is a "trade-off" between resistivity and opening time.

Finally, using the definition of  $\epsilon$ ,  $J_{SW}$ , and  $J_b$ , Eq. (23) can be expressed as

$$\frac{\epsilon}{\tau_p} = E_C f_0. \quad (24)$$

The relations derived in this section are used to relate the switch physics to the switch circuit characteristics outlined in Sec. V.A.

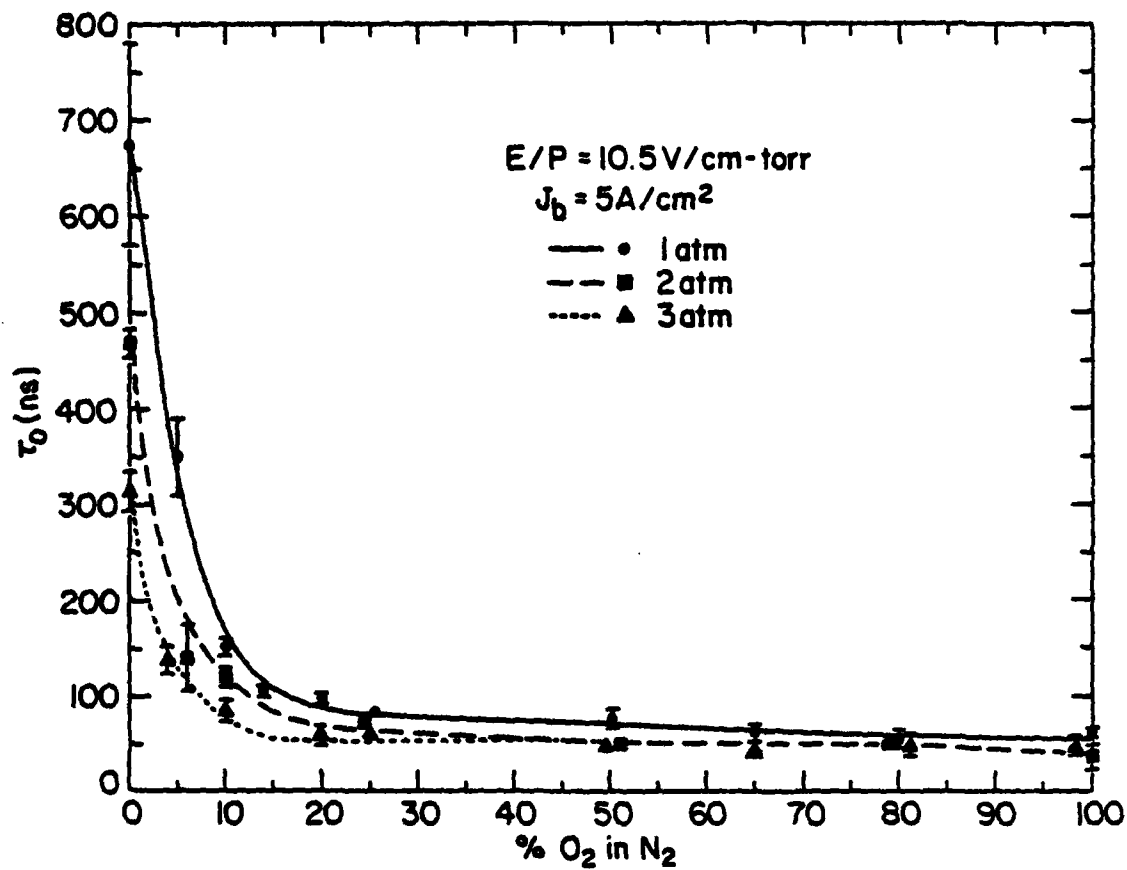


Fig. 7 — Plot of switch opening time,  $\tau_0$ , as a function of  $O_2$  concentration in  $N_2$  at  $E/P = 10.5 \text{ V/cm-torr}$  and  $J_b = 5 \text{ A/cm}^2$  for ambient pressure  $P = 1, 2$  and  $3 \text{ atm}$ .

### C. Design Procedure

In this section we combine the switch circuit requirements with the switch physics to develop a self-consistent procedure for obtaining the switch gas composition and pressure, the switch length, and switch area (radius) for a given switch gain.

First we obtain the factor  $k_0$  in Eq. (2), which when multiplied by the power delivered to the load gives the average power dissipated by the switch during the opening phase. During the time the switch is undergoing a transition from conducting to a nonconducting state ( $\tau_0$ ), the switch current is decreasing and the switch resistance is increasing. During  $\tau_L$  the switch current changes by  $I_{SW}$  ( $= I_L$ ) and switch voltage changes by  $V_L$ ; thus we define

$$k_0 \equiv \frac{\langle I_{SW} \rangle \langle V_{SW} \rangle}{I_{SW} V_L}, \quad (25)$$

where  $\langle I_{SW} \rangle$  and  $\langle V_{SW} \rangle$  are the average values of the switch current and voltage during  $\tau_0$ .

The time history of the voltage across the switch will depend upon the load voltage time behavior (see Figs. 1 and 2). For loads where the load voltage rises to its peak value in a time  $\approx \tau_0$  (i.e., resistive or inductive loads),  $\langle I_{SW} \rangle \approx 1/2 I_{SW}$  and  $\langle V_{SW} \rangle \approx 1/2 V_L$  so that

$$k_0 \approx 1/4. \quad (26)$$

For a capacitive load (Fig. 2a), the load voltage reaches its maximum in a time  $\tau_L = \tau_{CH}$ . In this case, we still have  $\langle I_{SW} \rangle \approx 1/2 I_{SW}$ . However,  $\langle V_{SW} \rangle \approx \langle I_{SW} \rangle \tau_0 / 2C = V_L \tau_0 / 4\tau_L$ . Thus, for a capacitive load,

$$k_0 \approx 1/8 (\tau_0 / \tau_L). \quad (27)$$

Once  $k_0$  is known, the opening time,  $\tau_0$  can be computed from Eq. (14a) for a choice of  $g_0$ . Knowing  $\tau_0$ , Eq. (18) can be used along with data on attachment and recombination rates, to make a judgement on whether the switch should be attachment or recombination dominated, thus suggesting a specific gas composition. The value obtained for  $\tau_0$  must be also consistent with the circuit requirements. If not, the choice of  $g_0$  must be modified.

We now set out to compute the switch pressure. Beginning with Eq. (14b) and substituting for  $E_C$  from Eq. (24), for  $\epsilon$  from Eq. (14c), for  $\tau_p$  from Eq. (18), and for  $\tau_0$  from Eq. (14a) we obtain

$$P^{-1} = \frac{g_0 g_C g_b s_B f_0}{k_0 k_p} \tau_L \frac{E_B^2}{P_0} \left( \frac{V_L}{V_b} \right) \left( \frac{\tau_L}{\tau_C} \right)^2. \quad (28)$$

The factors  $g_0$ ,  $g_C$ , and  $g_b$  are chosen so that  $P$  can be made small consistent with the constraint of Eq. (13). An optimum choice for  $g_0$ ,  $g_C$ , and  $g_b$  can be obtained by using the method of Lagrange undetermined multipliers,<sup>31</sup> with the result that  $g_0 \approx g_C \approx g_b = g$  (note that in some cases  $k_0$  and  $k_p$  can depend on the  $g$  factors). For example, if a  $\xi$  of 3 is chosen then  $g \approx 0.1$  and  $\eta = 0.75$ .

Once  $P$  is known, Eq. (1) gives the switch length

$$l = \frac{V_L}{s_B P (E_B^2 / P_0)}. \quad (29)$$

The value chosen for  $V_b$  in Eq. (28) can be combined with  $P$  and  $l$  to compute  $k_b$  of Eq. (4). Note that in order for the beam to traverse the switch length  $V_b$  will depend on the product  $Pl$ , as does  $V_L$ . Therefore, one can show that typically  $V_b \approx V_L$ , with  $k_b \approx 0.3$ .

The electron beam current to be injected into the switch can be obtained from Eq. (14c) and the definition of current gain,  $\epsilon$ :

$$\epsilon \equiv I_{SN}/I_b = g_b^{-1} \frac{V_b}{V_L} \left( \frac{\tau_C}{\tau_L} \right). \quad (30)$$

By substituting  $R_{SN}$  from Eq. (16) and  $I_b$  from Eq. (30) into Eq. (6) we arrive at the required switch area:

$$A = \frac{I_{SN} V_L (n\tau_L) g_C}{s_H (W_B^2/P_o) \pi l} \left[ 1 + \frac{k_O}{g_C} \left( \frac{\tau_O}{\tau_L} \right) + k_b \frac{g_b}{g_C} \right]. \quad (31)$$

The area thus computed insures that the switch will be large enough that the total energy per unit volume deposited in the switch is less than the deposited energy density required to lower the breakdown threshold.

The  $e$ -beam generator requirements are determined from  $V_b$ ,  $I_b$ , and  $A$ .  $I_b$  is computed from Eq. (30). The  $e$ -beam generator must actually provide a somewhat higher current than  $I_b$  to account for current lost to the structure supporting the vacuum-high pressure interface. The  $e$ -beam generator must also supply a beam of area  $A$ .

#### D. Design for Repetitive Closing Switch—Capacitive System

Taking the circuit parameters described in Table I, we apply the results of Sec. V.C to arrive at a switch design for the repetitive closing switch of Fig. 1.

For this case we choose  $\tau_{pp} = 15 \mu\text{s}$ , safety factors  $s_B = 0.75$ ,  $s_H = 0.5$ , and  $V_b = 200 \text{ kV}$ . As previously stated (Table II)  $I_{SN} = I_L = 20 \text{ kA}$ ,  $n = 5$ ,  $V_L = 200 \text{ kV}$ , and  $\tau_L = 40 \text{ ns}$ . Choosing  $\xi = 2$  gives  $g_O \approx g_C \approx g_b = 0.17$ . With  $\tau_C = \tau_L = 40 \text{ ns}$ , Eq. (30) requires  $\epsilon \approx 6$ . Because the load is not capacitive we substitute  $k_O$  from Eq. (26) into Eq. (14a) to compute  $\tau_O$ :

$$\tau_O \approx 4g_O\tau_L \approx 30 \text{ ns}. \quad (32)$$

It is not disturbing that  $\tau_O \sim \tau_L$  because the pulse line does most of the load pulse shaping; therefore, the major requirements are that  $\tau_O < \tau_{pp}$  and that  $\tau_{SR} \leq \tau_R$ . The second requirement can be easily met for an  $e$ -beam risetime  $\leq \tau_p$ .<sup>4</sup> We choose  $k_p$  in Eq. (18) to be  $\sim 5$  (attachment dominated) so that the plasma electron decay time  $\tau_p \approx 6 \text{ ns}$ . This can be achieved with a  $\text{N}_2\text{-O}_2$  gas mixture of 4:1.<sup>5</sup>

The switch pressure is given by Eq. (28) with  $E_B \approx 20 \text{ kV/cm}$ ,  $f_o = 2 \times 10^5 \text{ cm/V-s}$  for  $\text{N}_2\text{-O}_2$  and  $k_O = 0.25$  (Eq. (26)):

$$P \approx 1700 \text{ Torr} \approx 2.3 \text{ atm}. \quad (33)$$

The switch length is then (Eq. (29))

$$l \approx 5.9 \text{ cm}. \quad (34)$$

These  $l$ ,  $P$ , and  $V_b$  values are consistent with  $k_b \approx 0.3$ .

Equation (31) is then used to obtain the switch area (radius)

$$A \approx 2590 \text{ cm}^2 \quad (35)$$

$$(r \approx 29 \text{ cm}),$$

giving a switch current density of  $J_{SN} \approx 8 \text{ A/cm}^2$ . The  $e$ -beam current density is thus  $J_b \approx 1.3 \text{ A/cm}^2$ . From Eq. (16) we compute  $R_{SN} \approx 1.7 \Omega$  and from Eq. (15) we obtain  $\rho_o = 745 \Omega\text{-cm}$ .

Table III is a summary of the values of the switch parameters which, along with the required switch inductance ( $\leq 100$  nH), completely characterize the switch.

The  $e$ -beam generator is required to deliver  $\geq 20$  J/pulse with a very fast rise and decay time. The  $e$ -beam current density, however, is modest,  $\sim 1$  A/cm<sup>2</sup>.

### E. Design for Repetitive Opening Switch—Hybrid System

Taking the circuit parameters described in Table II, we apply the results of Sec. V.C to arrive at a switch design for the repetitive opening switch EBCS(O) of Fig. 2.

For this case:  $\tau_{pp} = 15$   $\mu$ s,  $\tau_{NC} = \tau_L = 2$   $\mu$ s,  $I_{SW} = I_L = I_o = 8$  kA,  $n = 5$ , and  $V_L = 200$  kV (Table II). We choose  $s_B = 0.75$ ,  $s_H = 0.5$ , and  $V_b \approx V_L = 200$  kV. Setting  $\xi = 4$  gives (Eq. (13))  $s_O \approx s_C \approx s_b = 0.08$ . With  $\tau_C \approx \tau_{pp} - \tau_L$ , Eq. (30) requires  $\epsilon \approx 80$ . Because of the capacitive load, we substitute  $k_O$  from Eq. (27) into Eq. (14a) to compute  $\tau_O$ :

$$\tau_O = \sqrt{8s_O} \tau_L \approx 1.6 \mu\text{s}. \quad (36)$$

Since  $\tau_O \sim \tau_L$ , a substantial fraction of the final charge voltage for the capacitor will be attained during the opening time. This presents no serious problems, because the major requirement is that the capacitor be charged in a time  $\leq \tau_{pp}$ . We choose  $k_p$  in Eq. (18) to be  $\sim 5$  (attachment dominated) so that  $\tau_p \approx 300$  ns, which can be readily attained using  $N_2$  with a small ( $\sim 1\%$ ) admixture of  $O_2$ .

The switch pressure is given by Eq. (29) with  $f_o = 2 \times 10^5$  cm/V-s for  $N_2$  and  $k_O = 0.1$  (Eq. (27)):

$$P = 5230 \text{ Torr} \approx 7 \text{ atm}. \quad (37)$$

The switch length is then (Eq. (29))

$$l = 1.9 \text{ cm}. \quad (38)$$

Equation (31) is then used to obtain the switch area (radius):

$$\begin{aligned} A &= 3000 \text{ cm}^2 \\ (r &\approx 31 \text{ cm}), \end{aligned} \quad (39)$$

giving a switch current density of  $J_{SW} \approx 2.6$  A/cm<sup>2</sup>. The  $e$ -beam current density is thus  $J_b \approx 0.03$  A/cm<sup>2</sup>. At this point the switch resistance can be computed as in Sec. V.D.

Table IV summarizes the values of the switch parameters, which, along with a required switch inductance ( $\sim 5$   $\mu$ H), completely characterize the switch.

The  $e$ -beam generator requirements are quite modest with only 2.6 J/pulse needed. This reduces the complexity of the  $e$ -beam pulse modulation. The pressure requirement may be relaxed by as much as an order of magnitude by choosing a gas with a higher mobility during conduction, e.g., a mixture of Ar with  $O_2$  or  $CH_4$  with an attaching gas ( $CO_2$ ). Alternately, use of these gases will increase the switch efficiency if the switch pressure can remain high, as is evident from Eq. (28). This is an area where more research is needed.

### VI. CONCLUDING REMARKS

We had three principal objectives in the present paper. The first was to review the principles of operation of electron-beam controlled switches, emphasizing the ability of these switches to recover and open rapidly under high applied voltage. This rather unique capability makes the EBCS attractive, particularly when compared with other switch candidates, as either a single pulse opening switch or as a switch for repetitively pulsed systems with high repetition rates.

Table III — Characteristics of Closing Switch  
for a Capacitive Pulser

A. Switch Parameters

gas	$N_2:O_2 \sim 4:1$
pressure, $P$	2.3 atm
length, $l$	5.9 cm
Area (radius), $A(r)$	$2590 \text{ cm}^2$ (29 cm)
Current Density, $J_{SW}$	$8 \text{ A/cm}^2$
energy gain (current gain), $\xi(\epsilon)$	2(6)
resistance during conduction	$1.7 \Omega$
voltage drop during conduction	34 kV

B. E-Beam Parameters

voltage, $V_b$	200 kV
current, $I$	3.5 kA
risetime $\leq \tau_r$	$\leq 2 \text{ ns}$
decay time $\leq \tau_d$	$\leq 30 \text{ ns}$

Table IV — Characteristics of Opening Switch  
for a Hybrid Pulser

A. Switch Parameters

Gas	$N_2:O_2 \sim 99:1$
Pressure, $P$	7 atm
length, $l$	1.9 cm
Area (radius), $A(r)$	$3000 \text{ cm}^2$ (31 cm)
current density, $J_{SW}$	$2.6 \text{ A/cm}^2$
Gain (current gain), $\xi(\epsilon)$	4(80)
Resistance during conduction, $R_{SW}$	$0.3 \Omega$
Voltage drop during conduction	2.4 kV

B. E-Beam Parameters

Voltage, $V_b$	200 kV
current, $I_b$	100 A
rise and decay time, $\leq \tau_p$	$\leq 100 \text{ ns}$

The second objective was to present a formalism for switch design. The formalism given emphasizes the overall energy-transfer efficiency of the switch, the fundamental circuit requirements, and the switch physics. Our analysis indicates that efficiencies of  $\approx 80\%$  should be achievable for the examples chosen. We point out that these efficiencies are conservative in that the switch designs utilize the well known but nonoptimum gases,  $N_2$  and  $O_2$ . Significant improvements in switch energy gain should result if  $N_2$  were replaced by a gas such as  $CH_4$  with high electron mobility, or if  $O_2$  were replaced by a gas such as  $C_2F_6$  in which the attachment rate increases rapidly with applied field.

The third objective was to illustrate the capabilities of the EBCS in a parameter regime of interest, both as an opening switch for inductive energy store, and as a fast closing switch. In the examples chosen, the opening switch would conduct for  $\sim 15 \mu s$  and open in  $\sim 1 \mu s$ ; the closing switch would close in  $\sim 5 ns$  and conduct for  $\sim 50 ns$ . The switch size in both cases was roughly one-half meter in diameter by a few cm in length.

Although single pulse operation has not been stressed in this report, it is important to note that the EBCS is capable of providing opening times substantially shorter than what can be achieved with wire fuses, the only available alternative for fast opening applications. New developments in erosion switches<sup>32</sup> may provide a fast opening time, but the conduction times are limited. Therefore, from the standpoint of the general development of inductive storage, the EBCS may make a significant contribution.

We stress that the performance of any EBCS is primarily limited by the desired switch efficiency and by the ambient switch gas pressure, as indicated by Eqs. (13) and (28). Choosing nominal values for  $k_0$ ,  $k_p$ ,  $s_B$ ,  $E_B/P_0$ , recalling the switch efficiency  $\eta = \xi/(\xi + 1)$ , and assuming  $V_b \approx V_L$ , Eq. (28) can be rewritten as

$$\left(\frac{\tau_C}{\tau_L}\right)^2 \approx 0.6 P \left(\frac{1-\eta}{\eta}\right)^3 f_o \tau_L. \quad (40)$$

The reader is reminded that  $f_o$  is proportional to the electron mobility. Equation (40) indicates that as  $\eta$  is made large,  $\tau_C/\tau_L$  becomes smaller. This type of relationship will exist for any opening switch, because there are always losses associated with the conduction phase.

As an example, we choose an energy efficiency of 80% ( $\eta = 0.8$ ),  $f_o = 2 \times 10^6$  cm/V-s, and assume a maximum practical gas pressure of 10 atm. Equation (40) then becomes

$$\left(\frac{\tau_C}{\tau_L}\right)^2 \leq \tau_L/(1 ns). \quad (41)$$

This condition precludes sub-nanosecond load pulse widths. That is, for a closing switch ( $\tau_L \approx \tau_C$ ),  $\tau_L \geq 1 ns$ . In the case of an opening switch this condition additionally limits the maximum allowed conduction time,  $\tau_C$ . For instance, for a load (open) time of  $\tau_L = 1 \mu s$ , the switch conduction time is limited to  $\tau_C \leq 30 \mu s$ . By reducing the switch efficiency to 50%, however, a conduction time of  $\tau_C \leq 250 \mu s$  could be realized. Equation (41), along with the similar equation for 50% efficiency, is displayed graphically in Fig. 8.

This report has not addressed all issues of concern to EBCS design and operation. We have not discussed, for example, the impact of electrode sheath effects, current conduction by ions, or vacuum interface problems. Nonetheless, none of these additional issues should seriously compromise the design performance. This statement is supported by experiments performed at NRL and elsewhere.<sup>1,4,6-8,13,14</sup> These experiments, which cover a wide parameter space, demonstrate that the EBCS does indeed open under high applied voltage and that the simple models used are adequate to explain the observed switch behavior.

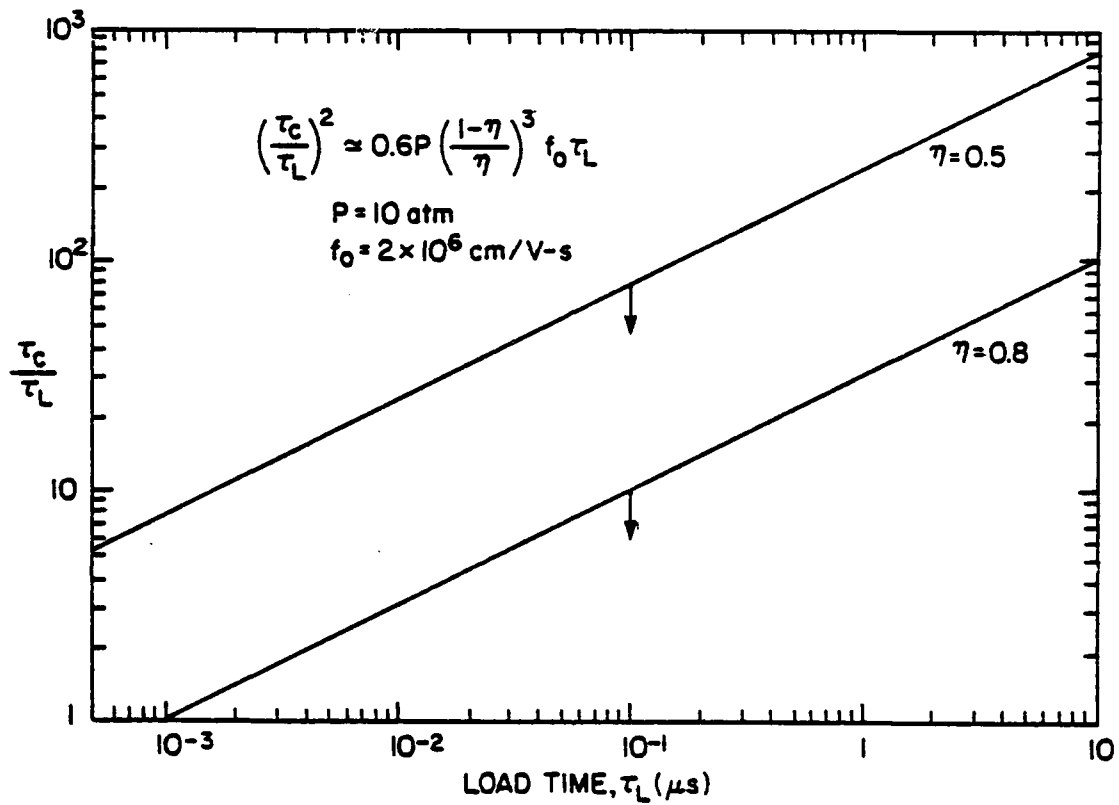


Fig. 8 -- Plot of  $\tau_c/\tau_L$  as a function of  $\tau_L$  based on Eq. (28) for switch efficiencies,  $\eta$  of 0.5 and 0.8

The authors wish to thank J. M. Cameron and H. Hall for their expert technical assistance in the design and operation of the experimental apparatus. This work was supported by the Naval Surface Weapons Center, Dahlgren, VA.

## VII. REFERENCES

1. R.O. Hunter, Proc. International Pulsed Power Conference, Lubbock, TX (1976), IC8:1-6.
2. J.P. O'Louglin, Proc. International Pulsed Power Conference, Lubbock, TX (1976), IIC5:1-6.
3. B.M. Kovalchuk and G.A. Mesyats, Sov. Tech. Phys. Lett., 2, 252 (1976).
4. K. McDonald, M. Newton, E.E. Kunhardt, M. Kristiansen, and A.H. Guenther, IEEE Trans. Plasma Sci. PS-8, 181 (1980).
5. R.F. Fernsler, D. Conte and I.M. Vitkovitsky, IEEE Trans. Plasma Sci. PS-8, 176 (1980).
6. P. Bletzinger, Proc. of Workshop on Repetitive Opening Switches, Tamarron, Colorado, Texas Tech University Rept. (April 1981), p. 128.
7. Lawrence E. Kline, Proc. of Workshop on Repetitive Opening Switches, Tamarron, Colorado, Texas Tech University Rept. (April 1981), p. 121.
8. R.J. Commisso, R.F. Fernsler, V.E. Scherrer, and I.M. Vitkovitsky, IEEE Trans. Plasma Sci., to be published (1982).
9. J. Benford, Physics International Co., San Leandro, CA, private communication (1980).
10. J. Salge, V. Braunsberger, and V. Schwartz, 1st International Conference on Energy Compression and Switching, Torino (1974).
11. I.M. Vitkovitsky, D. Conte, R.D. Ford, and W.H. Lupton, NRL Memorandum Report 4168 (1980).
12. R.D. Ford, D. Jenkins, W.H. Lupton, and I.M. Vitkovitsky, Rev. Sci. Inst. 52, 694 (1981).
13. V.E. Scherrer, R.J. Commisso, R.F. Fernsler, L. Miles, and I.M. Vitkovitsky, Third International Symposium on Gaseous Dielectrics, Knoxville, TN (1982).
14. V.E. Scherrer, R.J. Commisso, R.F. Fernsler, and I.M. Vitkovitsky, 1982 Fifteenth Power Modulator Symposium, Baltimore, MD (1982).
15. W.A. Barletta, Lawrence Livermore Laboratory Report, UCRL-87288 (1981).
16. T.R. Burkes, J.P. Craig, M.O. Hagler, M. Kristiansen, and W.M. Portnoy, IEEE Trans. Elect. Dev. ED-26, 1401 (1979).
17. E.J. Lauer and D.L. Birx, Third IEEE International Pulsed Power Conference, Albuquerque, NM IEEE Cat. No. 81CH1662-6 (1981), pg. 380.
18. I.D. Smith, G. Lauer, and M. Levine, 1982 Fifteenth Pulse Power Modulator Symposium, Baltimore, MD (1982).

19. D.L. Bix, et al., 1982 Fifteenth Pulse Power Modulator Symposium, Baltimore, MD (1982).
20. D.L. Bix, E.J. Laurer, L.L. Reginato, D. Rogers, Jr., M.W. Smith, and T. Zimmerman, Third IEEE International Pulsed Power Conference, Albuquerque, NM, IEEE Cat. No. 81CH1662-6 (1981), p. 262.
21. J.E. Eninger, Third IEEE International Pulsed Power Conference, Albuquerque, NM, IEEE Cat. No. 81CH1662-6 (1981), p. 499.
22. A.W. Freidman and J.E. Eninger, Third IEEE International Pulsed Power Conference, Albuquerque, NM, IEEE Cat. No. 81CH1662-6 (1981), p. 519.
23. C.A. Spindt, I. Brodie, L. Humphrey, and E.R. Westerberg, J. Appl. Phys. 47, 5248 (1976).
24. B. Fell, R.J. Commisso, V.E. Scherrer, and I.M. Vitkovitsky, J. Appl. Physics 53(4), 2818 (1982).
25. L.A. Miles, E.E. Nolting, I.M. Vitkovitsky, and D. Conte, IEEE Conference Record, 1980 Fourteenth Pulse Power Modulator Symposium, Orlando, FL (1980), p. 68.
26. N.W. Harris, F. O'Neill, and W.T. Whitney, Rev. Sci. Inst. 48, 1042 (1977).
27. R.D. Ford and I.M. Vitkovitsky, NRL Memo Report 3561 (1977).
28. D. Conte, R.D. Ford, W.H. Lupton, and I.M. Vitkovitsky, Proc. 7th Symposium on Engineering Problems in Fusion Research, Knoxville, TN, IEEE Pub. 77CH1267-4-NPS (1977), p. 1066.
29. S.A. Genkin, Yu. D. Kosolev, V.G. Rabothin, and A.P. Khuzeiv, Sov. J. Plasma Physics 7(3), 327 (1981).
30. S.C. Brown, *Basic Data of Plasma Physics* (MIT Press, Cambridge, 1967), pp. 87-94.
31. H. Goldstein, *Classical Mechanics* (Addison-Wesley, Reading, 1950), p. 41.
32. R.A. Meger, R.J. Commisso, G. Cooperstein, A.T. Drobot, and Shyke A. Goldstein, 1982 IEEE International Conference on Plasma Science, Ottawa, Canada, IEEE Cat. No. 82CH1770-7 (1982), p. 4.

### List of Symbols

- $A$  = switch area
- $E$  = electric field across the switch
- $E_B$  = electric field required for breakdown
- $E_C$  = electric field across switch during conduction
- $e$  = electronic charge
- $f_o$  =  $eS_o\mu P$
- $g_b$  = ratio of beam energy to load energy
- $g_C$  = ratio of energy dissipated during switch conduction to load energy
- $g_O$  = ratio of energy dissipated during switch opening to load energy
- $H_b$  = energy deposited by  $e$ -beam in switch gas by inelastic processes
- $H_C$  = energy deposited in switch during conduction
- $H_O$  = energy deposited in switch during opening
- $I_b$  =  $e$ -beam current
- $I_L$  = load current (=  $I_{SN}$ )
- $I_{SN}$  = switch plasma current
- $J_b$  =  $e$ -beam current density
- $J_{SN}$  = switch plasma current density
- $k_b$  = fraction of total  $e$ -beam energy deposited in switch gas from inelastic processes
- $k_O$  = fraction of load energy dissipated by switch during opening
- $k_p$  = ratio of opening time to characteristic loss time for switch plasma
- $L_o$  = inductance of storage inductor
- $L_{SN}$  = inductance of switch
- $n$  = number of pulses
- $n_p$  = switch plasma density
- $P$  = switch pressure
- $P_o$  = atmospheric pressure
- $r$  = switch radius
- $s_B$  = safety factor for static breakdown
- $s_H$  = safety factor for heating
- $S_o$  = ionization parameter
- $v$  = plasma drift velocity
- $V_b$  =  $e$ -beam voltage
- $V_L$  = voltage across the load
- $V_{SN}$  = voltage across the switch
- $W$  = energy per unit volume deposited in switch

- $W_B$  = energy per unit volume deposited in switch required for breakdown at pressure  $P$
- $W_B^0$  = energy per unit volume deposited in switch required for breakdown at atmospheric pressure
- $\epsilon$  = current gain
- $\epsilon_v$  = energy required for combination per electron-ion pair
- $\eta$  = switch efficiency
- $\mu$  = electron mobility
- $\xi$  = gain factor
- $\rho_0$  = switch resistivity at peak current
- $\tau_C$  = time interval during which switch is conducting
- $\tau_{CH}$  = capacitor charging time
- $\tau_{CH}^2$  = inductor charging time
- $\tau_{COM}$  = commutation time
- $\tau_L$  = load pulse width ( $\approx \tau_C$  for closing switch;  $\approx \tau_{NC}$  for opening switch)
- $\tau_{NC}$  = time interval during which switch is not conducting
- $\tau_p$  = characteristic loss time for plasma electrons
- $\tau_O$  = time interval during which switch changes from conducting to nonconducting
- $\tau_{FP}$  = time interval between pulses
- $\tau_R$  = rise time of load pulse
- $\tau_{SR}$  = time interval during which switch change from nonconducting to conducting

## THE CONTROL OF BREAKDOWN AND RECOVERY IN GASES BY PULSED ELECTRON BEAMS\*

V.E. Scherrer\*\*, R.J. Comisso+, R.F. Fernsler+,  
L. Miles++, and I. M. Vitkovitsky\*\*

\*Work supported by the Office of Naval Research and Naval Surface Weapons Center

\*\*Naval Research Laboratory, Washington, DC 20375

+Jaycor, Inc., Alexandria, VA 22304

++Naval Surface Weapons Center, White Oak, MD 20910

### ABSTRACT

Experiments in which a 150 keV electron-beam pulse is injected into test gas mixtures at atmospheric pressure are described. Electron attaching gases, including  $O_2$ ,  $CO_2$ ,  $CH_4$  and  $SF_6$ , are mixed with non-attaching base gases,  $N_2$  and Ar. The ionizing electron-beam current ( $1-100 A/cm^2$ ) provides a volume discharge between two electrodes. The discharge is used to determine the temporal behavior of gas resistivity as a function of beam current. Theoretical results for  $O_2:N_2$  mixtures agree with experimental values.

### KEY WORDS

Gaseous Dielectrics, Air Chemistry Code, Volume Discharge.

### INTRODUCTION

There is presently much scientific interest in, and a number of possible applications for, gaseous dielectrics in which the conductivity is controlled by an external source of ionization. When an electron beam (e-beam) is injected into a chamber containing a mixture of an attaching and a non-attaching gas, the ionization of the gas produced by the e-beam pulse competes with attachment and recombination processes controlling the conductivity of the gas. Thus, the discharge current is turned on and off in association with the e-beam pulse. This concept has application as a high power switch for fusion experiments and charged particle-beam production and has relevance to laser development and beam propagation. Use of electron beams to control gas conductivity was demonstrated by Koval'chuk and Mesyats (1976), Hunter (1976), and O'Loughlin (1976).

The objective of this study is to obtain basic data for volume discharges caused by e-beams and to compare this data with a theoretical model. In the experiment, a 150 keV pulse is applied to an e-beam diode producing an e-beam pulse that is injected into test gas mixtures. An ancillary capacitor connected to the test chamber drive the volume discharges. The ionizing e-beam current density was varied from 1 to  $100 A/cm^2$ . For  $O_2:N_2$  mixtures, resistivity and discharge current risetime and decay time agree with theoretical values.

## DESCRIPTION OF THE EXPERIMENT

A schematic of the facility is shown in Fig. 1. The system contains three principal parts: a high voltage pulser [Fell and colleagues (1982)], an e-beam diode electron accelerator, and a gas cell test chamber. In the pulser, a 20 kA current source is used to charge an inductive store with exploding wire fuses,  $F_1$  and  $F_2$ , serving as opening switches that produce a 200 ns(FWHM) 150 kV pulse to generate the e-beam.

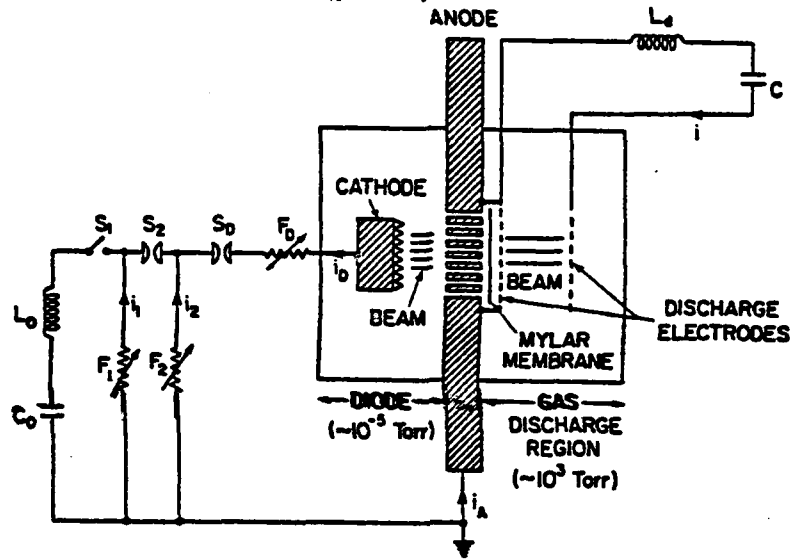


Fig. 1. Schematic diagram of experimental facility.

The test chamber is normally filled with a mixture of two gases at a pressure of 760 Torr. The resistance of the cell is determined by measuring the current through and the voltage across it. The circuit voltage is sustained by the capacitor C. The circuit is described by

$$V_0 = R(t) [i - i(e)] + L \frac{di}{dt} + \frac{1}{C} \int_0^t i dt, \quad (1)$$

where  $i$  is the net current flowing in the discharge circuit,  $V_0$  is the initial voltage on capacitor C,  $L$  is the circuit inductance, and  $i(e)$  is the electron beam current. The gas resistivity,  $\rho$ , is geometrically proportional to the resistance,  $R(t)$ .

## THEORY

Outlined here is a brief reformulation of the theory presented by Fernsler and colleagues (1980). Consider a volume discharge in which gas conduction is regulated solely by an externally applied ionizing electron beam and by the relevant gas chemistry. In the present experiments, where attachment is typically the dominant electron loss, the electron density evolves according to

$$\frac{dn}{dt} = \frac{J\sigma N}{e} - \alpha n, \quad (2)$$

where  $J$  is the beam current density,  $\sigma$  is the effective cross section for ionization by the electron beam,  $N$  is the neutral gas density,  $n$  is the electron density

and  $\alpha$  is the electron attachment rate. If  $J$  is applied as a square pulse of duration  $\tau$ , the electron density  $n(t)$  can readily be determined. Equivalently, for constant electron mobility  $\mu$  and constant attachment rate  $\alpha$ , the switch resistivity  $1/(en\mu)$  is given by

$$\rho(t) = \begin{cases} \frac{\alpha}{J\sigma N\mu} \left( \frac{e^{at}}{e^{a\tau} - 1} \right) & t < \tau \\ \frac{\alpha}{J\sigma N\mu} \left( \frac{e^{at}}{e^{a\tau} - 1} \right) & t > \tau \end{cases} \quad (3)$$

The minimum switch resistivity,

$$\rho_{\min} = \frac{\alpha}{J\sigma N\mu} \frac{e^{a\tau}}{e^{a\tau} - 1} \quad (4)$$

is thus limited by

$$(J\sigma N\mu \tau)^{-1} > \rho_{\min} > (J\sigma N\mu/\alpha)^{-1} \quad (5)$$

In the present experiments,  $\alpha$  is controlled by mixing a specified fraction of an attaching gas (e.g.,  $O_2$ ,  $SF_6$ , ....) with a non-attaching base gas ( $N_2$ , Ar).

Eqs. (2)-(4) provide a convenient basis for comparison to experiment. Alternately, numerical simulations coupling gas chemistry to the appropriate circuit and beam parameters may be used. Fig. 2 illustrates such a simulation using the air

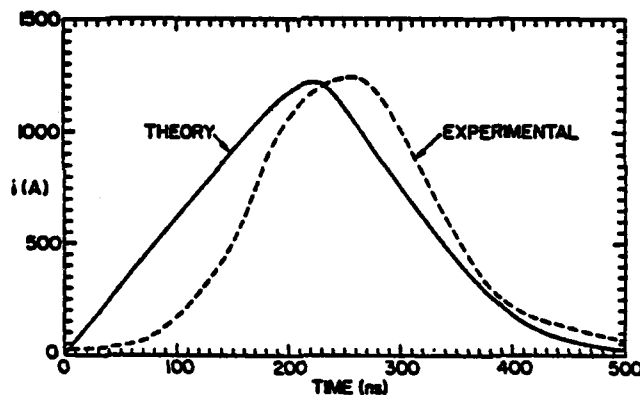


Fig. 2. Comparison of experimental and theoretical results.

chemistry code CHMAIR [Fernsler and others (1979)]. Similar calculations have been performed by Dzimianski and Kline (1979) for a variety of gas mixtures using a Boltzmann analysis to derive required transport coefficients and reaction rates. Simulations have also been performed by Lowke and Davies (1977) incorporating axial spatial variations to assess the effects of cathode fall and related phenomena.

We note that considerably altered behavior of  $\rho$  can often be obtained by choosing gases in which  $\mu$  decreases and  $\alpha$  increases with applied field. Such changes tend to obscure, however, the basic ionization and deionization processes, and can additionally result in unstable behavior as discovered by Douglas-Hamilton and Mani (1973).

## EXPERIMENTAL RESULTS

The preceding section describes the time dependence of the gas resistivity for the case of a square pulse electron beam injected uniformly into the gas. The analytic form of the resistivity is given by Eq. 3 for time intervals during and after beam injection. The derivation of Eq. 3 and 4 requires several assumptions that may be difficult to realize in practice. For these reasons we need to accumulate a data base for comparing experiment with a more realistic numerical calculation. We have carried out a systematic study of a number of gases. The resistivity,  $\rho$ , and falltime,  $\tau_F$ , were determined for each gas mixture and were plotted as a function of percent attaching gas. This was repeated for different values of electron current density from 1-100 A/cm<sup>2</sup>. In Fig. 3 we present a summary of  $\rho$  (evaluated at peak discharge current) as a function of percent of attaching gas for a narrow range of incident

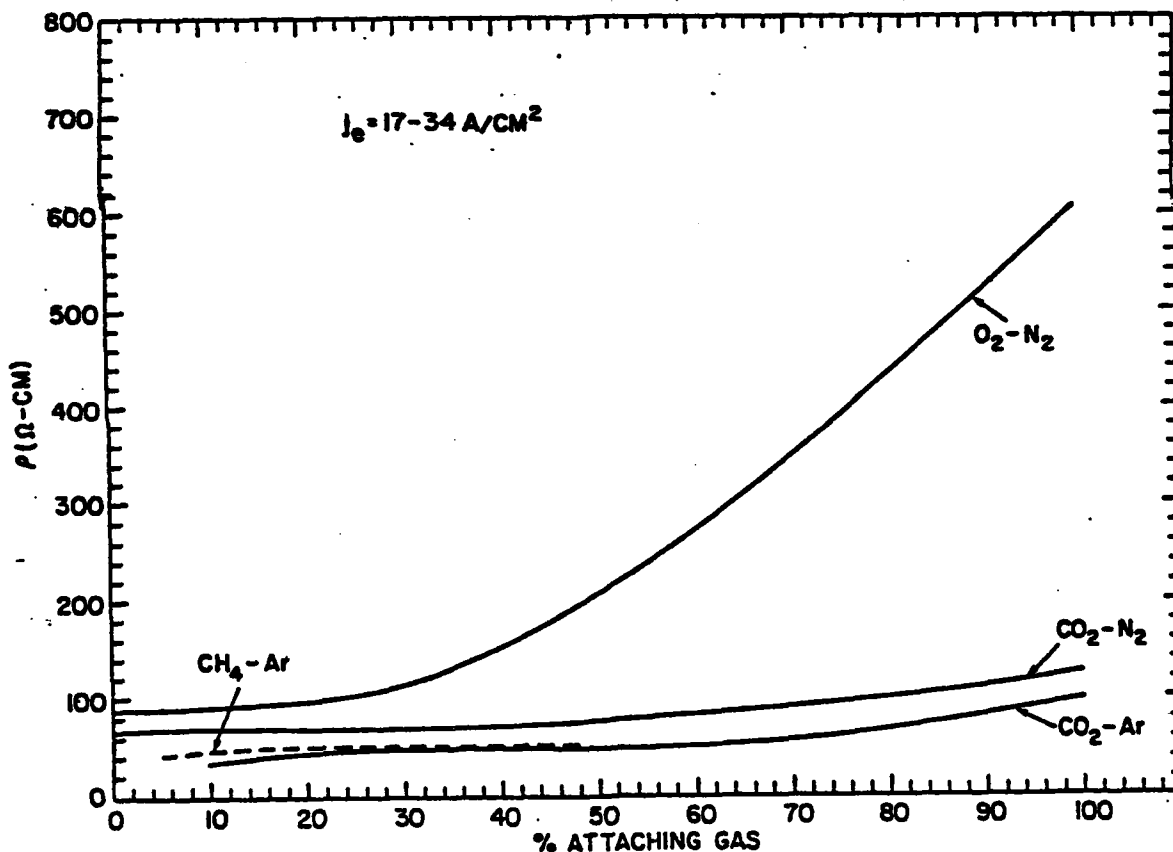


Fig. 3. Effect of gas mixtures on resistivity.

electron current densities (17-34 A/cm<sup>2</sup>). These results provide a comparison of the relative merit of gas combinations and percentages for producing low resistivity.

The current falltime,  $\tau_F$ , is presented in Fig. 4 for the same gas combinations and for the same incident electron current density as the previous figure. As a reference,  $\tau_F$  of the e-beam is also given. The measured falltimes as well as the discharge current risetime are governed not only by the magnitude and time variation of the beam current and the attachment rate, but also by circuit parameters.

In Fig. 4, only  $O_2$ -Ar (above 50%) and  $O_2$ - $N_2$  (above 30%) appear to be limited by the e-beam falltime. All other values of  $\tau_F$  are longer than the e-beam falltime and are determined by the gas properties. Because the voltage applied across the discharge electrodes is well below the level needed to support a self-sustained discharge, the gas recovers to the pre-discharge dielectric stress of  $\sim 10$  kV/cm.

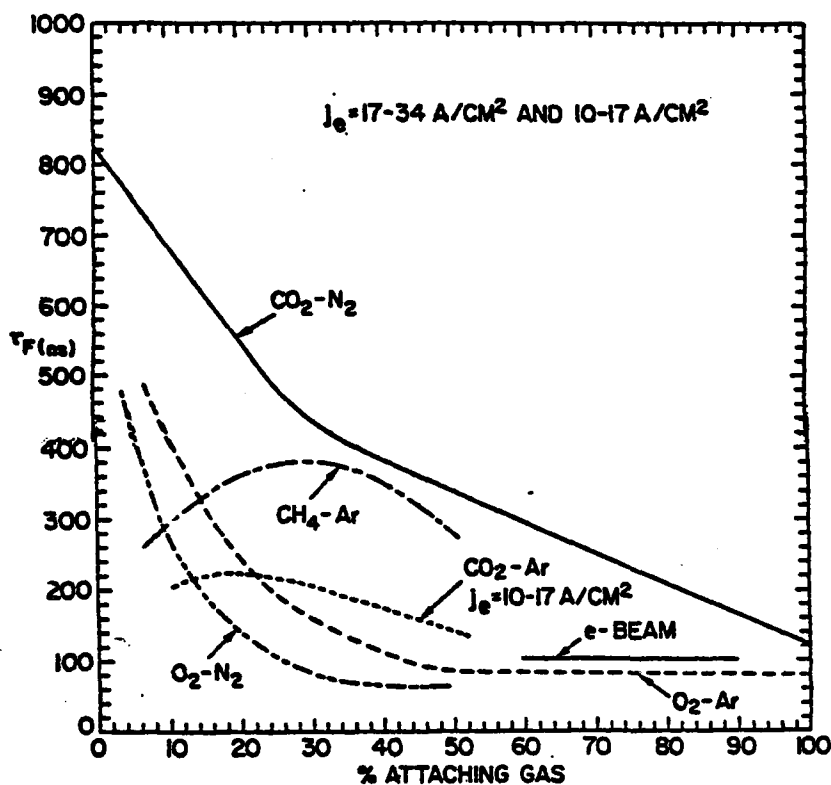


Fig. 4. Effect of gas mixture on current falltime.

#### REFERENCES

- Douglas-Hamilton, D.H., and S. A. Mani (1973). An electron attachment plasma Instability. *Appl. Phys. Lett.*, 23, 508-510.
- Dzimianski, J.W., and L.E. Kline (1979). High voltage switch using externally ionized plasmas. Westinghouse Electric Corp., Report DYD-555-85-AA.
- Fell, B., R.J. Comisso, V.E. Scherrer, and I.M. Vitkovitsky (1982). Repetitive operation of an inductively-driven electron-beam diode. *J. Appl. Phys.*, to be published (May).
- Fernsler, R.F., A.W. Ali, J.R. Greig, and I.M. Vitkovitsky (1979). The NRL CHMAIR code, Naval Research Lab. Memo. Report 4110.
- Fernsler, R.F., D. Conte, and I.M. Vitkovitsky (1980). Repetitive electron-beam controlled switching. *IEEE Trans. Plasma Sci.*, PS-8, 176-180.
- Koval'chuck, B.M. and G.A. Mesyats (1976). Rapid cutoff of a high current in an electron-beam-excited discharge. *Sov. Tech. Phys. Lett.* 2, 252-253.
- Hunter, R.O. (1976). Electron beam controlled switching. *Proc. IEEE First Int. Pulsed Power Conf.*, IC8:1-6.
- Lowke, J.J. and D.K. Davies (1977). Properties of an electric discharge sustained by a uniform source of ionization. *J. Appl. Phys.*, 48, 4991-5000.
- O'Loughlin, J.P. (1976). PFN design interface with e-beam sustained discharge. *Proc. IEEE First Int. Pulsed Power Conf.*, IIIC5:1-6.

MULTIPLE PULSE ELECTRON-BEAM CONTROLLED SWITCH

V.E. Scherrer, R.J. Cornisso\*,  
R.F. Fernuler\*, and I.M. Vitkovitsky

Naval Research Laboratory  
Washington, DC 20375

Summary

The electron-beam (e-beam) controlled switch is a promising opening switch candidate<sup>1</sup> for inductive storage pulsed power applications where repetitively pulsed (> 1 kHz) output power of  $\sim 10^{10}$  W is required. Several authors<sup>1-11</sup> have reported theoretical analysis and experimental results for e-beam controlled switches. The development of this switch requires a number of experiments to be performed to determine the gas conductivity, rate of change of conductivity, switch efficiency, and the effects of energy deposition in the gas on the switch recovery. Such experiments, which would establish the feasibility of the e-beam switch for high power applications, are being carried out with simple gas mixtures over a range of ambient gas pressures and electron beam current densities. Comparisons are made between experiment and theory<sup>1,2</sup> to understand the basic mechanisms involved in switch operation. Single pulse experiments are also used to provide a data base for establishing the repetitive capability of the switch. A typical design goal involves charging of a storage inductor over a period of several microseconds, voltage and current levels at the load of 200-500 kV and 10-100 kA, with a pulse-to-pulse separation of  $\sim 100$   $\mu$ sec. Initial experiments characterizing the performance of a second pulse have been carried out.

E-Beam Switch Concept

The principles of an e-beam controlled switch for repetitive operation are discussed in Ref.(1). An inductive storage system using an e-beam controlled switch to generate a pulsed high power output is shown schematically in Fig. (1). When the e-beam is turned on, the switch resistance drops to a low value, resulting in energy transfer from the source  $W_0$  to the inductor L. When the e-beam is turned off (and SW-2 is closed) the switch resistance becomes large and switch current is

shunted to the load  $R_L$ . After the pulse, SW-2 opens and the process is repeated for a second pulse by making the e-beam switch conduct again. The switch SW-2 is generally not required except for specific applications. The most significant problem associated with the use of such a switch is the energy loss by joule heating in the switch. To minimize this heating, the switch resistance must be as low as possible while the switch is conducting. Such heating can also lead to late time breakdown making repetitive pulse operation impossible. On the other hand, this switch promises to provide a repetitive opening capability with a very fast fall time of the switch current. Potentially, the opening time of the switch can be substantially faster than that achieved with fuse arrays.

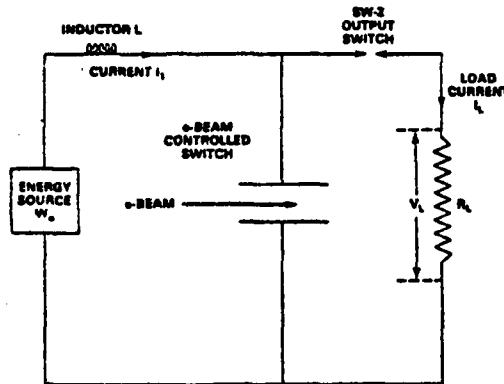


Figure 1. Schematic of an inductively driven pulser using an e-beam controlled switch.

A measure of the switch performance that determines how practical such a switch can be is the current gain,  $\epsilon$ . It is defined as the ratio  $(\bar{i}_n - \bar{i}_0)/\bar{i}_0$ , where  $\bar{i}_n$  is the total current flowing in the switch,  $\bar{i}_0$  is the injected e-beam current, and the bar indicates peak values. A current gain

of at least 10 atm considered necessary for a practical system.<sup>1</sup>

Theoretical predictions<sup>1</sup> indicate that the resistivity  $\rho$ , switch current fall time,  $\tau_F$ , and current gain  $\alpha$  depend on the ambient gas pressure. Limiting values of pressure depend upon the properties of the thin window between the evacuated ( $\sim 10^{-5}$  Torr) e-beam diode and the high pressure ( $\sim 10^3$  Torr) switch, electron energy requirements, and the strength of the switch chamber. A switch pressure of 10 atm appears feasible.

The upper limit of current density that can be switched in the repetitive pulse mode depends on energy deposition in the switch by joule heating. Excessive energy deposition is manifested in delayed breakdowns<sup>12</sup> which would preclude multiple pulse operation, as discussed later in detail.

#### Description of the Experiment

The experiment, shown schematically in Fig. (3), contains three principal parts: a high voltage pulser, consisting of a low voltage ( $< 10$  kV) source and a pulse-forming network; an e-beam diode; and a gas cell test chamber. In the pulser,<sup>13</sup> a 20 kA current

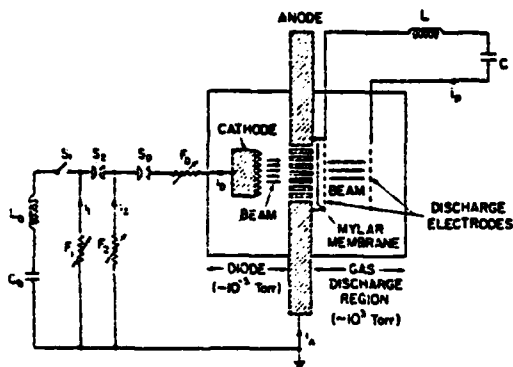


Figure 2 Schematic of the experiment

source charges an inductive store, with exploding wire fuses  $F_1$  and  $F_2$  serving as opening switches

that produce a 200 ns (FWHM), 200 kV pulse across the diode. The fuse  $F_3$  is chosen to open after 200 ns, limiting plasma generation in the diode. Two pulse-forming networks can be coupled to the diode for double-pulse studies of the e-beam switch.<sup>13</sup> The test chamber is isolated from the diode by a 0.005-cm mylar window and is normally filled with a mixture of two gases at a pressure of 1-3 atm. The resistance of the cell during discharge is determined by measuring the current through and voltage across it. The circuit voltage is sustained by the capacitor C. The circuit is described by:

$$V_0 = R(i_n - i_e) + L \frac{di_n}{dt} + \frac{1}{C} \int i_n dt, \quad (1)$$

where  $R$  is the switch resistance,  $V_0$  is the initial voltage on capacitor C, and  $L$  is the circuit inductance. We can neglect the last term in Eq.(1) (5% correction). At the time of peak  $i_n$  (i.e. when  $di_n/dt = 0$ ) the switch resistance is

$$R_0 = \frac{V_0}{i_n - i_e}. \quad (2)$$

The resistivity at peak net current,  $\rho_0$ , is related to  $R_0$  through the switch geometry. The fall time of the current through the switch is estimated from

$$\tau_F = \frac{L}{|V_2|} i_n, \quad (3)$$

where  $V_2$  is the transient voltage peak associated with the rise and fall of switch current and is indicated in Fig. (3).

The diagnostics used in the experiment include calibrated Rogowski loops and voltage dividers for measuring the diode voltage and current,  $V_D$  and  $i_D$  respectively; and the voltage across and net current through the discharge,  $V_d$  and  $i_n$  respectively. Blue cellophane and film techniques were used to verify the time integrated beam uniformity.

High-Voltage Experimental Data

For the switch concept that we have described, the following parameters are important: current gain, resistivity, switch current fall time and recovery characteristics. Also of importance is the effect of energy deposition on these parameters. Switch performance is expected to improve as the pressure is increased. Therefore, the experiments were focused on the accumulation of data to determine how  $\rho$ ,  $\tau_f^*$ , and  $c$  vary with gas composition and pressure. These measurements are also necessary to understand the basic physical processes involved in the switch and to provide input for theoretical analysis and scaling. We report primarily results for  $O_2-N_2$  mixtures because the atomic and molecular data are better established than for other gas mixtures.

An example of results for one discharge of the switch using a 20%  $O_2$ -80%  $N_2$  mixture at 1 atm pressure, is shown in Fig. (3). The incident e-beam current density,  $j_0$ , was 24 A/cm<sup>2</sup>. The top two traces show diode voltage,  $V_D$ , and current  $i_D$ , while the inferred e-beam current into the switch,  $i_0$ , is in the bottom section of the figure. The difference in decay time between  $i_D$  and  $i_0$  is due to plasma formation in the diode and the energy dependent transmission of electrons through the mylar window. Plasma current through the switch,  $i_p = i_D - i_0$ , and voltage across it,  $V_d$ , are shown in the center two traces.  $\rho$  is plotted as a function of time in the bottom section. The fast fall, low minimum resistivity ( $\sim 30 \Omega\text{-cm}$ ) followed by a fast rise, result in good switching performance.

The quantities  $\rho_0$ ,  $\tau_f^*$  and  $c$  are plotted as a function of percent  $O_2$  in  $N_2$  in Fig. (4) for  $j_0$  in the range 2.5-6.7 A/cm<sup>2</sup>. Shown also for reference are the beam rise and fall times,  $\tau_R$  and  $\tau_F$ . The gas pressure was 1 atm. The results indicate that  $O_2$  concentrations of 10-20% yield resistivities of 200-300  $\Omega\text{-cm}$ , a current gain over 10, and  $\tau_f^*$  about equal to that of the e-beam.  $E/P$ , where  $E$  is the applied electric field and  $P$  is ambient gas pressure, was 10.5 V/cm-Torr in this case. No late-time electrical breakdown was observed.

The scaling of  $\rho_0$  and  $c$  with electron beam current density is illustrated in Fig (5). A  $\rho_0$  as small as 20  $\Omega\text{-cm}$  is observed, but at the sacrifice

of current gain. These plots are the result of varying  $j_0$  over a wide range, using the same 20%  $O_2$  - 80%  $N_2$  mixture discussed earlier. The data in Fig. (5), demonstrate that  $j_0$  must be below 10A/cm<sup>2</sup> to approach  $c = 10$  for this gas mixture at  $P = 1$  atm.

Fig. (6) illustrates the effect on the net current in the discharge when the pressure is increased from 1 atm to 3 atm for a 20%  $O_2$  concentration in  $N_2$ , and  $E/P = 10.5$  V/cm-Torr.

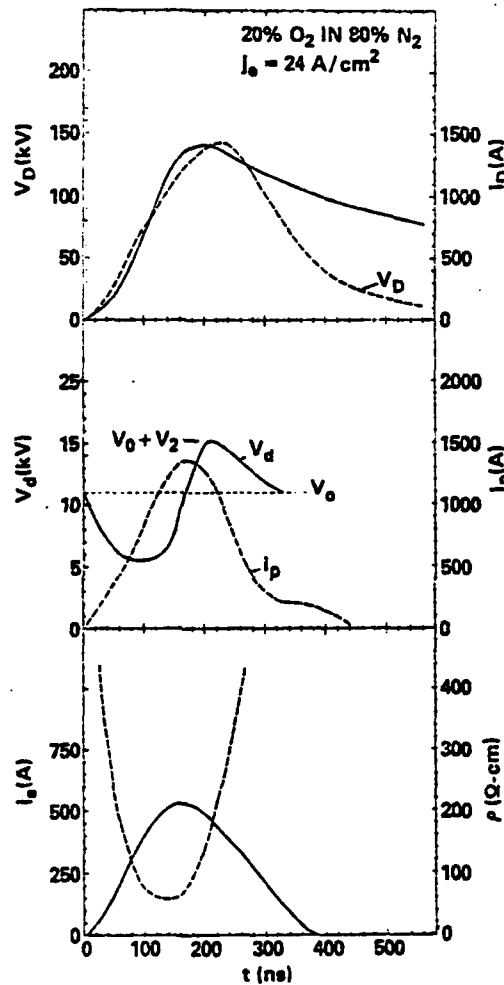


Figure 3. An example of measurements made on a single shot.

The input e-beam current was the same in both cases.

An illustration of how  $\rho_0$  changes with pressure is shown in Fig. (7) where  $\rho_0$  is plotted against P with constant E/P = 10.5 V/cm-Torr and  $j_0 = 5.0 \pm 0.3$  A/cm<sup>2</sup>. The data show that for O<sub>2</sub> concentrations up to 20%,  $\rho_0$  changes little with pressure. This is most likely because the duration

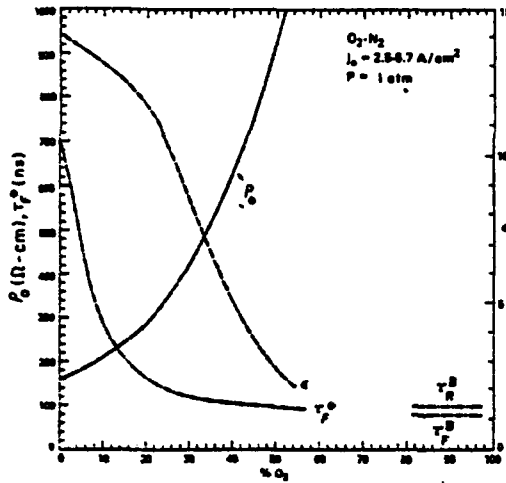


Figure 4. Dependence of  $\rho_0$ ,  $\tau_p$ , and  $c$  for various percentages of O<sub>2</sub>-N<sub>2</sub>.

of the e-beam pulse is too short for the discharge to reach equilibrium at the lower percentages of the attaching gas, as explained in what follows.

$\rho_0$  changes substantially with P for higher concentrations. In Fig. (8)  $\tau_p$  is plotted versus P for O<sub>2</sub> concentrations of 10, 20, and 50% in N<sub>2</sub>. E/P was 10.5 V/cm-Torr;  $j_0$  was  $5.0 \pm 0.3$  A/cm<sup>2</sup>.

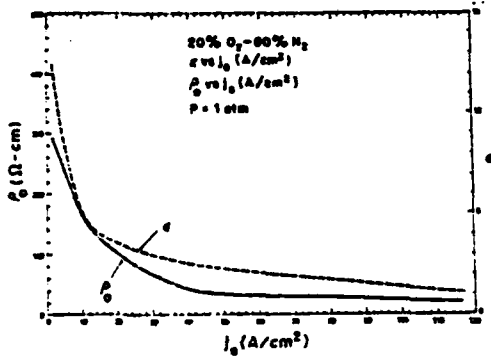


Figure 5. Illustration of change in resistivity,  $\rho_0$ , and current gain,  $c$ , as a function of beam current density,  $j_0$ .

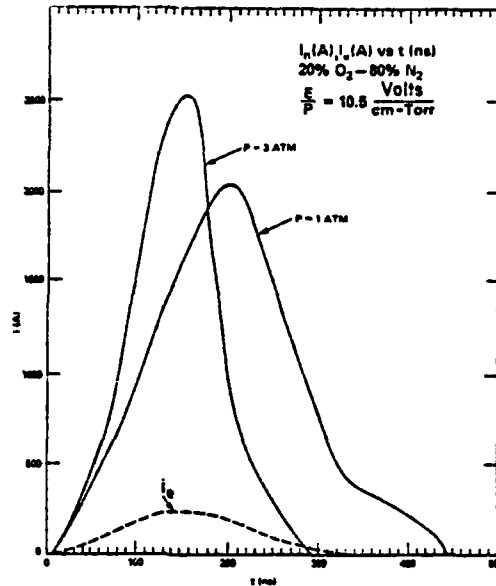


Figure 6. Effect of ambient gas pressure on switch current time history.

We illustrate the dependence of current gain on pressure with the data presented in Fig. (9) for 5% O<sub>2</sub> in N<sub>2</sub>. E/P was 10.5 V/cm-Torr and  $j_0$  was  $5.0 \pm 0.3$  A/cm<sup>2</sup> as before.  $c$  increases from 7.6 to 11.8 when pressure is increased from 1 to 3 atm.

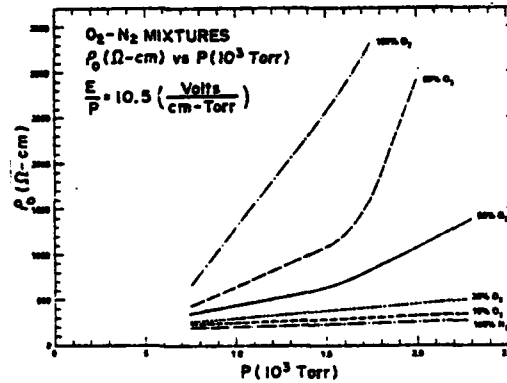


Figure 7. Effect of ambient switch pressure on  $\rho_0$ .

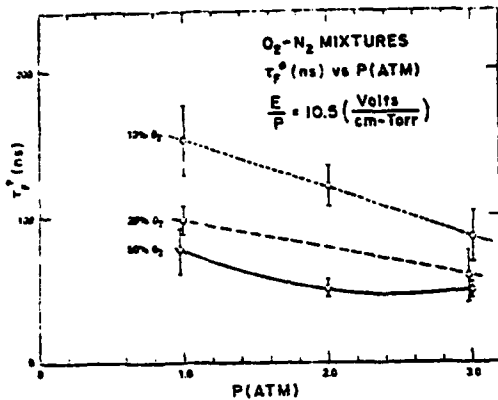


Figure 8. Effect of ambient switch pressure on  $\tau_f$ .

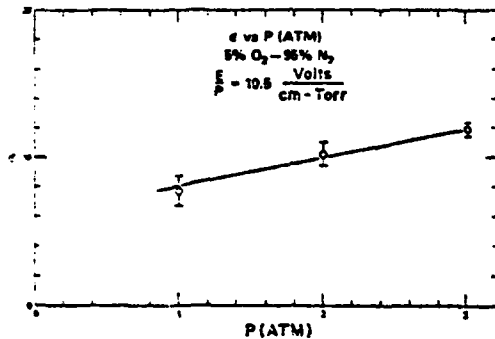


Figure 9. Effect of ambient switch pressure on current gain.

As Figs. (4)-(9) indicate, trade-offs exist between obtaining low resistivity  $\rho_0$ , short fall times,  $\tau_f$ , and high current gains,  $c$ . These trade-offs can be understood by expressing the continuity equation for the discharge plasma electron density,  $n_p$ , as

$$\frac{dn_p}{dt} = S j_0 P - n_p \tau_f^{-1} \quad (4)$$

where the beam ionization parameter  $S$  depends on the e-beam energy and gas composition and where

$\tau_f^{-1}$  characterizes the discharge plasma electron loss rate. The switch resistivity is given by

$$\rho = (en_p \mu)^{-1} \quad (5)$$

where  $\mu$  is the electron mobility. Minimum resistivity,  $\rho_{min}$ , is attained when the left-hand side of Eq. (4) goes to zero. This yields upon substitution in Eq. (5)

$$\rho_{min} \tau_f = (e S j_0 \mu p)^{-1} = \frac{f(E/P)}{j_0} \quad (6)$$

where the product  $(\mu p)$  is a function of gas composition and the field parameter  $E/P$ . Expressing the switch plasma current density as

$$j_p = E/\rho_{min} \quad (7)$$

leads to

$$c p_{min} = \frac{P}{j_0} f(E/P) \quad (8)$$

and

$$\frac{c}{\tau_f} = P \frac{E/P}{f(E/P)} \quad (9)$$

where switch current gain  $c = j_p/j_0$ . Breakdown limitations constrain the field parameter to  $E/P \leq 10$  V/cm-Torr.

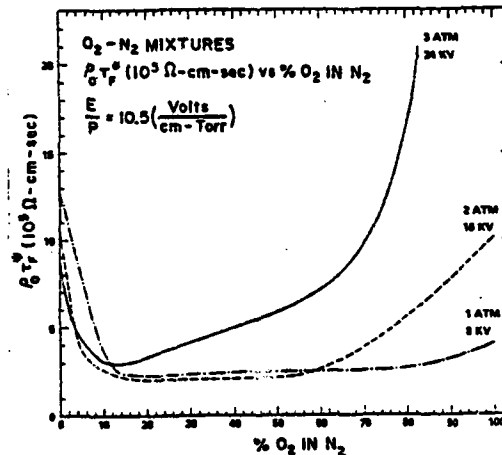


Figure 10. Effect of varying percent  $O_2$  in  $N_2$  and gas pressure on the product  $(\rho_0 \tau_f)$ .

AD-A143 233

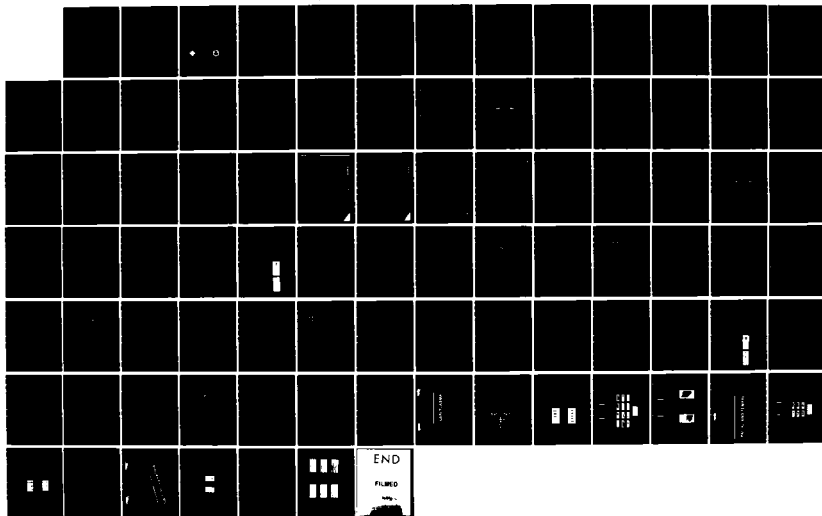
PLASMA SWITCH DEVELOPMENT(U) JAYCOR ALEXANDRIA VA  
R J COMMISSO 08 JUN 84 JAYCOR-J206-84-000/6220  
N00014-82-C-2114

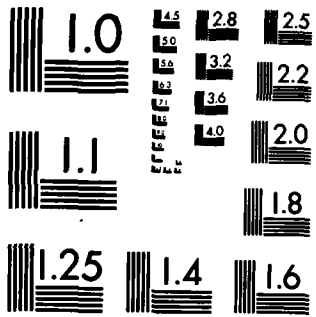
2/2

UNCLASSIFIED

F/G 20/7

NL





MICROCOPY RESOLUTION TEST CHART  
NATIONAL BUREAU OF STANDARDS-1963-A

Eqs. (6), (8), and (9) describe the qualitative behavior of e-beam controlled switches. These scaling relationships are valid, however, only if the e-beam pulse persists for a time longer than  $\tau_p$  and shuts off in a time shorter than  $\tau_p$ . The impact of this restriction can be seen by contrasting Eq. (6) with Fig. (10), in which the product  $\rho_0 \tau_p$  is plotted for three different gas pressures as a function of  $O_2$  concentration. Since electron mobility in  $N_2$  and  $O_2$  is similar, Eq. (6) predicts that  $\rho_{min} \tau_p$  is nearly constant independent of gas pressure,  $P$ , or  $O_2$  concentration. At low concentrations of the attaching gas  $O_2$ ,  $\tau_p$  becomes long compared with the beam duration, and hence  $\rho_0$  never reaches  $\rho_{min}$ . Similarly, at high concentrations and/or high pressures,  $\tau_p$  becomes smaller than the beam fall time; as a result the estimated switch fall time,  $\tau_p^*$ , approaches the beam fall time rather than  $\tau_p$ . This effect is also seen in the data in Fig. (4), where  $\tau_p^*$  approaches  $\tau_p^B$  at high  $O_2$  concentrations.

#### Late-Time Breakdown

One possible failure mode for the e-beam switch when operated repetitively is breakdown involving a self-sustaining arc from which the switch could not recover. We observe that in some cases breakdowns do occur late in time, well after the e-beam has been turned off. This phenomena is described with the aid of Figs. (11) and (12).

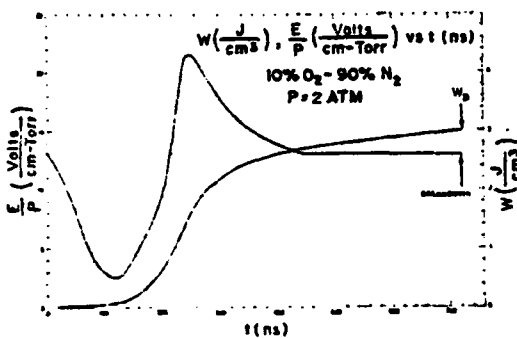


Figure 11. Plot of  $E/P$  and energy absorbed by the switch gas, as a function of time.

In one curve of Fig. (11) the parameter  $E/P$  is plotted versus time, beginning with the ambient  $E/P = 13$  V/cm-Torr.  $E/P$  decreases, during the rise of current in the switch, to a minimum of 2.5 V/cm-Torr. It then reverses, crosses the ambient line and peaks at 21.5 V/cm-Torr, before declining to the ambient of 13 V/cm-Torr at 440 ns. At a much later time, 720 ns, the switch breaks down discharging the system. The second curve is a plot of resistive energy deposited in the switch per unit volume,  $W$ . At the time of breakdown,  $W$  attains a value of  $W_B$ . The occurrence of breakdown at late times, i.e., long after  $E/P$  peaks, suggests that breakdown is influenced more by deposited energy than transient  $E/P$ .

This effect is seen in Fig. 12 in which a plot of  $W_B$  as a function of  $P$  for  $E/P = 11$  V/cm-Torr is shown for air and for a mixture of 10%  $O_2$  in  $N_2$ .

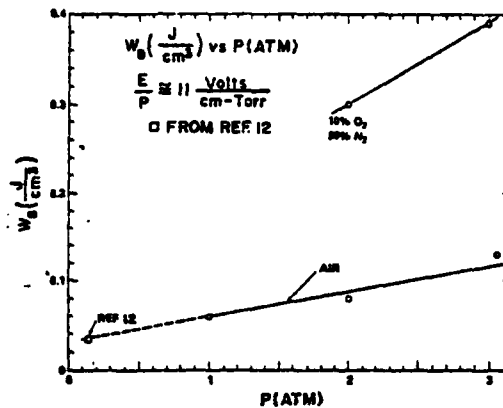


Figure 12. Breakdown energy per unit volume for 10%  $O_2$  in  $N_2$  and air.

Shown also on the curve is one point from Ref. 12 obtained in an experiment where  $P = 0.13$  atm. This point lies on a straight line extension of our data. The exact mechanisms responsible for late time breakdown will require further study.

#### Double-Pulse Experiments

Some of the problems associated with repetitive

DIGEST OF TECHNICAL PAPERS

4th IEEE Pulsed Power Conference

The Regent  
Albuquerque, New Mexico  
June 6-8, 1983



Editors



T.H. Martin  
Sandia National Laboratories  
Conference Chairman

M.F. Rose  
Naval Surface Weapons Center  
Chairman, Technical Program Committee

Conference Sponsors

IEEE Nuclear and Plasma Sciences Society  
IEEE Region 6  
IEEE Albuquerque Section  
Air Force Aero-Propulsion Laboratory  
Air Force Office of Scientific Research  
Army Research Office  
Defense Advanced Research Project Agency  
Department of Energy Office of Inertial Fusion  
Defense Nuclear Agency  
U.S. Army Electronics Research and Development Command  
Naval Sea Systems Command  
Naval Surface Weapons Center

The views and conclusions contained in this document are those of the authors and should not be interpreted as necessarily representing the official policies or endorsements, either expressed or implied, of the IEEE Nuclear and Plasma Sciences Society, IEEE Region 6, IEEE Albuquerque Section, Air Force Aero-Propulsion Laboratory, Air Force Office of Scientific Research, Army Research Office, Defense Advanced Research Project Agency, Department of Energy Office of Inertial Fusion, Defense Nuclear Agency, U.S. Army Electronics Research and Development Command, Naval Sea Systems Command, Naval Surface Weapons Center, or the U.S. Government. Abstracting is permitted with credit to the source. Libraries are permitted to photocopy articles in this volume beyond the limits of U.S. copyright law without fee if for private, noncommercial use of patrons. Instructors are permitted to photocopy isolated articles for noncommercial classroom use without fee. For other copying, reprinting, or republication permission, write to Director, Publishing Services, IEEE, 345 East 47th Street, New York, NY 10017. All rights reserved. Copyright © 1983 by The Institute of Electrical and Electronics Engineers, Inc.

Library of Congress Catalog Number 83-80951  
IEEE Catalog Number 83CH1908-3



## APPLICATION OF ELECTRON-BEAM CONTROLLED DIFFUSE DISCHARGES TO FAST SWITCHING\*

R.J. Comisso<sup>a</sup>, R.F. Fernsler<sup>a</sup>, V.E. Scherrer, and I.M. Vitkovitsky

Naval Research Laboratory  
Washington, DC 20375

### Summary

Recent investigations into the phenomena associated with electron-beam controlled diffuse discharges indicate a potential application for repetitive ( $> 10$  kHz, in a "burst" mode), high power ( $\sim 10^{10}$  W) switching. In such discharges the conductivity of the gas is regulated by the competition between beam ionization and attachment and recombination processes in the gas. Short opening times, limited in practice to the decay time of the electron beam, can be realized while high voltage is being applied to the switch. We report on one series of experiments using a  $N_2-O_2$  combination in which the time dependence of the discharge current at two pressures has been determined. The results are compared to a zero-dimensional numerical simulation where the gas chemistry is coupled to the discharge circuit. Experiments exploring the advantages of gases with different collision cross sections and the behavior of the overall discharge stability have also been performed. A formalism for switch design in which the switch gas mixture and pressure, switch area and length are estimated self-consistently for a given system efficiency is reviewed. The formalism is used to design a single pulse, 200 kV, 30 kA (6  $\Omega$ ), 100 ns FWHM inductive storage generator.

### Introduction

The successful implementation of inductive energy storage and its inherent benefits to pulse power applications<sup>1,2</sup> depends critically on the development of opening switches. These switches must be capable of conducting current during the charging period of an inductor and then become sufficiently resistive to divert the current flowing in the inductor to a load. The current commutation must occur on a time scale which is short compared to the inductor charging time and in the presence of an electric field across the switch that increases during the commutation process. Some applications require the switch to be capable of repetitively pulsed operation (see, for example, Ref. 3). Such a repetitively pulsed opening switch automatically satisfies the conditions required for operation as a repetitively pulsed closing switch.

Several authors<sup>4-7</sup> have reported on experiments and theoretical investigations in which an electron beam (e-beam) is used as an ionizing agent to sustain a diffuse (volumetric) discharge in a gas placed between two electrodes. The concept, as it might be used in a switching application, is illustrated in Fig. 1. In this scheme the gas resistivity at any time is determined by a competition between ionization provided by the beam and the various recombination and attaching processes characteristic of the specific gas mixture, pressure, and applied electric field. This, along with the volume discharge property, allows the gas to return to its original non-conducting state very quickly

once the source of ionization is removed. An arc discharge is avoided by proper switch design.<sup>8</sup> The switch length, pressure and area are maintained in such a way that self-sparking is avoided.

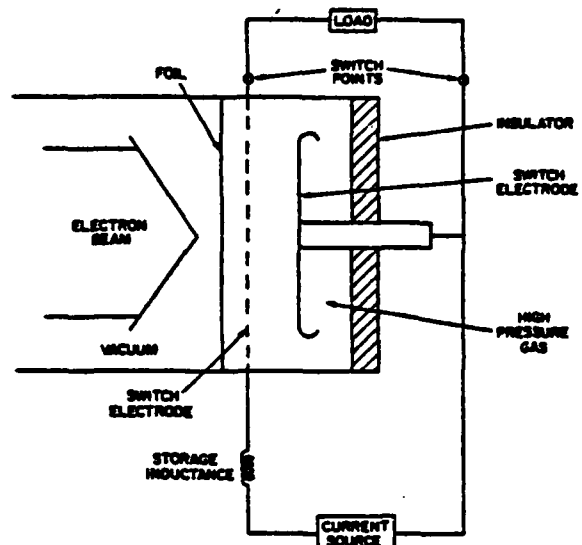


Fig. 1. Illustration of opening switch application for an e-beam controlled diffuse discharge.

In this paper we present some theoretical analyses and data from an e-beam controlled diffuse discharge experiment that are relevant to understanding the physics associated with the behavior and optimization of an e-beam controlled switch (EBCS). Included in this are general equilibrium scaling laws, the consequence of using gases which exhibit unusual collision cross section behavior, and stability of the discharge. Because of the reliability and accessibility of various cross section data, most of the experiments were performed with mixtures of  $O_2$  and  $N_2$ . Also reviewed is a design formalism<sup>8</sup> that self-consistently estimates the switch gas mixture, pressure, area, length and e-beam generator characteristics for a given system energy transfer efficiency, output pulse and number of pulses. Using this formalism we outline a design for an inductive storage system capable of delivering a single  $\sim 200$  kV,  $\sim 100$  ns full width at half maximum (FWHM),  $\sim 30$  kA pulse into a  $\sim 6 \Omega$  load.

### Description of Experiment

A schematic of the experimental apparatus is shown in Fig. 2. An inductively driven e-beam diode system, in which two exploding wire fuses are used in sequence as opening switches to

produce a high voltage pulse across the diode, provides the e-beam for the switch experiments. This system has been described in detail elsewhere. Generation of a second e-beam pulse can be accomplished by switching in a second set of fuses and switches (not shown in Fig. 2), which are similar to the set used in generating the first pulse. The 3-cm dia. cathode is constructed of saw blades. The anode plate is drilled with 0.5-cm dia. holes over an 8-cm dia. with a geometrical ratio of open area to total area of 0.68. At the typical charging voltages on  $C_0$  (240  $\mu\text{F}$ ) of  $\approx 9$  kV and with  $L_0 = 7$   $\mu\text{H}$ , pulses of  $\approx 180$  kV with  $\approx 200$  ns FWHM are produced. The beam current densities can be varied from 0.2 to 5 A/cm<sup>2</sup> by varying the anode-cathode separation. Because the e-beam pulse is so short, the discharge does not always have time to come to equilibrium. However, as long as the time histories of the beam current and voltage are known, investigations into how the basic physics of these discharges relate to EBCS applications and comparison to theory and numerical simulations can be carried out, as will be discussed in later sections.

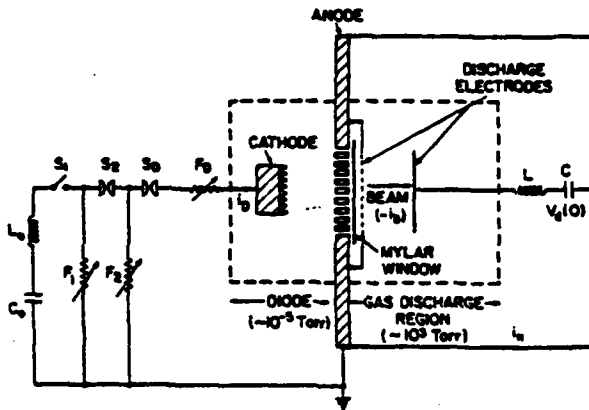


Fig. 2. Schematic of experimental apparatus.

Also schematically illustrated in Fig. 2 are the driving circuit and electrode structure for the gas discharge region. The current source driving the discharge in these experiments was a capacitor,  $C$  (1  $\mu\text{F}$ ), whose initial charging voltage  $V_d(0)$  could be varied from 0-30 kV. The system inductance was measured to be  $L = 430$  nH. The discharge electrode separation was 1 cm for all work discussed here. A copper screen of  $\approx 60\%$  measured current transmission was used as the ground electrode. The 50- $\mu\text{m}$  mylar window maintained a pressure differential between the discharge vessel and the evacuated ( $\approx 10^{-3}$  torr) e-beam diode region while allowing the high energy portion of the e-beam to enter the discharge chamber. The apparatus has been operated at pressures of 1-7 atm. A Rogowski loop, located between the screen electrode and mylar window, was used to measure  $i_b$ , the e-beam current flowing into the discharge region. Additional diagnostics for this experiment include a voltage divider to measure the voltage across the diode,  $V_D$ ; Rogowski loops to measure the diode current,  $i_D$ ; and a commercial current monitor located at the driving capacitor to measure the net current in the discharge circuit,  $i_p$ . Shown in Fig. 3 are representative time histories of  $V_D$ ,  $i_D$ ,  $i_b$  and  $i_p$

where  $i_p$  is the discharge plasma current, for a 20%  $\text{O}_2$  - 80%  $\text{N}_2$  mixture with a ratio of applied electric field to gas pressure of 10.5 V/cm-torr. Because the polarity of the discharge was such as to accelerate plasma and e-beam electrons in the same direction,  $i_p$  is related to  $i_n$  and  $i_b$  by

$$i_p = i_n - i_b \quad (1)$$

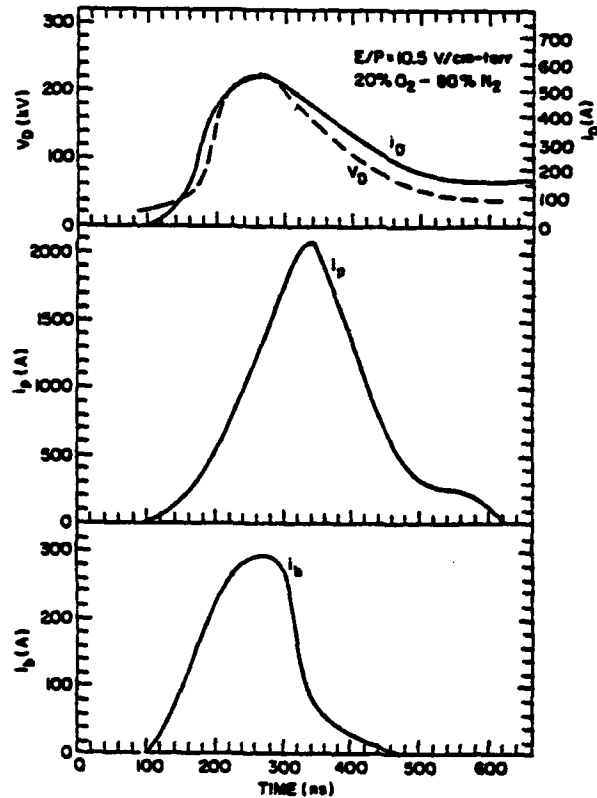


Fig. 3. Representative time histories of discharge parameters obtained from standard diagnostics.

The circuit equation for the discharge is

$$V_d(0) = R(i_n - i_b) + L \frac{di}{dt} + \frac{1}{C} \int_0^t i_n dt \quad (2)$$

where  $R$  is the discharge resistance. The discharge resistivity,  $\rho$ , is related to  $R$  through the discharge geometry only. Neglecting the last term in Eq. (2) ( $< 5$ -percent correction) we have at the time of peak  $i_n$  a discharge resistivity of

$$\rho_C = \frac{V_d(0)}{(i_n - i_b)} \left( \frac{\text{A}}{\text{I}} \right) \quad (3)$$

where  $A$  is the discharge area and  $z$  the discharge electrode separation.

The resistivity of the discharge during conduction is one important characteristic. Another important parameter is the current gain,  $\epsilon$ , defined as

$$\epsilon = \frac{i_n - i_b}{i_b} = \frac{i_p^0}{i_b^0} \quad (4)$$

where  $i_p^0$  and  $i_b^0$  are the peak values of  $i_p$  and  $i_b$  respectively. For a high energy transfer efficiency,  $\epsilon \gg 1$ . The current gain for the data in Fig. 3 is  $\epsilon = 7$ .

#### Theoretical Model

Various aspects of the theoretical concepts associated with controlled diffuse discharges as they relate to the EBCS have been discussed. In this section we give a cursory review of the physical model for the discharge. We describe a system in which a volumetric ionization source produces a very weakly ionized gas. Typically,  $n_p \sim 10^{-5} N_0$ , where  $n_p$  is the plasma electron density associated with the ionizing e-beam and  $N_0$  is the initial gas density. We assume electrode effects are not important, which is the case for applied voltages much greater than the sheath potential ( $< 1$  kV). Under these conditions the gas resistivity is determined by electron-neutral collisions, and the discharge potential is a linear function of the distance from the discharge electrodes.

We assume a two component gas mixture made up of a non-attaching base gas with some fraction of attaching gas. Because an attachment dominated recovery is desirable for EBCS applications, we will ignore recombination. Assuming further that density gradients are negligible, the continuity equation for  $n_p$  gives

$$\frac{dn_p}{dt} \approx S_0 J_b P - \alpha N_0 n_p \quad (5)$$

Here  $S_0$  is a beam ionization parameter,<sup>8</sup>  $J_b$  ( $\approx i_b/A$ ) is the e-beam current density,  $\alpha$  is the effective attachment rate coefficient ( $\text{cm}^3\text{-s}^{-1}$ ),  $P$  is the total gas pressure and  $N_0$  is the density of the attaching gas. The first term on the right hand side of Eq. (5) represents the source of discharge plasma electrons. The mechanism for discharge plasma electron loss is represented by the second term on the right hand side of Eq. (5).

The discharge plasma density is related to the discharge plasma current density through

$$J_p \approx i_p/A = n_p e v \quad (6)$$

where  $v$  is the electron drift speed,

$$v = \mu E \quad (7)$$

Here  $\mu$  is the electron mobility<sup>10</sup> and  $E$  is the electric field across the discharge. Thus the discharge resistivity during conduction is given by

$$\rho_c = \frac{E_c}{J_p} = (en_p \mu)^{-1} \quad (8)$$

where  $E_c$  is the electric field across the discharge during conduction.

We simulate the experiment by numerically solving a coupled set of rate equations, one for each ionic species, along with Eqs. (2) and (5). In this way  $n_p$  can be self-consistently obtained as a function of time for a given  $J_b$  and beam energy. It in turn may be used with Eq. (2) in Eqs. (6) and (8) to predict macroscopic observables in the experiment. An air-chemistry code, CHPAIR,<sup>11</sup> is used in solving Eq. (5). This allows many more atomic and molecular processes than those outlined here to be included. Comparisons between measured and calculated parameters will be discussed in the next section.

We replace the last term in Eq. (5) with a phenomenological expression,  $n_p/\tau$ , where  $\tau$  is the characteristic loss time for the discharge plasma electrons in the absence of ionization. Substituting  $n_p$  from Eq. (8) into Eq. (5), and noting that in equilibrium  $dn_p/dt = 0$ , Eq. (5) becomes

$$\frac{E_c}{\tau} = \left(\frac{E_c}{P}\right) f_0 P \quad (9)$$

where  $f_0 \approx e S_0 \mu P$  is essentially a constant for a given gas composition. For most gases  $f_0 \sim 10^7 - 10^8$  cm/V-s. Also,  $E_c/P$  will be approximately independent of pressure (see Sect. V). This analytic equilibrium scaling law has particular relevance for fast EBCS applications. In these applications one desires  $\epsilon$  to be large and  $\tau$  to be short. For a given gas composition, Eq. (9) indicates there is a "trade-off" between high  $\epsilon$  and small  $\tau$ , while suggesting that operation at high pressure and mobility is favorable.

#### Overview of E-Beam Controlled Discharge Results

In this section we review several aspects of the experimental results and theoretical analyses that are particularly relevant to the design of an EBCS.

Figure 4 shows a comparison of the measured and predicted net discharge current  $i$  as a function of time at pressures of 1 and 3 atm for a 20% O<sub>2</sub> - 80% N<sub>2</sub> mixture. The code uses the measured  $i_b$  and diode voltage,  $V_D$ , to predict the circuit behavior. The measured e-beam current was modified so that only those beam electrons with sufficient energy to traverse the switch were used in the calculations. Because the code is zero-dimensional, it can not accurately predict what happens when beam electrons do not traverse the entire switch length as a result of either insufficient initial directed energy or excess transverse energy. This effect is particularly evident in the 3 atm case. To improve this comparison the e-beam electron energy must be increased. In making this comparison the screen electrode transmission of 60% and the time response of the Rogowski loop measuring  $i_b$  were taken into account. The code result was also

shifted 5-10 ns in time. The uncertainties in the code and measurement are estimated to be = 15% each. As can be seen from Fig. 4, the code accurately tracks the measured net current to within these uncertainties and the limits of the model. By using the results presented in Fig. 4, the scaling relation Eq. (9) can be checked. The values of  $\tau$  obtained from the code are = 50 ns and = 20 ns for 1 and 3 atm respectively. Thus the ratio of  $(\epsilon/\tau)$  at 3 atm to  $(\epsilon/\tau)$  at 1 atm is = 4, compared to 3 from Eq. (9). The difference can be ascribed to the lack of equilibrium in the 1 atm. case.

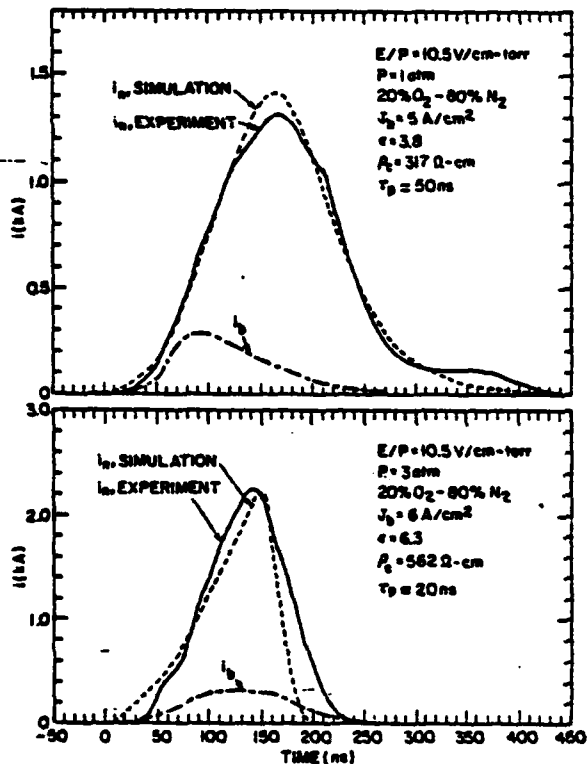


Fig. 4. Comparison of measured and calculated net discharge current for 1 and 3 atm.

The switch performance can be optimized by choosing a gas or gas combination that exhibits a mobility and attachment rate which strongly vary with the time dependent electric field across the switch.<sup>4,7,8,12</sup> An example of such optimization is illustrated in Fig. 5 where  $\rho_c$  for a 10% O<sub>2</sub> - 90% N<sub>2</sub> and 10% O<sub>2</sub> - 90% Ar mixture is plotted for 1 atm as a function of initial applied voltage across the discharge,  $V_d(0)$ . This is also the voltage across the discharge when  $\rho_c$  is evaluated (Eq. (3)). In an actual application we desire  $\rho_c$  to be low during conduction, i.e., when  $V_d$  is low and increase during opening, when  $V_d$  becomes larger. We see that the Ar-O<sub>2</sub> mixture shows markedly different behavior from the N<sub>2</sub>-O<sub>2</sub> mixture at different applied voltages. At low voltages ( $V_d(0) > 1$  kV, for  $V_d(0) < 1$  kV sheath effects dominate) the resistivity is 2 to 3 times lower for Ar-O<sub>2</sub> than N<sub>2</sub>-O<sub>2</sub>. As the voltage increases,

the opposite effect occurs with the resistivity for Ar-O<sub>2</sub> about 5 times higher than that for N<sub>2</sub>-O<sub>2</sub>.

A thorough analysis of this observation requires knowledge of the electron energy distribution, which we do not have at present. We

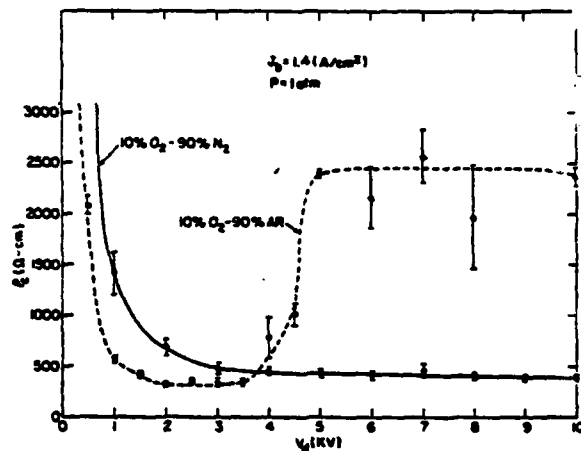


Fig. 5. Comparison of discharge resistivity,  $\rho_c$ , for Ar-O<sub>2</sub> and N<sub>2</sub>-O<sub>2</sub> mixtures as a function of initial voltage across discharge at 1 atm.

estimate<sup>13</sup> for the Ar case that the electrons have a mean energy ranging from 1-5 eV for the applied voltages in Fig. 5. This energy will be considerably lower in the N<sub>2</sub> case because of the accessibility of vibrational levels in N<sub>2</sub>. At the pressure indicated (1 atm), two body dissociative attachment will dominate three body attachment for electron energies of ~ 5 eV. Also the Ramsauer-Townsend<sup>14</sup> cross section for Ar is rapidly varying for electron energies between 0.5-5 eV. Thus the observed effect must be related to the higher mean electron energies in the Ar case, resulting in rapidly varying cross sections for momentum transfer and attachment. Control of the electron energy distribution is therefore desirable in switch applications, as has been emphasized by Christophorou and co-workers.<sup>14</sup>

Discharge stability is of concern in either the repetitive or single pulse mode. The discharge stability can be affected by several processes. Changes in electrical and chemical properties of the switch gas, can result from heating of the gas, or as a cumulative result of the length of the conduction period or duty cycle. It may be possible to avoid some of these potential problems with the proper gas mixture.<sup>15</sup> Any reduction of E/N, where N is the gas density, either local or global at any time can trigger avalanche ionization. For example, an attachment instability<sup>16-18</sup> has been suggested as a cause of local increase in  $\rho_c$ , which when accompanied by local heating and a consequent decrease in N during the conduction phase of an e-beam sustained discharge can result in a breakdown. Decreases in N resulting from heating at inhomogeneities in the discharge or at electrodes<sup>18,19</sup> has also been observed to cause breakdown.

Under certain conditions in our experiment a breakdown is observed sometime after the e-beam

controlled discharge plasma current has stopped flowing. This effect is illustrated in Fig. 6, where the time to breakdown,  $\tau_b$ , (measured from the initiation of  $i_p$ ), is plotted as function of the peak discharge plasma current,  $i_p^0$ . This data was taken with a 10%-90%  $N_2$  mixture at 1 atm. In order to observe this effect, the applied voltage must be 80-90% of the self break voltage. As seen in the figure,  $\tau_b$  increases rapidly as  $i_p^0$  (and the energy dissipated in the gas) is decreased. The measured times are of the order of acoustic transit times. This effect is not observed if the applied voltage is  $< 75\%$  of the breakdown voltage, and is being studied further at present.

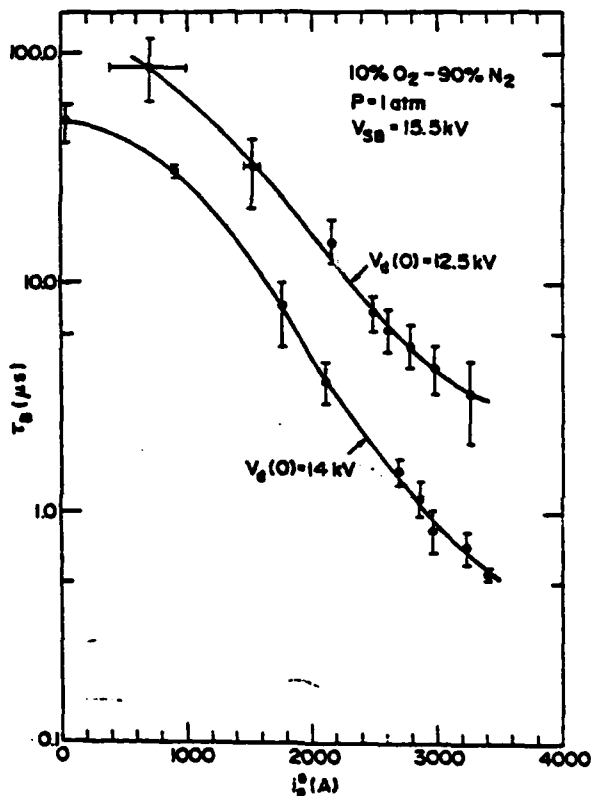


Fig. 6. Plot of time to breakdown, measured from the initiation of e-beam controlled discharge plasma current, as a function of peak e-beam controlled discharge plasma current,  $i_p^0$ .

#### Switch Design Formalism

The design of any EBCS must address two major concerns: (1) a required overall system efficiency must be satisfied; and (2) the self-sparking threshold must never be exceeded, so the switch gas can recover to its original dielectric strength. In this section we review a self-consistent procedure that can be used to estimate the switch gas composition, pressure, area, length, and e-beam generator characteristics for a given application. For details of this work, the reader should consult Ref. 8. This design formalism emphasizes the overall energy transfer efficiency of the switch-inductive store system, the circuit requirements, and the switch

physics. In what follows we assume the load pulse characteristics (current, voltage, FWHM) are specified a priori.

We begin by defining the energy transfer efficiency,  $\eta$ , as

$$\eta = \frac{n I_L^0 V_L^0 \tau_L}{(1/2) L I_{SW}^0{}^2 + n I_b V_b \tau_C} \quad (10)$$

Here  $n$  is the number of pulses,  $I_L^0$  and  $V_L^0$  are the (single pulse) peak current and voltage delivered to the load,  $I_b$  and  $V_b$  are the (single pulse) e-beam current and voltage,  $L$  is the storage inductance,  $I_{SW}^0$  is the peak switch current,  $\tau_L$  is the characteristic load pulse width, and  $\tau_C$  is the time interval during which the switch is conducting.

To elucidate better the energy loss terms, we rewrite Eq. (10) as  $\eta = \epsilon / (\epsilon + 1)$ , where  $\epsilon$ , the gain factor, is the ratio of the energy delivered to the load to the total energy used in making the switch conduct. Thus

$$\epsilon = \frac{I_L^0 V_L^0 \tau_L}{[k_0 I_L^0 V_L^0 \tau_0 + I_{SW}^0{}^2 R_{SW} \tau_C + I_b V_b \tau_C]} \quad (11)$$

where  $R_{SW}$  is the average switch resistance during conduction,  $I_{SW}$  is the average switch current during conduction, and  $\tau_0$  is the time interval during which the switch changes from conducting to nonconducting. The factor  $k_0$  is a dimensionless constant that when multiplied by the peak power delivered to the load gives the average power dissipated in the switch during the opening phase. For resistive or inductive loads  $k_0 = 0.25$ .

For reasonable energy efficiency ( $\eta > 0.5$ ) we require  $\epsilon > 1$ . Therefore, each term in the denominator of Eq. (11) must be sufficiently less than the numerator. Thus we set

$$k_0 I_L^0 V_L^0 \tau_0 = g_0 I_L^0 V_L^0 \tau_L \quad (12a)$$

$$I_{SW}^0{}^2 R_{SW} \tau_C = g_C I_L^0 V_L^0 \tau_L \quad (12b)$$

$$I_b V_b \tau_C = g_b I_L^0 V_L^0 \tau_L \quad (12c)$$

where  $g_0, g_C, g_b < 1$ , such that

$$\epsilon^{-1} = g_0 + g_C + g_b < 1 \quad (13)$$

The gas breakdown problem is avoided initially by satisfying the constraint

$$V_L^0 = s_B \frac{E_B}{P} (P_2) \quad (14)$$

Here  $V_L^0$  is the maximum expected voltage across the switch (i.e., the peak load voltage),  $E_B$  is the static breakdown electric field at atmospheric pressure  $P$ ,  $s_B < 1$  is a dimensionless safety factor, and  $P$  is the switch pressure. Additionally, cumulative heating of the gas must be sufficiently constrained so that any reduction

in switch gas density does not significantly lower the self-sparking threshold. Energy is deposited in the switch primarily by resistive heating during the conduction phase, by resistive heating during the opening phase, and by direct deposition by the e-beam. Thus, a second constraint to avoid breakdown is a

$$n [k_0 I_L^0 V_L^0 \tau_0 + I_{SW}^2 R_{SW} \tau_c + k_b I_b V_b \tau_c] = s_H \left( \frac{W_B}{P_0} \right) A(P_0) \quad (15)$$

Here  $k_b$  is the fraction of the beam energy deposited in the switch gas,  $s_H$  is a dimensionless safety factor, and  $W_B$  is the deposited energy per unit volume required for breakdown at atmospheric pressure.

We may now proceed to compute the switch pressure. Using Eqs. (12a,b,c) and (14), the definition of  $\epsilon$ , scaling relation Eq. (9), and recalling that  $E_c = I_{SW} R_{SW} / \epsilon$  we have

$$P^{-1} = \frac{g_0 g_c g_b s_B^2 f_0}{k_0 k_p} \tau_L \frac{E_B}{P_0} \left( \frac{V_L^0}{V_b} \right) \left( \frac{\tau_c}{\tau_0} \right)^2 \quad (16)$$

The factor  $k_p \approx \tau_0 / \tau_c$  is the number of  $\tau_c$  periods necessary for the switch to interrupt the current when the beam current is zero. Using Eq. (5) with the ionization term set to zero, one can show that  $k_p \approx 5$  for an attachment dominated switch.<sup>1,8</sup> The fraction of attaching gas can be estimated from the calculated pressure, required efficiency, and known attachment rates. The "g" factors in Eq. (16) are chosen so that P can be small (for ease of switch construction) consistent with the constraint of Eq. (13). An optimum choice for  $g_0$ ,  $g_c$ , and  $g_b$  can be obtained by using the method of Lagrange undetermined multipliers. This removes the implied arbitrary nature of Eq. (13). The result is  $g_0 = g_c = g_b$ . For example if n is chosen to be 0.75, then  $\epsilon = 3$  and  $g = 0.1$ .

Once P is known, Eq. (14) gives the switch length,  $\epsilon$ , and Eq. (15) gives the switch area, A. The switch dimensions thus computed insure that the switch will be large enough that the breakdown threshold will not be reached.

The e-beam generator requirements are determined from  $V_b$ ,  $I_b$ , and A.  $I_b$  is computed from Eq. (12c). The e-beam generator must actually provide a somewhat higher current than  $I_b$  to account for current lost to the structure supporting the interface between vacuum and high pressure. The e-beam generator must also supply a beam of area A. Note that in order for the beam to traverse the switch length  $V_b$  will depend on the product  $P\epsilon$ , as does  $V_L$ . Therefore, one can show that typically  $V_b = V_L$ , with  $k_b = 0.3$ .

#### Single Pulse System

In this section we outline the design of a single pulse, high power ( $\sim 6 \times 10^9$  W), inductive storage system presently under construction. The circuit requirements are presented first. The design procedure outlined in the previous section is then used to determine the switch parameters.

Figure 7 is a circuit diagram of the proposed system. The desired load pulse parameters are

peak load current of  $I^0 = 30$  kA, peak load voltage of  $V_L^0 = 200$  kV, and load pulse width of  $\tau_L = 100$  ns. This choice of parameters is relevant to several pulse power applications.<sup>3,8</sup> For technological reasons dealing with the beam decay time, we take  $\tau_c = 100$  ns. We chose the storage inductance charging time to be  $\tau_c = 10 \tau_L$  or 1  $\mu$ s. Thus the quarter period of the charging circuit (the switch conduction time) is 1  $\mu$ s, giving for a (typical) 1  $\mu$ F capacitor, a system inductance of  $L = 0.65$   $\mu$ H.  $I_{SW}$ , the peak value of the switch current, is  $\approx I^0$ . This gives a charging voltage for the capacitor of  $V_{SW}^0 = 25$  kV. The voltage produced is then  $V_L \approx \epsilon (I^0 / \tau_0) = 200$  kV.

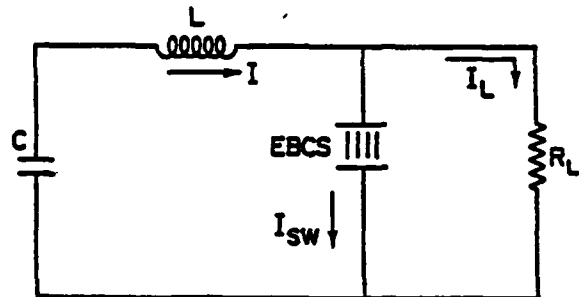


Fig. 7. Schematic of single pulse, inductive storage generator using an EBCS.

We choose an energy transfer efficiency of  $n = 0.5$ , assume the switch will be attachment dominated giving  $k_p = 6$ , take  $k_0 = 0.25$  for a resistive load,  $s_B = 0.75$ ,  $s_H = 0.5$ ,  $E_B = 20$  kV/cm, and  $W_B = 0.15$  J/cm<sup>3</sup>.<sup>8</sup> Then the results of the previous section can be used to obtain the following parameters:  $P = 12$  atm (Eq. (16)),  $\epsilon = 1$  cm (Eq. (14)), and  $A = 350$  cm<sup>2</sup>, radius = 10 cm (Eq. (15)). The current gain, from Eq. (12c) with  $g_0 = 0.3$ , is  $\epsilon = 30$ . This gives an e-beam current of  $I_b = 1$  kA. The beam decay time should be  $\ll \tau_0$ .

#### Conclusion

The results of this work indicate that the EBCS is a viable opening switch concept. Experiments with e-beam controlled discharges verify the conceptual understanding of the physics which govern the switch behavior. Discharge parameters may be optimized for switch application through proper choice of gas mixture and operating regime. Backed by this understanding an EBCS design procedure was outlined and a single pulse system was designed to demonstrate a high power ( $\sim 6 \times 10^9$  W) inductive store - opening switch system.

This work would not have been possible without the expert technical assistance of J.M. Cameron and H. Hall.

<sup>1</sup>Work supported by NSWC, Dahlgren, VA, and ONR, Arlington, VA.

<sup>2</sup>Jaycor, Inc., Alexandria, VA 22304.

### References

1. R.D. Ford, D. Jenkins, W.H. Lupton, and I.M. Vitkovitsky, *Rev. Sci. Inst.* **52**, 694 (1981).
2. S.A. Nesar and H.H. Woodson, *Proceedings of the Sixth Symposium on Engineering Problems of Fusion Research*, IEEE Pub. No. 75CH1097-5-NPS (1975), p. 316.
3. M.A. Barletta, Lawrence Livermore Laboratory Report UCRL-87288 (1981).
4. R.J. Comisso, R.F. Fernsler, V.E. Scherrer, and I.M. Vitkovitsky, *IEEE Trans. Plasma Sci.* **PS-10**, 241 (1982) and references therein.
5. L.E. Kline, *ibid.*, p. 224.
6. M.R. Hallada, P. Bietzinger, and W.F. Bailey, *ibid.*, p. 218.
7. R.F. Fernsler, D. Conte, and I.M. Vitkovitsky, *IEEE Trans. Plasma Sci.* **PS-8**, 176, (1980).
8. R.J. Comisso, R.F. Fernsler, V.E. Scherrer, and I.M. Vitkovitsky, Naval Research Laboratory Memo Report 4975 (1982). To be submitted to *Rev. Sci. Inst.*
9. B. Fell, R.J. Comisso, V.E. Scherrer, and I.M. Vitkovitsky, *J. Appl. Phys.* **53**, 2818 (1982).
10. S.C. Brown, *Basic Data of Plasma Physics* (MIT Press, Cambridge, 1967), pp. 87-94.
11. R.F. Fernsler, A.W. Ali, J.R. Grieg, and I.M. Vitkovitsky, Naval Research Laboratory Memo Report 4110 (1979).
12. L.G. Christophorou, S.R. Hunter, J.G. Carter and L.A. Mathis, *Appl. Phys. Lett.* **41**, 147 (1982).
13. J.W. Dzimianski and L.E. Kline, Final Technical Report No. 80-0120, Aero Propulsion Laboratory, Wright-Patterson AFB (1979).
14. J.B. Hasted, *Physics of Atomic Collisions* (American Elsevier, New York, 1972), pp. 306-310.
15. L. Christophorou, paper in this conference.
16. D.H. Douglas-Hamilton and Siva A. Mani, *Appl. Phys. Letter.* **23**, 503 (1973).
17. D.H. Douglas-Hamilton and S.A. Mani, *J. Appl. Phys.* **45**, 4406 (1974).
18. M.N. Andreeva, I.G. Perstantsev, V.D. Pis'mennyi, V.M. Polushkin, A.T. Rakhimov, M.A. Timofeev, and E.G. Treneva, *Sov. J. Plasma Phys.* **3** (6), 770 (1977).
19. S.A. Genkin, Yu. D. Korolev, V.G. Rabotkin, and A.P. Khuzeev, *Sov. J. Plasma Phys.* **7** (3), 327 (1981).

## STUDY OF GAS MIXTURES FOR E-BEAM CONTROLLED SWITCHES

V.E. Scherrer, R.J. Comisso, R.F. Fernsler,  
and I.M. Vitkovitsky

Naval Research Laboratory  
Washington, D.C. 20375

### ABSTRACT

An electron-beam sustained diffuse discharge has been suggested as a possible fast, high power, repetitive opening switch for compact pulsed power systems employing inductive storage. The dependence of gas resistivity at the time of maximum discharge current for an  $N_2-O_2$  mixture, an  $Ar-O_2$  mixture, pure  $CH_4$ , and  $CH_4$  with  $C_2F_6$  has been measured as a function of reduced electric field,  $E/N$ , at various pressures in such a discharge. Effects associated with  $E/N$  dependent mobility and attachment rate that are beneficial to switch applications have been observed.

### KEYWORDS

Diffuse discharge, opening switch, electron-beam controlled discharge, inductive storage.

### INTRODUCTION

There is presently much interest in the use of an electron-beam (e-beam) controlled diffuse discharge as a repetitive opening switch in an inductive storage pulsed power generator (Fernsler; 1980, Comisso, 1982; Hallada, 1982; Kline, 1982; Bletzinger, 1983; Comisso, 1983; Lowry, 1983; Comisso, 1984). The conductivity of this discharge is controlled by the competition between e-beam ionization and the various attachment and recombination processes characteristic of the gas or gas mixture. When the e-beam pulse is removed the gas may rapidly return to the normal, highly resistive state. This transition may be particularly rapid if attachment is the dominant loss process for discharge electrons (Fernsler, 1980; Comisso, 1982).

An important physics aspect of such an opening switch is the optimization of the gas mixture. Assuming that the electron mobility and attachment rates are independent of  $E/N$ , where  $E$  is the electric field across the switch and  $N$  is the gas density, one can show that the product of the opening time and the minimum discharge resistivity is a constant (Scherrer, 1982). The opening time is the time interval during which the discharge undergoes a change from low to high resistivity. This suggests that it may be difficult to realize a switch with both low resistivity during conduction and a short opening time. However, by choosing gas mixtures whose associated mobilities and attachment rates are strong functions of  $E/N$  it may be possible to satisfy these contradictory requirements, as has been suggested (Fernsler, 1980; Christophorou, 1982, 1983; Commisso, 1982, 1983, 1984). In this paper we compare the measured discharge resistivity during the conduction phase of several gas mixtures. The qualitative comparison of these data and of the discharge current waveforms demonstrates that indeed the gas mixture can be optimized to give a low resistivity at low  $E/N$  (conduction phase) with the resistivity increasing rapidly as  $E/N$  increases (opening phase).

#### DESCRIPTION OF EXPERIMENT

The apparatus has been described previously (Commisso, 1983). A schematic of the system is shown in Fig. 1. The system comprises three principal parts: a high voltage pulser (Fell, 1982), which uses fuses to produce a high voltage pulse; an e-beam diode, which provides the ionizing e-beam; and a gas cell test chamber, typically pressurized to 1-5 atm. At the typical charging voltage on  $C_0$  (240  $\mu$ F) of  $\approx 9$  kV and with  $L_0 = 7$   $\mu$ H, e-beam pulses of  $\approx 180$  kV with 200 ns FWHM are produced. The anode plate is drilled with 0.5-cm dia. holes over an 8-cm dia. with a geometrical ratio of open area to total area of 0.68.

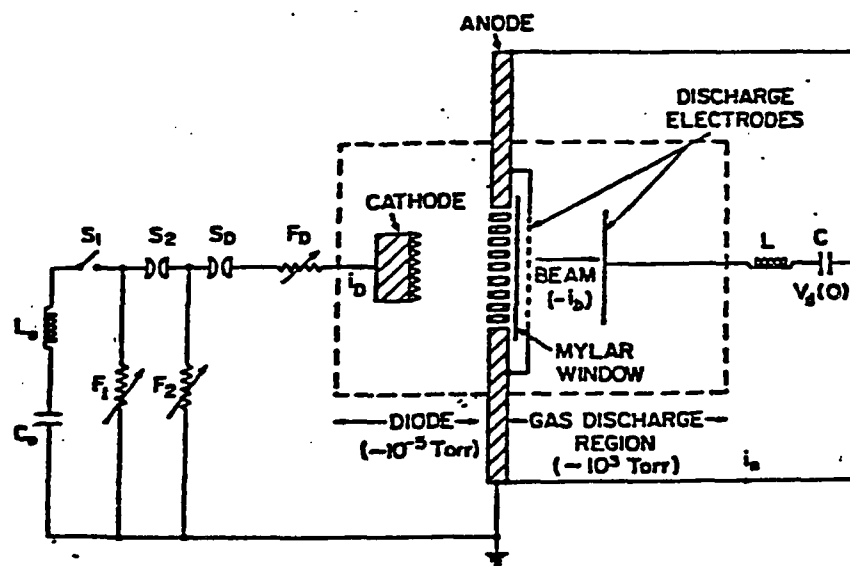


Fig. 1. Schematic of experimental apparatus.

The current source driving the discharge was a capacitor,  $C = 1 \mu\text{F}$ , charged at 0-30 kV. The discharge system inductance,  $L$ , was 430 nH. Unless otherwise stated, the discharge electrode separation was  $Z = 1 \text{ cm}$ . A 50- $\mu\text{m}$  mylar window maintained the pressure differential between the discharge vessel and the evacuated ( $\sim 10^{-4}$  torr) e-beam diode region while allowing the high energy portion of the e-beam to enter the discharge region.

### EXPERIMENTAL RESULTS

Figure 2 is a plot of the discharge resistivity,  $\rho_0$ , at peak discharge current as a function of  $E/N_0$ , where  $N_0$  is the ambient gas density and  $E \equiv V_d(0)/Z$  is the average electric field across the switch of electrode separation  $Z$  at the time of peak discharge current. The voltage across the switch at this time is simply the charge voltage of the ancillary capacitor,  $V_d(0)$  because the inductive correction to the discharge voltage may be neglected (Scherrer, 1982). For values of  $V_d(0) \lesssim 1 \text{ kV}$ ,  $E$  may be over estimated, as discussed later in the paper. The data shown are for 1:4 mixtures of  $\text{O}_2\text{-N}_2$  and  $\text{O}_2\text{-Ar}$  at ambient pressures of 1 and 5 atm. Note that for the  $\text{O}_2\text{-Ar}$  case there is a broad minimum at 6-8 Td for 1 atm and a strong minimum at 2-4 Td for 6 atm. The  $\text{O}_2\text{-N}_2$  data show no such minimum.

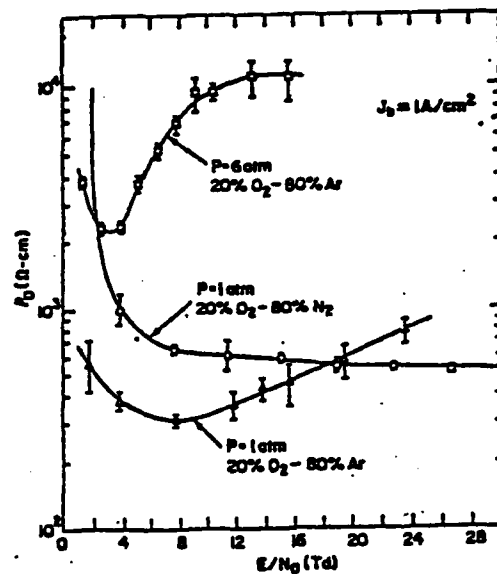


Fig. 2. Discharge resistivity (at peak discharge current),  $\rho_0$ , as a function of reduced field strength,  $E/N_0$ , for  $\text{O}_2\text{-N}_2$  and  $\text{O}_2\text{-Ar}$  mixtures at 1 and 5 atm.

In Fig. 3 we present data taken with 1 atm of  $\text{CH}_4$  both with and without 1% of the attaching gas  $\text{C}_2\text{F}_6$  (Christophorou, 1983). A broad minimum is observed at 18-21 Td. The addition of 1%  $\text{C}_2\text{F}_6$  increases the minimum resistivity

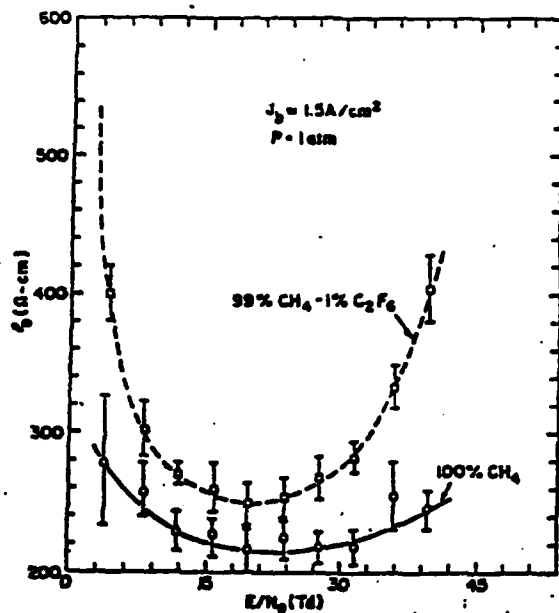


Fig. 3. Comparison of  $\rho_0$  as a function of  $E/N_0$  for CH<sub>4</sub> with and without 1% C<sub>2</sub>F<sub>6</sub> at 1 atm.

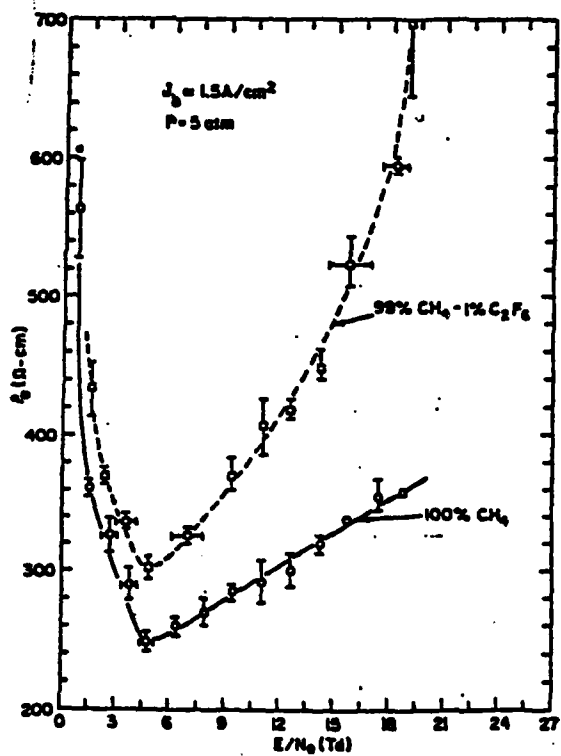


Fig. 4. Comparison of  $\rho_0$  as a function of  $E/N_0$  for CH<sub>4</sub> with and without 1% C<sub>2</sub>F<sub>6</sub> at 5 atm.

by ~ 10%. However, as  $E/N_0$  is increased the resistivity for the 1%  $C_2F_6$  case increases by more than a factor of 2.

This high  $E/N_0$  behavior is also observed for the same data taken at 5 atm, as shown in Fig. 4. The resistivity minimum has become more pronounced and moved to lower  $E/N_0 \sim 4-5$  Td.

Figure 5 is a representative time history of the discharge current compared pure  $CH_4$  and  $CH_4$  with 1%  $C_2F_6$ , both at 1 atm. The decay time (90% to 10%) of the discharge current for the 1%  $C_2F_6$  case is nearly an order of magnitude smaller than the 100%  $CH_4$  case.

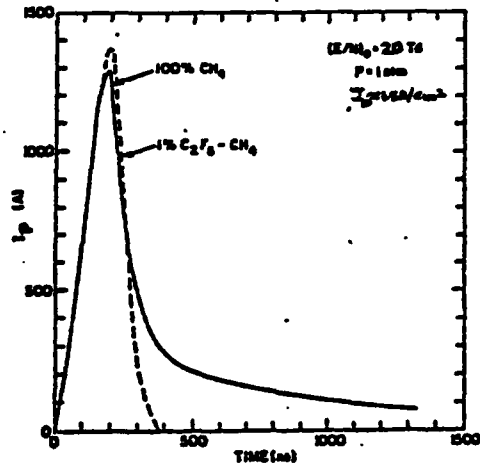


Fig. 5. Time history of discharge plasma current  $I_p$  for  $CH_4$  with and without 1%  $C_2F_6$  at 1 atm. Initial  $(E/N)_0 = 20$  Td.

#### DISCUSSION

Several aspects associated with the interpretation of these data bear discussion before proceeding. The magnitude of the resistivity quoted is obtained at the time of peak discharge current and is thus a minimum value for our particular choice of parameters. By varying  $E/N_0$  we attempt to simulate the transient variation of  $E/N$  in an actual switch as it evolves from the conduction to opening phase. However, in a real switch the e-beam would be absent during the opening phase making the value of the resistivity significantly higher than what is quoted here. Thus, the general trend of the data, rather than their actual magnitude, will be interpreted.

Another concern is the effect of the potential associated with the cathode sheath. At low values of  $E/N_0$ , the sheath potential ( $V_s \sim 1$  kV) is a significant fraction of the applied voltage  $V_d(0)$ . The effective field in the body of the discharge is therefore given by  $E = (V_d(0) - V_s)/Z$  rather than

$E \equiv V_d(0)/Z$ . This discrepancy is minimized over the same range of  $E/N_0$  by operating at higher pressure and/or larger electrode separation  $Z$ . In these cases  $V_d(0)$  must be increased to maintain the same  $E/N_0$  making the cathode sheath potential a smaller fraction of  $V_d(0)$ .

Using the appropriate Ohm's law and assuming an attachment dominated discharge in equilibrium ( $dn_p/dt = 0$ , where  $n_p$  is the discharge plasma electron density) the discharge resistivity is (Commisso, 1984)

$$\rho_0 = \left( \frac{N_a}{\sigma j_b} \right) \frac{\alpha}{\mu N_0} \quad (1)$$

Here  $\mu$  is the electron mobility,  $j_b$  is the e-beam current density,  $N_a$  is the density of the attaching gas,  $\sigma$  is the effective cross section for beam ionization, and  $\alpha$  is the attachment rate coefficient ( $\text{cm}^3/\text{sec}$ ). For a given gas and e-beam,  $\rho_0$  depends on  $E/N_0$  through the parameters  $\alpha$  and  $\mu$ .

For the  $O_2$ - $N_2$  mixture,  $\alpha$  and  $\mu$  depend only weakly on  $E/N_0$  (Dutton, 1975; Brown, 1967) as is observed in the data of Fig. 2. The apparent rapid increase in  $\rho_0$  at  $E/N_0 \lesssim 8$  Td is most likely a result of overestimating  $E$ , as discussed earlier. For example at  $E/N_0 = 8$  Td for 1 atm,  $E = 2$  kV/cm. If the sheath potential is  $\approx 1$  kV, the effective field is  $E = 1$  kV/cm (for  $Z = 1$  cm) and a more realistic value for  $E/N_0$  is  $\approx 4$  Td.

The situation in Fig. 2 is very different for  $O_2$ -Ar. Here  $\rho_0$  varies with  $E/N_0$  in such a way as to strongly enhance switching operation. That is,  $\rho_0$

increases with  $E/N_0$ . The minimum of  $\rho_0$  moves from  $\sim 6$ -8 Td for 1 atm to  $\sim 4$  Td for 6 atm. This is again mainly a cathode sheath effect, as outlined above. Estimates at 1 atm for the three body attachment rate, which is weakly  $E/N_0$  dependent, and the two body dissociative attachment rate, which is strongly  $E/N_0$  dependent, indicate they are comparable for a discharge plasma electron temperature of  $T_e = 1$  eV. At 6 atm three body attachment is dominant. Thus, from Eq. (1) the mobility must be  $E/N_0$  dependent as is expected because Ar exhibits a strong Ramsaur-Townsend behavior. The interpretation of the  $O_2$ -Ar data at 1 atm would be more straightforward if the electron energy as a function of  $E/N_0$  were known.

The  $CH_4$  data in Figs. 3 and 4 clearly show the effects of adding the attaching gas  $C_2F_6$ . The attachment rate for this gas is known to be  $E/N_0$  dependent (Christophorou, 1983). Although the minimum resistivity is higher by  $\sim 10$ -20%, the resistivity at higher  $E/N_0$  is greater by a factor  $\sim 2$  when 1% of  $C_2F_6$  is used. The same sheath effect is seen here as observed with  $O_2$ -Ar. The resistivity minimum at 5 atm has become very sharp and moved to 4 Td from the broad minimum at 18-21 Td with 1 atm. The quantitative agreement between the location of the minima in this case (again assuming a cathode sheath

potential of  $\sim 1$  kV) is not as good as the  $O_2$ -Ar case. Note that, as with Ar,  $CH_4$  exhibits a strong Ramsauer-Townsend effect.

The enhanced resistivity at higher  $E/N_0$  manifests itself as a shorter opening time, i.e., faster decay of the discharge plasma current  $I_p$ . This is demonstrated in Fig. 5 where  $I_p$  for 100%  $CH_4$  and 99%  $CH_4$ -1%  $C_2F_6$  at 1 atm is plotted as a function of time. The time from the 90% to 10% point is  $\sim 100$  ns with  $C_2F_6$ , compared with  $\sim 700$  ns without  $C_2F_6$ . The e-beam decay time is  $\sim 100$  ns.

### CONCLUSIONS

The data presented here demonstrate that an e-beam controlled discharge can be optimized for switching applications by choosing a gas mixture whose mobility and attachment rate are strong functions of  $E/N_0$ . The optimization allows a low resistivity during the conduction with a short opening time.

### ACKNOWLEDGEMENTS

The authors wish to thank H. Hall and J.M. Cameron for their expert technical assistance and Dr. L. G. Christophorou for suggesting the use of  $CH_4$  with  $C_2F_6$ . This work was supported by the office of Naval Research and the Naval Surface Weapons Center, Dahlgren, VA.

### REFERENCES

- Brown, S.C. (1967). Basic Data of Plasma Physics, MIT Press, Cambridge, 84.
- Bletzinger, P. (1983). Fourth IEEE Pulsed Power Conference, Albuquerque, NM, paper 3.3.
- Christophorou, L.G., S.R. Hunter, J.G. Carter, and R.A. Mathis, (1982). Appl. Phys. Lett. 41, 147-149.
- Christophorou, L.G., S.R. Hunter, J.G. Carter, S.M. Spyrou, and V.K. Lakdawala, (1983). Fourth IEEE Pulsed Power Conference, Albuquerque, NM, paper 32.1.
- Commisso, R.J., R.F. Fernsler, V.E. Scherrer, and I.M. Vitkovitsky, (1982). IEEE Trans. Plasma Sci. PS-10, 241-245.
- Commisso, R.J., R.F. Fernsler, V.E. Scherrer, and I.M. Vitkovitsky (1983). Fourth IEEE Pulsed Power Conference, Albuquerque, NM, paper 7.1.
- Commisso, R.J., R.F. Fernsler, V.E. Scherrer, and I.M. Vitkovitsky (1984). Rev. Sci. Instrum., to be published.
- Dutton, J. (1975). J. Phys. Chem. Ref. Data 4, 631-684.
- Fell, B., R.J. Commisso, V.E. Scherrer, and I.M. Vitkovitsky (1982). J. Appl. Phys. 53, 2818-2824.
- Fernsler, R.F., D. Conte, and I.M. Vitkovitsky (1980). IEEE Trans. Plasma Sci. PS-8, 176-180.
- Hallada, M.R., P. Bletzinger, and W.F. Bailey (1982).

IEEE Trans. Plasma Sci. PS-10, 218-223.  
Kline, L.E., (1982). IEEE Trans. Plasma Sci. PS-10, 224-233.  
Lowry, J.F., L.E. Kline, and J.V.R. Heberlein (1983).  
Fourth IEEE Pulsed Power Conference, Albuquerque, NM, paper 7.2.  
Scherrer, V.E., R.J. Comisso, R.F. Fernsler, and I.M.  
Vitkovitsky (1982). 1982 Fifteenth Power Modulator Symposium, Baltimore,  
MD. IEEE Cat. No. 82 CH1785-5, 146-152.

1982 ILLI INTERNATIONAL CONFERENCE ON PLASMA SCIENCE

MAY 17-19, 1987

Electron-beam Controlled Diffuse Discharges\*  
 V.E. Schurrer, R.J. Commins<sup>1</sup>, R.F. Formaler<sup>2</sup>,  
 L. Miles<sup>3</sup>, and I.N. Vitkovitsky, Naval Research  
 Laboratory -- Several experiments have demonstrated  
 that when an electron beam of appropriate energy and  
 current density is passed through a gas located  
 between two electrodes, the gas can be made to conduct,  
 even when the voltage across the electrodes is well  
 below the self-break-down value.<sup>1-4</sup> Conduction is  
 achieved when ionization processes associated with the  
 beam become more rapid than recombination and electron  
 attachment in the gas.<sup>5</sup> Thus, the time dependence and  
 magnitude of the resistivity of the gas can be controlled  
 by the electron beam. Moreover, if the beam  
 profile is uniform a volumetric discharge is produced  
 between the electrodes as is customarily done in the  
 electron beam sustained laser devices. By choosing a  
 proper mixture of electronegative and non-electro-  
 negative gases the discharge may be made to "turn off"  
 (quench conduction) very rapidly and remain non-  
 conducting against the applied electric field.<sup>5</sup> These  
 properties make such a discharge potentially useful as  
 a switching element (opening or closing) for pulsed  
 power generation.

We report on experiments to investigate the  
 properties of electron-beam controlled diffuse  
 discharges. An inductively driven electron-beam  
 vacuum diode (~150 kV, ~1.5 kA) that is capable of  
 producing either one or two beam pulses separated by  
 500 ns is used to study the conduction and recovery  
 properties of a variety of gases and gas mixtures.  
 The beam is injected through a 0.002" nylon vacuum  
 interface into the discharge region (2.1 Atm) where  
 conduction is achieved between two electrodes driven  
 by a 1 μF capacitor. Diagnostics include voltage and  
 current monitors, electron beam dosimetry, and  
 photography. To date, electronegative gases in-  
 cluding O<sub>2</sub>, Cl<sub>2</sub>, and SF<sub>6</sub> are used in mixtures  
 with non-attaching molecules such as H<sub>2</sub> and Ar.  
 Theoretical predictions<sup>5</sup> for the time history of the  
 discharge current and resistivity for the case of  
 O<sub>2</sub>-H<sub>2</sub> mixtures will be compared with experimental  
 results. The initial results for the discharge  
 current and resistivity appear to agree with ex-  
 pected discharge behavior. Current multiplication  
 (i.e., the ratio of the discharge current to the  
 electron beam current) of up to ~10 has been  
 observed.

\*Work supported by DARPA/Tehigrae.

<sup>1</sup>NAELM, Alexandria, VA 22304

<sup>2</sup>Naval Surface Warfare Center, White Oak, MD.

<sup>3</sup>R.C. Hunter, Proc. IEEE First Int. Pulsed Power  
 Conf., Lubbock, TX (1976), pp 1CB:1-6.

<sup>4</sup>J.P. O'Leary, Proc. IEEE First Int. Pulsed  
 Power Conf., Lubbock, TX (1976), 111CS:1-6.

<sup>5</sup>R.M. Kovalchuk and G.M. Nesyats, Sov. Tech.-  
 Phys. Lett., 2, (1975).

<sup>6</sup>K. McDonald, et. al., IEEE Trans. Plasma Sci.,  
 13-6, 181 (1985).

<sup>7</sup>R.F. Formaler, B. Conte and I.N. Vitkovitsky,  
 IEEE Trans. Plasma Sci. PS-8, 176 (1980).

<sup>8</sup>B. Fell, R.J. Commins, V.E. Schurrer and  
 I.N. Vitkovitsky, accepted J. Appl. Phys.,  
 May, (1982).

This form, or a reasonable facsimile, plus two Xerox copies must be received NO LATER  
 THAN FEBRUARY 15, 1982 at the following address: A.J. Alcock, Chairman, 1982  
 International Conference on Plasma Science, c/o National Research Council of Canada,  
 Ottawa, Ontario, Canada K1A 0R6.

Please refer to "First and  
 Final Call for Papers"  
 announcement for instructions  
 in preparing your abstract.

Subject category name:

Subject category number:

Prefer oral session

Prefer poster session

No preference

Special requests for  
 placement of this abstract

Submitted by:

(signature)

(same name typewritten)

(full address)

I am a member of the Committee  
 on Plasma Science and  
 Application

yes  no

Abstract Submitted  
For the Twenty-fourth Annual Meeting  
Division of Plasma Physics  
November 1 to 5, 1982

Category Number and Subject 1.12 Electron Beam/Plasma Interactions  
4.17 Other Applications

Theory  Experiment

Parameter Scaling in Electron-Beam Controlled Discharges. + V.E. Scherrer, R.J. Comisso\*, R.F. Fernsler\*, and I.M. Vitkovitsky, Naval Research Laboratory—The use of an electron beam to control the conductivity of a gas between two electrodes has potential application as a high power repetitive opening or closing switch.<sup>1,2</sup> An inductively driven e-beam diode is used to generate a 200-keV, 200-nA FWHM electron beam which is injected into a N<sub>2</sub>-O<sub>2</sub> gas mixture between two electrodes. The discharge resistivity at peak discharge current, the current gain (discharge plasma current/injected beam current), and opening time are determined as a function of percent attaching gas (O<sub>2</sub>), injected beam current (1-5 A/cm<sup>2</sup>) and ambient pressure (1-5 atm). The results are compared to computer simulations.

+Supported by NSWC, Dahlgren, VA and ONR, Arlington, VA  
\*JAYCOR, Inc., Alexandria, VA 22304

<sup>1</sup>R.F. Fernsler, D. Conte, and I.M. Vitkovitsky, *IEEE Trans. Plasma Sci.* PS-8, 176 (1980).

<sup>2</sup>R.J. Comisso, R.F. Fernsler, V.E. Scherrer, and I.M. Vitkovitsky, to be published, *IEEE Trans. Plasma Sci.* (1982).

- Prefer Poster Session  
 Prefer Oral Session  
 No Preference  
 Special Requests for placement of this abstract:  
 Special Facilities Requested (e.g., movie projector)

Submitted by:

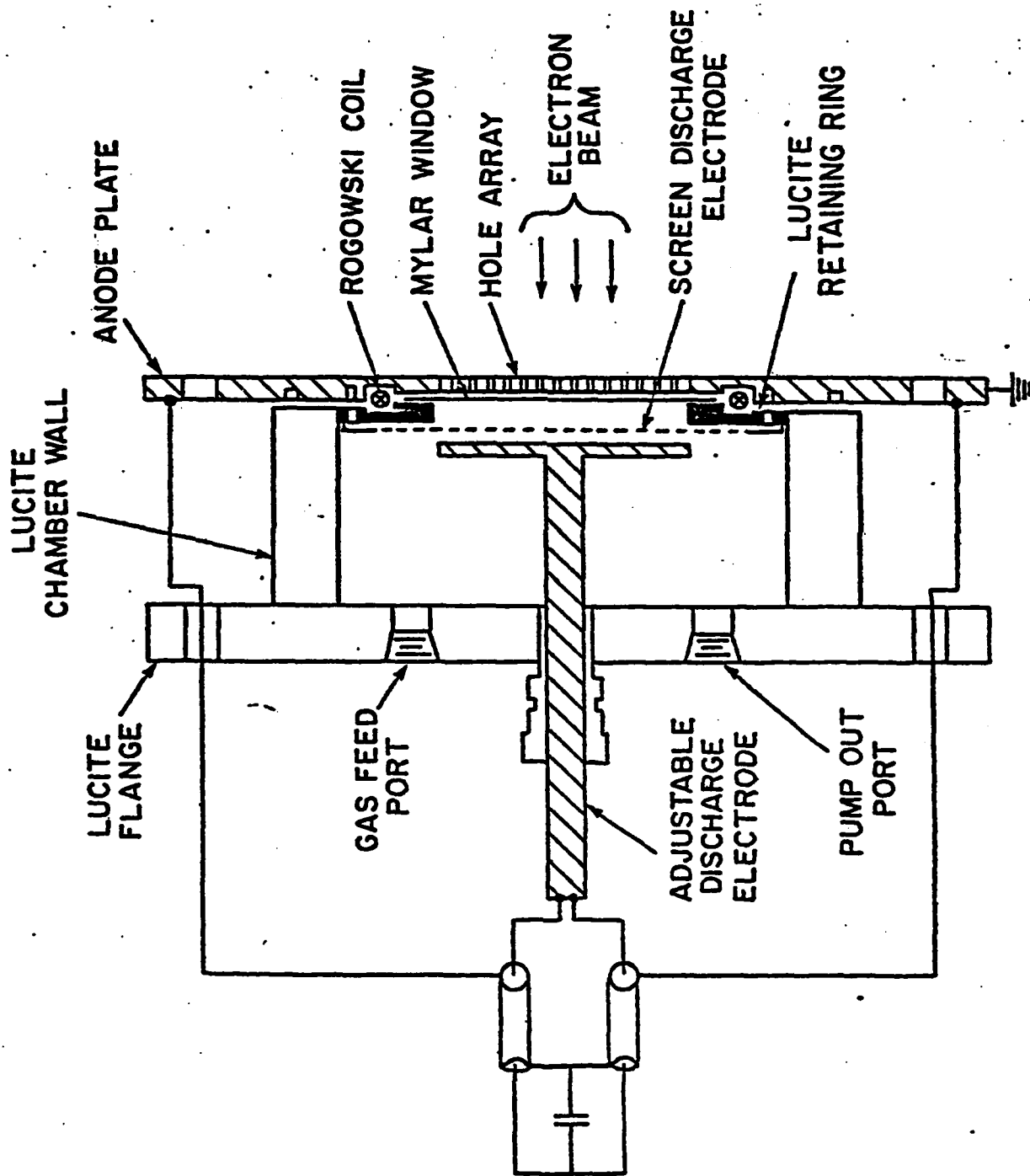
Robert J. Comisso  
(signature of APS member)

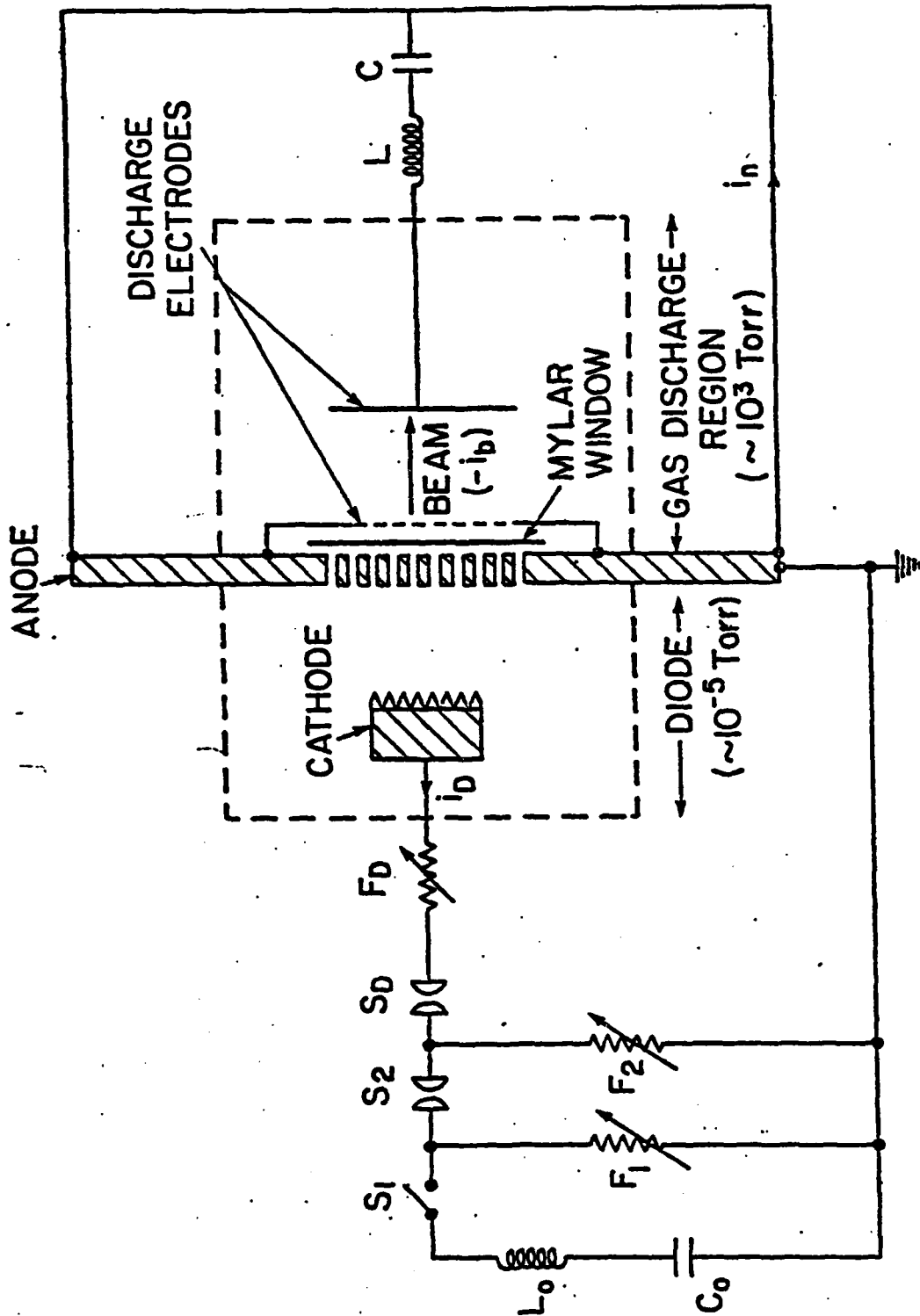
Robert J. Comisso

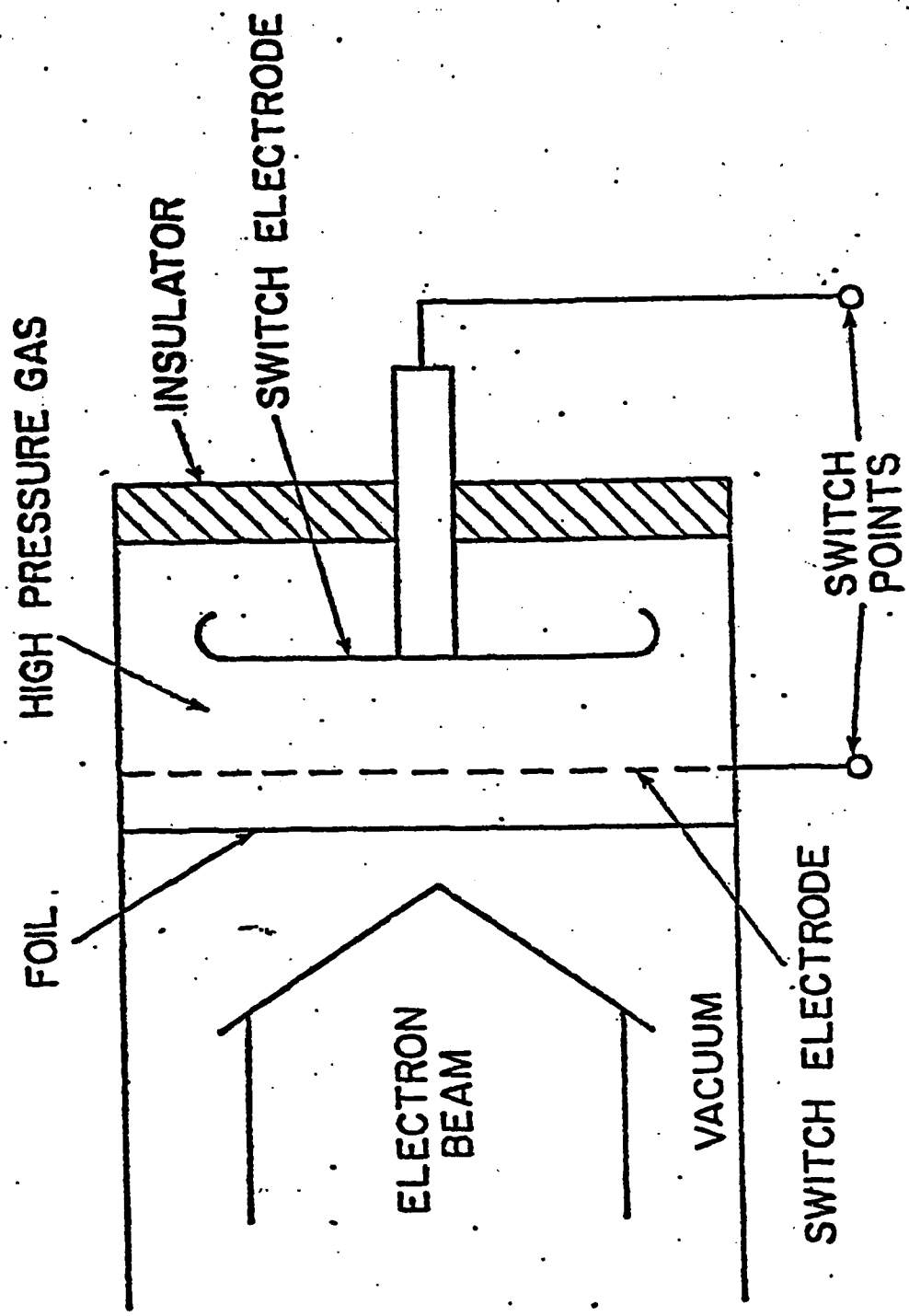
(same name typewritten)  
4555 Overlook Ave., S.W., Code 4770  
Washington, D.C. 20375  
(address)

This form, or a reasonable facsimile, plus *Two Xerox Copies* must be received  
NO LATER THAN NOON, July 30, 1982, at the following address:

Ms. Barbara Safarty  
Princeton Plasma Physics Laboratory  
P.O. Box 451  
Princeton, New Jersey 08544







• PRINCIPLES OF OPERATION:

- E-BEAM CONTROLS IONIZATION AND, THEREFORE, GAS CONDUCTIVITY
- ARC DISCHARGE IS NOT PERMITTED TO OCCUR!
- SWITCH VOLTAGE & STATIC BREAKDOWN VOLTAGE
- LOWERING OF SELF-SPARKING THRESHOLD AVOIDED BY  
PROPER CHOICE OF SWITCH VOLUME

• CONSEQUENCES:

- FAST OPENING UNDER HIGH APPLIED ELECTRIC FIELDS (LIMITED BY E-BEAM)
- REPETITIVE CAPABILITY
- VOLUME DISCHARGE
- LOW INDUCTANCE
- REDUCED ELECTRODE WEAR AND MECHANICAL SHOCK

THE CIRCUIT IS DESCRIBED BY:

$$V_0 = R(t)[i - i(e)] + L \frac{di}{dt} + \frac{1}{C} \int i dt$$

WHERE:

$i$  = NET CIRCUIT CURRENT

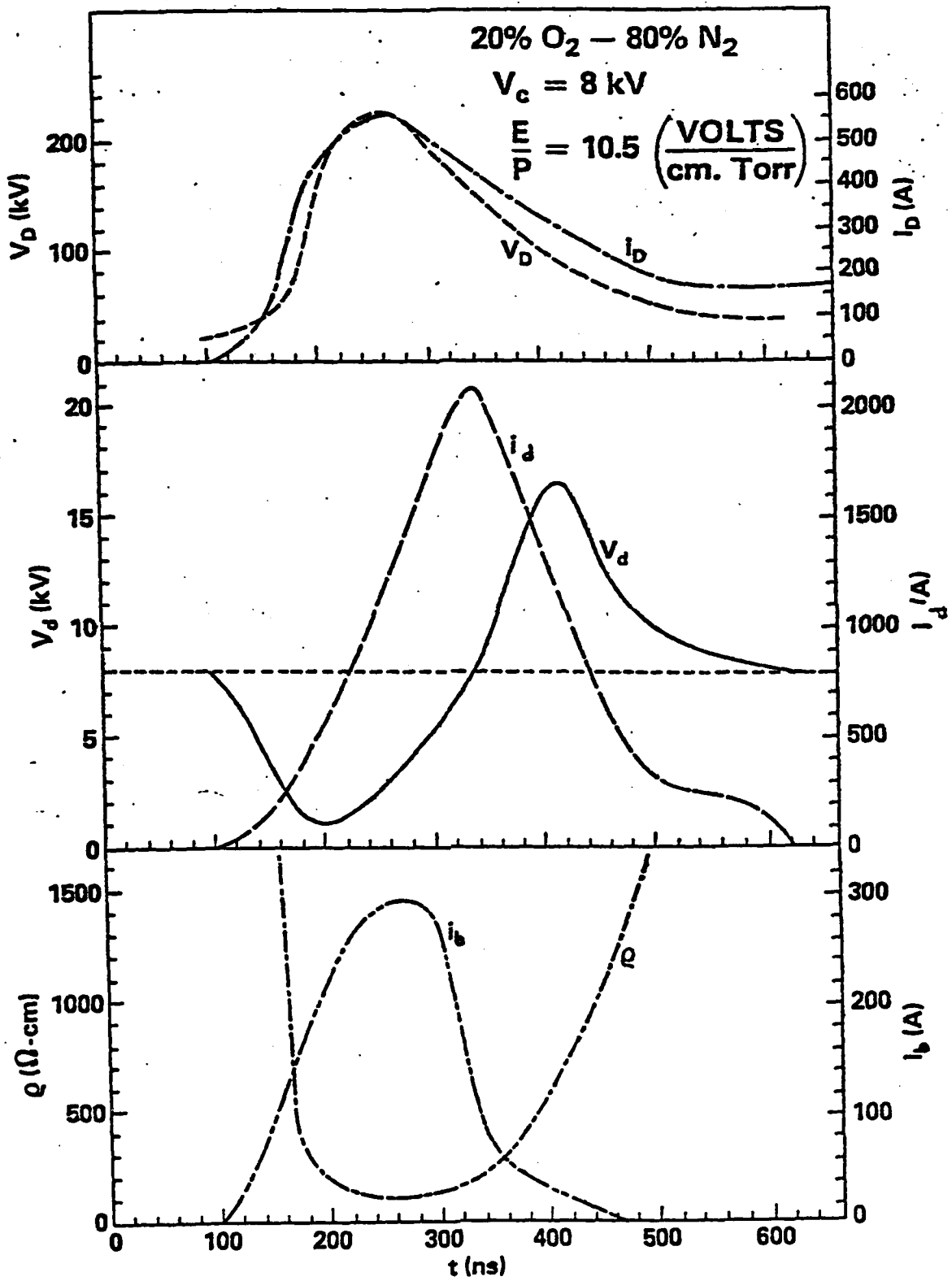
$V_0$  = INITIAL VOLTAGE ON C

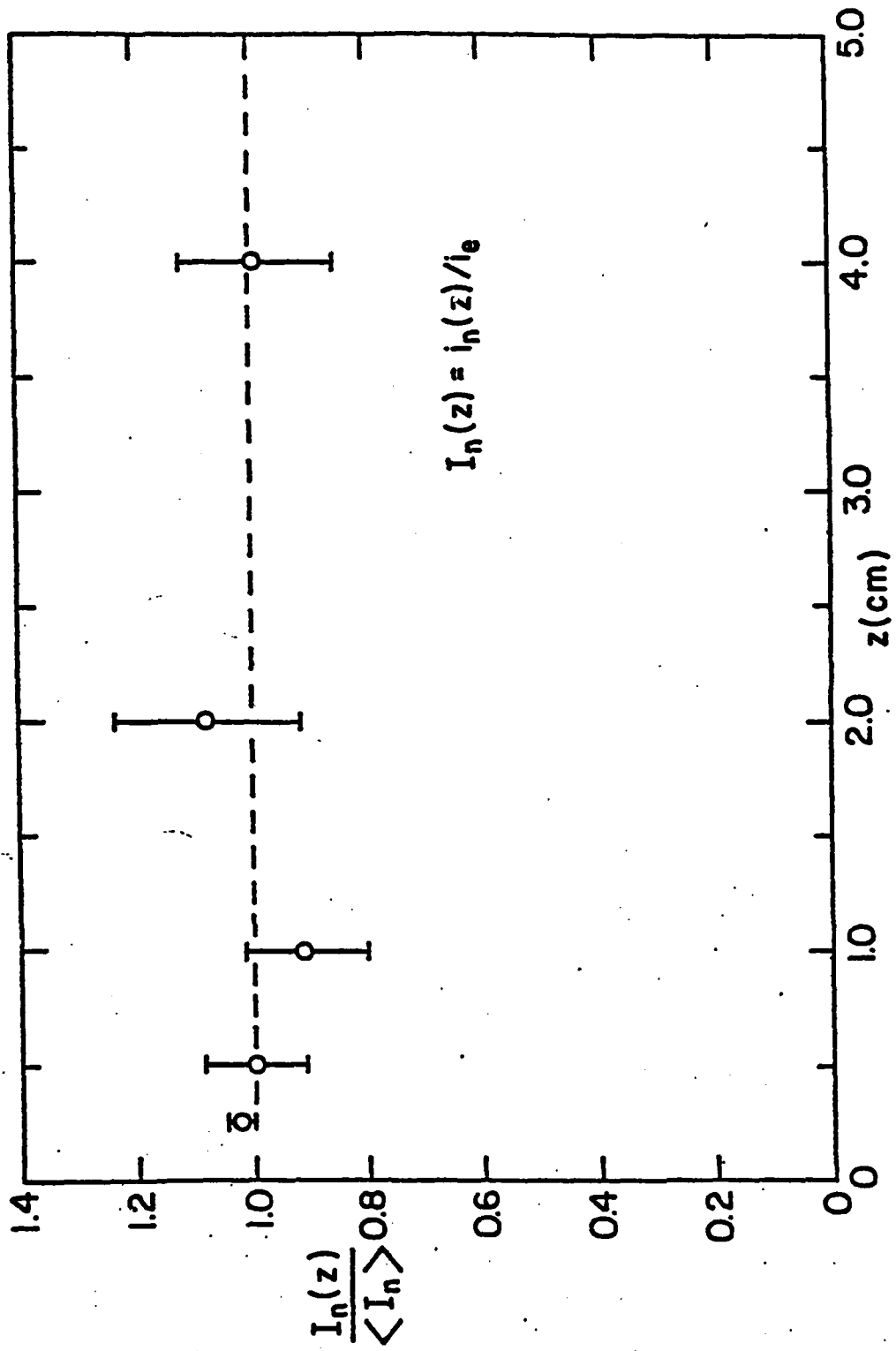
$L$  = CIRCUIT INDUCTANCE

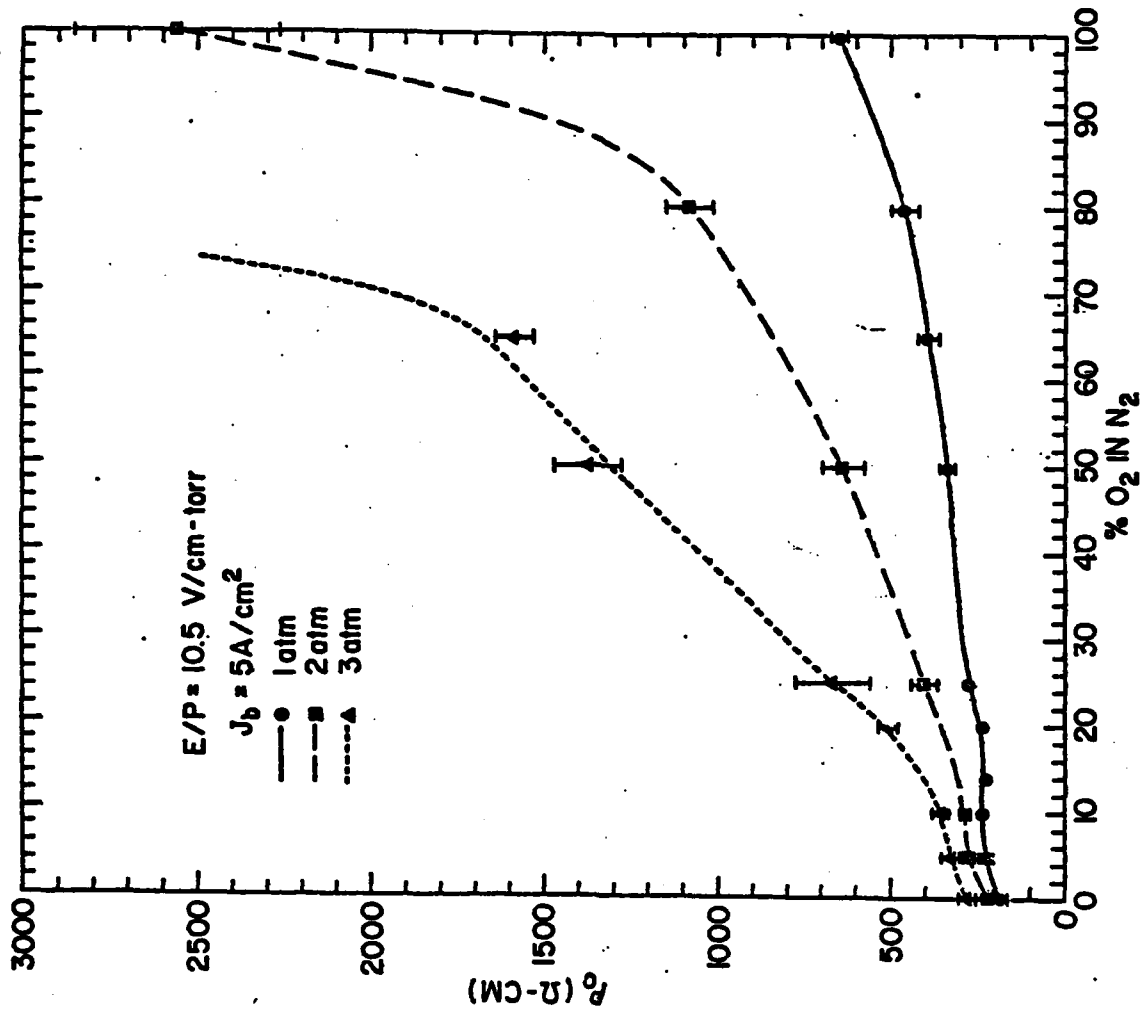
$i(e)$  = ELECTRON BEAM CURRENT

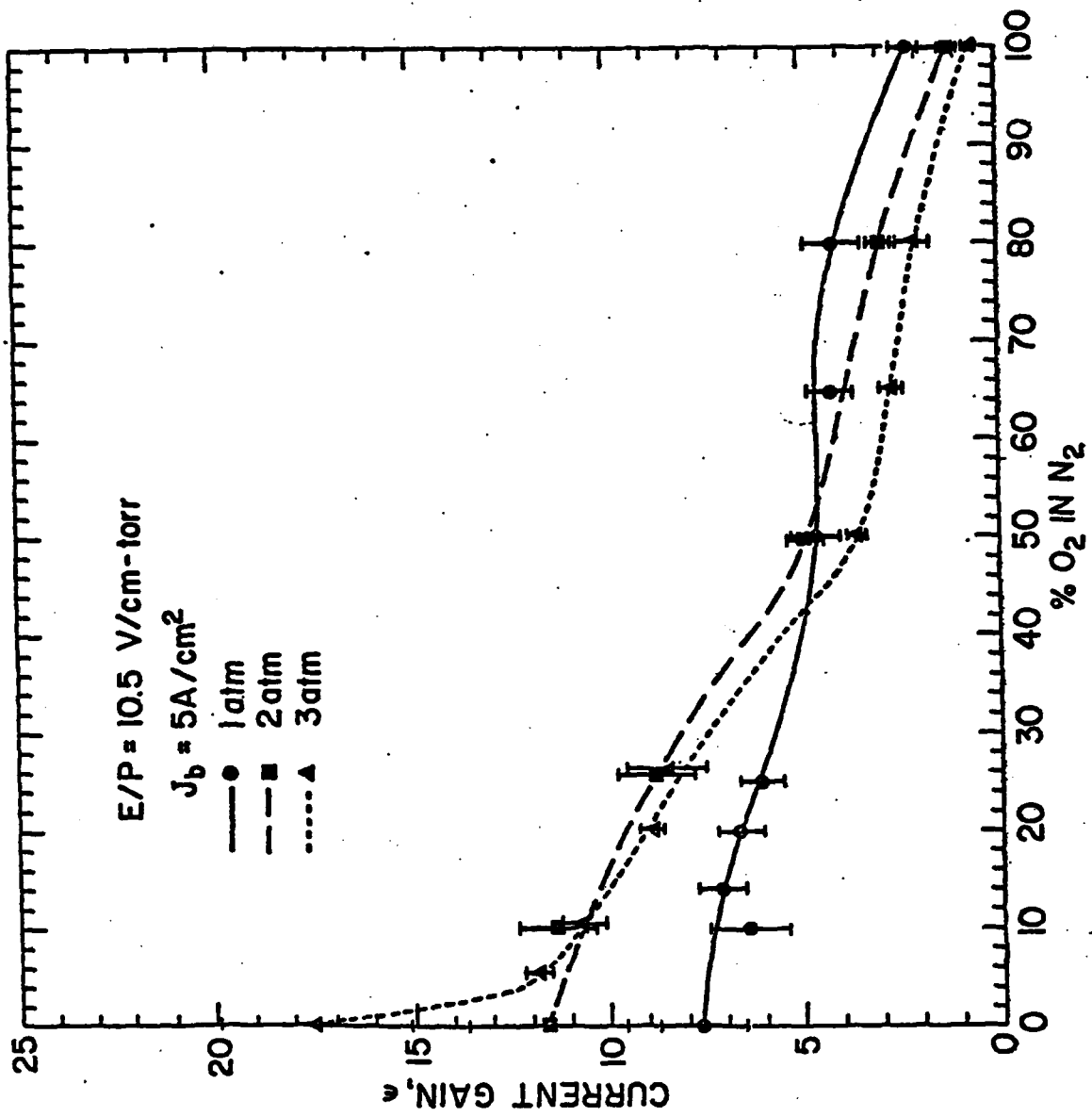
$R(x)$  = GAS RESISTANCE -

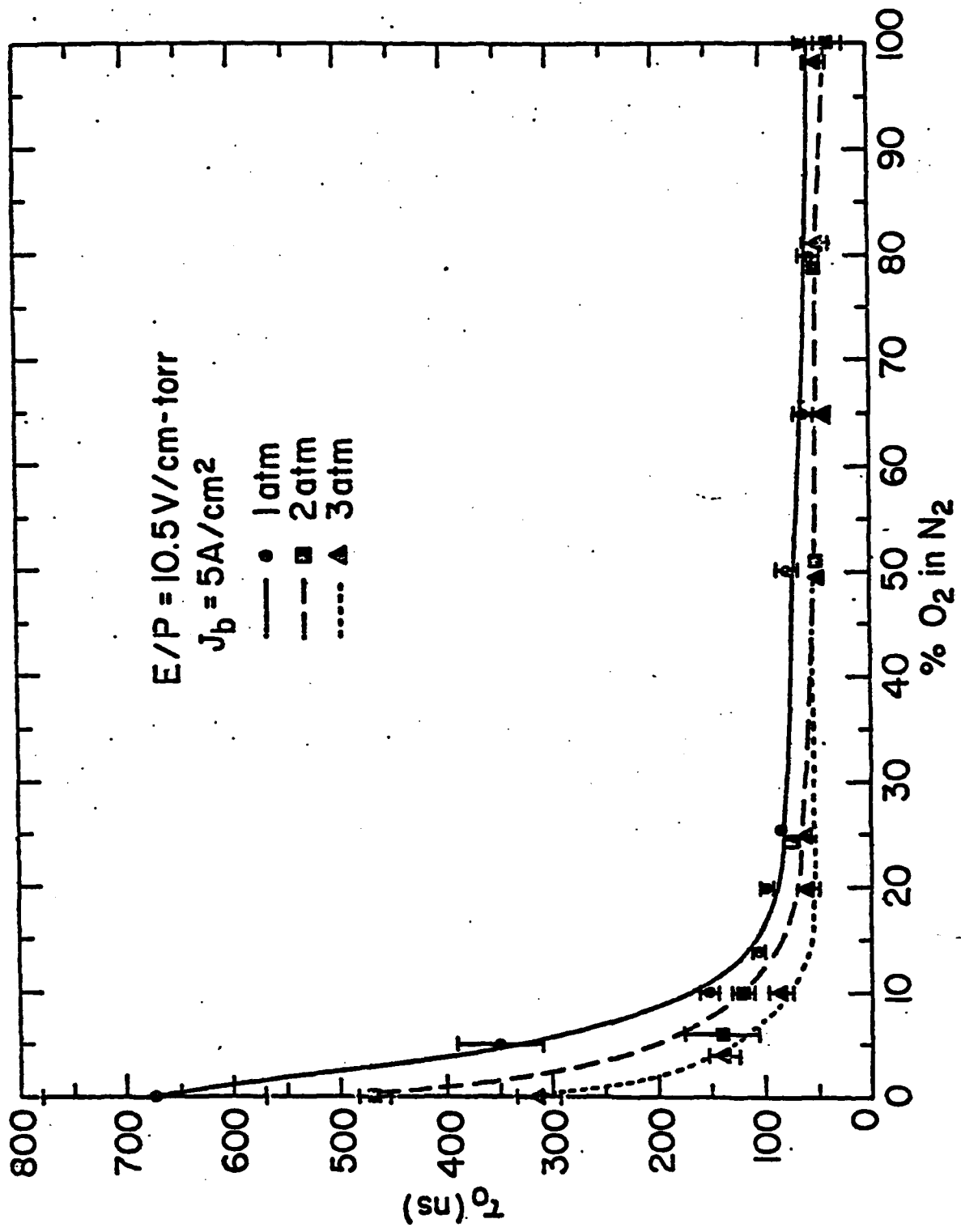
$\sim \rho(x)$  GAS RESISTIVITY

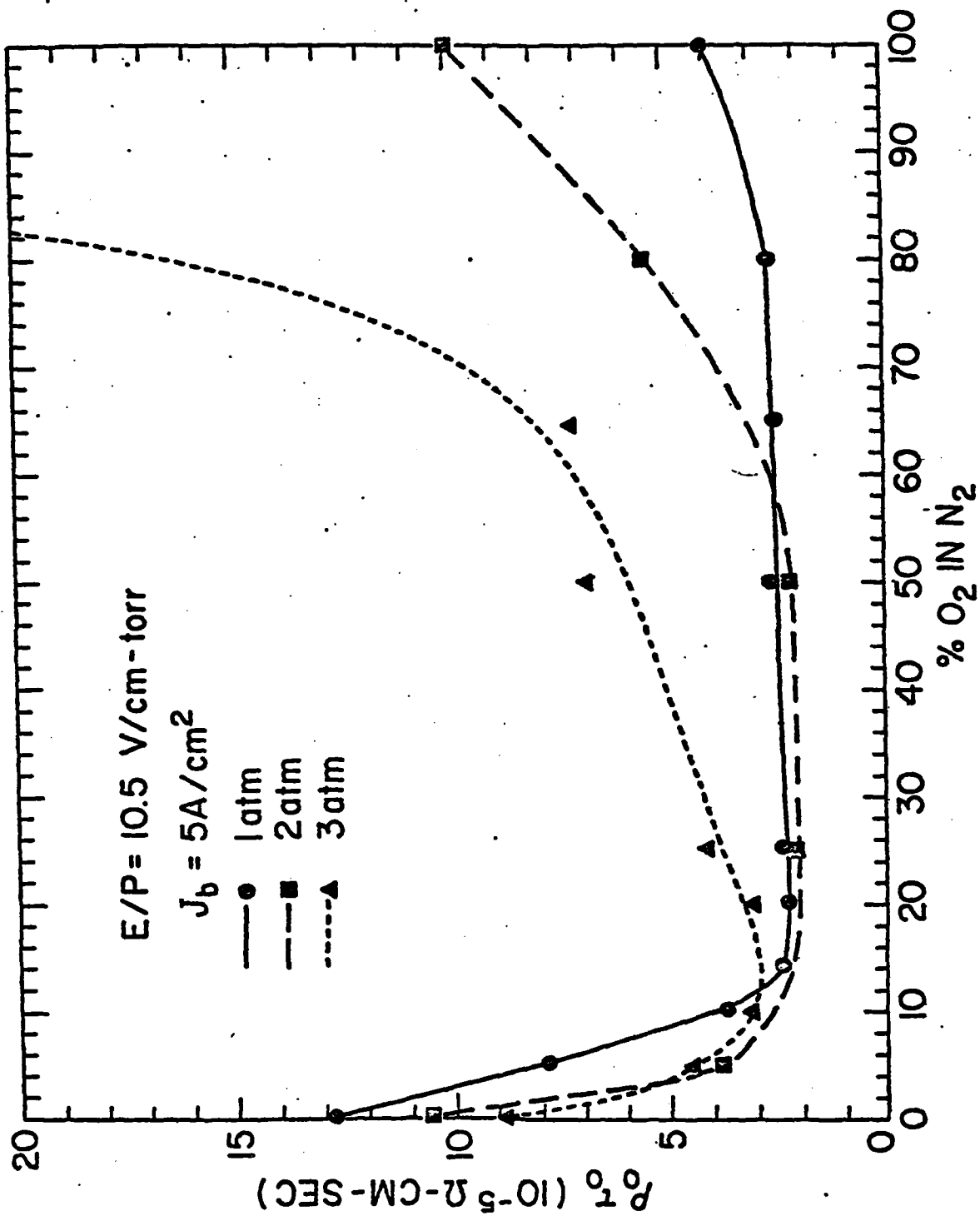


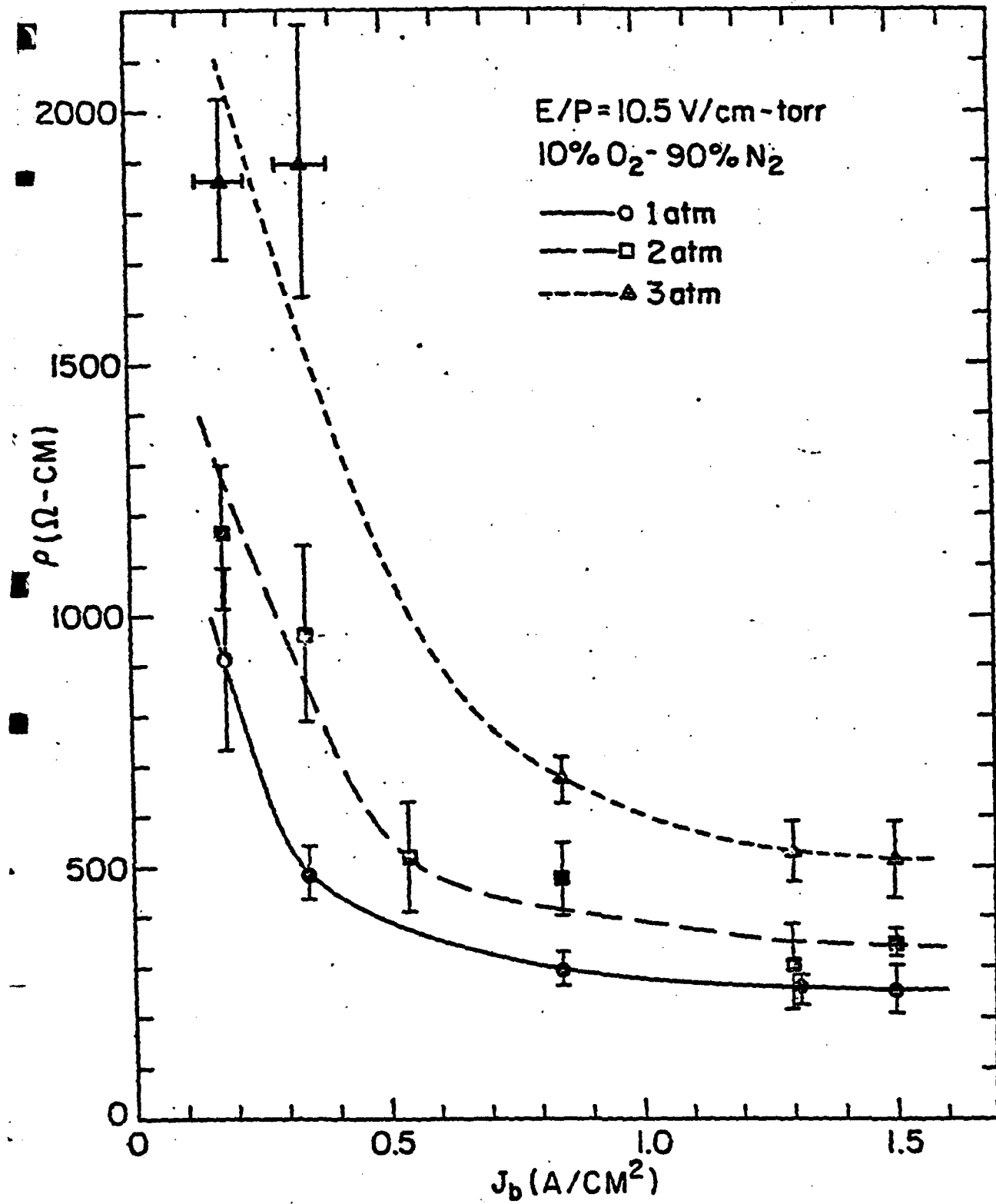


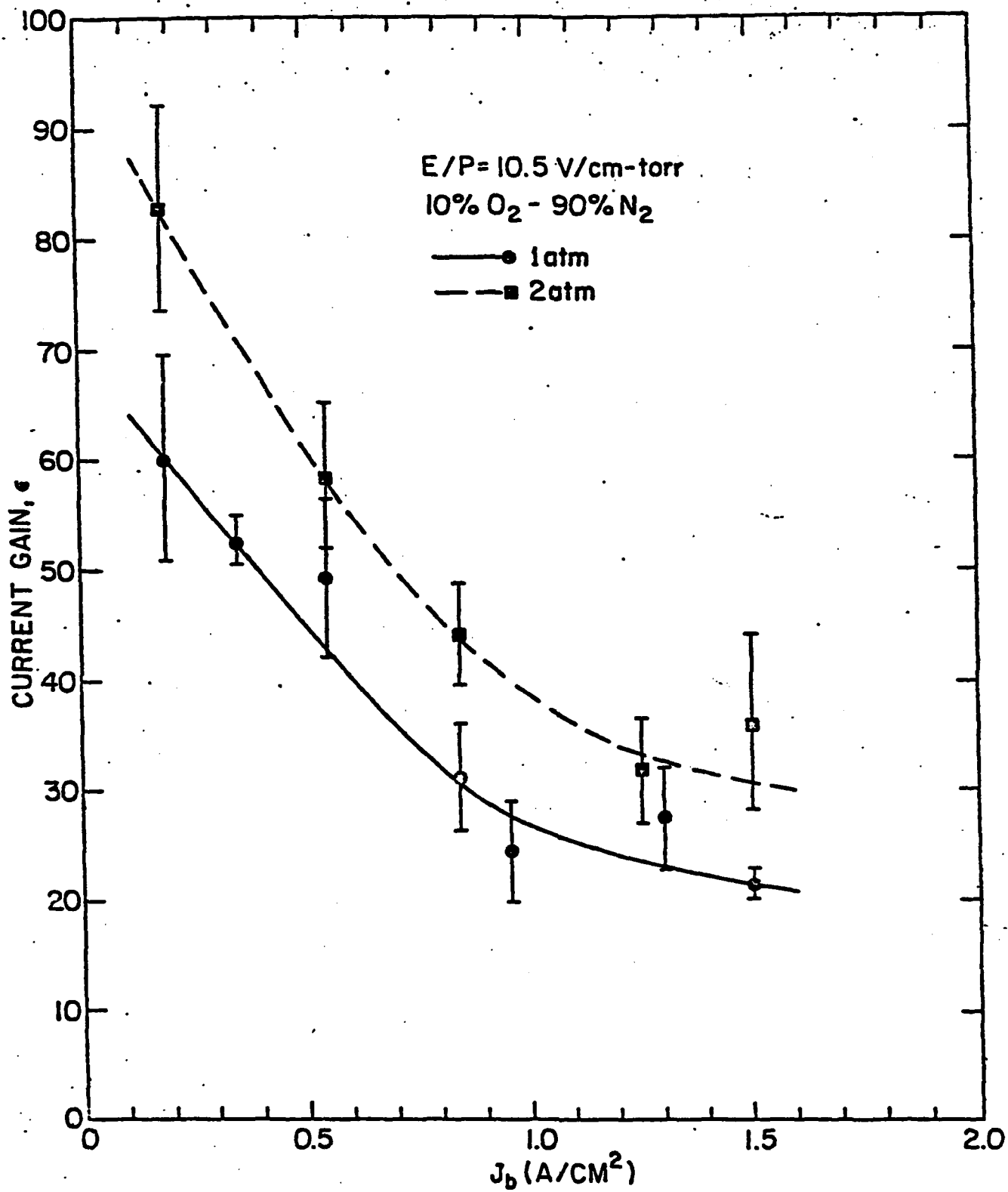


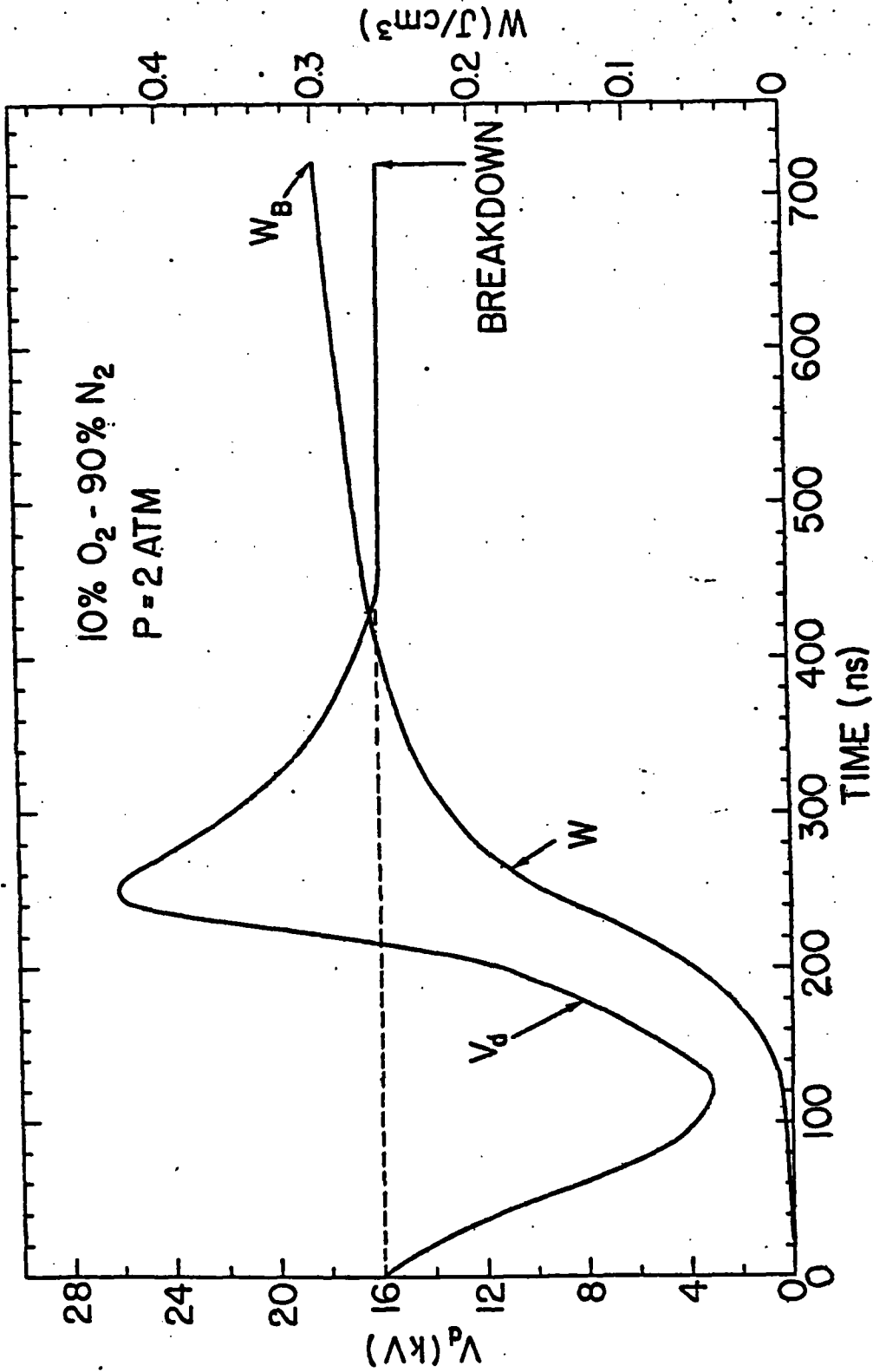


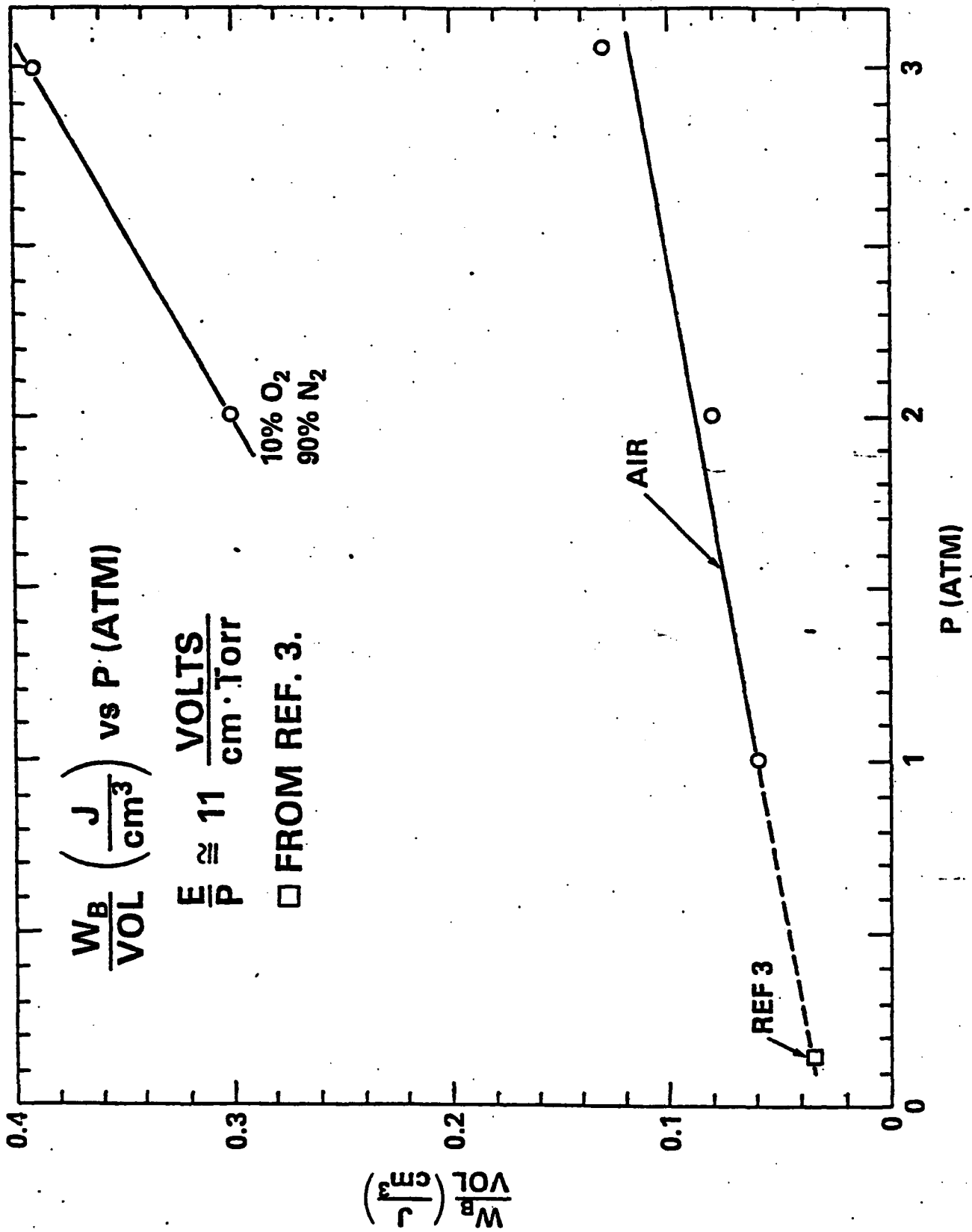












Studies of Electron-Beam Controlled Diffuse Discharges<sup>†</sup>, V.E. Scherrer, R.J. Commisso\*, R.F. Fernsler\*, and L.M. Vitkovitsky, Naval Research Laboratory, Washington, DC 20375 — When an electron beam of sufficient energy passes through a gas column at high pressure (~ 760 Torr) and voltage is applied across the column, a diffuse discharge can be formed. The conductivity of this discharge is dominated by electron-neutral collisions and is therefore controlled by the fractional ionization of the gas. The fractional ionization of the column is in turn determined by a competition between electron-beam (e-beam) ionization and recombination and (more importantly) attachment processes in the gas. When the electron beam ceases, the conductivity of the gas column can return quickly to that of the neutral gas. Investigations into these e-beam controlled diffuse discharges indicate potential application for repetitive (~ 10 kHz, in a "burst" mode), high power (~ 10<sup>10</sup> W) switching.<sup>1-3</sup> These applications include both opening and closing switches.<sup>4</sup>

Using N<sub>2</sub>-O<sub>2</sub> combinations at pressures ranging between 760 and 2,280 Torr we have studied the dependence of such discharge parameters as resistivity, current gain, and opening time on percentage of attaching gas, e-beam current density, and applied discharge voltage. These results are compared to zero-dimensional numerical simulations in which the gas chemistry is coupled to the discharge circuit.

Under certain conditions the gas is observed to breakdown after the e-beam ceases. The time interval between the e-beam turning off and the breakdown occurring can be varied. Experiments aimed at understanding this phenomenon will be discussed.

Other experiments, which use gases that exhibit the Ramsauer-Townsend<sup>5</sup> collision cross section behavior, have been performed.

† Work supported by Naval Surface Weapons Center, Dahlgren, VA

\* JAYCOR, Inc., Alexandria, VA 22304

<sup>1</sup> R.J. Commisso, R.F. Fernsler, V.E. Scherrer, and I.M. Vitkovitsky, IEEE Trans. Plasma Sci. PS-10, 241 (1982).

<sup>2</sup> L.E. Kline, IEEE Trans. Plasma Sci. PS-10, 224 (1982).

<sup>3</sup> M.R. Hallada, P. Hletzinger, and W.F. Baily, IEEE Trans. Plasma Sci. PS-10, 218 (1982).

<sup>4</sup> R.J. Commisso, R.F. Fernsler, V.E. Scherrer, and I.M. Vitkovitsky, NRL Memorandum Report 4975 (1982).

<sup>5</sup> J.B. Hasted, "Physics and Atomic Collisions," American Elsevier Publishing Co., NY (1972), p. 306.

MAY 23-25, 1983

SUBJECT CATEGORY:

ARC TECH-& GASEOUS EI

NUMBER: 14

X PREFER POSTER SE9

SUBMITTED BY:

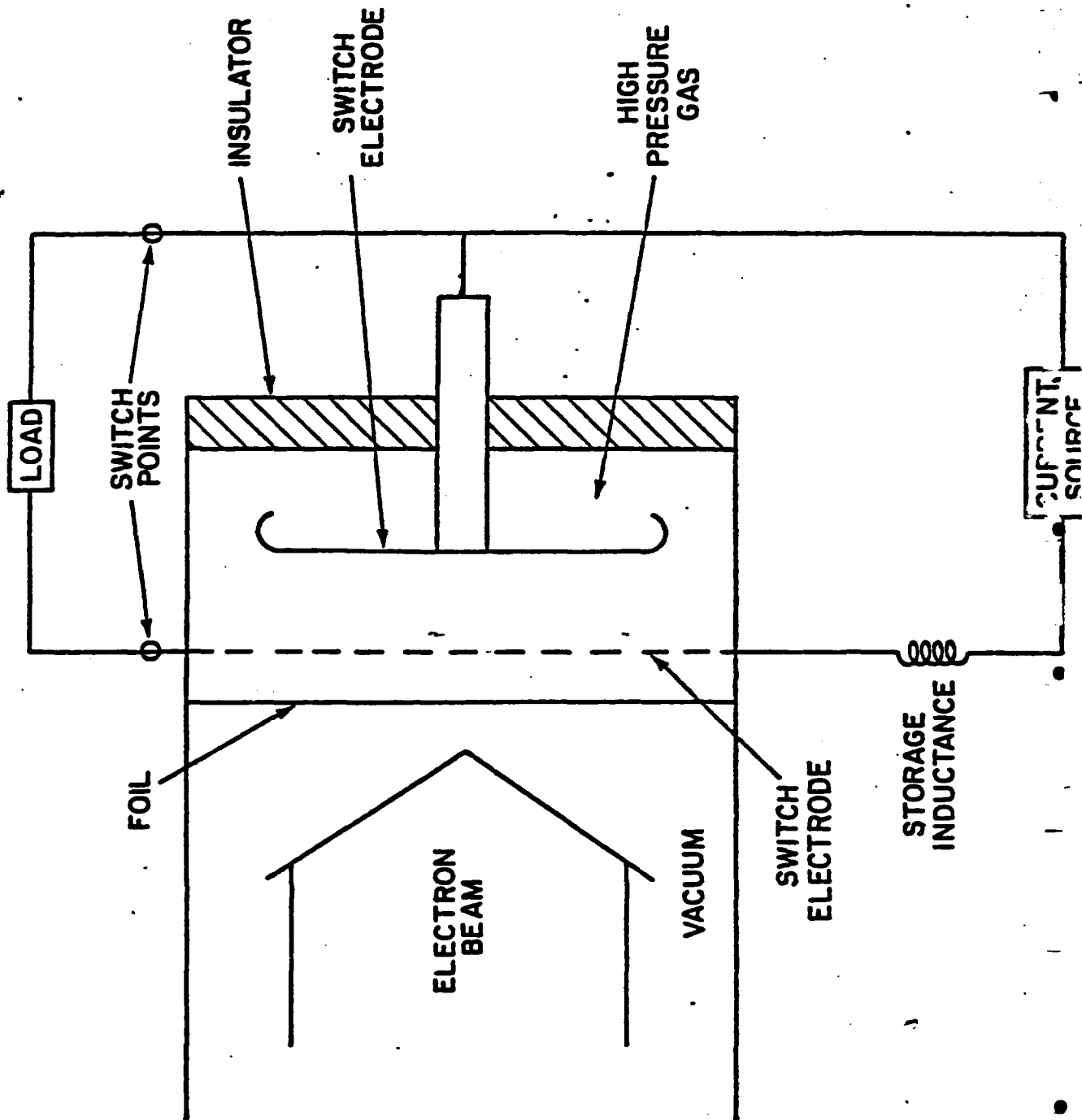
Robert J. Commisso  
Robert J. Commisso

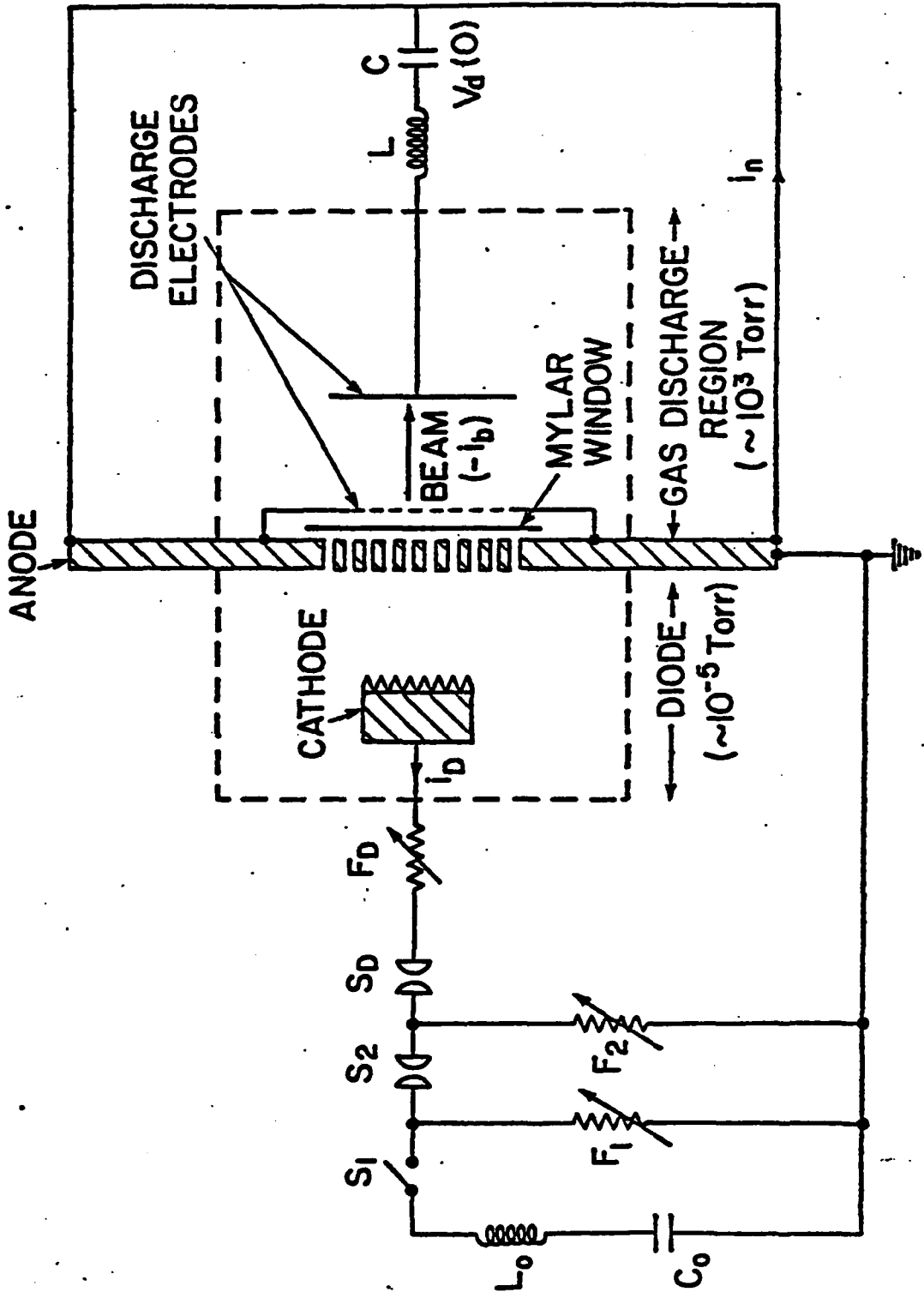
Code 4770

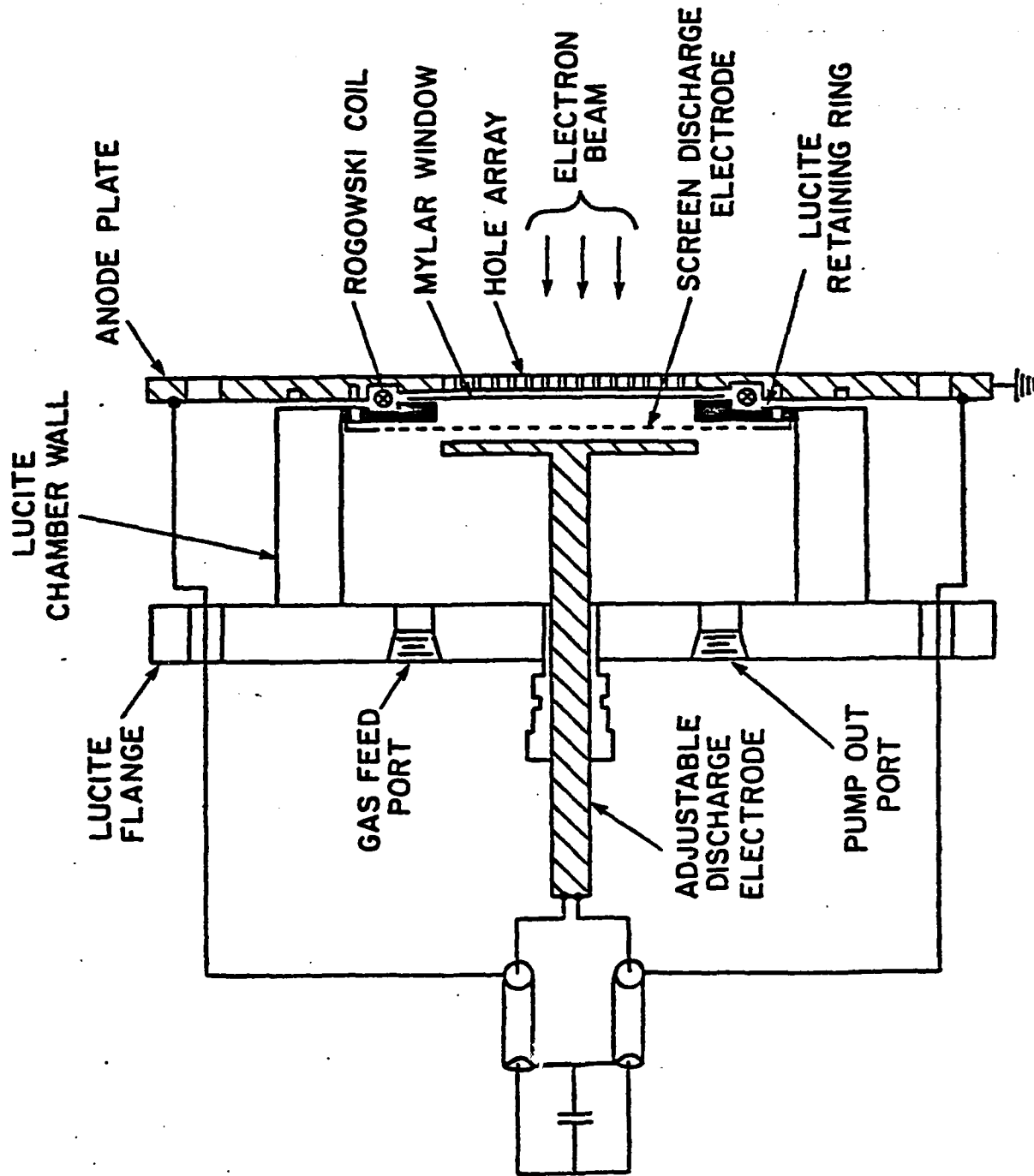
Naval Research Labor

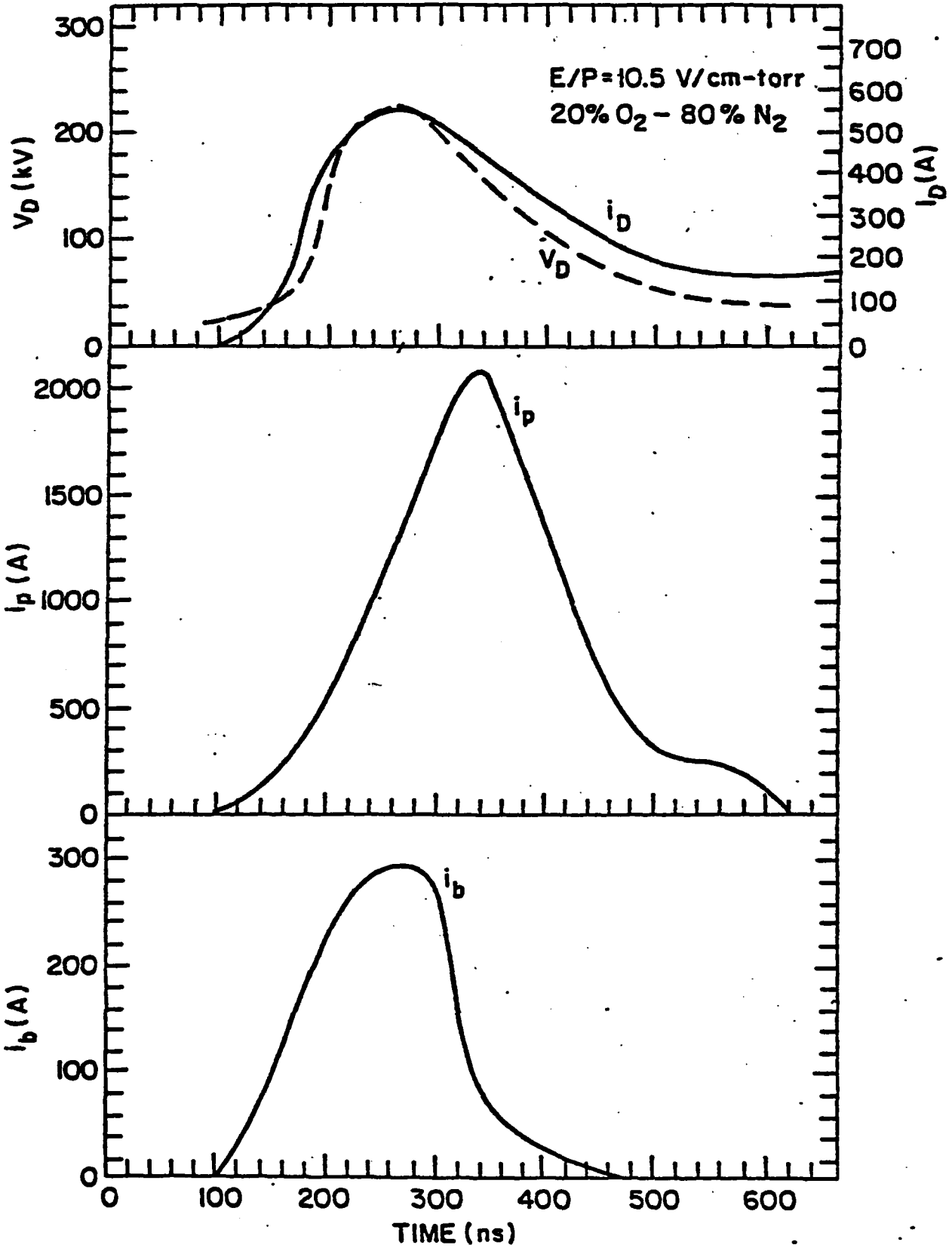
Washington, DC 20375

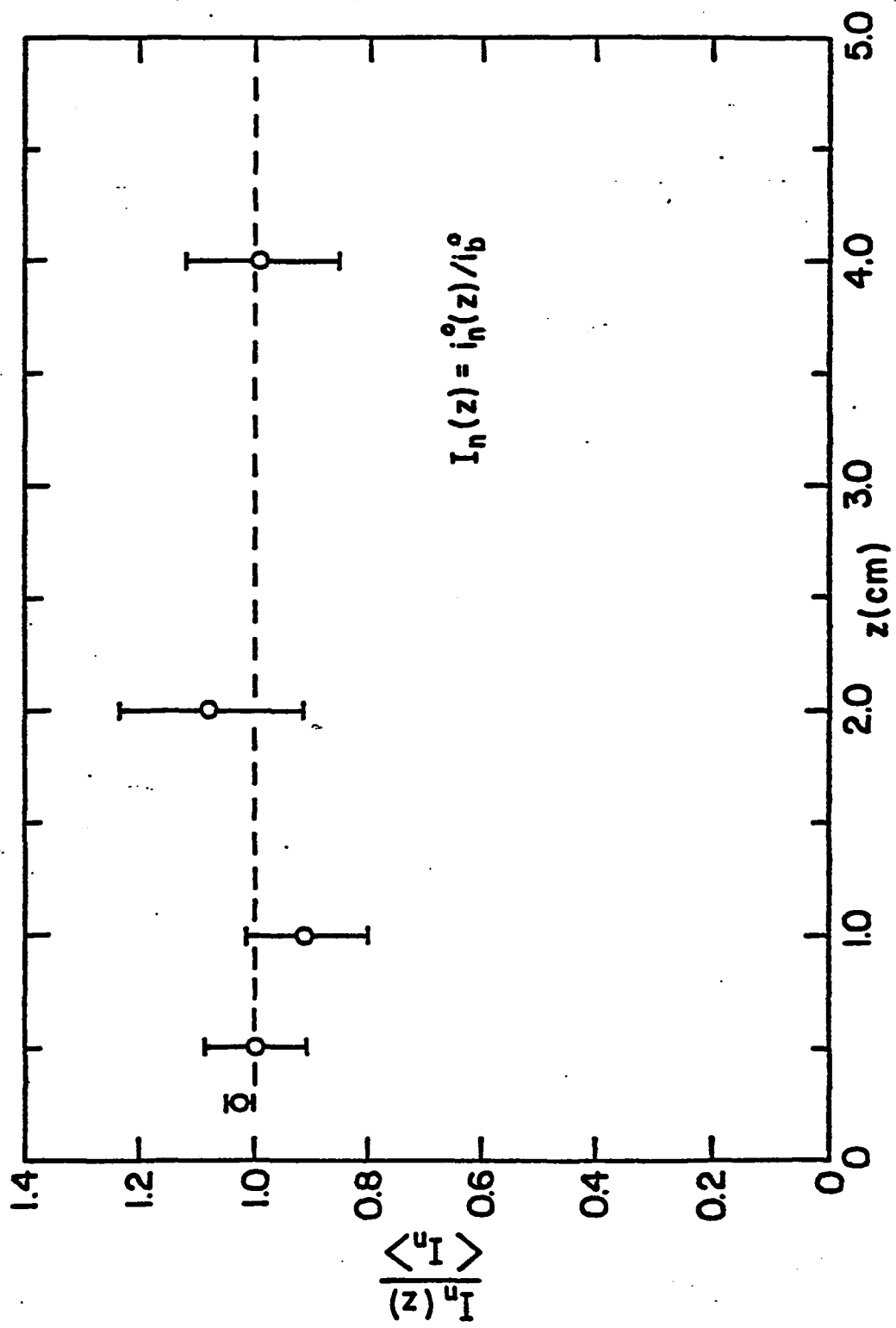
202-767-2468











## THEORETICAL MODEL

DISCHARGE PLASMA ELECTRONS:

$$\frac{dn_p}{dt} = S_0 J_0 P - [(\alpha_1 + \alpha_2 N_0) N_a + \beta N^+] n_p$$



OTHER SPECIES:

$$\left\{ \frac{dN}{dt} \right\}_A^{+, -, 0}$$

CHARGE CONSERVATION:

$$n_p + \sum_A N^- = \sum_A N^+$$

DISCHARGE PLASMA CURRENT:

$$J_p = n_p e v, \quad v = \mu E, \quad \mu = \text{ELECTRON MOBILITY}$$

CIRCUIT EQUATION:

$$V_d(t) = R(i_n - i_b) + L \frac{di_n}{dt} + \frac{1}{C} \int_0^t i_n dt$$

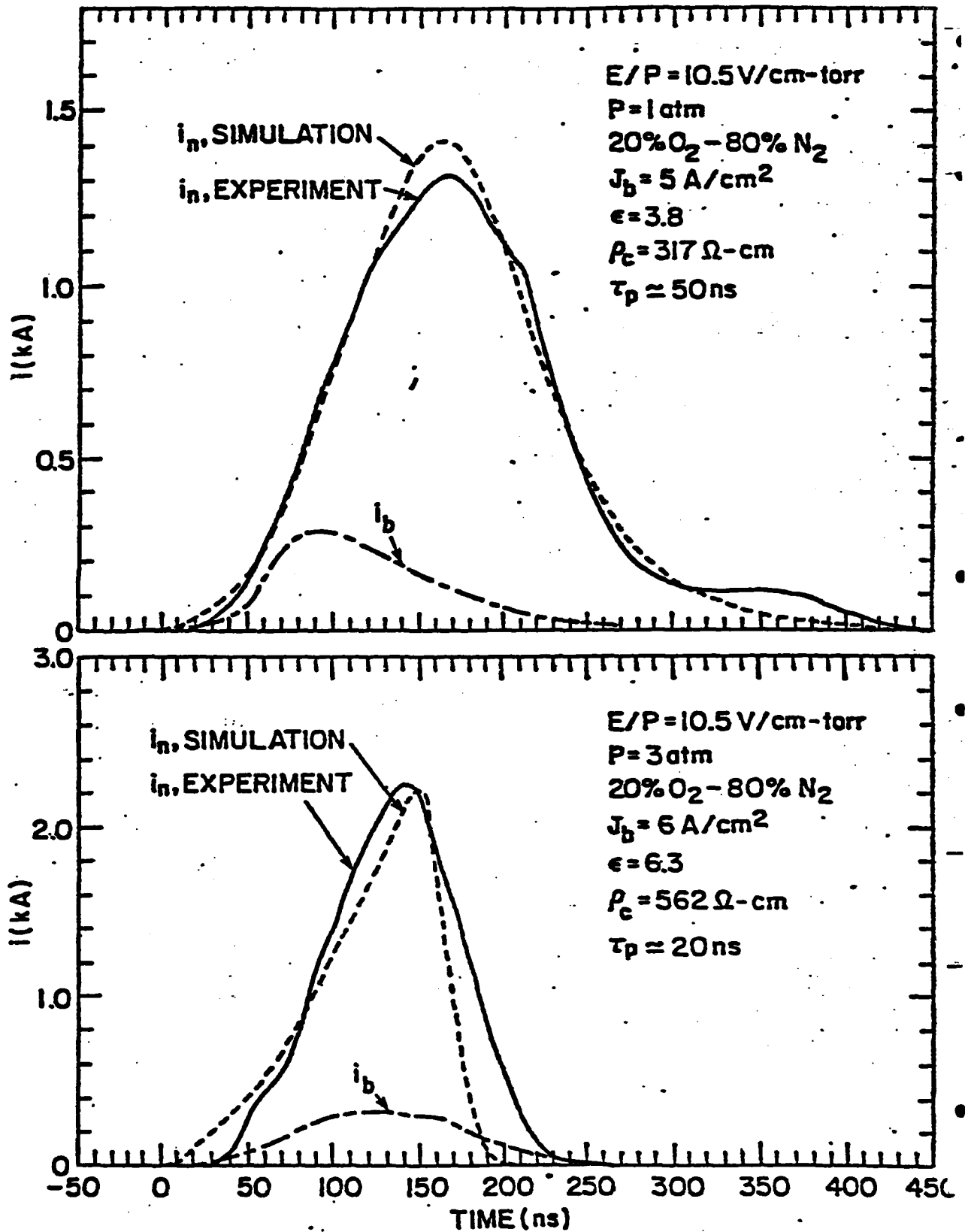
DISCHARGE RESISTIVITY:

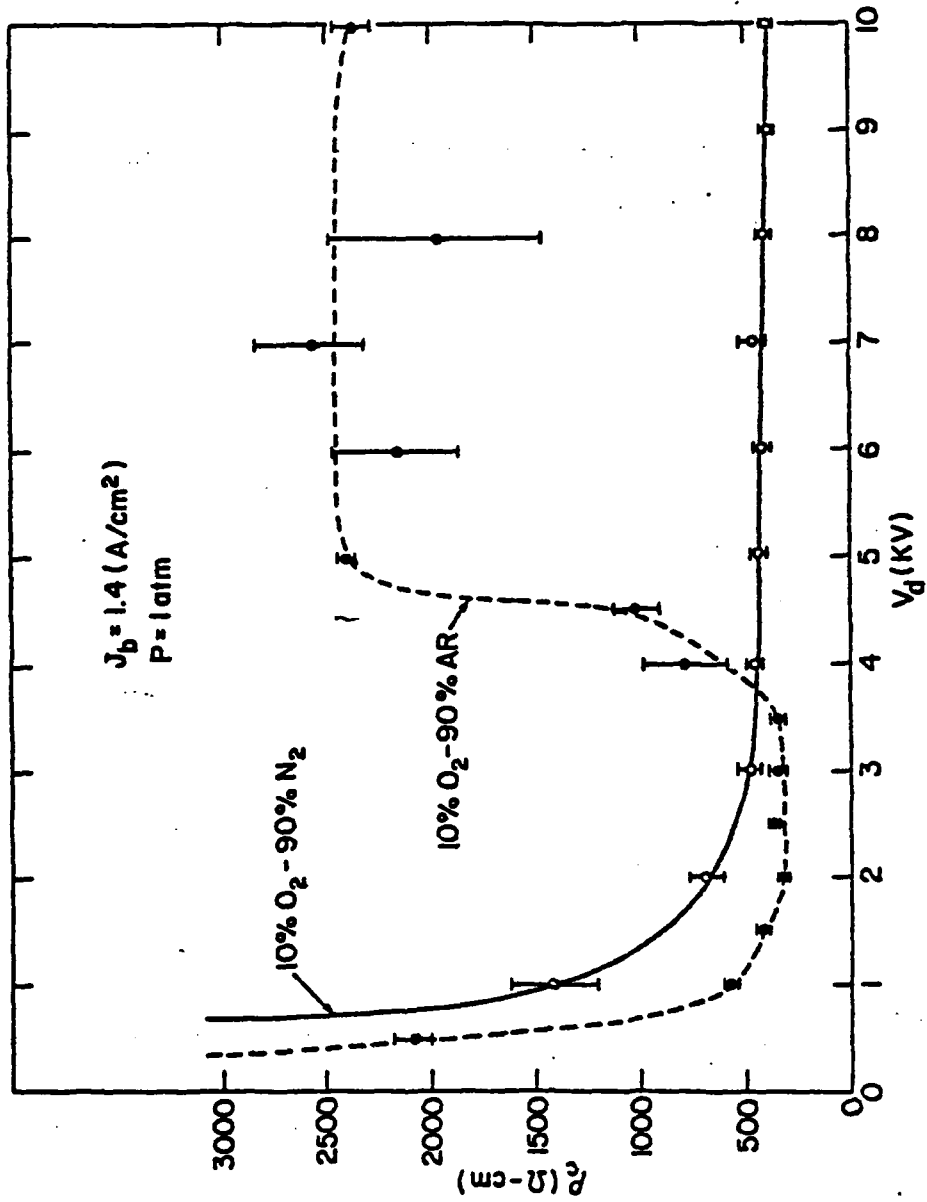
$$\rho_c = E_c / J_p = (e n_p \mu)^{-1}$$

IN EQUILIBRIUM:

$$\frac{dn_p}{dt} = 0$$

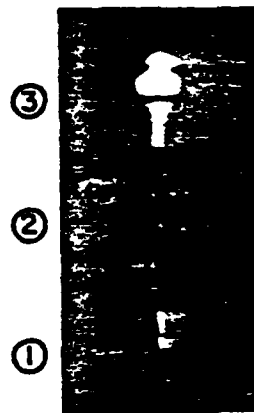
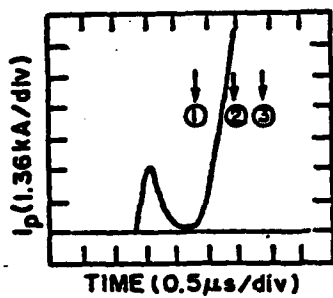
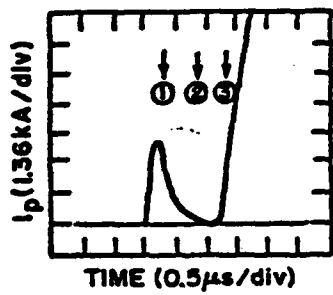
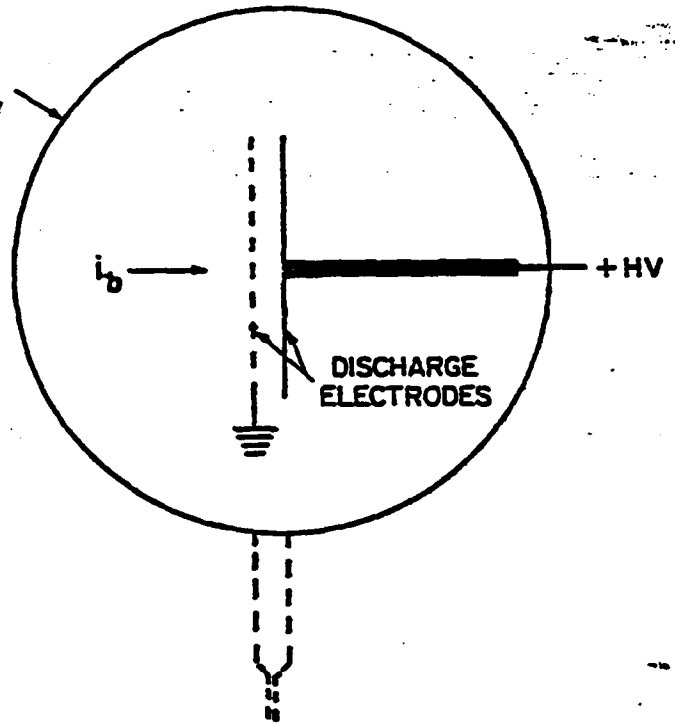
$$\Rightarrow \frac{E}{E_c} \propto P \quad (\text{FOR } E_c/P, \text{ GAS MIXTURE CONST.})$$





# FRAMING CAMERA PHOTOGRAPHY

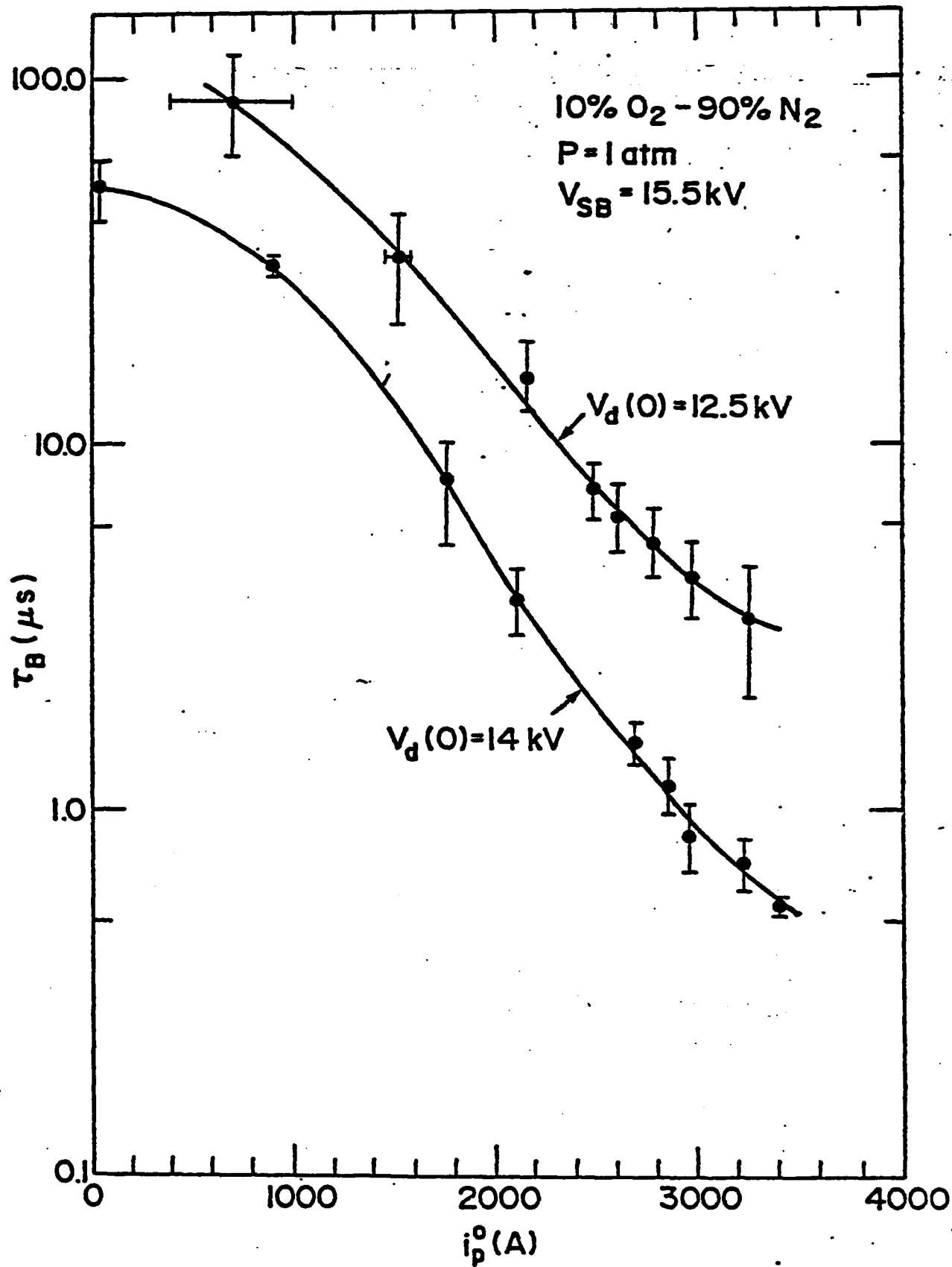
APPROXIMATE FIELD OF VIEW



f/20  
100ns EXPOSURE



f/22  
100ns EXPOSURE



## SUMMARY

1. DISCHARGE PARAMETERS SCALE AS PREDICTED BY THEORY/  
SIMULATION (CAN DESIGN SWITCHES WITH SOME CONFIDENCE).
2. DISCHARGE CHARACTERISTICS DESIRED FOR SWITCH  
APPLICATIONS MAY BE OBTAINED THROUGH OPTIMUM CHOICE  
OF GAS.
3. OBSERVED LATE TIME BREAKDOWN IS MOST LIKELY A RESULT  
OF LOCAL HEATING OR SURFACE EFFECTS.

Abstract Submitted  
For the Twenty-fifth Annual Meeting  
Division of Plasma Physics  
November 7 to 11, 1983

Category Number and Subject 4.14 OTHER APPLICATIONS

Theory  Experiment

Investigations Into Electron-Beam Controlled Diffuse Discharges.<sup>†</sup> V.E. SCHERRER, R.J. COMMISSO<sup>‡</sup>, R.F. FERNSLER<sup>§</sup>, and I.M. VITKOVITSKY, Naval Research Laboratory—The application of electron-beam controlled diffuse discharges to fast, high power, repetitive opening switches represents a possible solution to some of the switching problems associated with inductive storage.<sup>1,2</sup> We report on experiments in which the physics of these discharges relevant to switching applications is investigated. Various mixtures of Ar-O<sub>2</sub> and N<sub>2</sub>-O<sub>2</sub> are compared for switching applications. The dependence of energy deposition on discharge stability is also explored. Effects of long ( $\sim$  1 $\mu$ s) conduction time will be discussed.

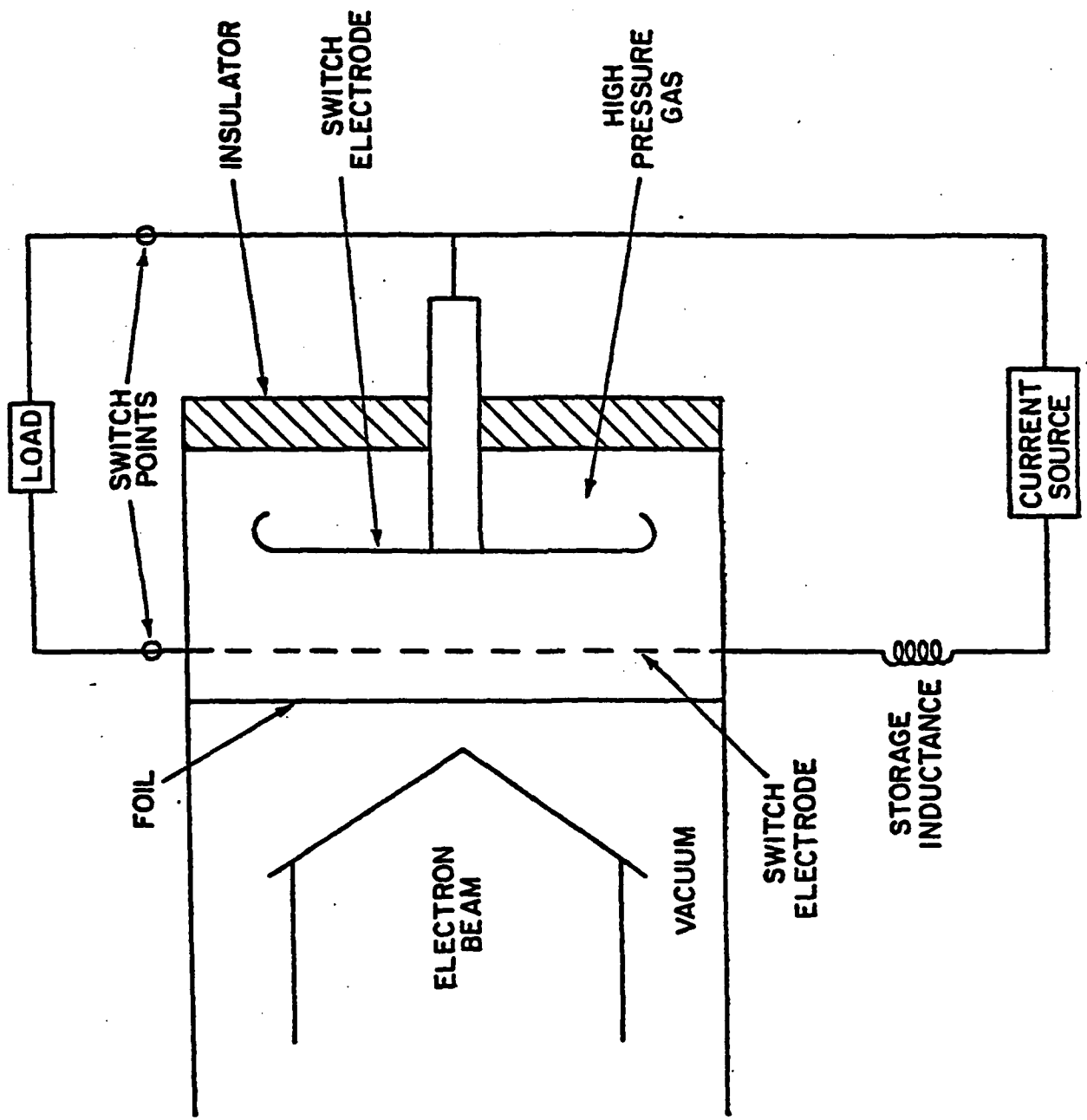
<sup>†</sup>Work supported by ONR, Arlington, VA and NSWC, Dahlgren, VA.

<sup>‡</sup>JAYCOR Inc., Alexandria, VA 22304.

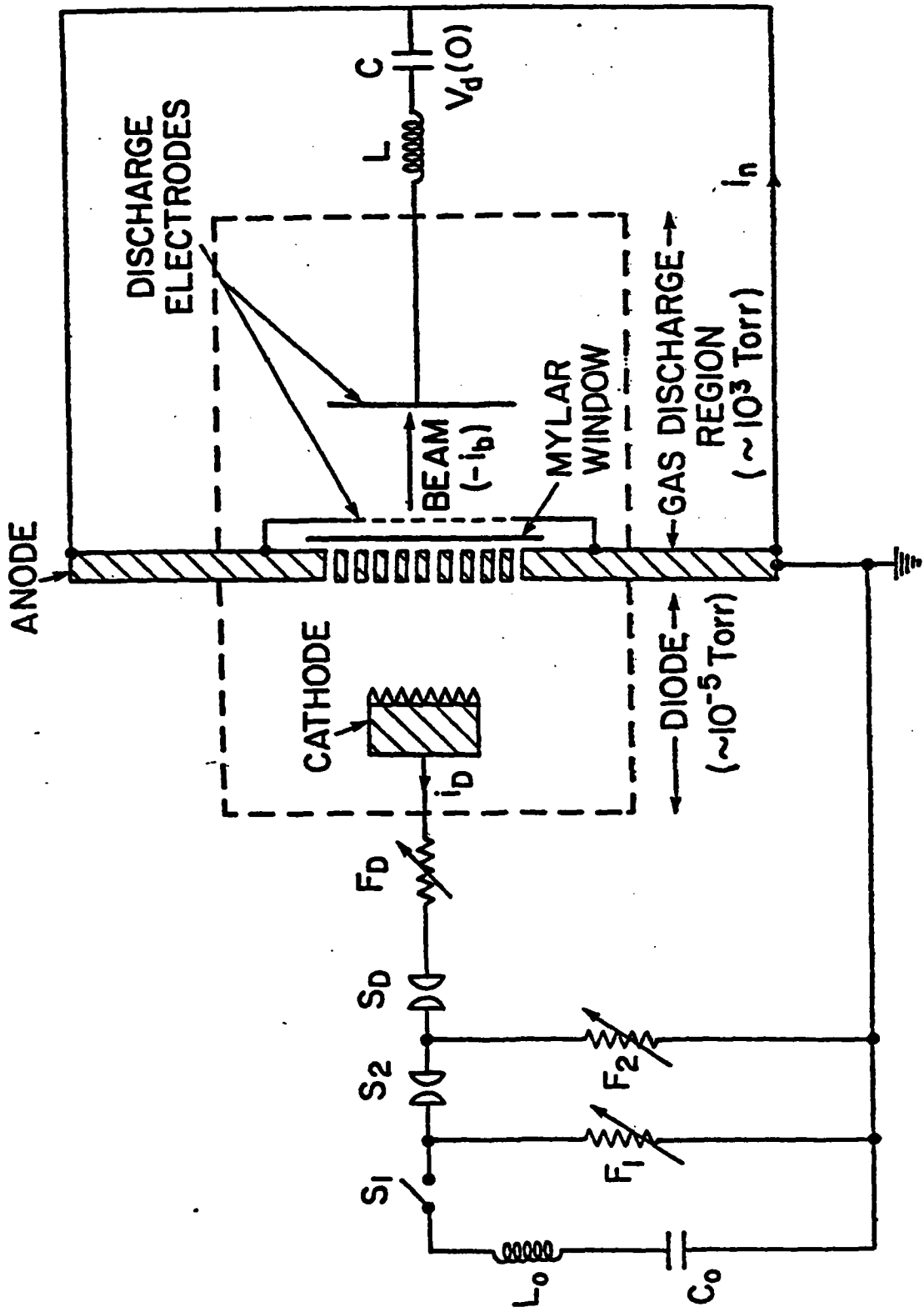
<sup>§</sup>R.F. Farnsler, D. Conte, and I.M. Vitkovitsky, IEEE Trans. Plasma Sci. PS-8, 176 (1980).

<sup>2</sup>R.J. Commisso, R.F. Farnsler, V.E. Scherrer, and I.M. Vitkovitsky, IEEE Trans. Plasma Sci., PS-10, 241 (1982), and references therein.

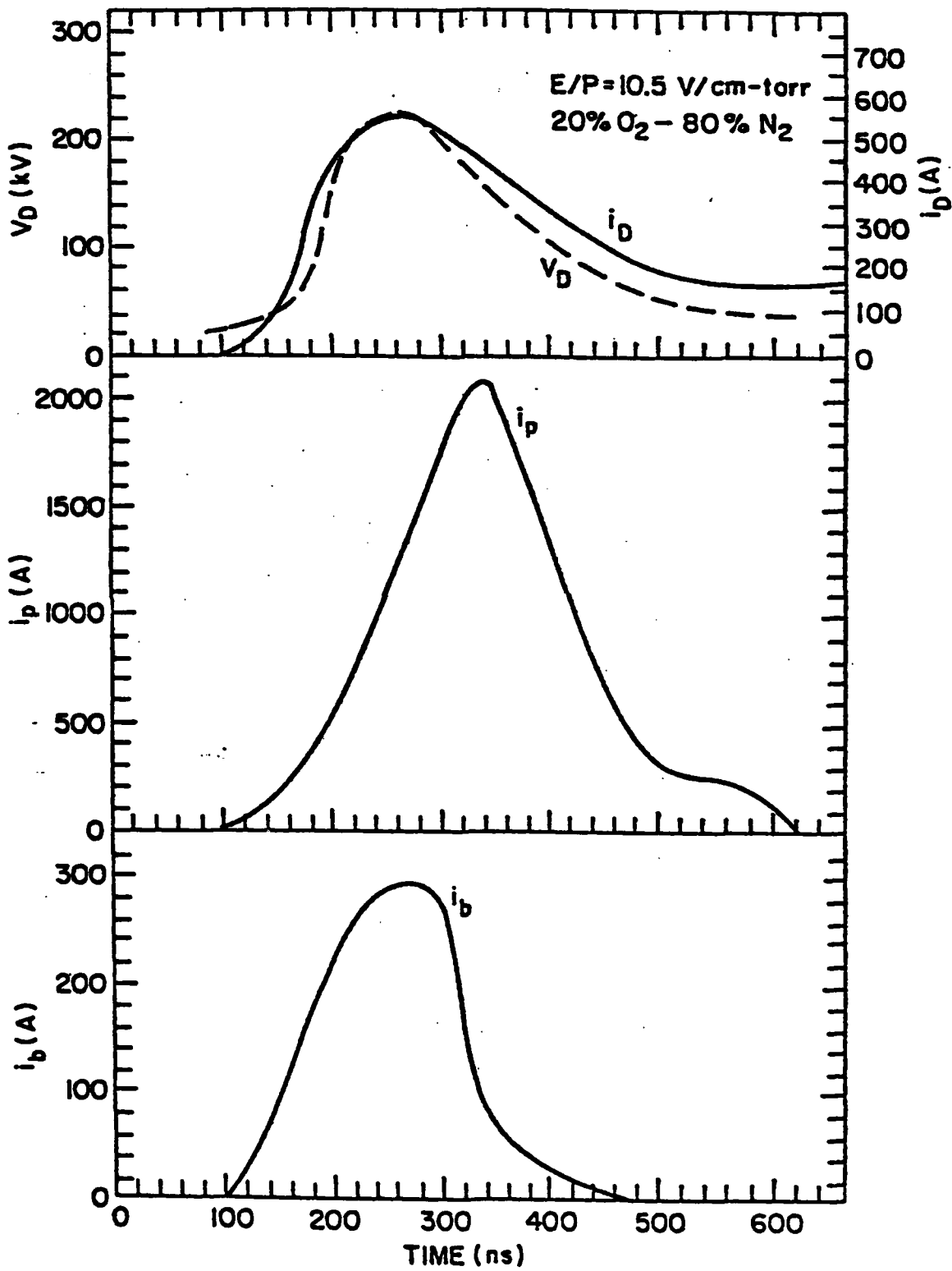
# CONCEPT

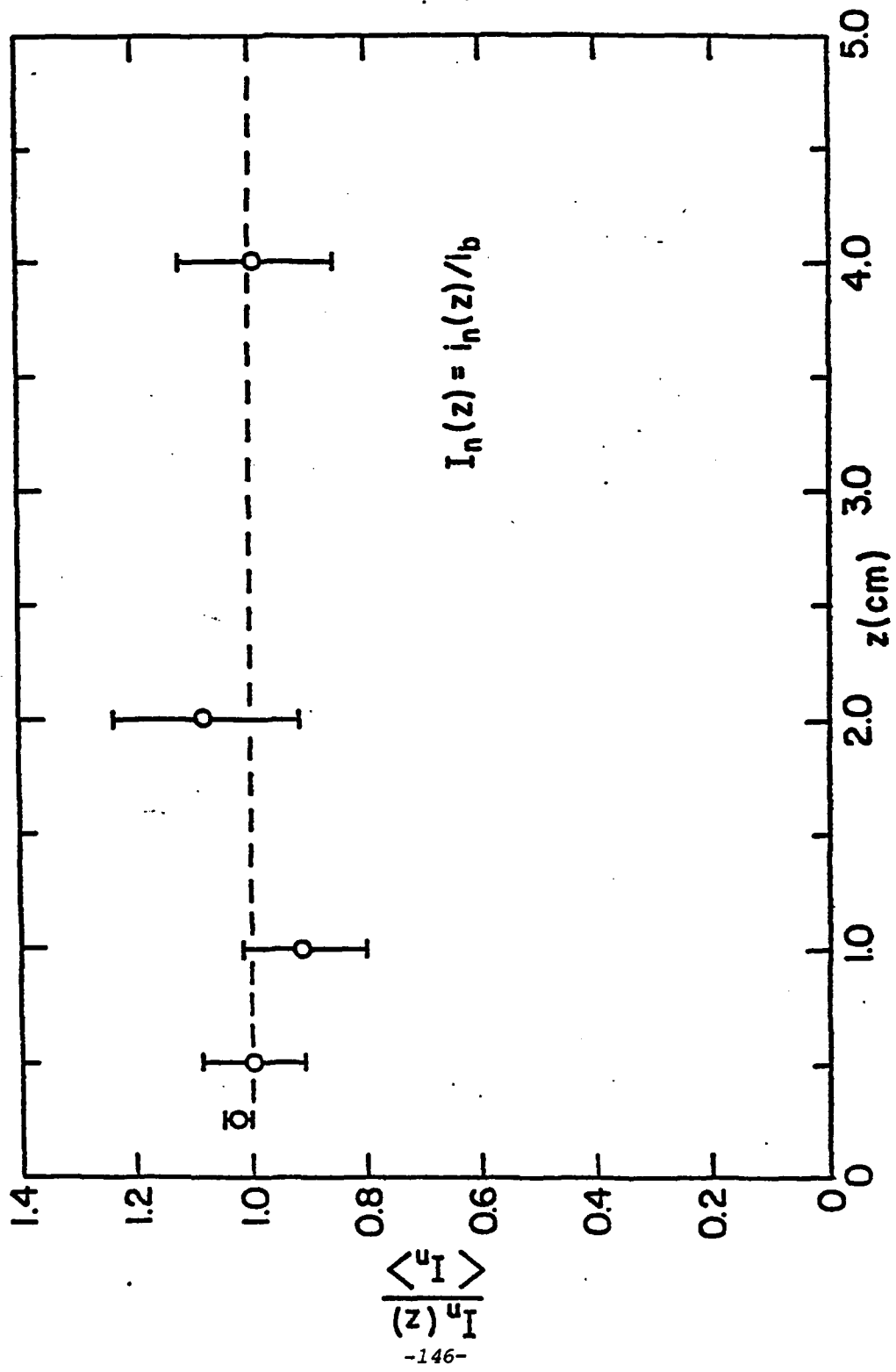


# APPARATUS



# TYPICAL EXAMPLE





# THEORY

## THEORETICAL MODEL

DISCHARGE PLASMA ELECTRONS:

$$\frac{dn_p}{dt} = S_0 J_0 P - \underbrace{[(\alpha_1 + \alpha_2 N_0) N_0 + \beta N^+]}_F n_p$$

$\alpha_1 \rightarrow 2$  - BODY DISSOCIATE ATTACHMENT :  $e + A_2 \rightarrow A^- + A$

$\alpha_2 N_0 \rightarrow 3$  - BODY ATTACHMENT :  $e + A + B \rightarrow A^- + B$

$\beta \rightarrow 2$  - BODY DISSOCIATIVE RECOMBINATION:  $e + A_2^+ \rightarrow A + A$

OTHER SPECIES:

$$\left\{ \frac{dN}{dt} \right\}_A^{+, -, 0}$$

CHARGE CONSERVATION:

$$n_p + \sum_A N^- = \sum_A N^+$$

CIRCUIT EQUATION:

$$V_0(t) = R \underbrace{(l_n - l_b)}_{l_p} + L \frac{di_n}{dt} + \frac{1}{C} \int_0^t i_n dt$$

DISCHARGE PLASMA CURRENT:

$$J_p \approx n_p e v; \quad v = \mu E, \quad \mu = \text{ELECTRON MOBILITY}$$

DISCHARGE RESISTIVITY:

$$\rho_c = E_c / J_p = (e n_p \mu)^{-1}$$

IN EQUILIBRIUM:

$$\frac{dn_p}{dt} = 0$$

$$\Rightarrow \frac{E}{l_p} \propto P f_0(P, \mu) \quad (\text{FOR } E_c/P \text{ CONSTANT})$$

THEORETICAL MODEL

ATTACHMENT

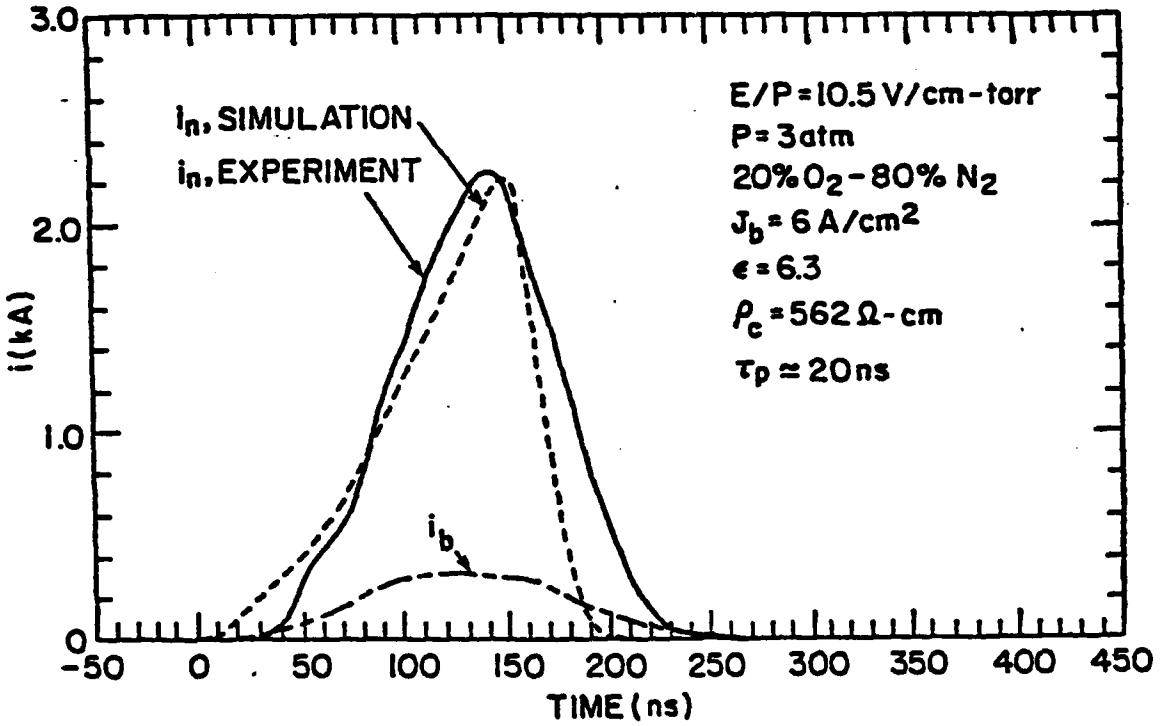
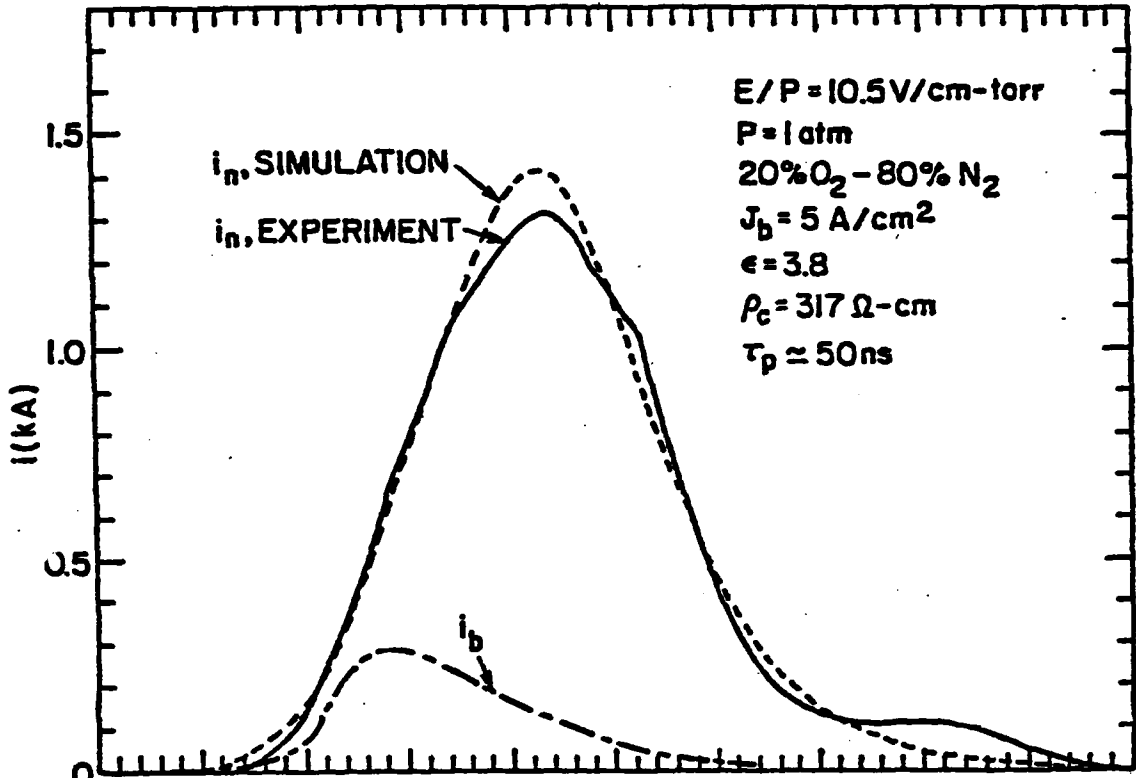
RECOMBINATION

$$\epsilon_a = \frac{S_0 l (W E) P}{\alpha N_a}$$

$$\epsilon_r = \left( \frac{S_0 P}{\beta J_b} \right)^{\frac{1}{2}} l (W E)$$

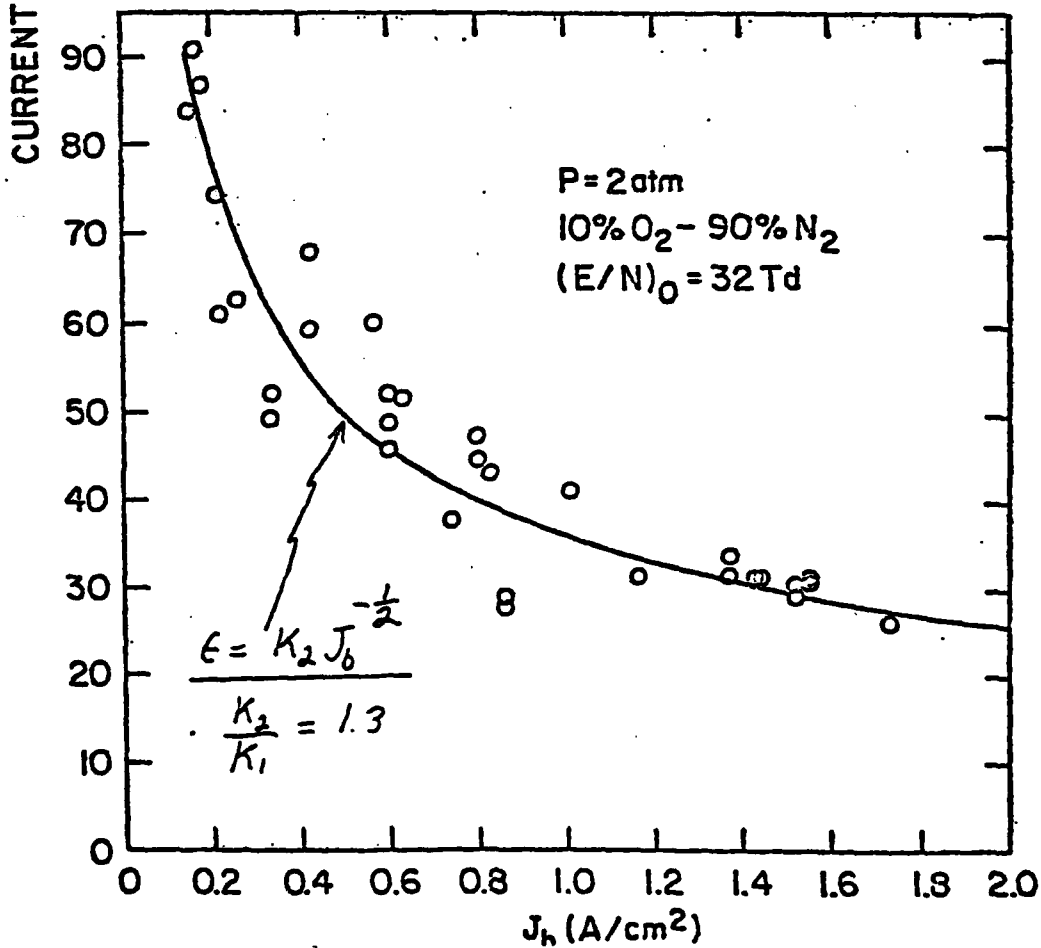
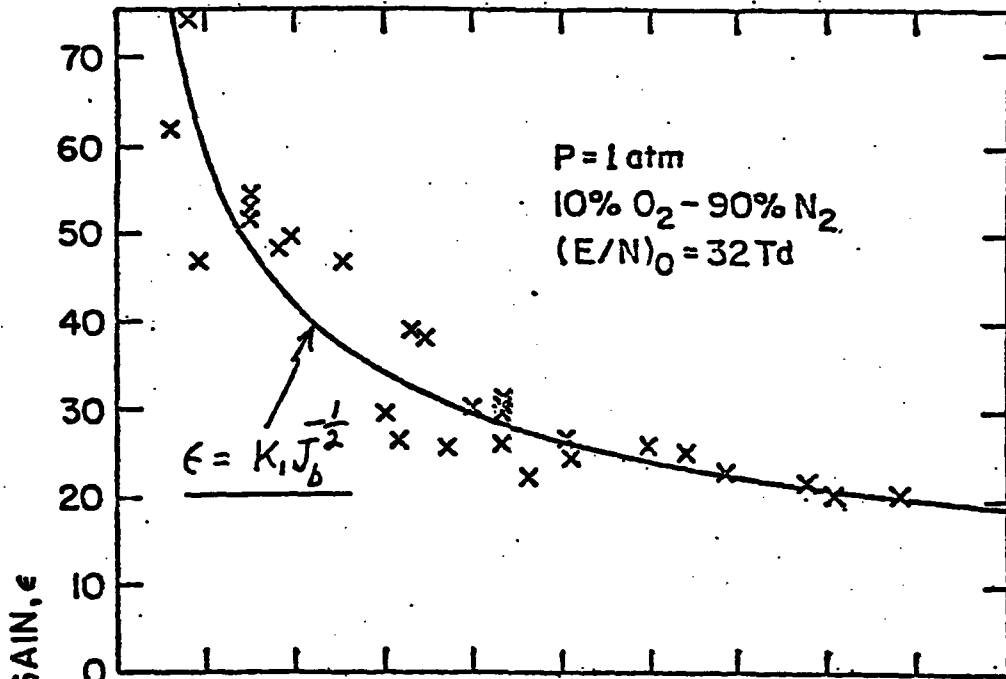
$$P_a = \frac{\alpha N_a}{S_0 l W P J_b}$$

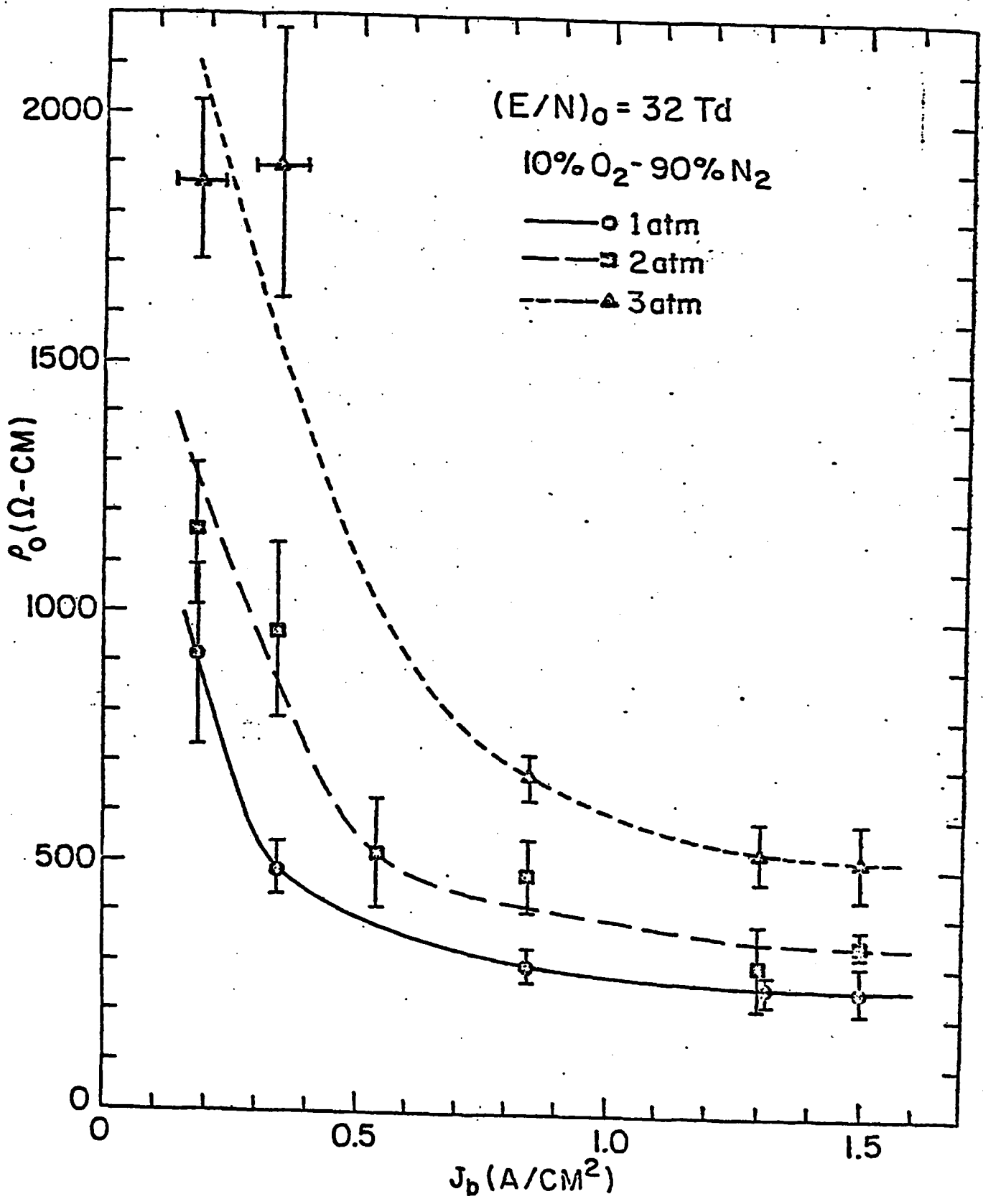
$$P_r = \left( \frac{\beta P}{S_0 J_b} \right)^{\frac{1}{2}} \frac{1}{l W P}$$

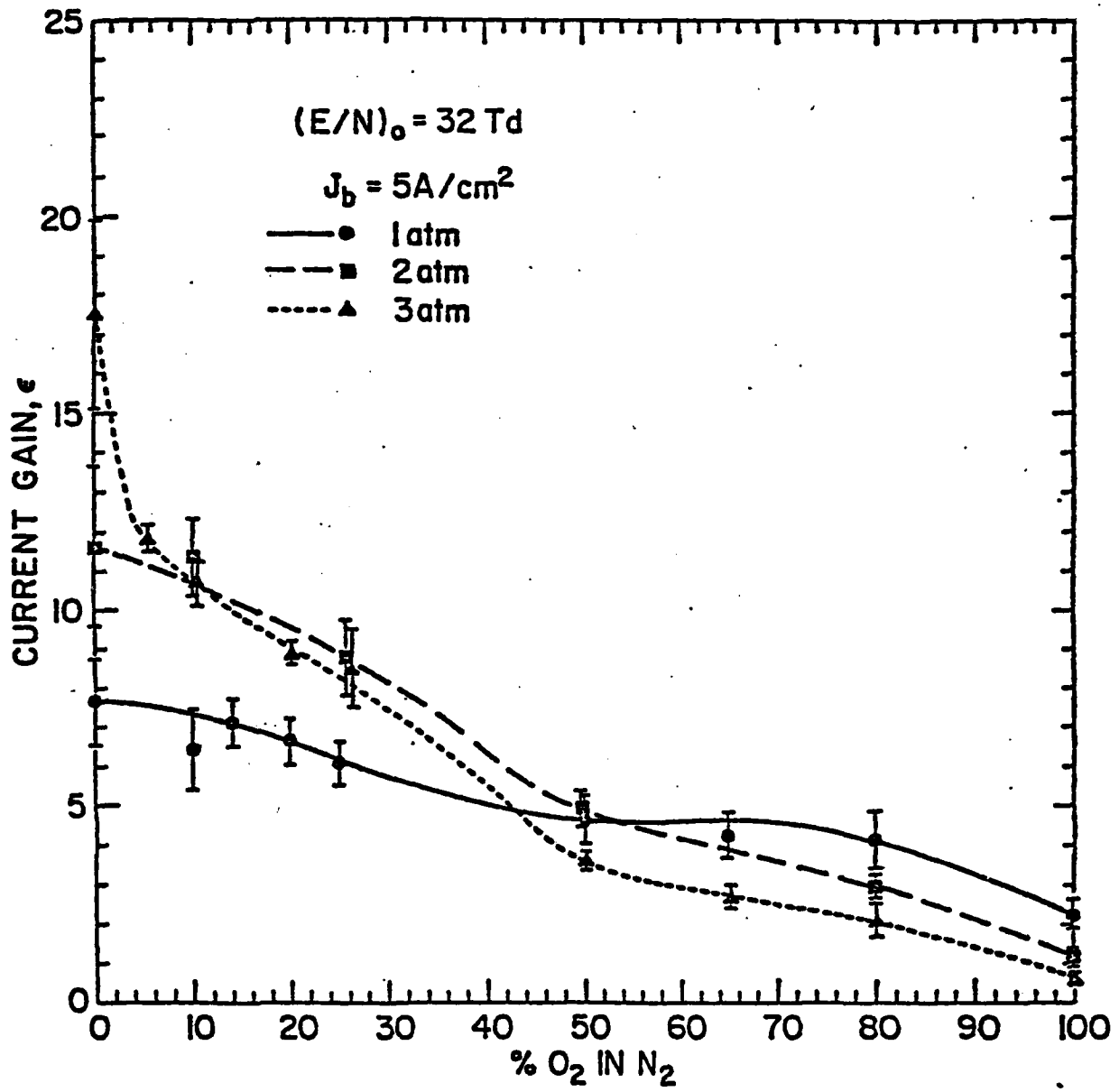


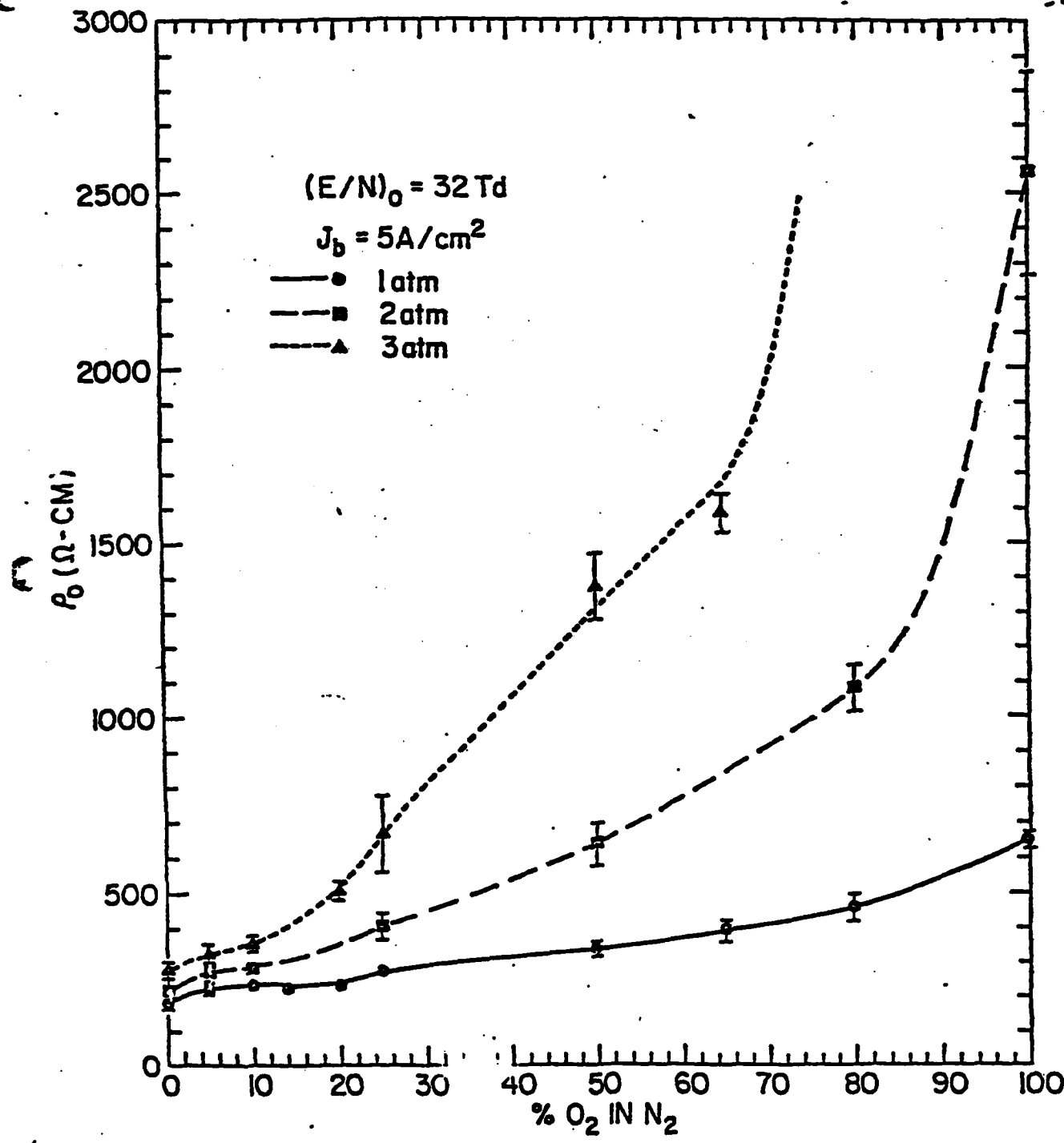
TIME (ns)

**DISCHARGE PARAMETER  
SCALING**

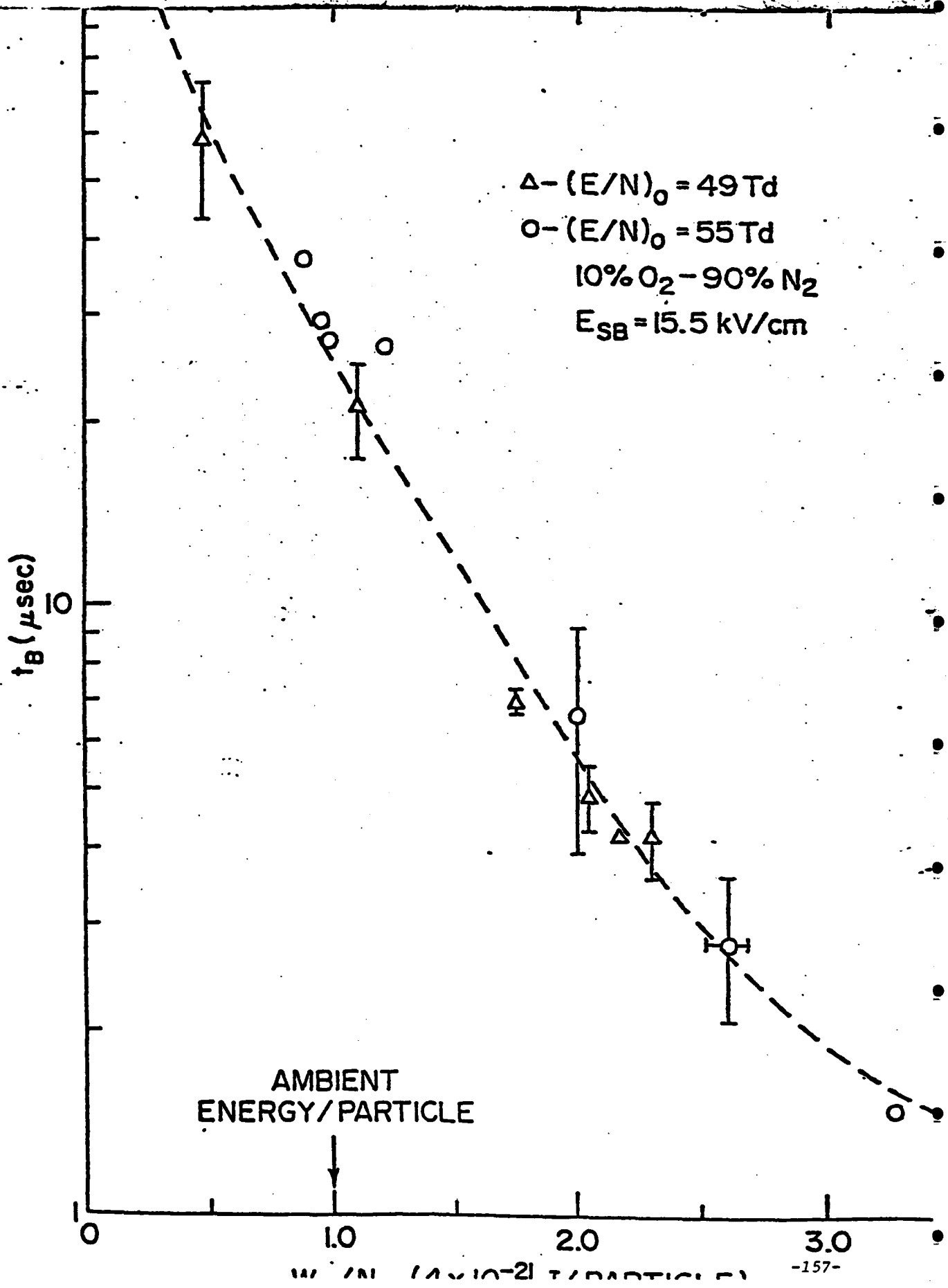








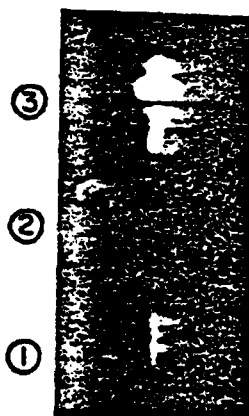
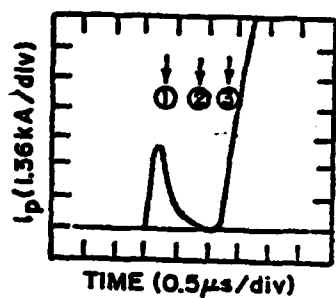
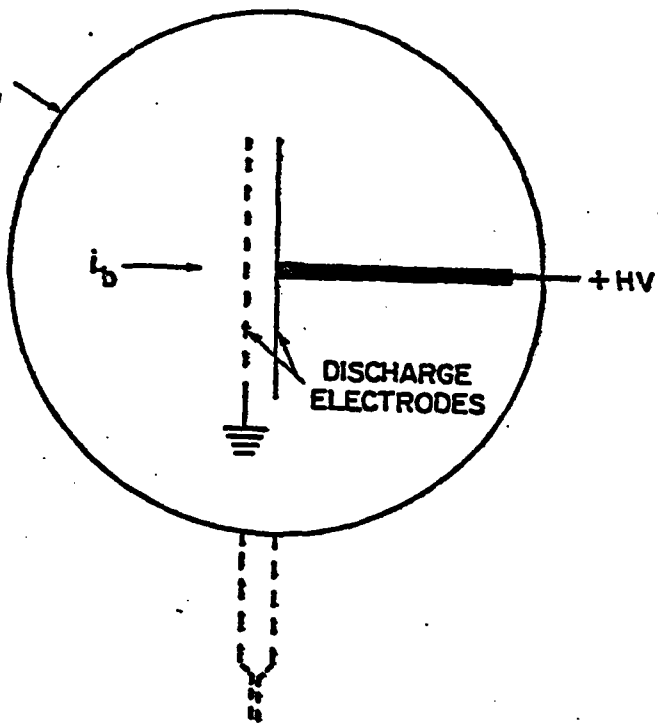
# DISCHARGE STABILITY



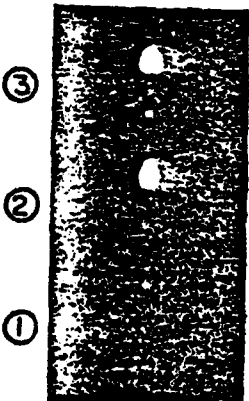
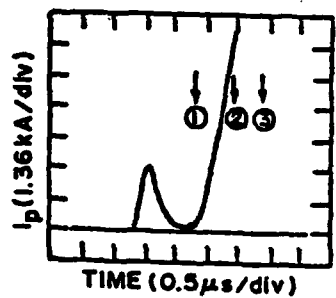
W (eV) ( $1 \times 10^{-2}$ ) / PARTICLE

# FRAMING CAMERA PHOTOGRAPHY

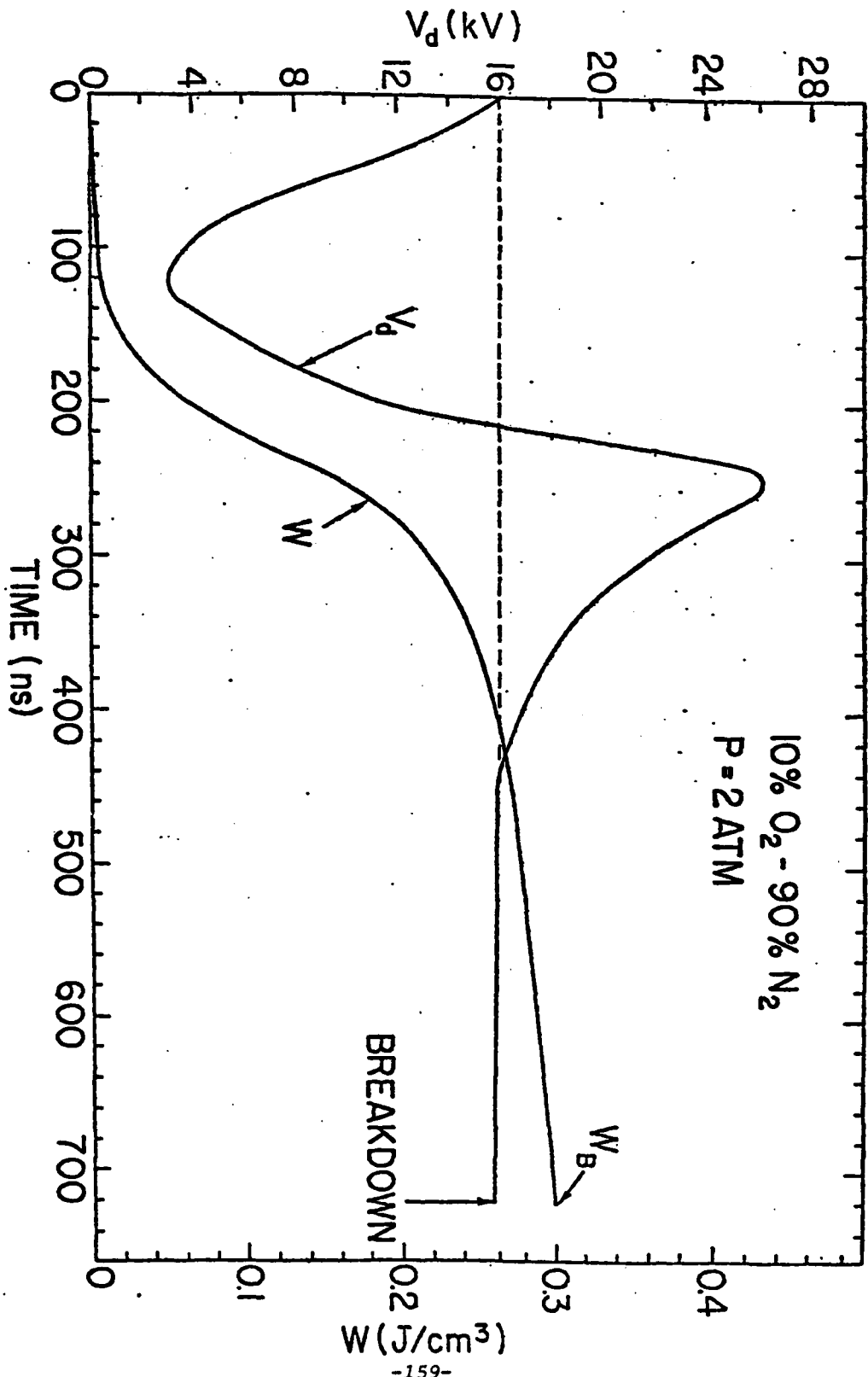
APPROXIMATE  
FIELD OF VIEW



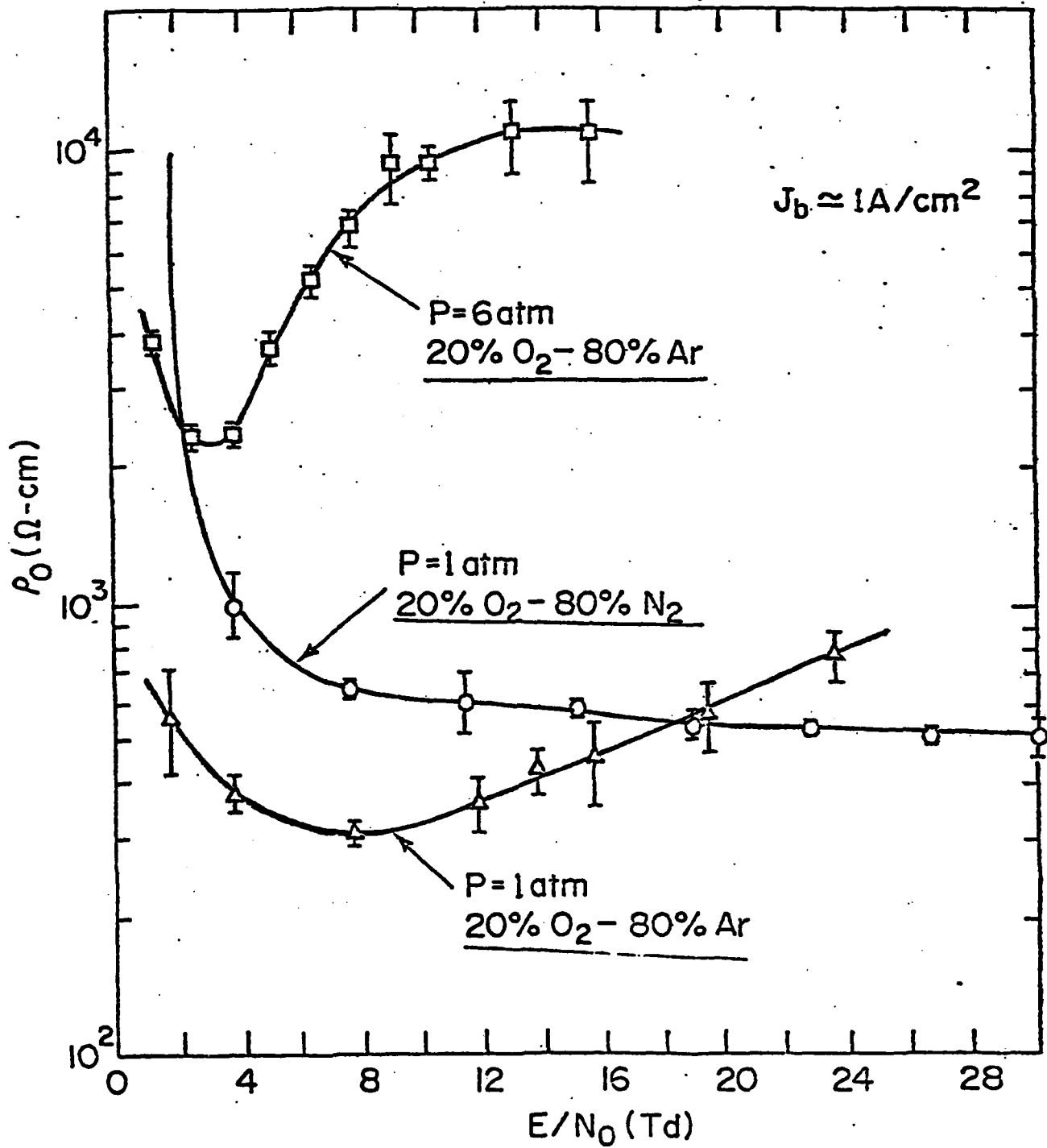
f/2.0  
100ns EXPOSURE



f/22  
100ns EXPOSURE



# GAS OPTIMIZATION



INTERPRETATION OF

$\rho_0$  VS.  $E/N$

NORMAL GAS ( $O_2-N_2$ ): CONSTANT  $\rho_0$

RISE AT LOW  $E/N$  DUE TO CATHODE SHEATH ( $V_c \sim 500V$ )

ANOMOLOUS GAS ( $O_2-Ar$ ): VARIABLE  $\rho_0$

RISE OF  $\rho_0$  WITH  $E/N$  DESIRABLE FOR SWITCHES

PROBABLE CAUSES:

RAMSAUER EFFECT ON MOBILITY  $\mu(E/N)$

AND/OR

DISSOCIATIVE ATTACHMENT RATE  $\alpha(E/N)$

PRESSURE SCALING OF  $\rho_0$  SUGGESTS BOTH PROCESSES PLAY  
A ROLE:

LOW  $P$ ,  $e+O_2 \rightarrow O+O^-$  WITH  $\alpha(E/N)$

HIGH  $P$ ,  $e+O_2+Ar \rightarrow O_2^-+Ar$  WITH  $\mu(E/N)$

# SUMMARY

1. WE HAVE PRESENTED A CONCEPT FOR AN E-BEAM CONTROLLED OPENING SWITCH, DESCRIBED EXPERIMENTAL AND THEORETICAL METHODS FOR INVESTIGATING IT, AND USED THESE METHODS TO OBTAIN EXPERIMENTAL AND THEORETICAL RESULTS.
2. EXPERIMENTAL RESULTS FOR 20%O<sub>2</sub>-80%N<sub>2</sub> AGREE WITH THOSE OBTAINED BY TIME DEPENDENT COMPUTER CODE SIMULATION.
3. OUR DISCHARGE APPEARS TO BE RECOMBINATION DOMINATED. THE IMPORTANT DISCHARGE PARAMETERS FOR SWITCH APPLICATIONS,  $\rho_0$  AND  $\epsilon$ , SCALE AS THEORY PREDICTS.
4. DISCHARGE INSTABILITY LEADING TO DELAYED BREAKDOWN CAN BE AVOIDED BY CHOICE OF OPERATING CONDITIONS.
5. PROPER CHOICE OF GAS CAN OPTIMIZE DISCHARGE FOR SWITCH APPLICATIONS.

APPENDIX II  
PAPER PRESENTED ON PDS  
REFERENCE 12

1982 IEEE INTERNATIONAL CONFERENCE ON PLASMA SCIENCE

MAY 17-19, 1982

Experiments with Plasma Switching.\* R.J. Comisso<sup>1</sup>, and I.M. Vitkovitsky, Naval Research Laboratory -- Application of inductive storage to present requirements for pulsed, high power generators demands a switch with the following ideal characteristics: it must conduct  $\geq 1$  MA of current at low resistance ( $\ll 1\Omega$ ) for a time on the order of  $1\mu$ s, open predictably (i.e., become resistive with respect to some load) in a time  $\leq 100$ ns, and remain open against a voltage of  $\geq 1$  MV. In practice, combining all of these requirements in a single device has proven to be extremely difficult. However, some success has been achieved by using several types of switches in succession to obtain the required power amplification.<sup>1</sup> One such component switch is the exploding wire fuse. It generally conducts for tens of microseconds, opens in  $\sim 150$ ns and can have recovery strengths of  $\sim 20$  kV/cm. The main disadvantages of the wire fuse are the joule heating losses and the necessity for physically replacing it after each use. In addition, the fuse opening time is about a factor of ten too long for some high power applications.

One possibility as an improvement over the wire fuse is the use of a plasma as a switch medium. Plasmas have been observed to conduct hundreds of kiloamperes of current for  $\leq 100$ ns and to open in tens of nanoseconds against several hundred kilovolts.<sup>2</sup> A plasma switch is also, at least conceptually, resettable; so that not only is replacement after each use not necessary but repetitively pulsed operation may be feasible.

In this paper we report an investigation to determine the feasibility of one scheme for a plasma switch. The scheme involves use of a deflagration plasma gun<sup>3</sup> as a source of helium plasma with high directed energy ( $\approx 10^7$  cm/s). The plasma so produced drifts through a vacuum region and then enters the gap between two electrodes that have a potential applied across them. The conduction and opening properties of the helium plasma in the electrode region are then studied. The diagnostics presently include voltage and current monitors, streak/framing camera, faraday cup probes, and spectroscopy. At present, the following operating parameters are used for the gun:  $V_G = 12$  kV,  $I_G = 200$  kA,  $C_G = 55$   $\mu$ F; and for the switch:  $V_S = 10$  kV,  $I_S \approx 10$  kA,  $C_S = 1.85$   $\mu$ F.

As observed with the streak/framing camera, the plasma gun ejects three, not totally distinct plasmoids; each correlated in time with an extremum of the gun current with each subsequent one moving more slowly than its predecessor. The first of these plasmoids has two components, each with a different speed. Based on the time of current initiation at the switch, a third component of the first plasmoid moving almost twice as fast as the fastest visible front is conjectured. No opening action has been observed as yet, probably as a result of excess plasma and poor plasma spatial distribution. The effects of limiting apertures and of a crowbar on the gun are being investigated.

\*Work supported by Office of Naval Research. <sup>1</sup>JAYCOR, Inc., Alexandria, VA 22304

<sup>1</sup>R.D. Ford, D. Jenkins, W.H. Lupton, and I.M. Vitkovitsky, Third IEEE Int. Pulsed Power Conf., Albuquerque, NM (1981) paper 7.2.

<sup>2</sup>C.W. Mandel and S.A. Goldstein, J. Appl. Phys. **48**, 1004 (1977).

<sup>3</sup>D.Y. Cheng, Nuc. Fus. **10**, 305 (1970).

This form, or a reasonable facsimile, plus two Xerox copies must be received NOT LATER THAN FEBRUARY 15<sup>TH</sup>, 1982 at the following address: A.J. Alcock, Chairman, 1982 International Conference on Plasma Science, c/o National Research Council of Canada, Ottawa, Ontario, Canada K1A 0R6.

Please refer to "First and Final Call for Papers" announcement for instructions in preparing your abstract.

Subject category name:

Subject category number:

- Prefer oral session
- Prefer poster session
- No preference
- Special requests for placement of this abstract

Submitted by:

(signature)

(same name typewritten)

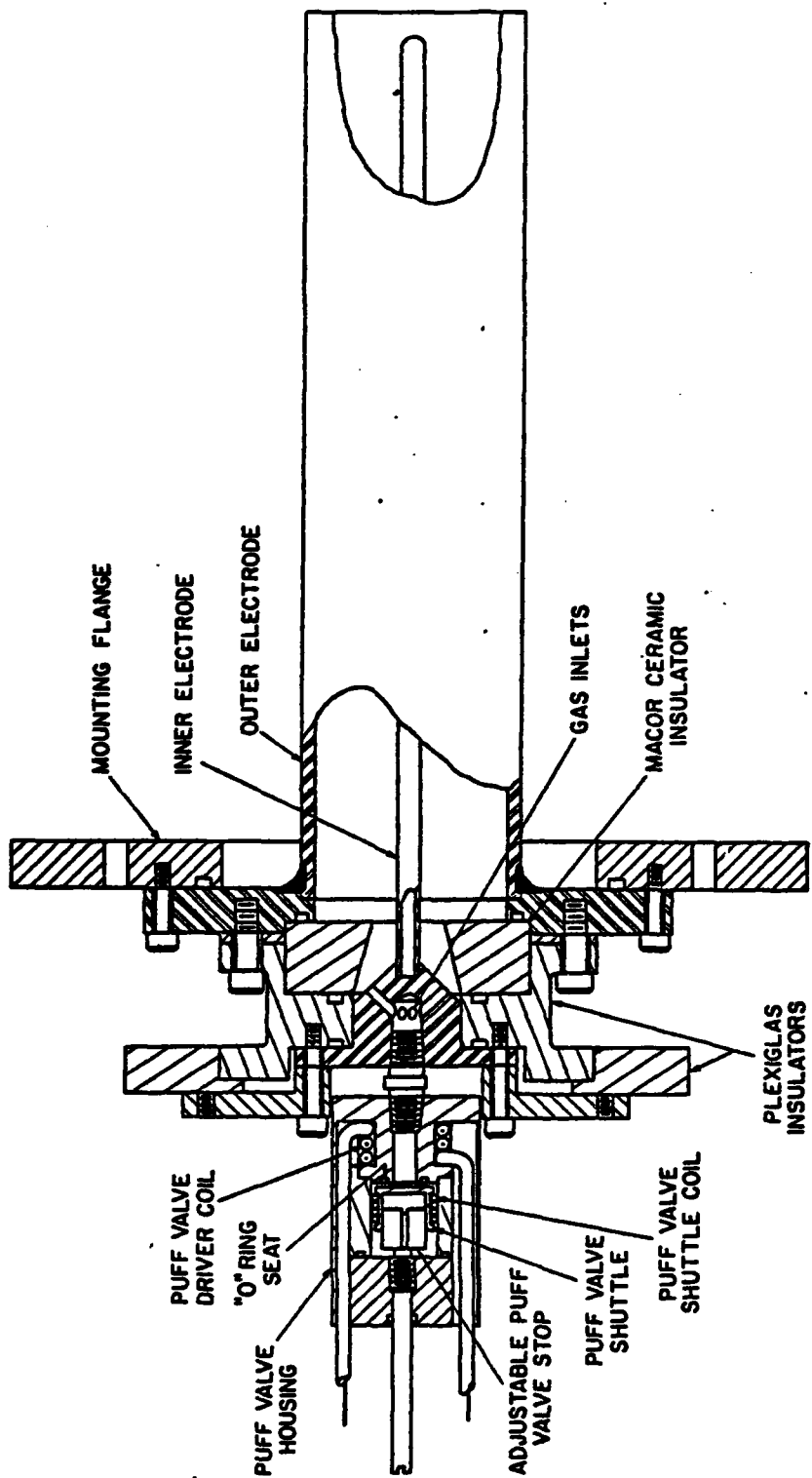
(full address)

I am a member of the Committee on Plasma Science and Application

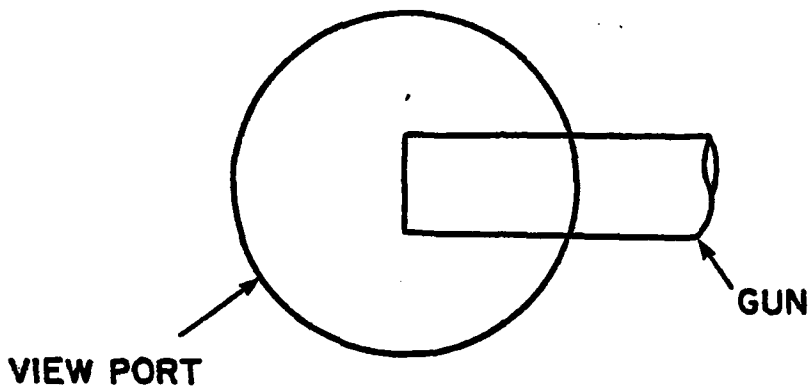
- yes  no

N.B. FOLDS CAN BE AVOIDED BY TYPING ON A XEROX COPY OF THIS FORM.

# GUN PLASMA

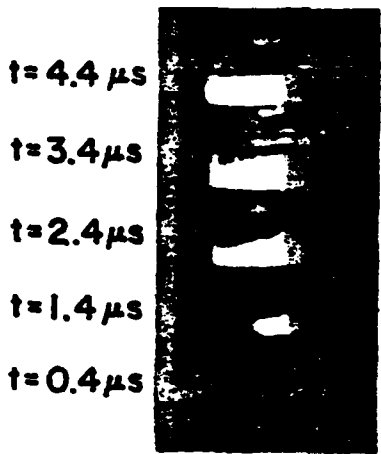


CAMERA FIELD OF VIEW

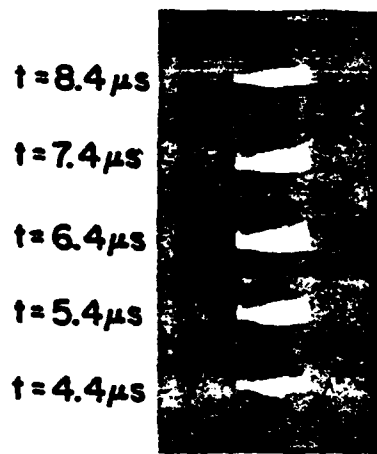


$V_G = 12 \text{ KV}$

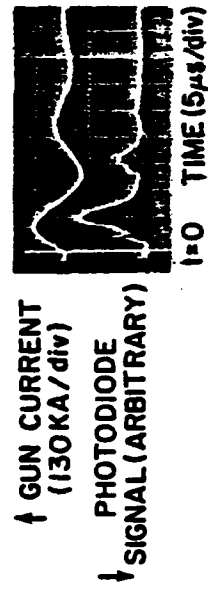
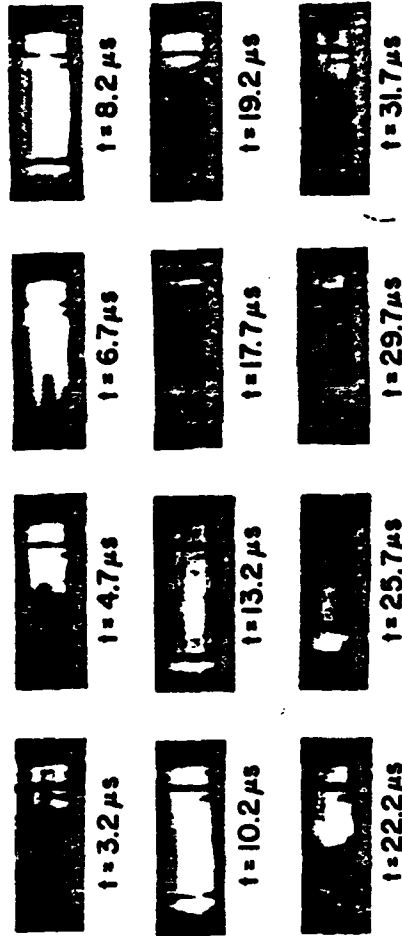
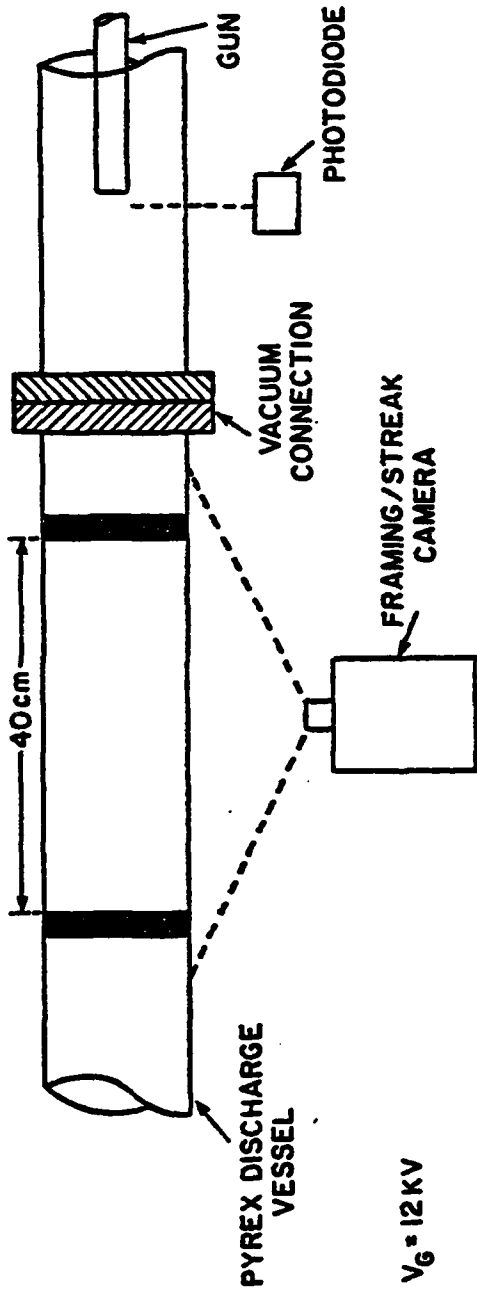
f/8

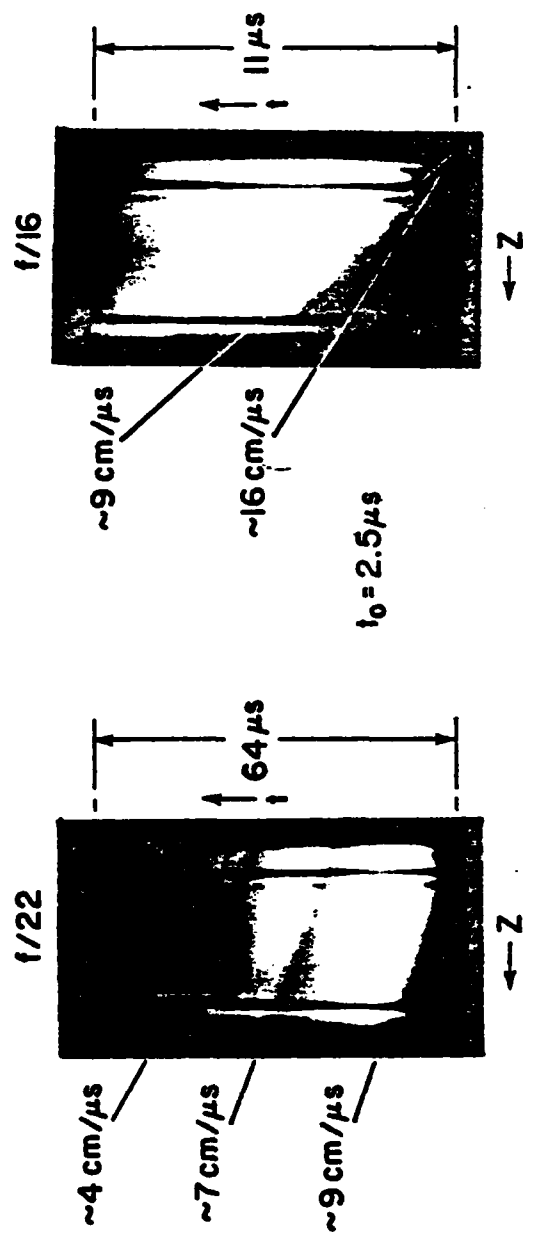
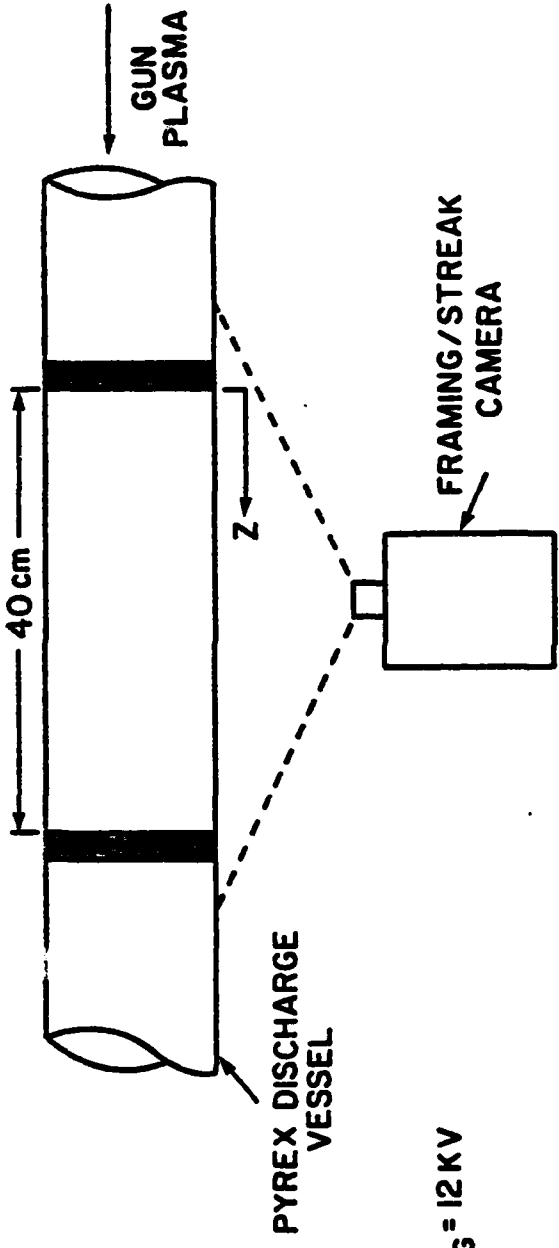


f/16



$t=0 \rightarrow$  GUN CURRENT INITIATION (10 μs half period)

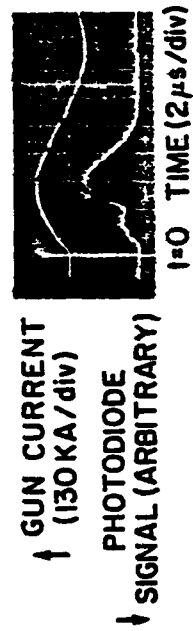
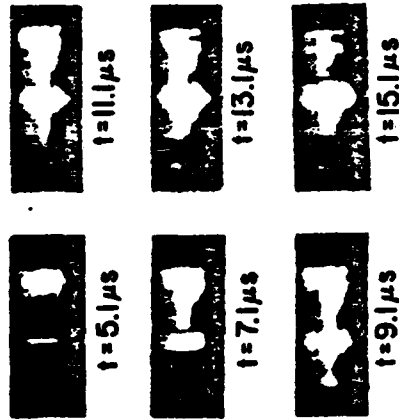
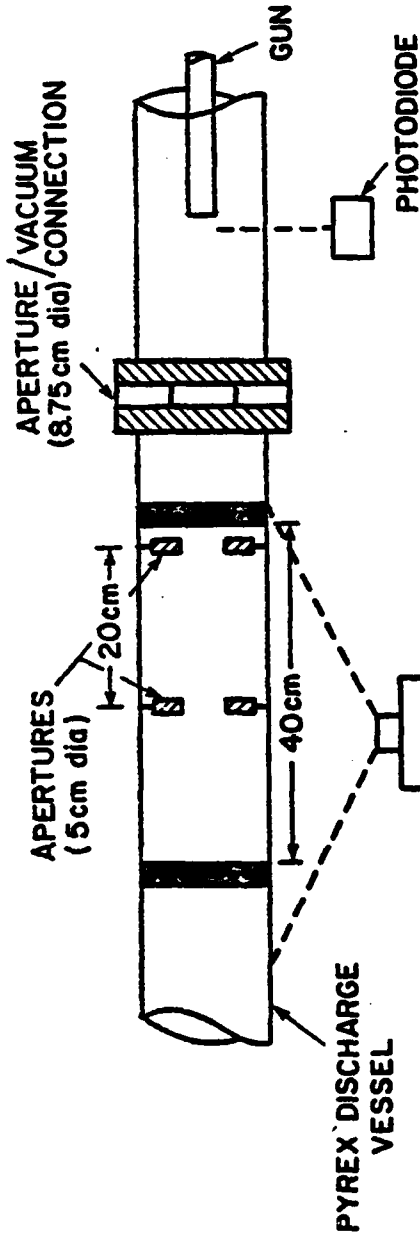


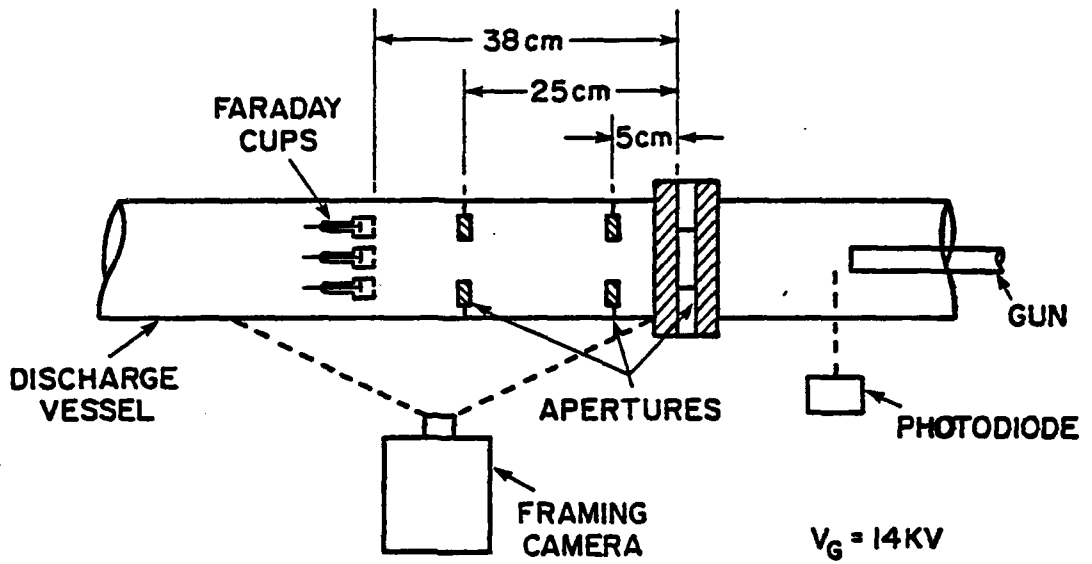




# SPACIAL AND TEMPRO

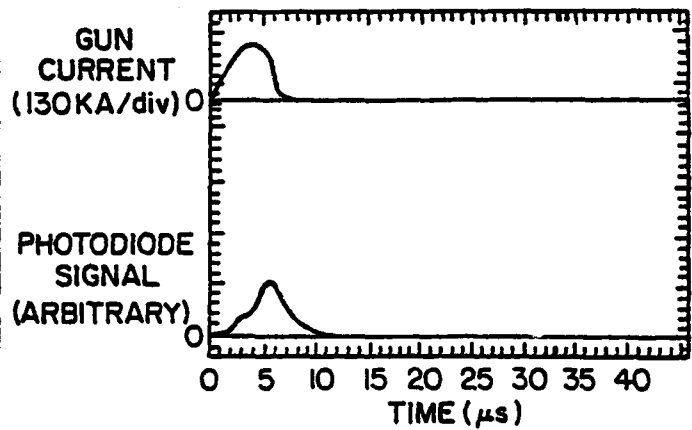
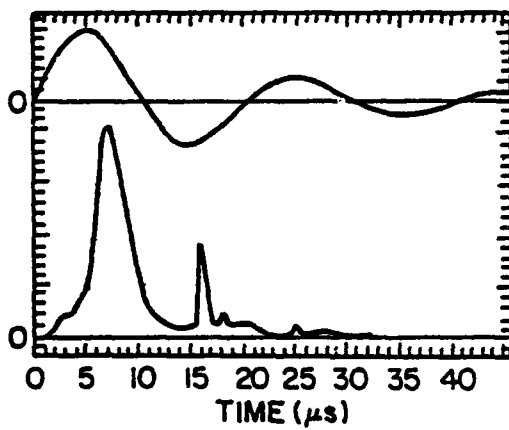
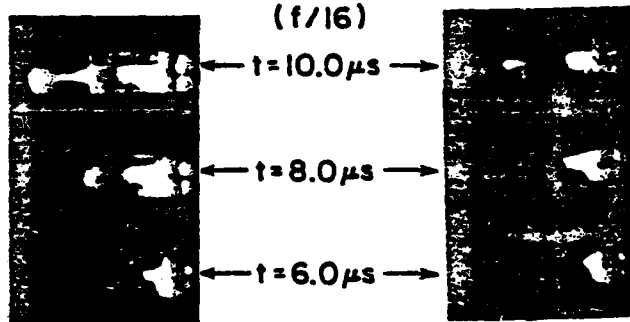






FULL DISCHARGE

FUSE



## Summary of Faraday Cup Results (with apertures)

1. Fastest plasma component (not seen optically).

$$\langle v_0 \rangle = 32 \text{ cm}/\mu\text{s} \quad \langle n_0 \rangle_i \approx 6.2 \times 10^{12} \text{ cm}^{-3}$$

2. Fast plasma component (seen optically)

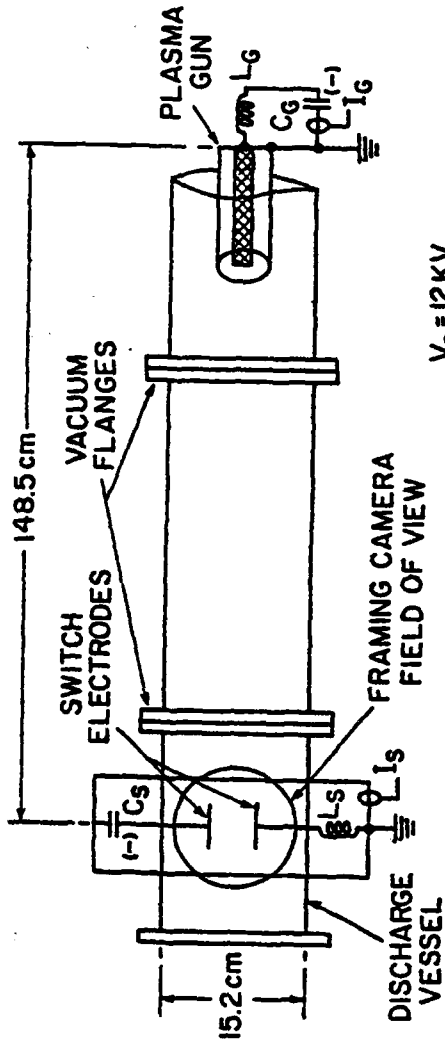
$$\langle v_1 \rangle \approx 84 \text{ cm}/\mu\text{s} \quad \langle n_1 \rangle_i \approx 7.4 \times 10^{15} \text{ cm}^{-3}$$

$$\langle v_2 \rangle \approx 18.5 \text{ cm}/\mu\text{s} \quad \langle n_2 \rangle_i \approx 1.6 \times 10^{16} \text{ cm}^{-3}$$

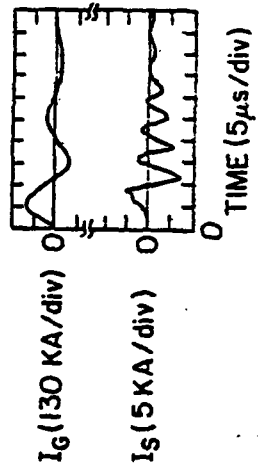
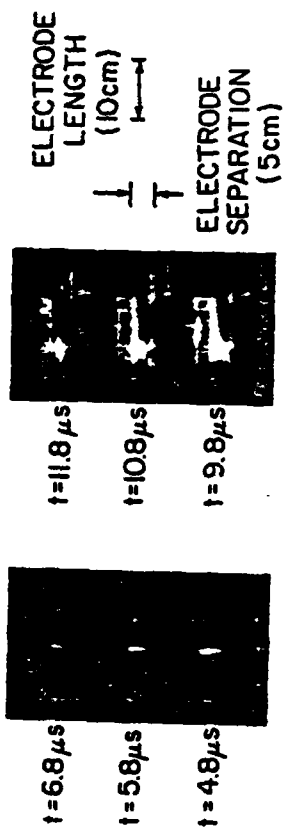
3. Slower components are not azimuthally symmetric and not temporally reproducible.

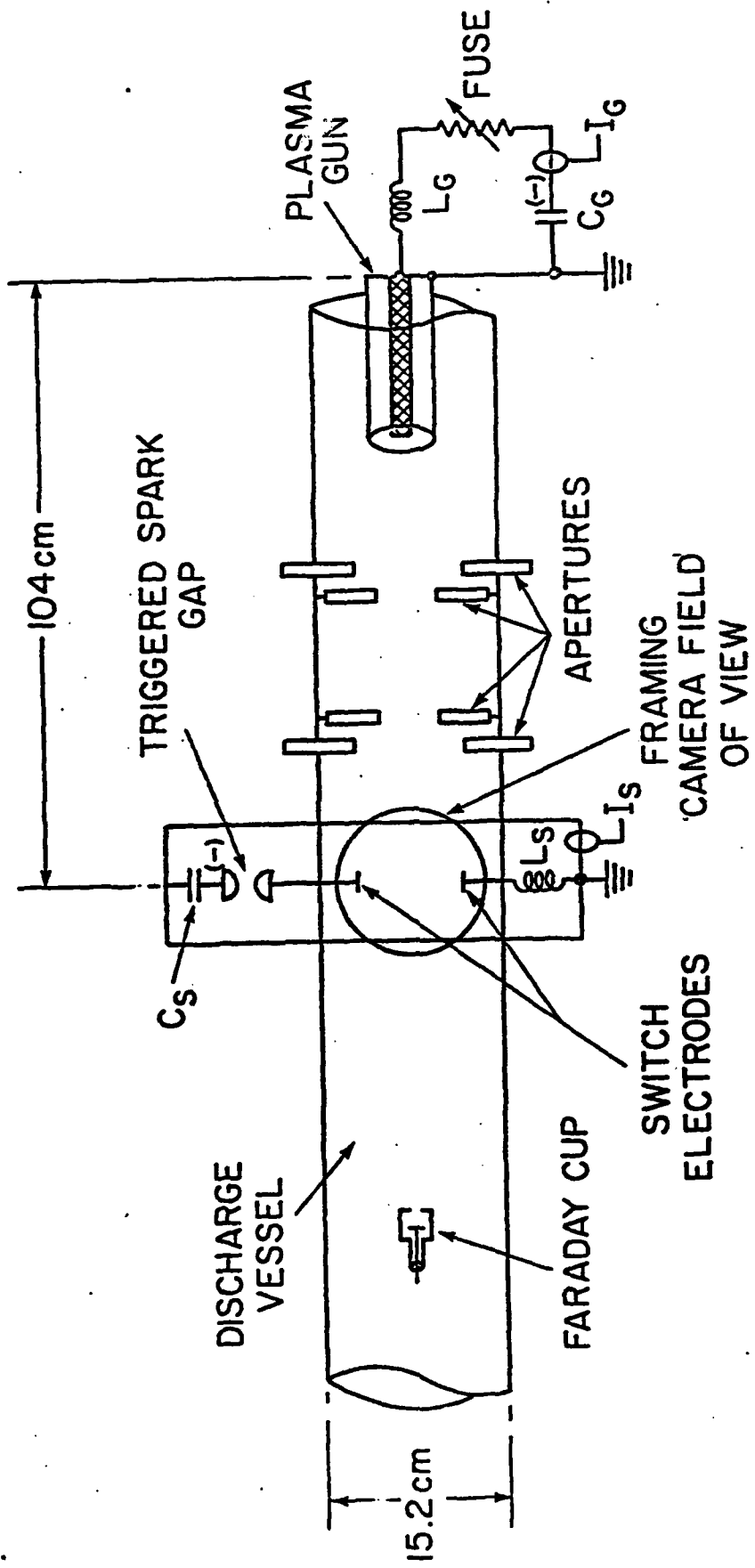
4. When gun is operated with fuse, there is no apparent change in the faraday cup signals. (may be a result of plasma wall interaction). (may be a result of detailed plasma ejection mechanisms in gun).

# SWITCH OPERATION



(f/4)





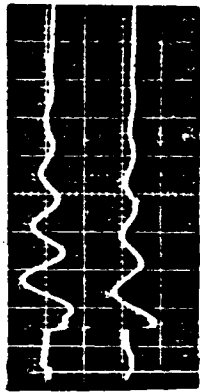
FULL DISCHARGE

$\Delta t_{SD} = 2.5 \mu s$



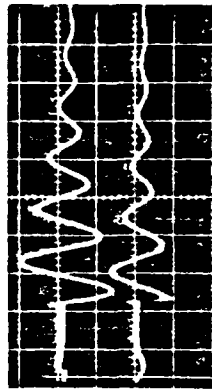
t=0

$\Delta t_{SD} = 5.5 \mu s$



t=0

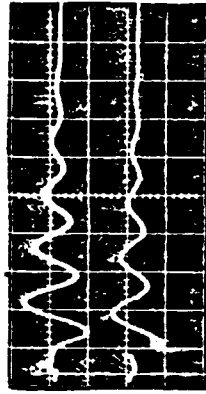
$\Delta t_{SD} = 9.5 \mu s$



t=0

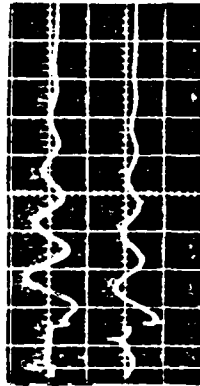
FUSE

$I_s$  (10KA/div)  
 $V_{sc}$  (8KV/div)  
5  $\mu s$ /div



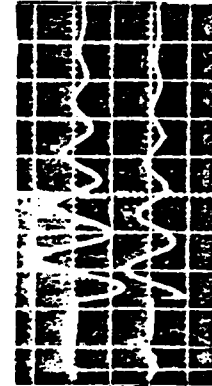
t=0

ELECTRODE  
LENGTH  
3cm



t=0

ELECTRODE  
SEPARATION  
9cm



t=0

$V_G = 14KV$   
 $V_{sc}(0) = 10KV$

**END**

**FILMED**

**8-84**

**DTIC**